PPPL-Q--42

DE86 008595

Annual Report Covering the Period October 1, 1983 to September 30, 1984

Princeton University
Plasma Physics Laboratory
Princeton, New Jersey

PPPL-Q-42

Edited by
Carol A. Phillips

Unless otherwise designated, the work in this report is funded by the United States Department of Energy under Contract DE-AC02-76-CHO-3073.

Printed in the United States of America

CONTENTS

PREFACE

During FY84, experimental research on the Tokamak Fusion Test Reactor (TFTR) confirmed the favorable size-scaling of energy confinement in large ohmic-heated tokamak plasmas. Initial auxiliary-heating studies were carried out with neutral-beam injection and adiabatic compression. Substantial progress was also made towards full-parameter machine operation and towards the development of technical capabilities for the deuterium-deuterium and deuterium-tritium $Q \sim 1$ experiments.

The Princeton Large Torus (PLT) extended its ion cyclotron range of frequencies (ICRF) heating experiments to the 4-MW power level, producing ion temperatures above 4 keV. Lower-hybrid current drive was advanced to plasma regimes in the 10^{13} cm^{-3} density range, by means of a new 2.45-MHz source. The problem of intense focal limiter heating during long-pulse radio-frequency discharges was addressed successfully by introduction of a rotating limiter system.

The reconfiguration of the Poloidal Divertor Experiment (PDX) into the Princeton Beta Experiment (PBX) resulted in a doubling of the achievable beta value: stable tokamak plasmas with average β's above 5% were reached for the first time. The bean-shaped tokamak was found to enter readily into the favorable H-mode plasma-confinement regime.

The predicted stabilization of spheromak plasmas by means of external figure-eight coils was demonstrated successfully on the S-1 device, with a resultant improvement in plasma parameters. A promising new ICRF-type heating technique, based on the ion Bernstein wave, was developed on the Advanced Concepts Torus (ACT-I).

The single-pass gain in the Soft X-Ray Laser Experiment has been advanced to 6.5 (corresponding to a level of stimulated emission 100 times larger than spontaneous emission) for the 182-Å line of a carbon plasma. A small experiment on the spin-polarization of hydrogen, which is aimed at investigating the prospects for polarized fusion-reactor plasmas, has reached the 28% polarization level in atomic hydrogen of 10^{12} cm^{-3} density.

Theoretical studies in the area of lower-hybrid-driven current ramp-up have produced remarkably detailed agreement with the PLT experiments. New predictive capabilities for MHD stability and transport have been developed in support of "two-dimensional" experiments, such as the PBX and S-1, as well as advanced "three-dimensional" concepts, such as the Heliac high-beta stellarator. Sophisticated new codes are also being developed to treat edge-plasma phenomena and atomic effects in the vicinity of tokamak divertors and limiters.

The national design effort in support of a Tokamak Fusion Core Experiment (TFCX), which was coordinated by PPPL, led to the publication of a TFCX Preconceptual Design Report in July, 1984.

PRINCIPAL PARAMETERS ACHIEVED IN EXPERIMENTAL DEVICES (Fiscal Year 1984)

Parameters	Tokamak Facilities			Alternate Concept Facilities	
	TFTR	PBX	PLT	S-1	ACT-I
R (m)	2.56	1.45	1.32	0.40	0.59
a (m)	0.82	0.4	0.42	0.25	0.1
I_p (MA)	1.5	0.5	0.7	0.4	—
B_T (T)	3.9	1.0	3.3	0.4	0.57
τ_{AUX} (sec)	0.5	0.3	0.3	—	dc
P_{AUX} (MW)					
NB	1.5, (80 keV)	7, (50 keV)	1.5, (40 keV)	—	—
ICRF	—	—	4.0, (30 MHz)	—	0.002
LH	—	—	0.6, (800 MHz) 0.6, (2.45 GHz)	—	0.2
n(0) (cm^{-3})*	0.6×10^{14}	10^{14}	0.8×10^{14}	3×10^{14}	3×10^{12}
T(0) (keV)*	3.5	4.0	4.0	0.06	0.04
τ_E (msec)*	300	40	40	0.25	0.2

*These highest values of n, T, and τ were not achieved simultaneously.

TOKAMAK FUSION TEST REACTOR

During the first full year of experimental operations (FY84), a very considerable effort continued on the fabrication, installation, and commissioning of neutral-beam systems, on the high-power-capability internal armor, and on the addition of increasingly sophisticated diagnostics. Major efforts also continued towards providing downstream capability in the areas of tritium systems, remote handling, and shielding. Progress in all these areas is reported in detail in the following sections and briefly summarized here.

Figure 1 illustrates the division of the available operating time among the various activities. As the Tokamak Fusion Test Reactor (TFTR) gradually assumes its final form, machine availability for experimental operations is rising steadily towards levels equal to or exceeding those anticipated at the time of design authorization.

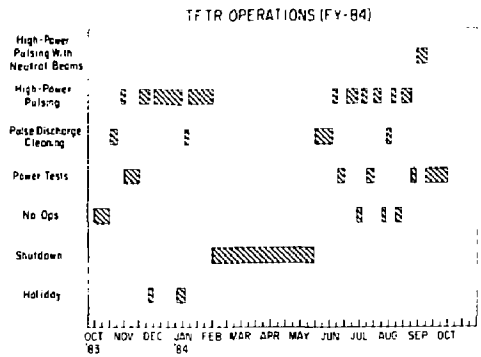

Fig. 1. Division of available time for various activities. (85X3065)

During 1984, the TFTR Facility continued to extend its operating capability towards design-rated parameters. The toroidal-field (TF) coil system was tested and now operates routinely at 56 kA (4.0 T). The power supplies are ready to support full-field (73 kA, 5.2 T) integrated system tests. The ohmic-heating coil circuit was operated at full current in both mode A (24 kA) and mode B (20 kA). During this period, the interrupter mode of operation was successfully commissioned, resulting in a large increase in available volt-seconds, and the equilibrium-field (EF) circuit was tested at 24 kA. This year also saw the successful resolution of the motor generator (MG) bearing runout problems, so that TFTR now has an operational pulsed-power capability of 950 MVA with 4500 MJ of deliverable energy. This was a major milestone for the project.

The 1984 spring shutdown was carried out according to plan. Major activities included installation of two neutral beamlines and the addition of prototype protective armor to the inside of the vacuum vessel. All shutdown tasks were completed on schedule, and the vacuum vessel was pumped down at the end of April. After a series of power tests and several weeks of pulse-discharge cleaning, normal high-power operation resumed in June.

In this first full year of TFTR experimental operation, there was significant progress on experimental studies of confinement during ohmic heating and plasma compression, as well as on initial experiments using neutral-beam heating. In addition, a review of the projections for TFTR $Q \sim 1$ capability was carried out. Planning activities for pellet injection and lower-hybrid current drive were also initiated.

The TFTR-ORNL (Oak Ridge National Laboratory) collaboration began during the summer of 1984. The ten on-site ORNL-ISX (Impurity Study Experiment) physicists immediately began to make important contributions to the TFTR Project.

The TFTR was operated at plasma currents up to $I_p = 1.4$ MA, toroidal fields up to $B_\phi = 2.7$ T, and plasma durations up to 4 sec. As indicated in Fig. 1, there were two major operational periods, a winter 1983-1984 run period and a summer 1984 run period. The conditioning for the summer 1984 run period involved a two-week bakeout of the entire torus, including the pumping ducts, at 150°C. While the vessel was hot, 50 hours of glow-discharge cleaning ($p = 0.7$ Pa, $I \simeq 15$ A) and 70 hours (45,000 pulses) of pulse-discharge cleaning were performed. For the winter 1983-1984 run period, the graphite movable limiter was coated with TiC (titanium carbon). Titanium was the major metallic impurity, with a relative concentration of n_{Ti}/n_e as high as 5×10^{-3} in low-density plasmas. Because of difficulties with the adhesion, the TiC coating was removed during the shutdown period. With the TiC removed, the titanium impurity radiation was reduced by a factor of 40. The nickel, from the Inconel inner-wall limiter, increased modestly. However, all the metallic impurities decreased substantially at higher densities. Both X-ray pulse-height analysis and visible bremsstrahlung measurements indicate a significant reduction in Z_{eff} at low densities with the removal of the TiC coating.

Considerable progress was made on the studies of confinement during ohmic heating. The energy

confinement time is evaluated at the end of the current and density flattops. At this time, plasma discharges in TFTR typically reach equilibrium and the surface voltage approaches a value in the range of 0.8-1.4 V, depending on the plasma parameters. The total energy confinement time τ_E is defined as the energy stored in the ions and electrons divided by the ohmic input power with, if necessary, a very small correction for the rate of change of the stored energy. Density scans were conducted for plasma currents of 0.6 to 1.4 MA and for toroidal fields of 1.8 and 2.7 T. The results can be represented by

$$\tau_E \propto \bar{n}_e q^{1.1}$$

The movable limiter was used to form plasmas of different minor radii. Density scans were made for a = 0.83, 0.69, 0.55, and 0.41 m at R = 2.55-2.65 m, B_ϕ = 2.7 T, and q ≃ 2.7-3.3. The density limit, radiation fraction and profile, Z_{eff} range, and electron temperature profile shape of all these discharges are similar. The combined confinement results are in reasonable agreement with the relation $\tau_E \propto \bar{n}_e R^2 aq$ and are similar to previous results. A more detailed discussion is in the section on Experimental Research.

Initial studies of major-radius compression in TFTR have concentrated on demonstrating plasma control during the compression phase, on evaluating scaling laws for plasma parameters during compression of ohmically heated discharges, and on studying the evolution of a freely expanding plasma. In these experiments with full compression, the density profile follows the expected scaling ($n_e \propto C^2$, $a \propto C^{-1/2}$) until the plasma reaches the inner wall, when a slight broadening and loss of central density occurs, although the total particle count is conserved within the accuracy of measurement. However, the electron temperature profiles exhibit significant deviations from ideal scaling ($T_e \propto C^{4/3}$). The increase in the central ion temperature is more nearly in accordance with the expected adiabatic scaling.

It is worth noting that the compression process constitutes a powerful form of auxiliary heating, providing ~2.9 MW average total power (compared with 0.6 MW ohmic power before compression), with a peak instantaneous power exceeding 5 MW. The apparent degradation of confinement is not inconsistent with that observed with other forms of auxiliary heating at comparable P_{heat}/P_{oh}. Measurement of the evolution of the electron temperature and electron density profiles during the free expansion of a partially compressed plasma should provide considerable insight into confinement processes.

Installation and commissioning of hardware continued to be the dominant activity in the neutral-beam area in FY84. An important milestone was achieved with the operation of the TFTR Neutral Beam Test Cell (NBTC) in the first half of FY84. This was a significant step forward since here, for the first time, three sources were operated simultaneously into a single beamline, and no significant source-to-source interaction was observed. These test operations were followed by the injection of modest power into TFTR near the end of the fiscal year. Another important milestone was achieved when modifications to the modulator/regulator allowed full 120-keV operation into a dummy load.

The first injection results (concerning rotation, radiation, confinement, etc.) were achieved during the last week of August 1984. Power levels were modest, at best, beginning at 0.6 MW and gradually increasing to ~1.5 MW with one beamline and three ion sources. The maximum ion temperature, as measured by the TiXXI K_α diagnostic, of 3.2 keV was achieved in a low-density discharge with P_{inj} = 1.15 MW. Electron heating has been weak, perhaps because it is masked by the density rise. As expected, the energy confinement time (τ_E) deteriorates with additional power over the very limited range of power and electron density that was studied. Confinement enhancements such as profile shaping, etc. and a wider range of heating power must await the future.

The long-pulse ion-source upgrade for TFTR has progressed well during the past year. The first prototype ion source is scheduled for delivery to the Lawrence Berkeley Laboratory (LBL) for testing at the Neutral Beam Engineering Test Facility (NBETF) in August 1985. Present plans call for a complete retrofit of the TFTR neutral-beam system with the long-pulse sources in the late summer of 1986. The 2-sec capability of these ion sources and the modified beamline system give a much improved margin of success in achieving the Q = 1 [deuterium-deuterium (D-D) equivalent] demonstration.

In the area of diagnostics, operational testing, addition of new hardware during the shutdown period, and development of downstream items were hampered somewhat by a shortage of engineering manpower. Nevertheless, real progress was made as is shown in Table I in the section on Diagnostics. In particular, a significant advance in obtaining full spatial electron density and temperature profiles at a single time was made with the commissioning of the Thomson scattering system. This system uses television data-handling to provide profiles along the horizontal midplane. Another diagnostic for electron temperature measurement is the Fourier-transform spectrometer that was developed in association with the University of Maryland. In addition, the ion temperature measurement capability was augmented by the implementation of an X-ray crystal spectrometer. A grating spectrometer (SOXMOS) in the very soft X-ray region was of considerable importance in studying the low-Z impurity lines (oxygen and carbon).

An essential ingredient for increased diagnostic capability was the enhancement of CICADA computer capabilities and the associated CAMAC interface equipment, together with better software for collecting and analyzing data. The CICADA system is growing towards 10 megabytes of data capacity per discharge, about 70% of which is plasma diagnostic information.

An important activity in FY84 was the design and procurement of the internal vacuum vessel hardware. Major subcontracts were awarded for the complete

surface pumping system, the bumper limiters, and the "final" protective plates required for operation with four neutral beams. Subcontractors were monitored very closely by Princeton Plasma Physics Laboratory (PPPL) staff and, as a result, difficult schedules were maintained. Delivery of all items will be on time for installation during the spring 1985 shutdown.

Looking ahead to confinement enhancement techniques to help assure $Q \sim 1$ demonstration both in D-D and deuterium-tritium (D-T), PPPL initiated a pellet injection program. In May 1984, ORNL presented a preliminary design for a tritium pellet injector (TPI). This led to the establishment of a formal project to implement pellet fueling on TFTR. The first element of the project is the repeating pneumatic injector (RPI), which is an upgrade of an existing device at ORNL. Oak Ridge National Laboratory will provide the RPI, with a TFTR-compatible control system, to PPPL in March 1985. The next element will be the deuterium pellet injector (DPI) that utilizes eight gun barrels instead of one. It is scheduled for delivery in May 1986. Final design of the tritium pellet injector (TPI) is expected to begin in FY86, after sufficient data has been obtained from RPI performance and the DPI fabrication and testing activities.

Further progress was made in the areas of tritium, shielding, and remote handling. The installation of the tritium-handling equipment was completed during this period. Major studies were performed by Grumman Aerospace Corporation/Ontario Hydro, Bechtel National, Incorporated, and Burns and Roe/Los Alamos Technical Associates as the first stage of a multiyear tritium commissioning contract scheduled to be awarded in FY85 to the team that produces the best study.

Improvements in the shielding of the Test Cell were made. They allow for extended D-D and D-T experiments without violating the design radiation dose at the site boundary, while maintaining adequate protection of the electronics in the Test Cell Basement. .

Preparation for the remote-handling capability for TFTR was resumed in FY84. Activity was restricted to the maintenance of parts with a high probability of required change (e.g., components exposed to plasma at high power levels). This task was given to a team from Canadian industry, supported by engineers of the Hanford Engineering Development Laboratory (HEDL). Toward the end of the year, an agreement between the Canadian Fusion Fuels Technology Project (CFFTP) and PPPL was ready for signature. The agreement covers the full scope of a five-year program.

The TFTR staff continued the management of the Lithium Blanket Module (LBM) Project which is sponsored by the Electric Power Research Institute (EPRI). The LBM is an approximately 80×80×80 cm^3 module representative of a helium-cooled, lithium-oxide, fusion-reactor blanket module which will be installed on TFTR in late FY86. The two most important accomplishments in FY84 were: (1) GA Technologies, Incorporated (GAT), under contract to PPPL, completed 80% of the fabrication and assembly of the components of the blanket module, and (2) tritium extraction tests at PPPL showed conclusively that lithium oxide is a suitable breeding material for this experiment.

Safety and environmental matters continue to require a significant fraction of TFTR engineering time and have continued to be important considerations in the planning, testing, and operating activities of the TFTR Project. As an example, written procedures were required for all component installations, integrated systems testing, operational testing, and lifting activities. A primary consideration in developing these procedures was that all safety implications be addressed and that procedures be reviewed and approved by the Project and Operational Safety Office (P&OS) prior to implementation.

Finally, the Ebasco/Grumman industrial team provided engineering, design, and construction services, as well as installation and assembly support, to TFTR during the FY84 period. This support was provided in the areas of shielding, safety analysis, electrical systems, neutral beams, diagnostics, surface pumping, CICADA (Central Instrumentation, Control, and Data Acquisition), and construction.

FACILITIES OPERATIONS

During 1984, the TFTR Facility continued to extend its operating capability towards design-rated parameters. The toroidal-field coil system was tested and now operates routinely at 56 kA (4.0 T). This is especially significant because it required power supply operation at high-current levels in a four-parallel configuration where problems of current balancing had to be resolved. The power supplies are now ready to support full-field (73 kA, 5.2 T) integrated system tests. The ohmic-heating coil circuit was operated at full current in both mode A (24 kA) and mode B (20 kA). During this period, the interrupter mode of operation was successfully commissioned, resulting in a large increase in available volt-seconds. The equilibrium-field circuit was successfully tested at 24 kA, the maximum current available until the EF power supply paralleling task is completed (scheduled for the 1985 shutdown).

This year saw the successful resolution of the motor generator bearing runout problems, the installation and testing of the second MG (Fig. 2), and the routine operation of both MG sets in the synchronized mode. The TFTR now has an operational pulsed-power capability of 950 MVA with 4500 MJ of deliverable energy. This was a major milestone for the project.

On the tokamak itself, the 150°C bakeout capability was extended to both "R" and "C" pumping ducts (Fig. 3), and electrical heaters were added to the port covers. The 150°C bakeout is now a routine part of vacuum vessel conditioning after machine openings.

The spring 1984 shutdown was carried out according to plan. Major activities included installation of two neutral beamlines and the addition of prototype protective armour to the inside of the

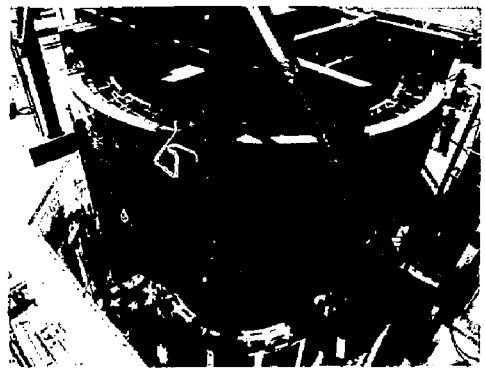

Fig. 2. Motor Generator Unit No. 2 stator installation on February 22, 1984. The weight of the stator plus associated rigging was 690,000 lbs. The lifting and setting of the stator was successfully accomplished in 16 hours. (84E0723)

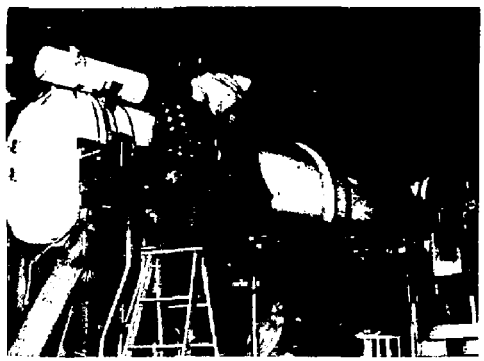

Fig. 3. Installation of hot air bakeout system piping and thermal insulation on the TFTR vacuum pumping ducts. (84E0927)

vacuum vessel. The TF busbars were modified to improve their insulation resistance and to increase the contact area at the coil power feeds. With these improvements, the TF circuit is now ready for operation at design levels. Poloidal-field (PF) lead stem and bus work supports were added to permit operation at extended design levels. All shutdown tasks were completed on schedule and the vacuum vessel was pumped down at the end of April. After a series of power tests and several weeks of pulse-discharge cleaning, normal high-power operation resumed in June.

During FY84, a program of upgrades for the vacuum control system was initiated. When this work is completed in FY85, the vacuum control system will provide improved equipment protection and alarm capability.

The designs for fire and gas seals successfully completed qualification tests. These seals will be used to close Test Cell penetrations and provide a negative pressure capability for tritium operation.

The Engineering Department Systems Engineering Group continued the integrated systems test effort, planning and executing power tests to extend the operating parameter regime of TFTR. In parallel with this test program, an analysis program was initiated with TFTR Engineering Analysis Division staff and a contract with Grumman Aerospace Corporation. The objective of this analysis effort is to take advantage of margins in design and "as-built" configurations to extend the operating parameter regime of the facility to levels in excess of design values.

Scheduled operations for TFTR fall into two major categories, high-power discharges and pulse-discharge cleaning. In FY84, during high-power discharge operation, 60% of scheduled operation time was charged to downtime and only 40% to uptime. This low availability factor was due primarily to problems with the energy conversion system equipment. A comprehensive circuit analysis and modification program is underway to correct deficiencies. The pulse-discharge cleaning mode of operation had a 56% availability factor reflecting, at least in part, improvements that were implemented in the capacitor charge and discharge circuitry. For FY84, TFTR had 1,498 high-power discharges (at plasma currents up to 1.8 MA) and 92,645 pulse-discharge cleaning shots.

Fiscal year 1984 also saw the formation of the TFTR Operations Review Committee (ORC), a group consisting of representatives from the various TFTR divisions and from the Project and Operational Safety Office. The purpose of this group is to provide a formal review and approval process for TFTR Administrative, Systems Operating, General Operating, Alarm, and Emergency Procedures.

The TFTR Operations Center continues to provide support in the area of documentation and control for the project. Central Files (over one million documents) were relocated to C-Site. The 25,380 aperture card system for drawings continues to be maintained and updated.

NEUTRAL BEAMS

Installation and commissioning of hardware continued to be the dominant activity in the neutral-beam area in FY84. Operation of the TFTR Neutral Beam Test Cell (NBTC) began in the first half of FY84 and was followed by injection of modest power into TFTR near the end of the fiscal year. More detailed discussions of the year's activities follow under the system headings below.

Mechanical Systems

The highlight of accomplishment in this area was the move and installation of the second neutral beamline (N4) on TFTR during the spring 1984

shutdown. This completed the two-beamline complement required for the summer 1984 operating period (Fig. 4).

One serious problem that surfaced during this reporting period was the inability to obtain additional pivot-point bellows that were free of leaks. These bellows allow positioning of the beamlines, for different injection angles, in order to optimize heating for various plasma major radii. The bellows were originally fabricated of Inconel 718 to provide an adequate margin of safety in the fully extended beamline position and to allow both bakeout at 250°C and 17 psi differential pressure. While the first production unit (installed on Beamline N3) was leak tight, subsequent units were not, due to cracks that always accompanied any attempts at repair. During the 1984-1985 run period, Beamline N4 had to be installed with a short stainless steel bellows that allowed only a fixed injection angle.

Since the original specifications have now been reduced, i.e., bakeout at 150°C maximum and electrical bakeout blankets (for the neutral beam duct) that result in ~15 psi as the maximum differential pressure, Inconel 625 can be substituted as the fabrication material. This material does not require heat treatment to achieve the necessary strength. PPPL procured stampings of the new material and is welding the bellows. These will be shipped to the Lawrence Berkeley Laboratory for incorporation into the complete duct assemblies. Beamlines N4 and N3 will be retrofitted with the new bellows during the 1985 opening.

Cryogenic Systems

Several runs of the 225-watt helium refrigerator were made during the year in preparation for and in support of operations with the Neutral Beam Test Cell. When it became apparent that start-up of the larger (1070-watt) refrigerator for TFTR neutral-beam operations was to be delayed into FY85, several attempts were made to supplement the bulk liquid helium (LHe) requirements for operations during the fall by using the 225-watt refrigerator. These were all unsuccessful since the line losses were too great to allow this unit to make liquid in the beamline. Operations during FY84 (and into FY85) were achieved through purchase of bulk LHe in 1000-

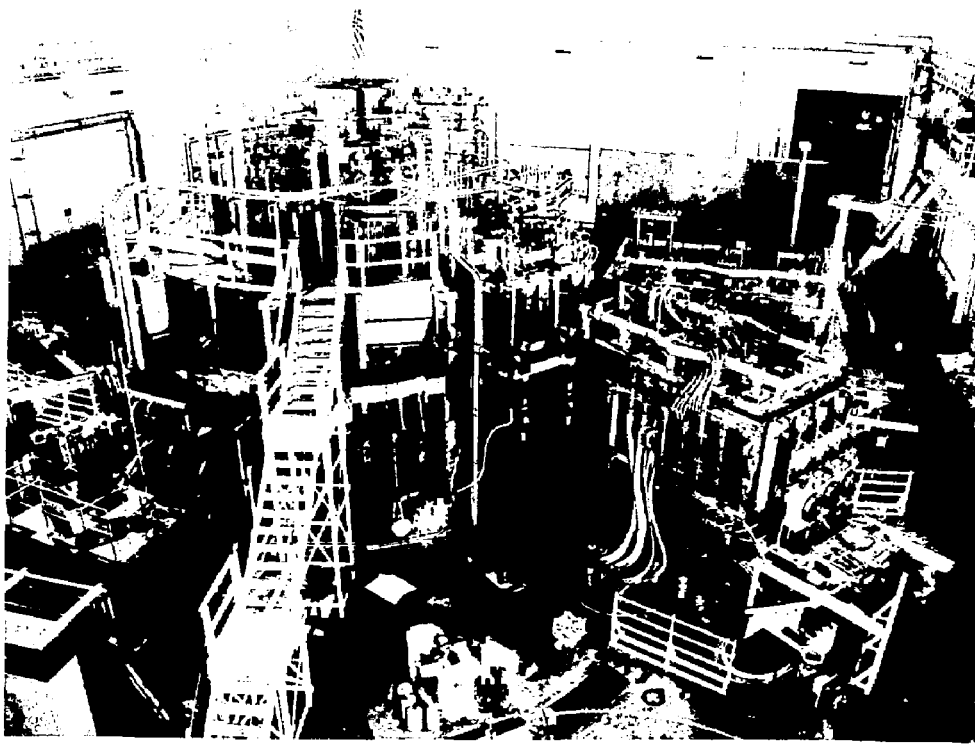

Fig. 4. The TFTR and complement of two neutral beamlines (at the right). (84E0691)

gallon and 2000-gallon dewars with a temporary transfer line piped into the cryogenic transfer system. The 225-watt compressor system was used successfully to reduce the helium vapor pressure below atmospheric in order to achieve ~4°K panel temperature and hydrogen vapor pressure of $<10^{-6}$ Torr.

Electrical Power Systems

Installation of the neutral-beam power-system hardware progressed actively during the January-June 1984 opening and access period. Six high-voltage enclosures (HVE's) and the flexible transmission lines, which attach the HVE's to the ion sources, were installed in the Test Cell Basement (Figs. 5 and 6). While this exercise was not without the sort of minor problems associated with any "first-time" fit-up, it was a substantial accomplishment, considering the complexity and extremely tight quarters in which the units must reside.

Fig. 5. The TFTR neutral-beam high-voltage enclosures installed in the Test Cell Basement. (84E0763)

Commissioning of power systems continued throughout the year with the first complete system (N5-C) put through its integrated dummy load acceptance test in January 1984. Two more systems followed in March 1984 to complete the NBTC power system complement.

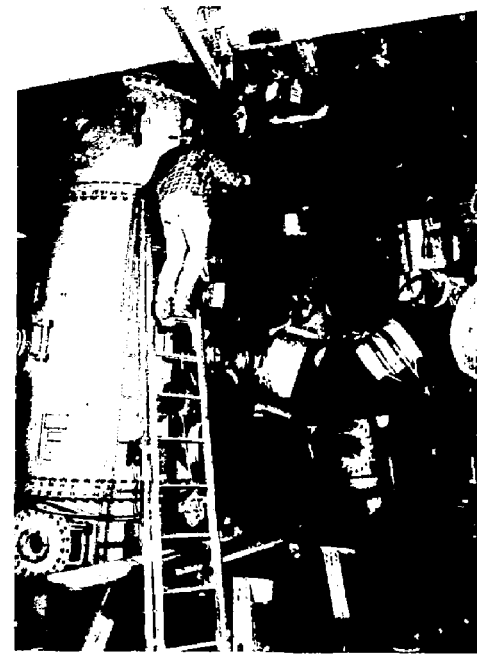

Fig. 6. A TFTR neutral-beam high-voltage flexible transmission line being connected to one of the high-voltage enclosures. (84E0822)

The first of the TFTR neutral-beam power systems (N3-C) was completed in July and N3-A, N3-B, and N4-B were completed by the end of September. Completion of N4-A and N4-C (which will allow two-beamline, six-ion-source operation on TFTR) was delayed into FY85, due primarily to hardware problems and limited manpower resources.

The voltage limitations and noise susceptibility of the original hardware led to a subcontract with RPC Industries to redesign and rebuild the modulator/regulators. An important step in this subcontract was the successful demonstration of reliable system operation at 120 kV into a dummy load in January 1984. This was made possible by a replacement of the weakest link (from a voltage hold-off standpoint) with a new filament-isolation transformer procured by RPC (Fig. 7).

A complete system rebuild of one modulator/regulator unit took place in August 1984, and successful testing to demonstrate repetitive blocking with the proper sequence of events by the unit at 120 kV took place in September. Hardware started to arrive for the upgrade of the remaining 12 systems. This work will start during the spring 1985 shutdown. It will begin with the systems N5 and N2, not now used in TFTR operations, and then include the N3 and N4 systems. By August 1985, there should be

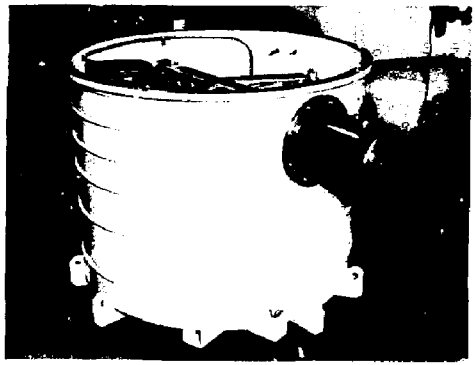

Fig. 7. One of the twelve TFTR neutral-beam filament-isolation transformers. (83E1547)

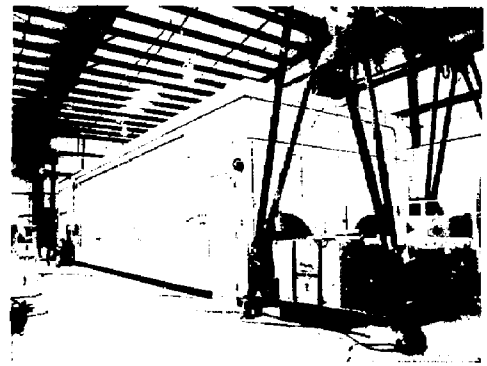

Fig. 8. The clean room constructed for ion-source assembly and repair. (84E0592)

12 systems capable of reliable 120-kV operation. During the operational period of August 1984 to April 1985, an administrative voltage limit of 80 kV was in effect, due to the present system shortcomings.

Systems Engineering

The new nine-bit analog-to-digital and digital-to-analog (A/D-D/A) all-fiber-optic data links performed well. Some initial operational problems were experienced that resulted in component damage by ion-source faults. These were later traced to grounding techniques within the high-voltage enclosures. While delivery and installation of the new data links was often a pacing item in being able to commission a power system and the changeover was expensive, a comparison of the new data link output with the old Transrex units leaves no doubt that it was worth both the money and delay.

The 11-channel ion-source fault detectors performed very well during Neutral Beam Test Cell and TFTR operations. They have adequate flexibility and response times to assure good ion-source protection, subject to achieving proper response by the power system.

The CICADA interface with the NBTC progressed to the point of waveform acquisition and display. In addition, thermocouple temperature profiles were successfully acquired to allow a beam "footprint" to be observed on the target tank beam dump approximately 36 ft away. Preliminary optical multichannel analyzer (OMA) data was obtained from a 50-keV H^0 beam, which gave reasonable species ratios.

Research and Development

The clean room for ion-source assembly and repair was completed (Fig. 8). It has been used extensively for the ion-source initial assembly and for refilamenting sources from the NBTC for TFTR. The Boice xyz-coordinate measuring machine was assembled by a field representative, with TFTR checkout and personnel training provided. So far this year, eight ion sources have been assembled, leak checked, and hi-potted prior to installation on TFTR or the NBTC.

The long-pulse ion-source upgrade for TFTR has progressed well during the past year. The Lawrence Livermore National Laboratory (LLNL) was appointed lead laboratory to handle the procurement. In the spring of 1984, a decision to adopt the Lawrence Berkeley Laboratory (LBL) ion-source design was made by all of the potential users [PPPL, LLNL, and GA Technologies, Incorporated (GAT)]. A contract for fabrication was awarded to RCA during the summer. Several meetings between users and LBL were held to harden design criteria and maximize commonality. The long-pulse sources will be supplied in two variations: a 12-cm by 48-cm focused version to LLNL and GAT and a 12-cm by 43-cm (masked) unfocused version to PPPL. The choice of the 12-cm by 43-cm variation by PPPL was made on the basis of a cost trade-off between minimizing the amount of beamline rework, apertures, beam-deflection magnet, valves, calorimeters, and beam dumps versus attaining sufficient power for a Q = 1 (D-D equivalent) demonstration in FY87. The first prototype ion source is scheduled for delivery to LBL for testing at the Neutral Beam Engineering Test Facility in August 1985. The second unit is to come to PPPL for systems testing during the winter of 1985-1986. Present plans call for a complete retrofit of the TFTR neutral-beam system with the long-pulse sources in the late summer of 1986. The 2-sec capability of these ion sources and the modified beamline system gives a much improved margin of success in achieving the Q = 1 (D-D equivalent) demonstration.

Operations

The NBTC became operational with a single source in Januury 1984, albeit with the very modest power level of 20 kV and 6 A. Other sources were installed during February and March following the completion of the integrated power system tests. Considerable

problems and delays occurred due to the tendency of the RCA switch tube to oscillate (internally) on accel "turn-on" plus the fact that a water leak developed in the ion-source 5C suppressor grid (a prototype unit). Consequently, three-source operation was not achieved until April 2, 1984, two days late for the milestone. During April, adequate system isolation, such that a fault in one source did not affect the other two, was demonstrated. Also, adequate power (~60 keV) was obtained to demonstrate CICADA readout of the target thermocouples for achieving beam power profiles and to obtain OMA analysis of the species mix. The NBTC operations were not continued beyond the end of April because all manpower resources were needed to get the TFTR neutral-beam systems commissioned and operational for August 1984.

The first injection results (concerning rotation, radiation, confinement, etc.) for TFTR were achieved during the last week of August 1984. Power levels were modest, at best, beginning at 0.6 MW and gradually increasing to ~1.5 MW with one beamline and three ion sources. These preliminary results were reported at the September 1984 IAEA London meeting[1] and were followed with a system description and performance assessment at the SOFT conference at Varese.[2] As expected, the energy confinement time (τ_E) deteriorates with additional power over the very limited range of power and electron density that were studied. Confinement enhancements, such as a wide range of available power, profile shaping, etc., must await the future.

TECHNICAL SYSTEMS

Tokamak Engineering

Major subcontracts were awarded for the complete surface pumping system, the bumper limiters, and the "final" protective plates required for operation with four neutral beams. The surface pumps utilize zirconium-aluminum (ZrAl) modules as the pumping medium. The limiters and protective plates have water-cooled Inconel backing plates on which are mounted graphite tiles.

Fabrication of 40 surface pumping panels was subcontracted to Grumman Aerospace Corporation, and the associated power supplies were subcontracted to the Grim Corporation. The bumper limiters and "final" protective plates were subcontracted to the McDonnell Douglas Corporation. There are 60 bumper limiter panels and 9 protective plates (see Figs. 9 and 10). Subcontractors were monitored very closely by PPPL staff and, as a result, difficult schedules were maintained and the delivery of all

Fig. 9. Bay Q bumper limiter plate with uncoated tiles. (85E0512)

items will be on time for installation during the spring 1985 shutdown.

The associated cooling water systems for both the bumper limiters and the protective plates were designed and are being fabricated and assembled at PPPL. These systems distribute chilled water to all the backing plates and incorporate instrumentation to measure inlet and outlet water temperatures and flow rates. Safety devices are provided to shut off the water supplies in the event a leak develops inside the vacuum vessel.

There were 186 thermocouples included in the design of the bumper limiters and "final" protective plates. They will be used to monitor the heat inputs to the protective armor.

During the January to March 1984 shutdown, the 11 "initial" protective plates and cooling water system were installed and checked out. These plates have functioned, without problems, to protect the vacuum vessel wall during initial operations with two neutral beams.

Pellet Injectors

In May 1984, the Oak Ridge National Laboratory (ORNL) presented a preliminary design for a tritium pellet injector (TPI). This led to the establishment of a formal project to implement pellet fueling on TFTR. The result is a project that has all of the essential elements of development that will be required to inject trit . nto TFTR for the D-T demonstration.

The first element of the project is the repeating pneumatic injector (RPI), which is an upgrade of an existing device at ORNL. The Oak Ridge National Laboratory will provide the RPI, with a TFTR compatible control system, to PPPL in March 1985. PPPL will be responsible for the facility interfaces, installation, and operation. The RPI is capable of firing a single pellet of hydrogen or deuterium at 1600-1900 m per sec or a series of pellets (more than 2 per sec) at slightly reduced velocity.

The next element in the project is the deuterium pellet injector (DPI) that utilizes eight gun barrels instead of one. This configuration adds greater flexibility in fueling control. It is being designed to replace the RPI in the spring of 1986 and is intended for use during the D-D equivalent Q =1 demonstration. The original mounting stand and peripheral services (control, cryogenic, vacuum, electrical, etc.) from the RPI will remain for the DPI.

Final design for the tritium pellet injector (TPI) is expected to begin in FY86, after sufficient data has been obtained from RPI performance and the DPI fabrication and testing activities.

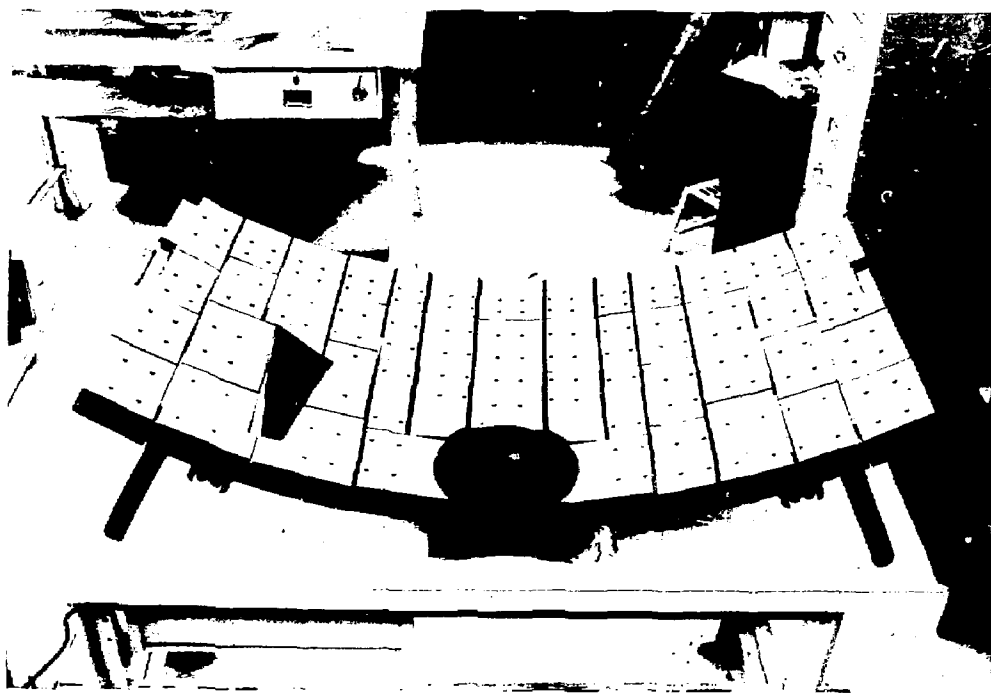

Fig. 10. Bay F protective plate with TiC-coated carbon tiles. (85E0513)

During the period from May to October 1984, PPPL conducted a preliminary design of TPI installation requirements on TFTR. In addition, the design of the RPI installation was initiated.

Lithium Blanket Module Program

The Lithium Blanket Module (LBM) Program is being sponsored by the Electric Power Research Institute (EPRI). The LBM is an approximately 80×80×80 cm^3 module, it is representative of a helium-cooled, lithium-oxide, fusion-reactor blanket module, and it will be installed on TFTR in late FY86. The two most important accomplishments in FY84 were: (1) GA Technologies, Incorporated (GAT), under contract to PPPL, completed 80% of the fabrication and assembly of the components of the blanket module, and (2) tritium extraction tests at PPPL showed conclusively that lithium oxide is a suitable breeding material for this experiment.

Some 650 kg of lithium-oxide powder, meeting rigid specifications for size distribution and purity, was delivered to GAT by Cerac, Incorporated in 1984. The powder was used to manufacture 15,000 pellets, which were assembled into 700 rods (about 75% of the total required). An aluminum canning process for test pellets was successfully developed.

Figure 11 shows a view of the LBM under construction, with about 75% of the rods in place. The completely assembled LBM will be delivered to PPPL in early 1985 for acceptance testing.

A neutronically thin cover plate, to be used over the TFTR port housing the LBM, was designed by McDonnell Douglas Corporation and fabrication was initiated.

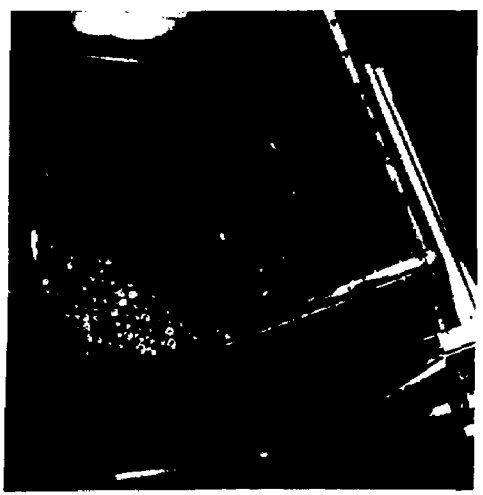

Fig. 11. The Lithium Blanket Module assembly with about 75% of the rods in place. (85E0315)

The final Monte Carlo neutron and photon code (MCNP code) models for the TFTR LBM system were completed by GAT. EG&G Idaho completed work on dosimetry, material qualification, and on interfacing the dosimetry counting equipment to the PPPL computers that will be used for data analysis and comparison with MCNP code predictions.

Fabrication of the new tritium thermal extraction and counting apparatus at PPPL was completed. Small lithium metal samples and LBM-type pellets were irradiated in the Argonne National Laboratory thermal reactor and in the Coupled Fast Reactivity Measurement Facility fast neutron reactor at the Idaho National Engineering Laboratory (INEL). Many experiments were carried out to investigate tritium release rates. These experiments validated the choice of Li_2O as a breeding material and also provided new insight into the nature of tritium migration in Li_2O pellets.

Nuclear Engineering

TFTR nuclear engineering work in FY84 focused primarily on three sections:

- tritium technology for TFTR,
- improvements of the radiation shield of the Test Cell, and
- remote-handling technology for maintaining TFTR.

Tritium

The installation of the tritium-handling equipment was completed during this period, and additional engineering personnel were recruited to the TFTR Tritium Section in preparation for tritium operations in TFTR.

A new 200-ft meteorological tower was erected at C-Site and placed in service to collect on-site meteorology data (wind speed, direction, and atmospheric stability), and equipment to sample the stack effluents from TFTR was procured.

Under contract to PPPL, development of a real-time tritium monitor for TFTR was initiated at the Los Alamos National Laboratory (LANL). This monitor has on-line sampling capability for discriminating between tritium gas, tritium water vapor, and neutron-activated air. An investigation of the requirements for a global radiation monitoring system was started.

Major studies were performed by Grumman Aerospace Corporation/Ontario Hydro, Bechtel National, Incorporated, and Burns and Roe/Los Alamos Technical Associates as the first stages of a multiyear tritium commissioning contract to be awarded in FY85 to the team that produces the best study.

Shielding

Improvements in shielding of the Test Cell were made. They allowed for extended D-D and D-T

experiments without violating the design radiation dose at the site boundary while maintaining adequate protection of electronics in the Test Cell Basement. Accordingly, a modular concrete lining of the Test Cell was designed, and some of the numerous penetrations of the Test Cell floor were filled with a radiation shielding material. The latter is a PPPL development that is easy to install in the presence of complex equipment inside the penetration, easy to drill through if new equipment has to be installed, and is inexpensive. A boron coating of the entire Test Cell Basement floor was added, which will cut down the thermal neutron flux experienced by the electronics.

The quality of shielding depends upon the accuracy of the radiation transport analysis. Neutron measurements (flux and spectra) were prepared in order to check the calculated predictions in the basement. The detectors were calibrated (with INEL and ORNL cooperation) relative to a californium standard and to an ORNL linear accelerator with calibrated yield and spectrum.

Remote Handling

Preparation for the remote-handling capability for TFTR was resumed in FY84. Activity was restricted to the maintenance of parts with a high probability of required change (e.g., components exposed to plasma at high-power levels). This task was given to a team from Canadian industry, supported by engineers of the Hanford Engineering Development Laboratory.

Numerous studies on remote handling for TFTR have been executed over the years. This time the main thrust is towards experimental studies involving: demothballing of the M-3 Mock-Up of TFTR and upgrading it for demonstrations; time studies of the "hands-on" maintenance (see Fig. 12) of in-vessel components (e.g., limiter tiles) under the assumption of a mildly activated, tritium-contaminated TFTR; implementation of a computer interface between the master and the slave arms of a manipulator (Tele-Operator Systems Corporation) to provide for higher flexibility and reliability (done by ORNL); removal and attachment of a port cover by a gantry-mounted robot (see Fig. 13). Demonstrations of the remote exchange of the movable limiter, surface pumping panels (together with HEDL), and tiles are in preparation. These activities require development work as well as the design and acquisition of some novel hardware. By largely using standard industrial equipment, such as robots, experience will be gained in the trade-off between the use of state-of-the-art equipment, development of new tools, modification of TFTR, or highly adaptive tooling. Further information is expected concerning the required dynamic response of the various components.

Towards the end of the year, an agreement between the Canadian Fusion Fuels Technology Project and PPPL was ready for signature. The agreement covers the full scope of a five-year program. In preparation for this collaboration, a work breakdown structure

Fig. 12. An example of "hands-on" maintenance. (84E1176)

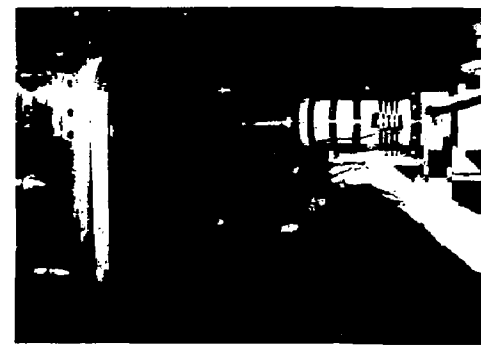

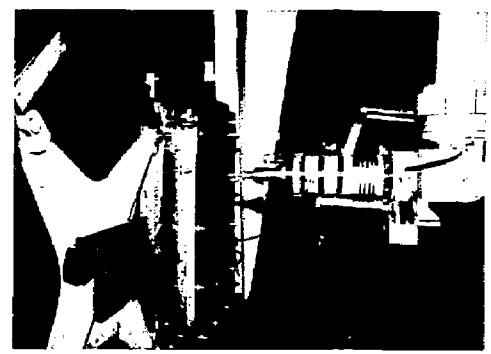

Fig. 13. The top photo depicts a scale of the robot's size. The bottom photo shows port-cover bolts being removed by the robot. (85E0511)

(WBS) and a cost and schedule measuring system were developed.

SAFETY AND ENVIRONMENTAL MONITORING

Safety of personnel and property, as well as possible environmental impacts, continued to be important considerations in the planning, testing, and operating activities of the TFTR Project. A program (initiated in CY82) of analyses to determine the concentrations of radioactive pollutants in the air and groundwater at the TFTR site was continued. Analyses of nonradioactive pollutants in surface waters were increased to ten locations and performed in-house in CY84. These same ten locations were analyzed for radioactive pollutants, starting with in-house measurements in March. These analyses are a part of a program to establish a reference baseline for the TFTR Facility prior to significant operating activity and to carry out the continuing environmental monitoring required to comply with state and federal regulations. In May 1984, PPPL published its Second Annual Environmental Report for CY83.

Four real-time prompt-gamma ionization-chamber monitors were in operation at the exclusion zone boundary (EZB), and eight others of lower sensitivity were placed in close proximity to the Test Cell. All monitors are utilized whenever the tokamak is in operation. The CICADA software development and subsequent testing are now being finalized. Passive thermoluminescent dosimeter (TLD) monitors were placed inside and outside the Test Cell to measure bremsstrahlung radiation emission levels and profiles for comparison with predicted doses during tokamak operation. A program for neutron measurement through penetrations was initiated. The TLD data collected was found to be an important diagnostic for machine operation as well as for safety applications. Temporary "Bonner Sphere" neutron monitors were put in place for D-D runs. Permanent real-time neutron monitors will be installed in FY85.

Required written procedures were prepared for all component installations, integrated systems testing, operational testing, and lifting activities. A primary consideration in developing these procedures was that all safety implications be addressed and that procedures be reviewed and approved by the Project and Operational Safety Office (P&OS) prior to implementation. A system of noting what safety documentation [Final Safety Analysis Reports (FSAR's), Safety Requirements (SR's), and Operational Safety Requirements (OSR's)] was affected by Engineering Review Board (ERB) actions was implemented by P&OS. The Area Safety Coordinator Program, which began in FY83, has become an important program to cover each area of the TFTR complex in order to help in maintaining a safe working environment and a safety awareness on the part of all project staff.

DIAGNOSTICS

For TFTR Diagnostics, the year had three distinct parts. There was a period of operational testing and plasma measurement using the diagnostics installed for the ohmic-heated plasma operation period that ended in January.[3-5] This was followed by a three-month opening of the tokamak vacuum vessel during which considerable hardware fabrication and installation work was completed. Finally, the remainder of the year was spent in bringing on-line new or enhanced diagnostics in parallel with bringing two neutral beams into operation. In this last period, there was some delay in the scheduled operation of some diagnostics because of shortages of engineering manpower in the preparation of the equipment.

Table I gives a full list of diagnostics functioning on TFTR for operation with heating by two neutral beams. The diagnostics are listed so as to identify the principal plasma measurement for which they are used; details about temporal or spatial resolution or additional plasma information obtainable in each case is omitted. An asterisk identifies diagnostics whose full operational capability had not been achieved at the end of the year.

One of this last set of diagnostics is the far-infrared (FIR) multichannel interferometer that measures the plasma density integrated along vertical chords. This system is mounted on a tripod vibration-isolation stand, one of whose legs passes up the center column of the tokamak. The lasers, the CO_2 laser and the two methyl-alcohol lasers which it pumps (located in a box below a beam splitter box, which creates five interferometer paths), are shown in Fig. 14. This equipment occupies the full 18-ft height of the diagnostic basement under the tokamak. This instrument is a good example of the sheer size of equipment necessary for TFTR and thus exemplifies the required design need for mechanical rigidity, capability for alignment, and extreme care to avoid magnetic coupling. The associated electronic equipment to provide reasonable levels of control and data taking is a further major undertaking.

Another example of the size of diagnostic equipment required for TFTR can be seen in Fig. 15, where a graphite three-pin Langmuir-calorimeter probe for TFTR is shown beside an alumina-insulated probe for the C-Stellarator. The size of the TFTR probe is necessary for survival in the outer scrape-off region of the plasma, while the small probe could penetrate the ohmically heated stellarator plasma without perturbing it. Edge plasma data for TFTR is now being obtained.

Table I. Diagnostics Available for TFTR Operation with Two Neutral Beams.

Plasma Parameter Measured	Diagnostic	Location of Measurement
Electron Density	1-mm Interferometer[a]	Horizontal Midplane
	Multichannel Far-Infrared Interferometer[b]	5 Vertical Chords
Electron Temperature	TV Thomson Scattering	Radial Profile
	ECE Heterodyne Radiometer	Radial Profile
	X-Ray Pulse-Height Analyzer	Horizontal Midplane
	ECE Fourier Transform Spectrometer	Radial Profile
Ion Temperature	Charge-Exchange Analyzer	2 Horizontal Chords
	X-Ray Crystal Spectrometer	Horizontal Midplane
	Multichannel Visible Spectrometer	2 Horizontal Midplane
Impurity Concentration	Interference Filter Array (HAIFA)	18-Chord Array, 4 Toroidal Locations
	Ultraviolet Survey Spectrometer (SPRED)	Horizontal Midplane
	Soft X-Ray Spectrometer (SOXMOS)	Horizontal Midplane
Radiated Power	Bolometer Arrays	19 Horizontal, 19 Vertical Chords
	Wide-Angle Bolometers	6 Toroidal Locations
Magnetic Properties	Rogowski Loops	2 Toroidal Locations
	Voltage Loops	6 Poloidal Locations plus Saddle
	B_r/B_p Loops	2 Sets of 26 Pairs, External
	Diamagnetic Loops	2 Toroidal Locations
Wave Activity	Internal Mirnov Loops	19 Coils, Internal
	X-Ray Imaging System	64 Horizontal Arrays
Fusion Products	Epithermal Neutrons	4 Toroidal Locations
	Proton Detectors[b]	4 Vertical Locations
	Neutron Activation System[b]	2 Toroidal Locations
	2-Channel Collimator[b]	1 Toroidal Location
	Neutron Fluctuation Detector	1 Toroidal Location
Plasma Edge/Wall	Plasma TV/Infrared TV	Periscopes at 3 Toroidal Locations
	Neutral Beam Pyrometer[b]	2 Toroidal Locations
	Probes	2 Horizontal, 1 Vertical[b]
Miscellaneous	Hard X-Ray Monitors	5 Wall Locations
	Torus Pressure Gauges[c]	2 Toroidal Locations
	Residual Gas Analyzers[d]	2 Toroidal Locations
	Vacuum Vessel Illumination	3 Toroidal Locations
	Laser Impurity Injector	1 Toroidal Location
	Glow Discharge Probes	2 Toroidal Locations

[a]P.C. Efthimion, G. Taylor, W. Ernst, *et al.*, "A One Millimeter Wave Interferometer for the Measurement of Line Integral Electron Density on TFTR," Rev. Sci. Instrum. *56* (1985) 908.

[b]These diagnostics were not fully operational on September 30, 1984.

[c]P.H. LaMarche, H.F. Dylla, D.K. Owens, *et al.*, "Neutral Pressure and Gas Flow Instrumentation for TFTR," Rev. Sci. Instrum. *56* (1985) 981.

[d]H.F. Dylla, W.R. Blanchard, R.J. Hawryluk, *et al.*, "First-Wall and Limiter Conditioning in TFTR." J. Nucl. Mater. *128&129* (1984) 861.

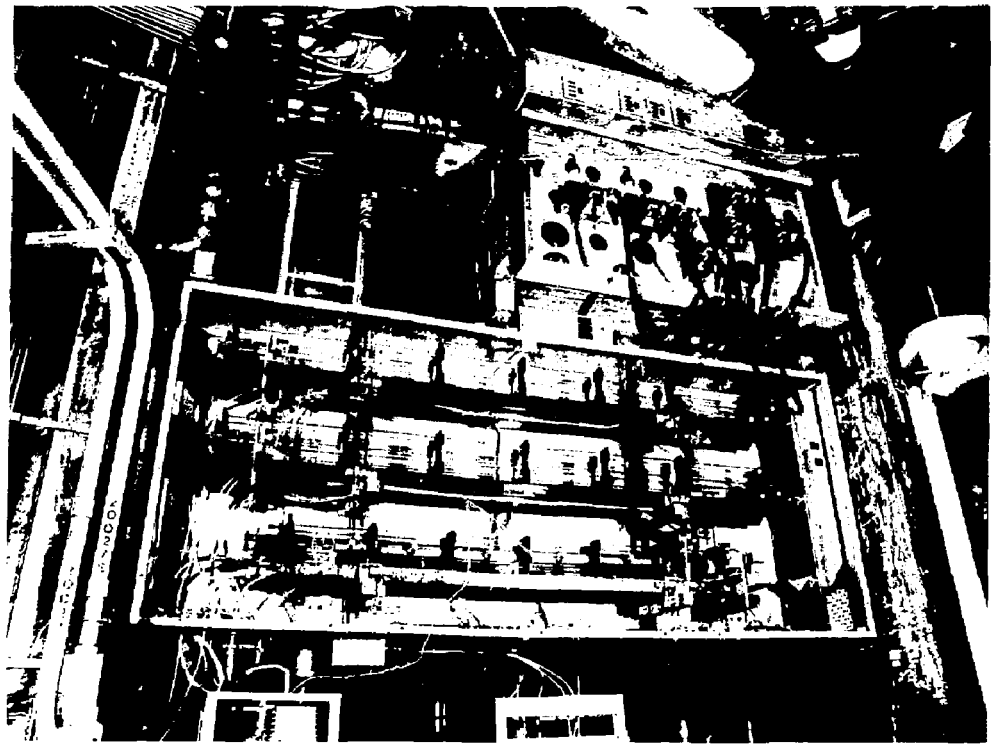

Fig. 14. The three lasers of the far-infrared multichannel interferometer mounted alongside the beam-splitter box in the basement under TFTR. (84E1375)

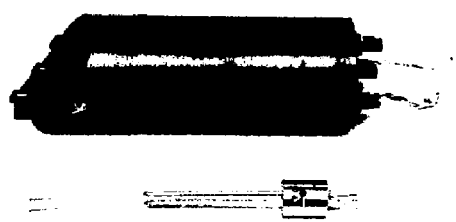

Fig. 15. A three-pin Langmuir-calorimeter probe head for measurement of TFTR edge plasmas compared with a head used for central plasma measurements in the C-Stellarator. (84E0780)

A significant advance in obtaining full spatial electron density and temperature profiles at a single time was made by commissioning the Thomson scattering system.[6] This system uses television data-handling to provide profiles along the horizontal plane. A line diagram of the instrument is shown in Fig. 16; the light from the ruby laser (mounted in the TFTR Basement) is focused at the center of the plasma in a narrow horizontal beam. The scattered light is collected by a mirror under the tokamak onto multifiber-optical bundles that take the light to a spectrometer and recording tube. Proper windows, shutters, and beam and viewing light dumps are provided in the vacuum vessel. The power of this instrument is revealed in the experimental data shown in Fig. 17. The data are shown for three cases of a precompression plasma (the plasma at large major radius), postcompression plasma (the plasma has been moved inward to a small major radius), and for a large centrally located plasma. In each case, the data is obtained in a single plasma pulse.

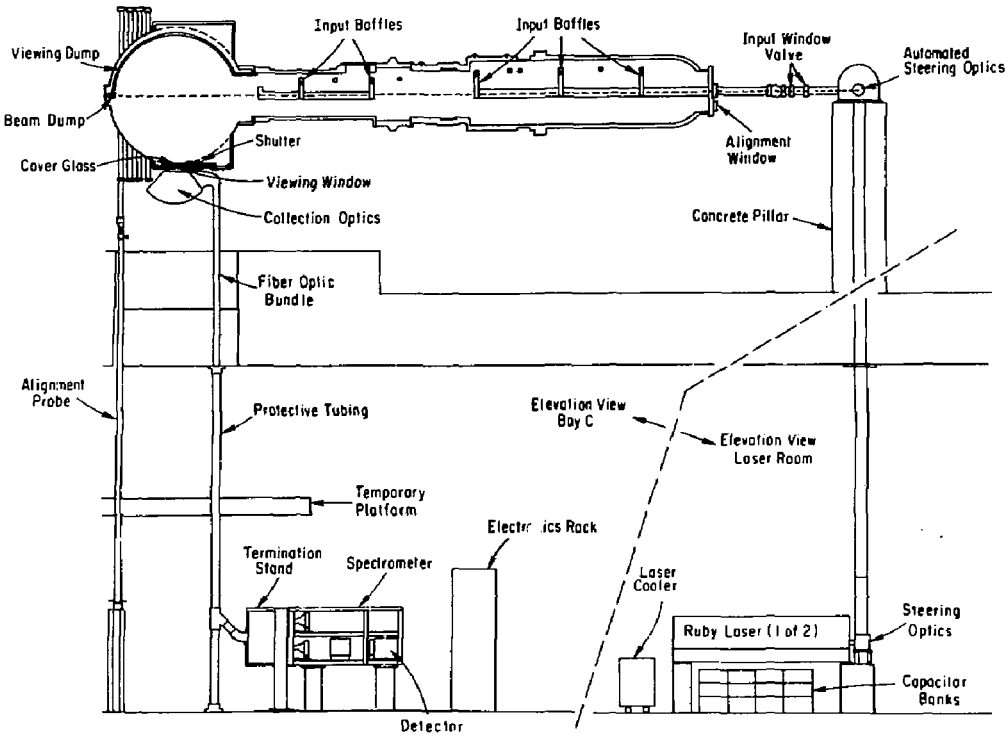

Fig. 16. The layout of the Thomson scattering system showing the long optical paths and major components of this system.

Another diagnostic for electron temperature measurement is the Fourier-transform spectrometer that was developed in association with the University of Maryland. This instrument can measure a full spatial profile 72 times per second with a time resolution of 11 msec. This made it particularly useful in the study of free-expanding plasmas after a modest compression had been provided magnetically. Figure 18 shows electron temperature profiles during a free-expanding plasma after compression start-up at 2.5 sec; the expansion typically lasts 40 msec. The instrument is used in conjunction with the heterodyne radiometer[7,8] to characterize the expansion very thoroughly.

The ion temperature measurement capability was augmented by the implementation of an X-ray crystal spectrometer.[9] This instrument is mounted on the horizontal midplane, but views through its beryllium window at about 11° to the radial so that it can measure toroidal motion of the impurity species during tangential neutral-beam injection. This instrument was set up for looking at the K_α resonant line of helium-like titanium. Figure 19 shows resonance line profiles at various times and the interpretation of the Doppler width and shift used to evaluate ion temperature and toroidal motion throughout a beam-heated plasma pulse. The neutron measurements (from deuterium plasmas) and charge-exchange measurements[10] were enhanced to provide alternative ion temperature measurements.

A grating spectrometer (SOXMOS) in the very soft X-ray region, using a multichannel detector identical to that used in the longer wavelength survey instrument (SPRED), was of importance in studying the low-Z impurity lines (oxygen and carbon). This instrument requires full calibration to achieve its full usefulness in assigning the impurity concentrations, but it has already provided valuable information on relative impurity changes under different plasma conditions. It occasionally provides information about bursts of impurities during a plasma pulse, such as that shown in Fig. 20, where a "flake" of zirconium fell into the plasma.

Measurement of the power accountability of tokamak plasmas is difficult and has often produced puzzling results. For radiated power measurement on

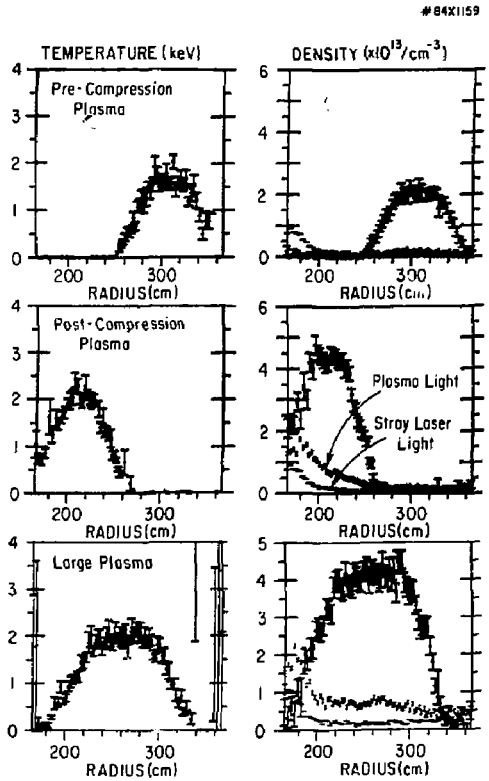

Fig. 17. Electron temperature and density profiles obtained at a single time during the pulse by Thomson scattering for three ohmic discharges: a) precompression plasma, b) postcompression plasma, and c) large-radius plasma.

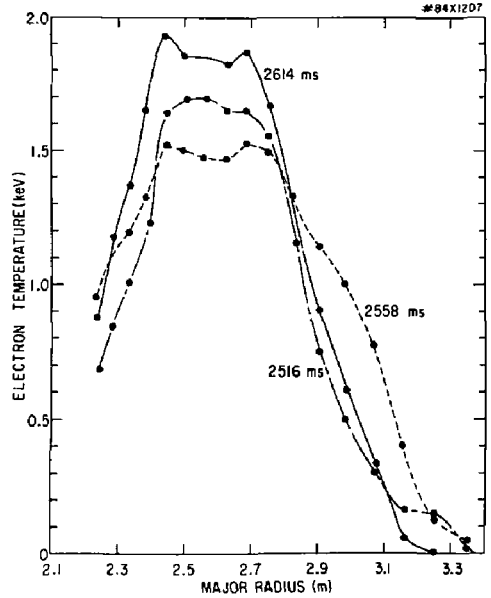

Fig. 18. Electron temperature profiles measured by the Fourier-transform spectrometer at three times during the free expansion of an ohmic plasma after compression.

TFTR, there is a visible bremsstrahlung telescope array at one toroidal location with single telescopes at other loctations to account for toroidal variations. There are also two arrays of bolometers, one viewing vertically and the other horizontally, with occasional wide-angle collecting bolometers at other toroidal locations. The spatial measurements from the two bolometer arrays during a large plasma pulse and after Abel inversion for the same time[11] are shown in Fig. 21. This type of data is used to infer the ratio of total radiated power to the input power.

The X-ray imaging system for carrying out plasma tomography was operated with about 60 chordal views. Figure 22 is a photograph of the top section of this instrument's vacuum box. It shows foil ladders and their support frame, which allow foils of different thickness to be moved across the detectors to enhance the instrument dynamic range. The frequency response of the detectors was limited to 2 kHz, because of the late delivery of transient digitizers with 100-kHz capability. Nevertheless, significant studies of relatively slow sawteeth were possible. An example is shown in Fig. 23 of sawteeth with a period of about 100 msec, for which it was possible to measure the electron temperature profile by the heterodyne radiometer at the time of maximum and minimum emissivity. Very significant heat pulse propagation is apparent. The presence of the foils enables the possibility of using two neighboring detectors, with different foil thicknesses, to determine an electron temperature by the difference in the X-ray absorption. This technique was used effectively.

An adaptation of the standard plasma TV (and infrared) periscope optical systems has been used for inspection of the inside of the vacuum vessel on a routine basis. Simple probe mechanisms are used to move lamps, operable in air or under vacuum, inside the vacuum vessel wall. A photograph of one set of the internal vacuum vessel components, taken at medium magnification (20° field of view), is shown in Fig. 24. Magnification to a 5° field of view is possible.

An essential ingredient for increased diagnostic capability was the enhancement of CICADA computer capabilities and the associated CAMAC interface equipment, together with better software for collecting and analyzing data. The CICADA system is growing towards 10 megabytes of data capacity per discharge, about 70% of which is plasma diagnostic information.

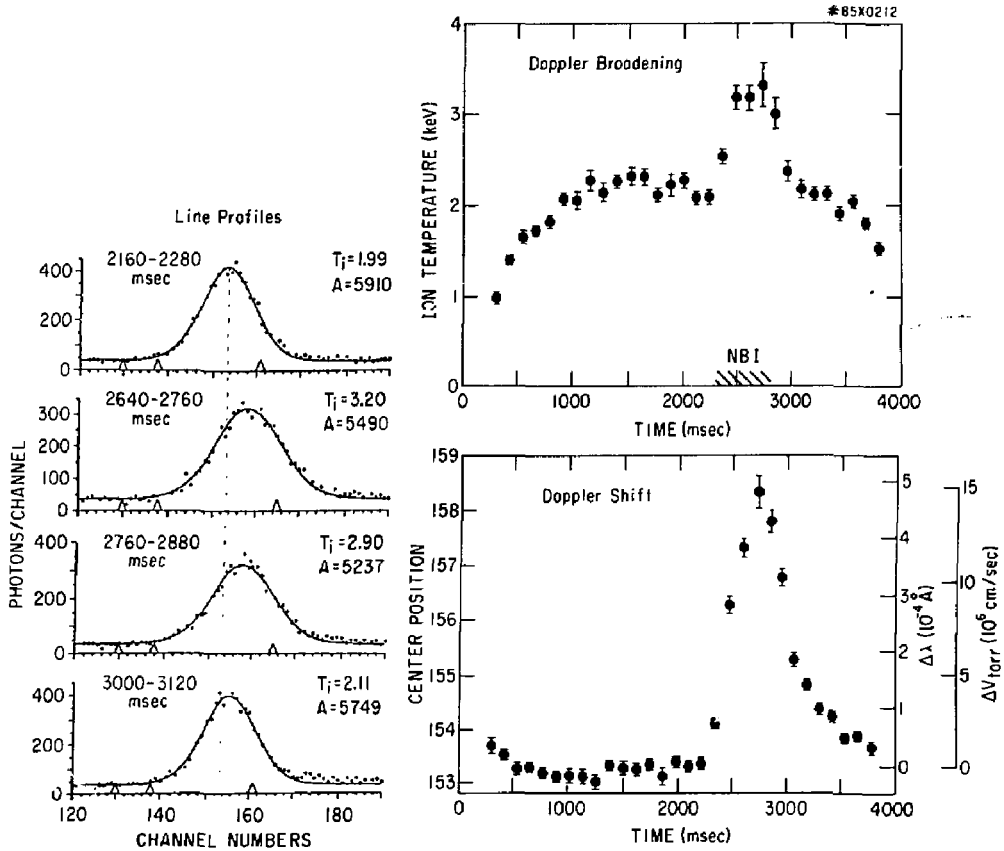

Fig. 19. Measurement of ion temperature and plasma rotation by the X-ray crystal spectrometer. Spectra at various times and the inferred central ion temperature and plasma rotations are shown as functions of time.

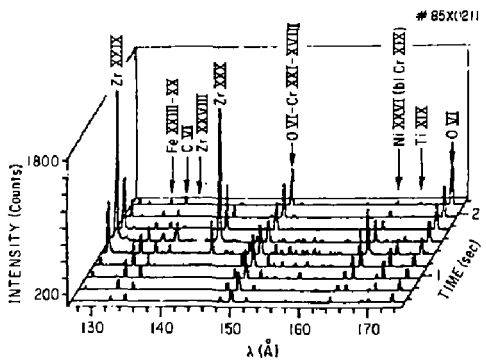

Fig. 20. The time variation of the far-ultraviolet spectra from the soft X-ray spectrometer showing the effect of a "flake" of zirconium.

The major fabrication projects during this year were the diagnostic neutral beam and a three-channel X-ray crystal spectrometer for installation under the tokamak. Progress on the electrical work was good for the diagnostic neutral beam, with most of the major power components having been contracted for manufacture. There was more difficulty in obtaining manpower and containing costs in the mechanical work, though the installation during mid-1985 is still confidently expected. The X-ray crystal instrument will be delivered on schedule.

As the TFTR Project has moved closer to tritium operation, a greater emphasis has been placed on developing a program for measurement of fusion products. This has resulted not only in increased neutron flux measurement techniques, but also in studies of gamma measurement,[12] in the installation of proton detectors (to study burn-up of fusion products), and in a thorough study of potential α-particle measurements. The emphasis for the last

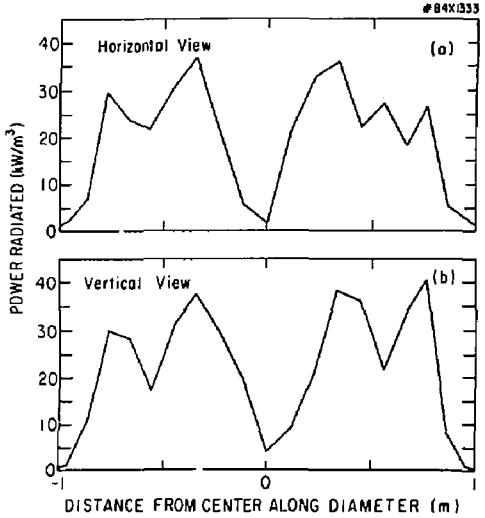

Fig. 21. Abel-inverted profiles of the power radiated by the plasma measured by 19-channel bolometer arrays on top and outside the torus.

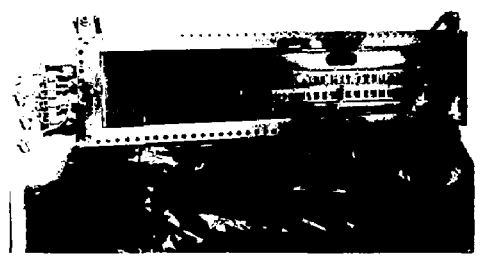

Fig. 22. The top cap of the X-ray imaging system showing the arrangement of movable foils in front of the 64 detectors. (84E0968)

mentioned has been on finding relatively cheap evaluation techniques; the most attractive is a charge-exchange recombination spectroscopy technique that will be used in conjunction with the diagnostic neutral beam. This is a powerful technique for thermalized α-particles. The techniques for looking at fast α-particle losses are still being evaluated.

Very little attempt was made in FY84 to prepare diagnostics for the unpleasant neutron radiation environment that will emerge with neutral-beam heating, even with deuterium plasmas. Some careful code calculations for the radiation background levels and for some specific idealized local shielding geometries were completed, but detailed shielding

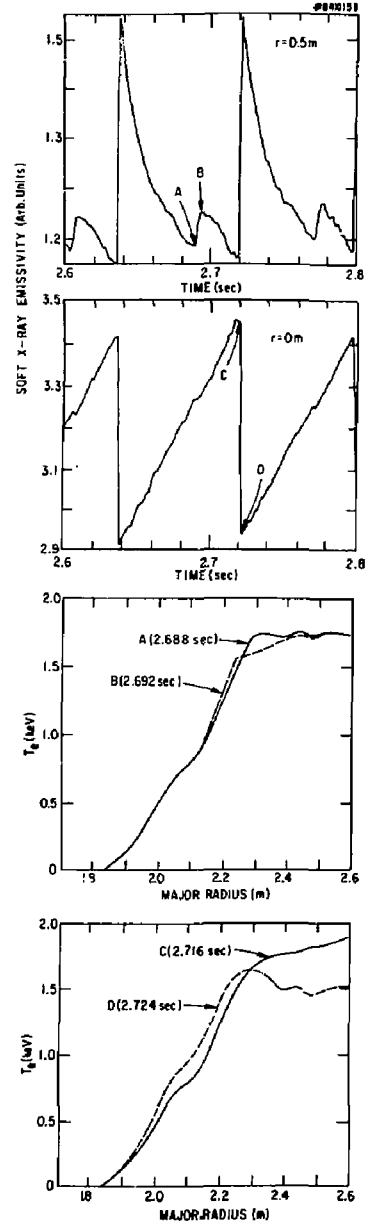

Fig. 23. Sawteeth observed at two chords through the plasma. Radial profiles of the electron temperature taken by the heterodyne radiometer at the times marked by letters show the changes in temperature distribution for large and small sawteeth.

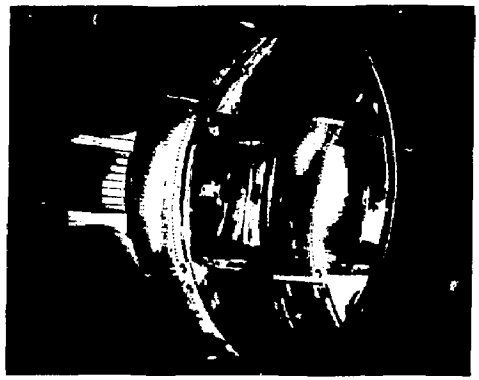

Fig. 24. Photograph of the movable limiter (left) and other hardware inside the TFTR vacuum vessel taken with 20° field of view through one of the plasma TV periscopes.

design remains largely to be done. The relocation of electronic equipment is also under consideration.

The diagnostic systems on TFTR were brought on-line with only relatively minor schedule slippages. They have provided very good physics information for all the TFTR plasma-operating conditions.

EXPERIMENTAL RESEARCH

Fiscal year 1984 was the first full year of TFTR experimental operation. There was significant progress on experimental studies of confinement during ohmic heating and plasma compression, as well as on initial experiments using neutral-beam heating. In addition, a review of the projections of TFTR Q ~ 1 capability was carried out. Planning activities for pellet injection and lower-hybrid current drive were also initiated.

The TFTR-ORNL (Oak Ridge National Laboratory) collaboration began during the summer of 1984. The ten on-site ORNL-ISX (Impurity Study Experiment) physicists immediately began to make important contributions to the TFTR Project.

Physics Operations

The TFTR was operated at plasma currents up to I_p = 1.4 MA, toroidal fields up to B_ϕ = 2.7 T, and plasma durations up to 4 sec. There were two major operation periods, a winter 1983-84 run period and a summer 1984 run period. The conditioning for the summer 1984 operational period involved a two-week bakeout of the entire torus, including the pumping ducts, at 150°C. While the vessel was hot, 50 hours of glow-discharge cleaning (p = 0.7 Pa, I ≈15 A) and 70 hours (45,000 pulses) of pulse-discharge cleaning were performed. All discharge cleaning was done in hydrogen, except the last 12 hours of pulse-discharge cleaning, which was performed in deuterium. The only significant modifications to the internal vacuum vessel hardware prior to the summer run period were the installation of graphite protective plates for two neutral beamlines and the removal of the TiC coating from the graphite limiter. The coating was removed because sections of the coating were damaged during the winter run period.

Enhanced pumping speed is provided by ZrAl getter modules. The pumping speed was 110 m³ per sec with six modules, compared with 10 m³ per sec for the turbomolecular pumps. Little systematic work was done to assess the effectiveness of the getters; thus far there has been no observable change on the gas fueling rate, density limit, impurity concentration, or plasma confinement.

Impurities and Radiation

The TFTR movable limiter consists of three water-cooled Inconel blades covered with graphite tiles. The limiter provides the wide range, in the plasma minor and major radii, necessary to study confinement-size scaling. For the winter 1983-1984 run period, the graphite movable limiter was coated with TiC. Titanium was the major metallic impurity with a relative concentration of n_{Ti}/n_e as high as 5×10^{-3} in low-density plasmas. Figure 25 shows a comparison of

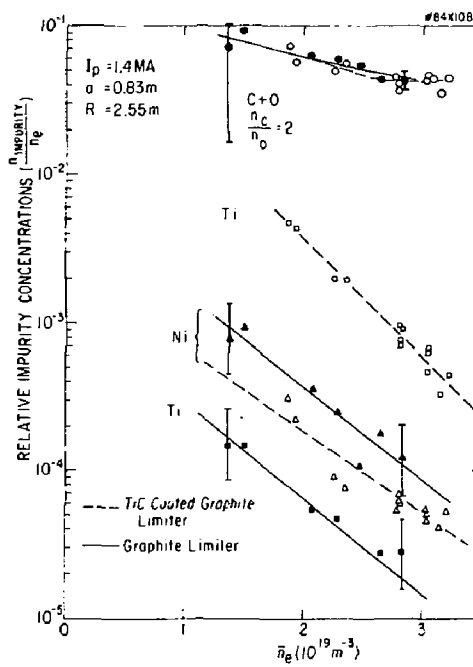

Fig. 25. Comparison of relative concentration of the metallic and low-Z ion impurities for the TiC-coated graphite limiter. The error bar represents the absolute accuracy of the measurements.

the metallic and low-Z concentrations measured for the graphite and TiC-coated limiter by X-ray pulse-height analysis (PHA) as a function of density for $I_p = 1.4$ MA, $a = 0.83$ m, and $R = 2.55$ m. After the TiC was removed, the titanium was reduced by a factor of 40. The nickel from the Inconel inner-wall limiter increased modestly. However, all the metallic impurities decreased substantially at the higher densities. In contrast, the concentration of low-Z ions showed no measurable change and did not have a strong variation with density.

The removal of the titanium had a noticeable effect on the plasma Z_{eff}. A comparison of Z_{eff}, measured by X-ray pulse-height analysis and visible bremsstrahlung, is shown as a function of density for the 1.4 MA plasma in Fig. 26. Also shown is Z_{eff} from the summer run period for the 1-MA plasmas. Both measurements indicate a significant reduction in Z_{eff}, with the removal of the TiC coating, at low densities. As reported by Hawryluk *et al.*,[13] Z_{eff} decreases with increased density and minor radius and increases with increased plasma current. This trend is observed for all density and current scans. Regression fits indicate Z_{eff} is approximately proportional to the ratio of the average-current density to the plasma density. Z_{eff} is as low as 2.5-3 at high density and currents of 1.0-1.4 MA. Impurity Z_{eff} measurements consistently lie between the estimates obtained from the Spitzer and the neoclassical resistivity models.

Confinement Studies During Ohmic Heating

The energy confinement time is evaluated at the end of the current and density flattops (2.8-3.1 sec). At this time all plasma discharges in TFTR reach equilibrium and the surface voltage approaches a value in the range of 0.8-1.4 V, depending on the plasma parameters. The confinement time is calculated with either the time-dependent transport analysis code TRANSP or the time-independent equilibrium code SNAP. The total energy confinement time τ_E is defined by

$$\tau_E = \frac{(W_e + W_i)}{[P_{oh} - (d/dt)(W_e + W_i)]},$$

where W_e and W_i are the electron and ion stored energies and P_{oh} is the ohmic input power.

For the largest plasmas ($a \simeq 0.83$ m, $R \simeq 2.55$ m), density scans were conducted for plasma currents of $I_p = 0.6$, 0.8, 1.0, 1.2, and 1.4 MA at $B_\phi = 2.7$ T. For any current, the confinement time increases with density, reaching a maximum of 0.3 sec. A maximum line-averaged density of $\bar{n}_e = 3.35 \times 10^{19}$ m^{-3} was obtained. At fixed density, the confinement time decreased with increasing current ($\tau_E \propto I_p^{-1.1}$). A limited number of discharges at $I_p = 0.8$ MA and $B_\phi = 1.8$ T indicated that the confinement time

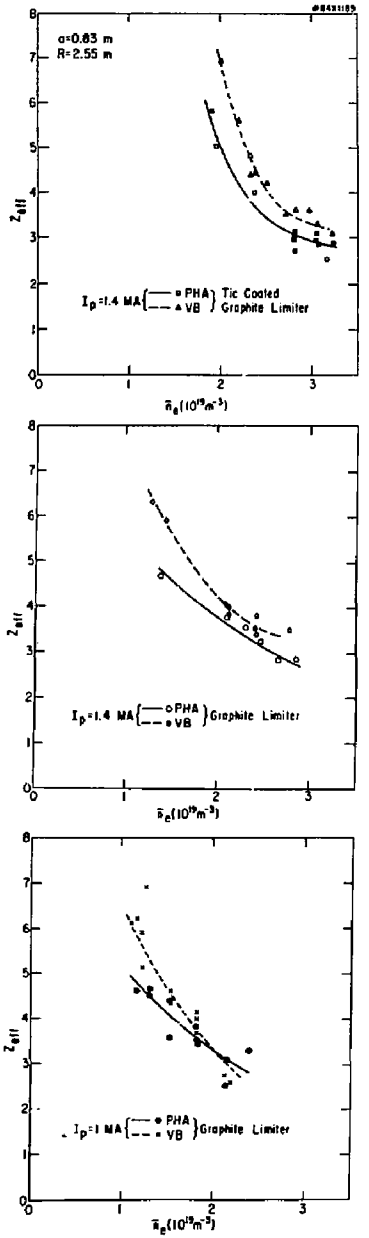

Fig. 26. Comparison of Z_{eff} measured by X-ray pulse-height analysis and visible bremsstrahlung as a function of density at $I_p = 1.4$ MA for the TiC-coated graphite and the uncoated graphite limiter, as well as Z_{eff} for the uncoated graphite limiter at $I_p = 1.0$ MA.

depends on the ratio of B_T/I_P. The results can be represented by the expression

$$\tau_E \propto \bar{n}_e q^{1.1} \quad .$$

Scans at 1.4 MA, taken with the bare graphite limiter, show a 20% improvement in the confinement time compared to the TiC-coated limiter.

Plasma-Size Scaling

The movable limiter was used to form plasmas of different minor radii. Density scans were made for a = 0.83, 0.69, 0.55, and 0.41 m at R = 2.55-2.65 m, $B\phi$ = 2.7 T and q ≃ 2.7-3.3. The density limit, radiation fraction and profile, Z_{eff} range, and electron temperature profile shape of all these discharges are similar. When $\bar{n}_e \lesssim 2\times10^{19}$ m^{-3}, the total energy confinement time is linear with density for plasmas of all sizes. However, both the a = 0.41 and 0.55 m plasmas show signs of saturating as $\bar{n}_e$ increases beyond this value. Figure 27 shows the gross energy confinement time as a function of $\bar{n}_e q$ for plasmas with radii a = 0.83, 0.55, and 0.41 m, studied during the summer run period. The q dependence was adopted from the studies of the a = 0.83 m plasmas. The q range for

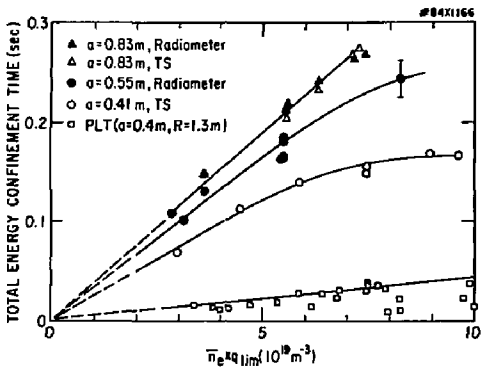

Fig. 27. The total energy confinement time versus $\bar{n}_e q$ for plasmas with a = 0.83, 0.55, and 0.41 m. Note that there are sets of points for the a = 0.83 m plasmas from the confinement using the Thomson scattering profiles and the analysis using scanning radiometer profiles.

the smaller plasmas is limited (2.7-3.3). The inferred minor-radius scaling depends on which minor radii plasmas are compared. The a = 0.83 and 0.55 m plasmas imply a very weak dependence ($\tau_E \propto a^{0.2}$), while the a = 0.55 and 0.41 m discharges imply $\tau_E \propto a^{1.1}$. The weakening of the scaling for the larger plasmas is consistent with the size-scaling experiments conducted last winter (Hawryluk *et al.*[13]) and may be related to the proximity of the plasma to the vessel wall for the larger plasmas, or to the greater relative importance of ion conduction in the smaller plasmas. A similar weakening of the a scaling near the vessel wall was observed by Ejima *et al.*[14] Comparing the 0.41-m TFTR plasmas with those from PLT (Princeton Large Torus)[15](a = 0.4 m, R = 1.3 m) implies $\tau_E/\bar{n}_e q \propto R^2$. However, the PLT data were taken at q ≃ 4-7, and PLT confinement did not show a systematic variation with q.

In the 0.41-m plasmas, ion conduction is consistent with the neoclassical model at all densities. Because the electron-ion temperature difference is somewhat larger, smaller limits may be set on the neoclassical multiplier of 1 to 3. Ion conduction is more apparent in the small plasmas because the electron conduction scales approximately as a, whereas ion conduction in the banana regime scales as $a^{-3/2}$.

The combined confinement results are shown in Fig. 28, with the confinement time plotted as a function of $\bar{n}_e R^2 aq$. The confinement results of PLT are also included. This scaling is similar to that of Pfeiffer and Waltz[16] and Alcator,[17] but the q dependence observed on TFTR is included. The TFTR results are also consistent with the T-11 scaling[18] of $\tau_E \propto R^{2.5}a^{0.4}$.

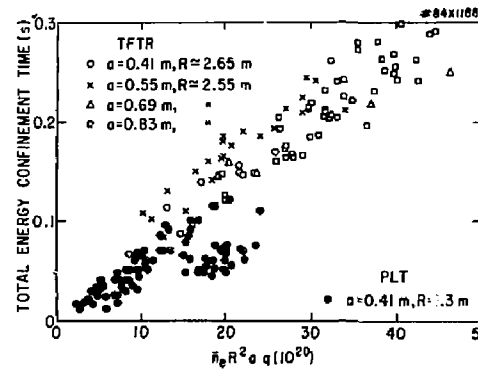

Fig. 28. The total energy confinement time versus $\bar{n}_e R^2 aq$ for PLT and TFTR ohmic confinement results.

Toroidal Compression Experiments

Initial studies of major-radius compression in TFTR have concentrated on demonstrating plasma control during the compression phase, evaluating scaling laws for plasma parameters during compression of ohmically heated discharges, and studying the evolution of a freely expanding plasma.

In the compression experiments, a deuterium plasma of small minor radius (typically a ≃ 0.55 m) is established at a large major radius (R ≃ 3.05 m) on the graphite movable limiter. The plasma is then compressed rapidly (~20 msec) in major radius by programming a step decrease in the reference position for the feedback control system and

simultaneously discharging capacitor banks in the equilibrium-field system to augment the rectifier power supplies. In full compression experiments, the plasma is brought into contact with the Inconel bellows cover plates, which form the small major-radius limiter, and maintained for ~1 sec at the final position ($R \simeq 2.10$ m, $a \simeq 0.48$ m). In free-expansion experiments, the plasma is rapidly moved part way across the vessel and allowed to slowly expand until it contacts the limiters.

For the standard compression scenario, the time evolution of the Thomson scattering electron density and temperature profiles during compression are shown in Figs. 29 and 30. Calculated profiles based on adiabatic scaling of the precompression profiles are shown for comparison. The density profile follows the expected scaling ($n_e \propto C^2$, $a \propto C^{-1/2}$) until the plasma reaches the inner wall when a slight broadening and loss of central density occurs, although the total particle count is conserved within the accuracy of measurement. However, the electron temperature profiles exhibit significant deviations from ideal scaling ($T_e \propto C^{4/3}$). Measurements of the central electron temperature using pulse-height analysis of the X-ray spectrum (accumulated over several shots) also show that the central electron temperature does not scale adiabatically. Interpretation of the electron temperature data is complicated by the occurrence of a large sawtooth oscillation towards the end of compression. This feature is always present, but the magnitude and timing of the sudden drop in central electron temperature varies from shot-to-shot, depending (at least in part) on the phase of the sawtooth prior to compression; consequently, there is a large scatter (±200 eV) in the $T_e(0)$ values at the end of compression. To reduce sensitivity to sawtooth effects, the electron temperature scaling has been examined in terms of the total electron stored energy, which for a single Thomson scattering profile is known to within 10%. At the end of compression, the electron stored energy is ~78% of the value expected for ideal scaling, with only a small scatter associated with the sawtooth and shot-to-shot reproducibility.

The increase in the central ion temperature is more nearly in accordance with the expected adiabatic scaling (Fig. 31). A detailed analysis of the strong compression discharges was made using the TRANSP code with measured R(t), $T_e(R)$, $n_e(R)$, and Z_{eff} data as input. Good agreement is obtained between measured and calculated neutron fluxes by assuming 1 × Chang-Hinton neoclassical transport for the ions. The defect in central ion temperature

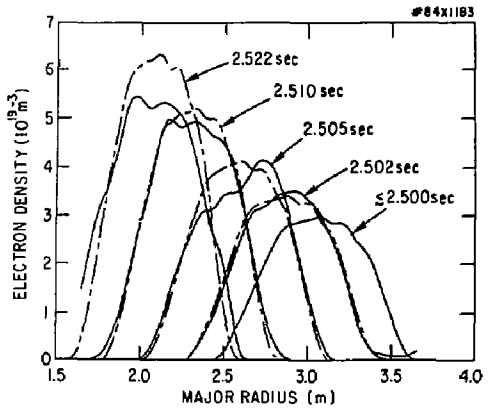

Fig. 29. Thomson scattering measurements of the electron density profile evolution during a full compression discharge. The dotted curves indicate the predicted ideal adiabatic scaling of the density.

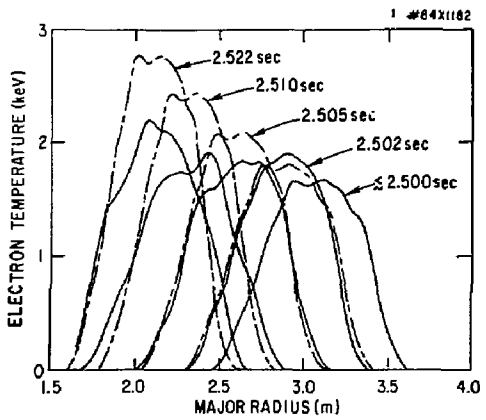

Fig. 30. Thomson scattering measurements of the electron temperature profile evolution during a full compression discharge. The dotted curves indicate the predicted ideal adiabatic scaling of the temperature.

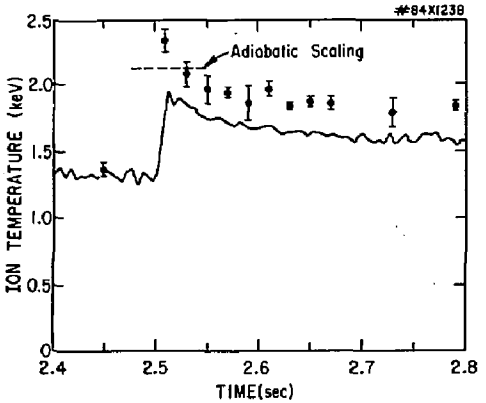

Fig. 31. Time evolution of the charge-exchange and neutron measurements of the central ion temperature for a full compression discharge.

(as inferred from the neutron flux), relative to adiabatic scaling, and the cooling of the ions after compression are accounted for by ordinary ion heat conduction, electron-ion coupling, and a significant convection term associated with the loss of central particles. The data suggests enhanced electron heat transport during the compression process. Averaged over the first 20 msec of compression, the gross energy confinement time is ~80 msec, to be compared with a value of 215 msec prior to compression. It is worth noting that the compression process constitutes a powerful form of auxiliary heating, providing ~2.9 MW average total power (compared with 0.6 MW ohmic power before compression), with a peak instantaneous power exceeding 5 MW. The apparent degradation of confinement is not inconsistent with that observed with other forms of auxiliary heating at comparable P_{heat}/P_{oh}. It should also be noted that although the TFTR electron heating results are similar to those for ATC,[19] in the latter case the precompression energy confinement time and the compression time were of comparable magnitude in contrast with the TFTR experiments.

Free-Expansion Experiments

The evolution of the measured electron temperature and density profiles during the free expansion of a partially compressed discharge are shown in Fig. 32. There are several striking aspects of the free-expansion phase. At first, the electron temperature profile broadens rapidly, reaching maximum width in ~50 msec after the start of compression (the compression time is ~20 msec). Then, the temperature profile contracts and within ~150 msec after the start of compression the temperature profile is similar to that of a high-q_a discharge formed at the same location without compression. In addition, the electron density in the center decreases rapidly after compression as particles move to the outer region of the discharge. During the free-expansion phase, the temperature profile is temporarily broader than the density profile, contrary to what is usually observed in tokamak discharges.

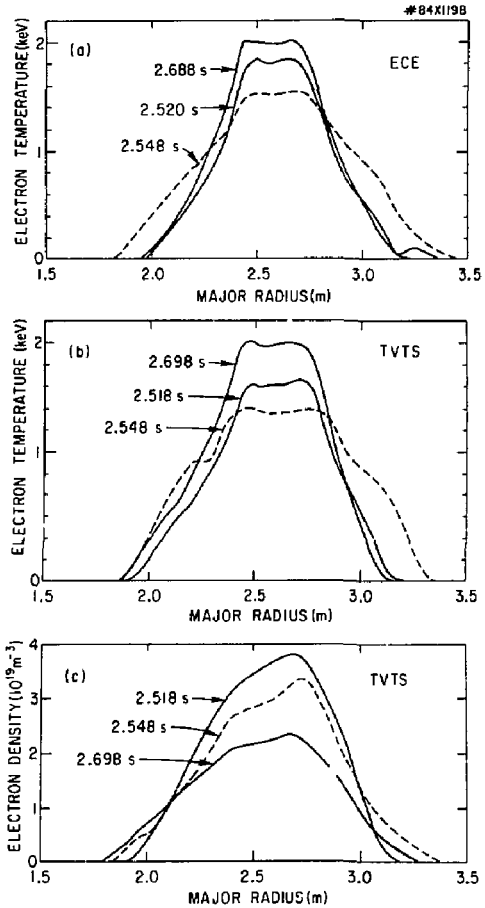

Fig. 32. Electron cyclotron emission measurements using the Michelson interferometer and Thomson scattering electron temperature and density profile measurements of a free-expansion discharge.

Initial Neutral-Beam Heating

Two neutral beamlines were installed for co-injection on TFTR during the spring of 1984. During September 1984, one beamline with three sources was operated at voltages up to 55 kV and 0.5-sec pulses of ~1.5 MW in hydrogen.

Figure 33 shows the time evolution of the ion temperature measured by Doppler broadening of TiXXI K_α line radiation and by neutron emission for a 1.0-MA discharge with $\bar{n}_e = 2.5 \times 10^{19}$ m^{-3}. In order to obtain agreement between the two ion temperature measurements, it was necessary to assume that the density rise observed during injection was due to hydrogen from the fast ions and beamlines, rather than due to recycling of the working gas. A similar assumption was required on PLT. Charge-exchange measurements were not available for this particular discharge but, in general, show satisfactory agreement with the other diagnostics. The maximum ion temperature of 3.2 keV, measured by the TiXXI K_α diagnostic, was achieved in a low-density discharge with $P_{inj} = 1.15$ MW. Electron heating was weak, perhaps because it is masked by the density rise. In addition, calculations indicate that the injected power transferred from the beam ions to the electrons in the core of the discharge is a small fraction of the ohmic input power. Typically, at higher densities the electrons heat by ~100-200 eV evenly across the discharge. This constitutes a modest broadening of the electron temperature profile shape.

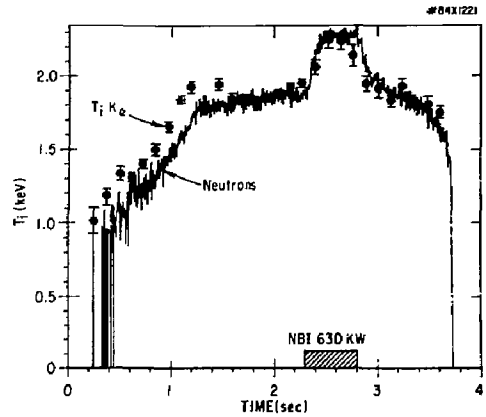

Fig. 33. The time evolution of the ion temperature measured by Doppler broadening of TiXXI K_α line radiation and by neutron emission for a 1.0-MA discharge with $\bar{n}_e = 2.5 \times 10^{19}$ m^{-3}.

Preliminary transport analyses of several discharges were performed using the PPPL transport analysis codes SNAP and TRANSP, as well as the ORNL analysis code ZORNOC. Figure 34 shows the resulting thermal confinement times. The trend of confinement degradation with increasing power is clearly confirmed. Because of the closeness of T_e and T_i and the low injection power levels, it is difficult to determine whether the ions or the electrons (or both) contribute to the degradation of the global confinement time with increasing power. At the lowest densities, core radiation may also play a significant role. There is no evidence of enhanced MHD activity to suspect anomalous loss of fast ions.

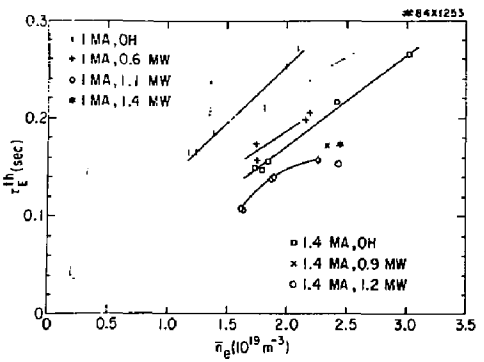

Fig. 34. Energy confinement time measured from kinetics versus line-averaged density for ohmic shots and for beam shots at the end of the heating pulse. Electron temperature and density profiles are from Thomson scattering, ion depletion from pulse-height analysis and visible bremsstrahlung impurity measurements, ion temperature from titanium K_α Doppler broadening and neutron emission. Typical uncertainty, ±15%.

EBASCO/GRUMMAN SUBCONTRACT

The Ebasco/Grumman industrial team provided engineering, design, and construction services as well as installation and assembly support to TFTR during the FY84 period. This support was provided in the areas of shielding, safety analysis, electrical systems neutral beams, diagnostics, surface pumping, CIC, ADA, and construction. Following is an elaboration on the accomplishments in each of these areas.

Shielding

The Ebasco efforts for Q = 1 equivalent shielding were concentrated in two areas. The first was the design and installation of radiation shielding in numerous penetrations of the Test Cell floor and the boron coating of the entire Test Cell Basement floor and selected areas of the data acquisition rooms. The second was the design and fabrication contract award for a modular concrete lining for the Test Cell. In addition, designs were completed for the installation of these liners and also for the installation of the radiation shielding in the remainder of the penetrations in both the machine and Test Cell floors.

Safety Analysis

Ebasco Nuclear Safety coordinated the publication of the TFTR Final Safety Analysis Report (FSAR). Assistance was provided to PPPL in identifying impacts of all approved TFTR configuration changes on safety documentation (i.e., FSAR's, OSR's and SR's) as well as on Operating Manuals and Maintenance Manuals.

The PPPL Radioactive Waste Management Plan was prepared in accordance with the requirements of DOE Order 5820.2 (Radioactive Waste Management), for formal transmittal to DOE in December 1984.

Information was compiled for PPPL on the existence and quality of relevant electric utility offsite meteorological and radiological monitoring programs and data within a 50-mile radius of TFTR. This information was needed by PPPL to determine the necessity for establishing its own such programs to satisfy DOE requirements.

Ebasco Nuclear Safety presented a paper entitled "Safety Review and Approval Process for the TFTR," at the 10th Symposium on Fusion Engineering in December 1983.

Guidance was provided, as needed, on the implementation of TFTR nuclear safety criteria and on potential impacts on the project of federal and state legislation.

Electrical Systems

During FY84, electrical design services were provided for the following systems.

- Surface Pumping System: Upgrading and trouble shooting of the surface pumping system (SPS) prototype that was put in operation during FY83 was carried out. The SPS full system electrical and control design, and equipment and material procurement were accomplished in preparation for system installation during 1985.
- Protective Plate Cooling Water System: The control system for the protective plate cooling water system was designed, fabricated, and installed. The system is operational and can be controlled from CICADA or the local control cabinet.
- Bumper Limiter Cooling Water System: The control system design for the bumper limiter cooling water system was completed. The system will be operated by a programmable controller. The equipment will be installed during FY85.
- Energy Conversion System: The emergency stop systems for the energy conversion system and the neutral beam system were designed and the equipment procured, installed, and commissioned. In addition, nine design specifications were issued, about 100 control wiring diagrams were revised, and ten new drawings were generated for modifications to the ECS equipment.
- Neutral Beam Power Supply System: Design and installation procedures were issued for the Kirk key system, bending magnets, grounding sticks, water-skid grounding system, control and instrumentation isolation system, SF_6 detection system, power receptacles, jib crane, and cryogenic area exhaust fans.
- Miscellaneous: Design and installation procedures were issued for the following: tritium system, neutron detectors, and bakeout heaters.

Neutral Beams

Early in the first quarter of FY84, Ebasco/Grumman began preparation for the installation of the second neutral-beam assembly, Neutral Beam No. 4. All work packages were completed by January 1984.

Installation of water, auxiliary gas, and cryogenic jumper subsystems began in January. Neutral-Beam Assembly No. 3 was repositioned in February, prior to the start of major assembly operations. Also, in February, the neutral-beam vacuum enclosure and the transition duct were delivered to the Test Cell. In March, the transition duct was installed and the vacuum enclosure was prepared for positioning on its support structure. Installation of the high-voltage enclosures in the Test Cell Basement was started. By May 1984, all neutral-beam mechanical installation was complete in the Test Cell and Test Cell Basement.

Diagnostics

The design engineering and most of the procurement activity for the X-ray crystal spectrometer was completed in FY84. The beryllium windows, screens, and vacuum vessel adaptors were fabricated in time for installation by the end of the shutdown. The crystal mounts, crystal table material, and the Lucite crystal enclosure were delivered prior to the end of FY84. Procurement of the helium bag was started, with delivery anticipated in CY85.

Ebasco was responsible for the mechanical engineering, design, and installation of the tokamak interface and support structure for a near-ultraviolet spatial scanning spectrometer (FLOPSY). Work was initiated in November 1983. The hardware was installed at TFTR on schedule in September. The optical train is a fiberglass tube, open to the atmosphere, which contains several lenses that carry emission through the Test Cell floor to the spectrometer located in the basement.

Ebasco provided the mechanical engineering design and installation of the periscope and optical train for the Fourier-transform spectrometer. The periscope is attached to the vacuum vessel and is open to the vacuum vessel interior. A highly polished aluminum mirror on a rotary-motion feedthrough reflects the electron cyclotron emission from the plasma through a quartz window in the optical train. The mirror can be rotated 180° to view a calibration cryostat through a second quartz window. It was installed and turned over to PPPL in time for the operational run in the summer.

First Wall Thermocouple Instrumentation Systems

During FY84, installation and check out of the "initial" protective plates and neutral-beam thermocouple systems were completed.

Design and procurement of equipment and cables for the "final" protective plates, "final" surface pumping system, and bumper limiter thermocouple systems were initiated and completed. Installation and "end-to-end" thermocouple test procedures for these were identified and initiated. These systems are scheduled for completion in FY85.

Plotting and archiving requirements for the "final" first wall instrumentation systems were identified and forwarded to CICADA for implementation during FY85.

Construction Activities

The construction activities were very diversified and ranged from standard craft skills to highly specialized and precision work. Much of the work required special staging because TFTR is operational and access is limited to nonoperational periods. To

circumvent this problem, an extensive amount of prefabrication work was accomplished in nonrestricted areas. In spite of these constraints, the construction activities for all released work were completed on or ahead of schedule.

Among the tasks completed were the upgrading of the vacuum vessel bakeout system and torus vacuum pumping system, as well as the radiation shielding in the machine floor and addition of borate to the data acquistion room floor tiles. The main part of the construction effort was concentrated on the installation of all ancillary systems and equipment for the operation of two neutral-beam boxes for Lines No. 3 and No. 4. Although neutral-beam box No. 3 was installed in FY83, it was now completed with the installation of all piping (including cryogenics, water, gas, and air) and electrical systems. Neutral-beam box No. 4 was installed during the winter opening of the Test Cell. Also, during that time, the high-voltage enclosures were installed in the Test Cell Basement.

The following neutral-beam support systems were also completed: surge rooms, modulator/regulators, high-voltage transformer yard, main transmission lines, 1000-watt refrigeration system, and water systems.

Central Instrumentation, Control, and Data Acquisition

Ebasco/Grumman supplied an average of 15 engineers to the CICADA group to supplement their staff during FY84. These engineers worked under the direction of PPPL staff and applied their skills to system software development, applications software development, and hardware system documentation.

References

[1]H.P. Eubank, J. Bell, M.G. Bell, *et al.*, "Neutral Beam Heating in TFTR—Projections and Initial Results," in *Plasma Physics and Controlled Nuclear Fusion Research 1984* (Proc. 10th Int. Conf., London, 1984), Vol. *I*, IAEA, Vienna (1985) 303.

[2]B.A. Prichard, Jr., H.P. Eubank, L.R. Grisham, *et al.*, "Neutral Beam Heating Systems for TFTR—Initial Operating Results," in *Symposium on Fusion Technology 1984* (Proc. 13th Symp., Varese, Italy, 1984), Vol. *I*, Pergamon Press, New York (1985) 703.

[3]P.C. Efthimion, N. Bretz, M. Bell, *et al.*, "Confinement Studies of Ohmically Heated Plasmas in TFTR," in *Plasma Physics and Controlled Nuclear Fusion Research 1984* (Proc. 10th Int. Conf., London, 1984), Vol. *I*, IAEA, Vienna (1985) 29.

[4]J.L. Cecchi, M.G. Bell, M. Bitter, *et al.*, "Initial Limiter and Getter Operation in TFTR," J. Nucl. Mater. *128&129* (1984) 1.

[5]P.C. Efthimion, M.G. Bell, W.R. Blanchard, *et al.*, "Initial Confinement Studies of Ohmically Heated Plasmas in the Tokamak Fusion Test Reactor," Phys. Rev. Lett. *52* (1984) 1492.

[6]D. Johnson, D. Dimock, B. Grek, *et al.*, "TFTR Thomson Scattering System," Phys. Rev. Lett. *56* (1985) 1015.

[7]G. Taylor, P.C. Efthimion, M.P. McCarthy, *et al.*, "Fast Scanning Heterodyne Receiver for the Measurement of the Time Evolution of the Electron Temperature Profile on TFTR (I)," Rev. Sci. Instrum. *55* (1984) 1739.

[8]G. Taylor, P.C. Efthimion, M.P. McCarthy, *et al.*, "Fast Scanning Heterodyne Receiver for the Measurement of the Time Evolution of the Electron Temperature on TFTR (II)," Rev. Sci. Instrum. *56* (1985) 928.

[9]K.W. Hill, M. Bitter, M. Tavernier, *et al.*, "The TFTR Horizontal High-Resolution Bragg X-Ray Spectrometer," Rev. Sci. Instrum. *56* (1985) 1165.

[10]A.L. Roquemore, G. Gammel, G.W. Hammett, *et al.*, "Application of an E||B Spectrometer to PLT Charge Exchange Diagnostics," Rev. Sci. Instrum. *56* (1985) 1120.

[11]J.F. Schivell, "Performance of the TFTR Bolometers," Rev. Sci. Instrum. *56* (1985) 972.

[12]S.S. Medley, F.E. Cecil, D. Cole, *et al.*, "Fusion Gamma Diagnostics," Rev. Sci. Instrum. *56* (1985) 975.

[13]R.J. Hawryluk, M.G. Bell, M. Bitter, *et al.*, "Recent Results from TFTR," in *Heating in Toroidal Plasmas* (Proc. 4th Int. Symp., Rome, 1984), edited by H. Knoepfel and E. Sindoni, Vol. *II*, International School of Plasma Physics and ENEA, Varenna (1984) 1012.

[14]S. Ejima, T.W. Petric, A.C. Riviere, *et al.*, "Scaling of Energy Confinement with Minor Radius, Current and Density in Doublet III Ohmically Heated Plasmas," Nucl. Fusion *22* (1982) 1627.

[15]R.J. Hawryluk, K.Bol, N. Bretz, *et al.*, "The Effect of Current Profile Evolution on Plasma-Limiter Interaction and the Energy Confinement Time," Nucl. Fusion *19* (1979) 1307.

[16]W. Pfeiffer and R.E. Waltz, "Empirical Scaling Laws for Energy Confinement in Ohmically-Heated Tokamaks," Nucl. Fusion *19* (1979) 51.

[17]B. Blackwell, C.L. Fiore, R. Gandy, *et al.*, "Energy and Impurity Transport in the Alcator C Tokamak," in *Plasma Physics and Controlled Nuclear Fusion 1982* (Proc. 9th Int. Conf., Baltimore, 1982), Vol. *II*, IAEA, Vienna (1983) 27.

[18]V.M. Leonov, V.G. Merezhkin, V.S. Mukhovatov, *et al.*, "Ohmic-Heating and Neutral-Beam Injection Studies on the T-11 Tokamak," in *Plasma Physics and Controlled Nuclear Fusion* (Proc. 8th Int. Conf., Brussels, 1980), Vol. *I*, IAEA, Vienna (1981) 393.

[19]K. Bol, R.A. Ellis, H. Eubank, *et al.*, "Adiabatic Compression of the Tokamak Discharge," Phys. Rev. Lett. *29* (1972) 1495.

PRINCETON LARGE TORUS

Supplementary heating by radio-frequency (rf) has many attractive features for a working fusion reactor. From the physics viewpoint, rf waves are capable of penetrating to the center of large, high-density plasmas. An attractive feature from the engineering viewpoint is that the high-power generators could be located outside the radiation area where they would be easily accessible for maintenance. Also, present-day rf technology is capable of providing the required power. Another key advantage of rf is the ability to drive current in a plasma. The rf current drive could simplify a tokamak reactor design by reducing cyclic stresses, by allowing a more rugged first wall, and by eliminating some of the poloidal-field coils.

The research program on the Princeton Large Torus (PLT) continued to be directed towards evaluating rf heating and current-drive methods relevant for fusion reactors. Significant progress was made in FY84 in upgrading the high-power rf systems to pursue this goal. The level of engineering and construction in support of the PLT program was intense in FY84 and the planned array of rf sources is now available for a thorough exploration of rf heating and current-drive techniques for potential reactor use.

A major accomplishment in FY84 was plasma heating at the 4-MW level, in the ion cyclotron range of frequencies (ICRF), with stable discharge conditions and with the plasma energy content continuing to scale linearly with rf power. Ion temperatures of >4 keV were achieved at a line-averaged density of 3.5-4 $\times$ 10^{13} cm^{-3}. Successful results on PLT over the past few years are largely responsible for making ICRF the heating method of choice in the design of future reactors such as the International Tokamak Reactor (INTOR) and the Tokamak Fusion Core Experiment (TFCX).

A new 2.45-GHz lower-hybrid system was installed and commissioned. Initial results at this higher frequency have shown current-drive effects well above the density $\bar{n}_e \sim 7 \times 10^{12}$ cm^{-3} which limited the old 800-MHz system.

In addition to the two mainline rf efforts, experiments with ion Bernstein wave heating at 90 MHz are set to begin, and preparations for fast-wave current-drive experiments at 80 and 800 MHz are well underway. Studies continued in the areas of limiter design and materials, X-ray spectroscopy, fusion products, impurity transport and spectroscopy, and fast-ion charge-exchange in support of the experiments in rf heating and confinement.

MAJOR ACTIVITIES

The typical "run week" consisted of two days for ICRF, two days for lower-hybrid (LH), and the remaining day going to either ion cyclotron resonance heating (ICRH), neutral beam + ICRH, LH, or to an auxiliary experiment. In addition, auxiliary experiments often were carried out in a "piggyback" mode. In FY84, PLT had approximately 14,000 high-power discharges, with 113 "run days" for experimentation, and has continued to operate reliably.

ICRF Heating Experiments on PLT

In FY84, primary emphasis was placed on studies of high-power fundamental minority ^{3}He heating at 30 kG. This regime was selected since it exhibits the highest heating efficiencies on PLT and should permit the highest temperatures to be obtained. Intensely heated D-^{3}He plasmas are desired to permit rf performance optimization under conditions relevant for TFTR and the hot plasma rf regimes envisioned in the ignition devices.

A plan to prepare for 6-MW capability at the single frequency of 30 MHz was developed in FY83. Basically, the goal was to use the "old" 25-MHz system (Unit 3) and the two newer 42-MHz systems (Units 1 and 2 originally built for 55 MHz) on one set of experiments for very high-power ICRF applications. Each system was estimated to be capable of around 2 MW at the 30-MHz frequency. Completion of the system in August 1984 resulted in 6-MW capability in dummy load with the power division as follows: Unit 1, 2.25 MW; Unit 2, 2.25 MW; Unit 3, 1.5 MW.

A major advance in early 1984 was the acquisition and testing of a novel cone-type antenna feedthrough (bushing) constructed from the PPPL design made in 1982 (Fig. 1). These cone bushings, which connect the rf transmission system to the antenna inside the vacuum enclosure of PLT, were tested to over 100-kV rf voltage standoff on a test stand. Upon installation of the new bushing on PLT in February 1984, the power-handling capability of a single antenna was raised to >1.4 MW from a previous level of ~0.6 MW. Indeed, the 1.4-MW level was source limited, and to date the new cone-bushing has not arced during high-power PLT operation. Eight high-power coils were installed on PLT in May 1984 with the new

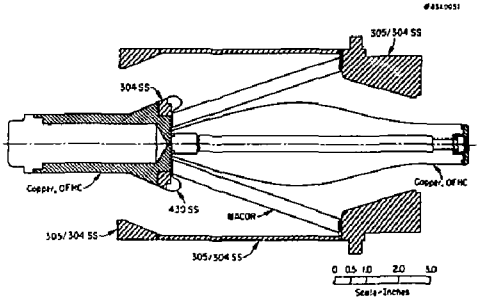

Fig. 1. The Princeton Plasma Physics Laboratory ICRF cone bushing.

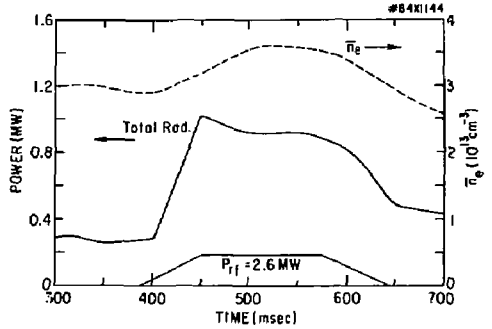

Fig. 2. Line-averaged electron density (dotted line) and total power as a function of time for P_{rf} = 2.6 MW.

feedthroughs. Thereby, the capability of utilizing the full source power was achieved.

Experiments during FY84 continued to extend our evaluations of the quantitative effects produced during ICRF heating. The effects of recycling, impurity influx, production and loss of energetic ions, and wave propagation and mode conversion properties continued to be stressed as reported at the Rome Conference[1] in March 1984. Of particular importance in FY84 was the achievement of ~4 MW delivered at 30 MHz to the PLT antennas in the D-^{3}He regime. As reported at the London Conference[2] in September 1984, for powers up to 3 MW, this was accomplished for stable discharge conditions. At the 4-MW level, ion temperatures in excess of 4 keV were obtained at densities in the range of 3.5-4 × 10^{13} cm^{-3}.

Typical parameters of the target ohmic plasma were a central electron temperature T_{eo} ~ 1.5 keV, a central ion temperature T_{io} ~ 1 keV, and a line-averaged density $\bar{n}_e$ ~ 2-4 × 10^{13} cm^{-3}. The plasma current was maintained in the range of 500-600 kA. Previous studies show that the plasma current in PLT must be maintained at values above 300 kA to prevent a precipitous drop in the ion-heating efficiency and the simultaneous influx of impurities. The value of Z_{eff} derived from the measured electron temperature and density profiles was in the range 1-1.5.

One characteristic feature of ICRF in PLT is a density increase during the rf pulse. This is shown in Fig. 2 where the time evolution of $\bar{n}_e$ is shown for 2.6 MW of rf power into the plasma. It was found that the density increase tends to saturate with rf power. It was also found that the density during the ICRF pulse depends very weakly on the target plasma density so that low-density discharges are strongly perturbed by the rf and, therefore, are more difficult to control at large power levels.

An increase in the charge-exchange outflux of low-energy (<1 keV) neutrals was observed during the ICRF heating pulse. This flux is apparently toroidally uniform and was measured to be linearly dependent on ICRF power, and about equal to 10^{15} cm^{-2} sec^{-1} MW^{-1}. An increase in the H_α emission was also measured at several locations around the torus. These observations suggest that the density increase caused by ICRF is predominantly due to an increase in recycling at the vacuum vessel wall, although a small fraction of the density increase is due to an influx of impurities (see below). It was also found that the charge-exchange outflux increases significantly for plasma currents below ~300 kA. This current threshold effect parallels that for impurity influx and suggests that fast-ion losses may trigger the increase in recycling.

Minority concentrations $\eta = n_{^3He}/n_e$ of 10% or smaller were used in the ICRF experiments. The density of ^{3}He was estimated from the increase of $\bar{n}_e$ produced by the injection of ^{3}He into the discharge. Study of the mode conversion of fast-magnetosonic waves into ion Bernstein waves indicates that this is a good estimate of the ^{3}He concentration in the central part of the plasma torus. In this study, density fluctuations at the ICRF frequency were detected with scattering of microwaves at a fixed position on the midplane. The magnetic field necessary to localize the ion Bernstein wave with a well-defined wave vector inside the scattering region was measured. The measurements at several values of the wave vector were then fitted to the kinetic dispersion relation. The only free parameter was the minority concentration. The values obtained for η agree (within ±20%) with those estimated from the changes of $\bar{n}_e$ induced by the puffing of ^{3}He.

Three techniques have been used for determining the deuterium ion temperature T_i: charge-exchange measurements, Doppler broadening of impurity line radiation, and neutron emission measurements. This redundancy is necessary because each method has intrinsic uncertainties.[2] Ion heating versus time from these measurements is shown in Fig. 3 for a discharge with $\bar{n}_e$ = 3.8 × 10^{13} cm^{-3} and 2.6 MW of coupled rf power.

The spectroscopic results of Fig. 4 reveal not only that most of the deuterium depletion is caused by oxygen and carbon impurities (in addition to that attributable to ^{3}He), but that the bulk radiation (Fig. 2) is caused by these lighter impurities in the periphery of the plasma. The higher Z impurities give a radiation contribution from the central region of ~0.2-0.3 W

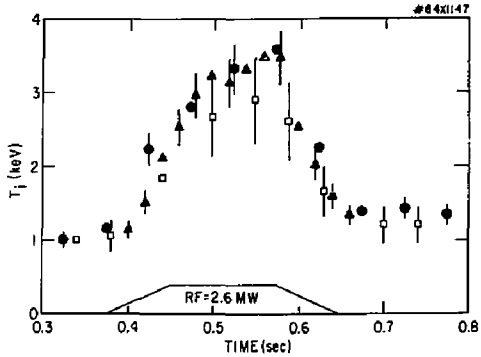

Fig. 3. Time evolution of the central ion temperature derived from charge-exchange (squares), Doppler broadening of the FeXXV line (circles), and neutron emission (triangles) for P_{rf} - 2.6 MW and $n_e(0) = 5 \times 10^{13}$ cm^{-3}.

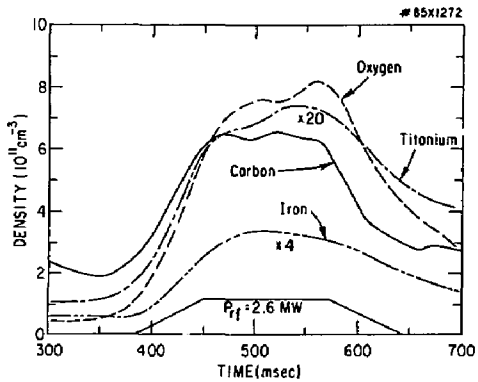

Fig. 4. Time evolution of impurities for P_{rf} = 2.6 MW and $\bar{n}_e = 3.8 \times 10^{13}$ cm^{-3}.

cm^{-3} and contribute somewhat to the value of Z_{eff} which almost doubles during the rf pulse for the case shown.

Figure 5 shows the radial profiles of T_i derived from Doppler broadening measurements for several values of rf power and $\bar{n}_e \simeq 3.8 \times 10^{13}$ cm^{-3}.

The electron temperature T_e was obtained from measurements of the plasma emission at the second harmonic of the electron cyclotron frequency and from Thomson scattering of laser light. Figure 6 shows the time evolution of T_e at four radial locations for the 2.6-MW case. The central value of T_e is strongly modulated by the sawtooth relaxation. Thomson scattering radial profiles show that large rf powers flatten the central part ($r \lesssim 20$ cm) of the density and temperature profiles.

Figure 7 (top) shows the quantity $p_e = n_e(0)dT_e(0)/dt$ at the beginning of a sawtooth oscillation as a function of rf power for a constant value of $\eta \sim 0.07$. If the electron thermal losses in the center of the discharge

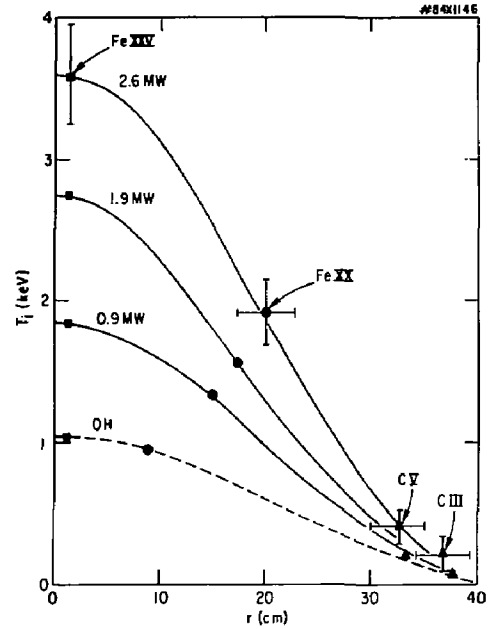

Fig. 5. Radial profiles of deuterium ion temperature from Doppler broadening of impurity lines for $\bar{n}_e = 3.8 \times 10^{13}$ cm^{-3}.

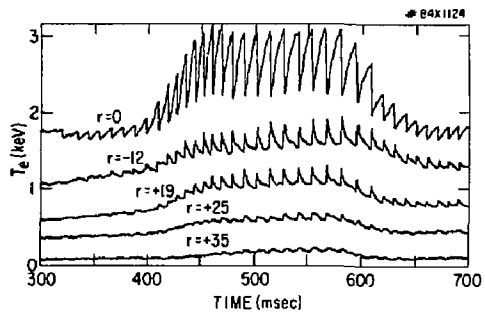

Fig. 6. Time evolution of T_e derived from second-harmonic electron cyclotron emission at different radial locations for P_{rf} = 2.6 MW and $\bar{n}_e = 3.8 \times 10^{13}$ cm^{-3}.

over the first part of the sawtooth period are neglected, p_e is a measure of the central power deposition to the electrons. These data indicate that p_e increases with rf power and has a value of ~1 W cm^{-3} at 2 MW. It was also found that the value of p_e is a growing function of η [Fig. 7 (bottom)]. This must be considered a clear indication that other processes (i.e., mode conversion), besides collisions with the hot minority component, play a role in the ICRF heating.

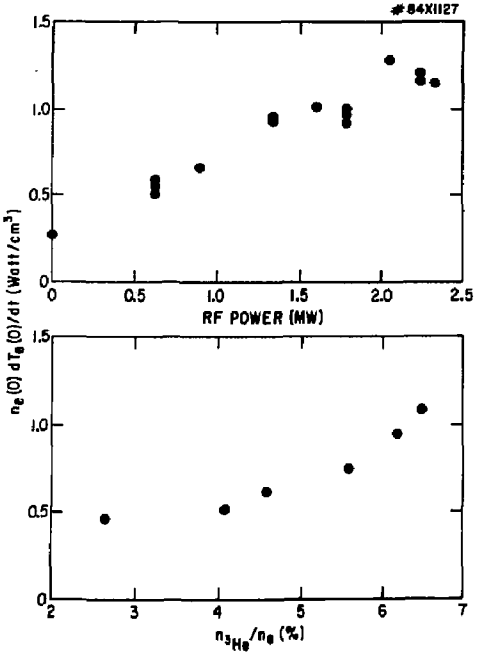

Fig. 7. Values of $p_e = n_e(0)dT_e(0)/dt$ as a function of rf power (top) and as a function of $\eta = n_{^3He}/n_e$ for P_{rf} = 1.8 MW (bottom).

The results of Fig. 8 indicate that no catastrophic ion energy loss was encountered as the ICRF power to the antennas was raised to the 3-MW level. Energy content up to the 4-MW level (not shown in Fig. 8) continues to increase approximately linearly with rf power.

Plasma confinement time, defined by $\tau_E = \epsilon_{tot}/(P_{oh} + P_{rf})$, decreases to approximately 2/3 of the ohmic value at $P_{rf} \simeq 2$ MW and then remains approximately constant with further increases in rf power. The value of τ_E for large P_{rf} must, in fact, be considered a lower limit since the fraction of P_{rf} coupled to the plasma core may not be 100%, and the fraction of power lost by the fast minority ions is not known.

It is noteworthy that while the radiation loss does increase with the application of rf power, the fraction of radiated power is similar to that in ohmic plasmas. Consequently, during rf heating, radiation losses remain a small part of the total power balance.

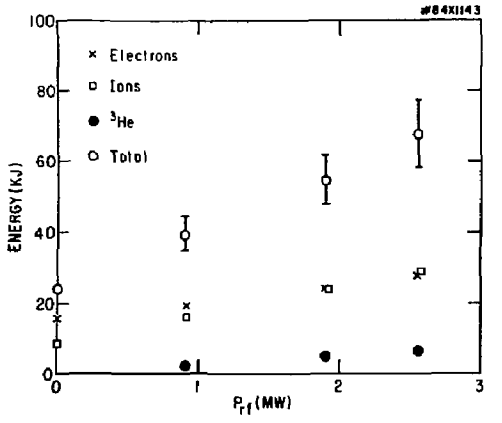

Fig. 8. Energy of plasma components as a function of rf power (^{3}He energy from quasi-linear theory).

Lower-Hybrid Current-Drive Experiments on PLT

Lower-hybrid current-drive continues to be the most successful method for maintaining plasma current in long-pulse tokamak discharges. Also, evidence obtained on PLT and discussed in last year's Annual Report indicated that lower-hybrid waves could do more than just maintain a constant current; these waves could start up the plasma current without the aid of the ohmic-heating transformer and could ramp up the current with surprising efficiency.[3-5] Such application of rf-driven ramp-up could eliminate the need for a costly and complex ohmic-heating system in subsequent fusion reactors, and so it is essential to understand the relatively high ramp-up efficiencies observed on PLT (>20%) in order to extrapolate to larger tokamak devices.

Figure 9 shows the current ramp-up efficiency measured as a function of the rf power. Before delving into the esoteric features of this work, it should be pointed out that there is no evidence of any decrease in efficiency at the highest available rf power levels.

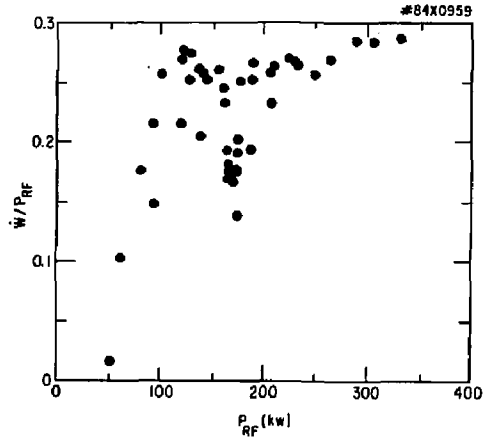

Fig. 9. Efficiency of conversion of rf energy into poloidal-field energy versus rf power.

Before this data was taken, fear of such a decrease was extant in both the theoretical and experimental communities.

The specter of low efficiency had its origin in the physics of the so-called reversed current. As the current ramps up faster, a reversed electric field increases and inevitably drives a current which counters the one trying to be increased. In the midst of these concerns, the PLT lower-hybrid group began a very fruitful cooperation with PPPL theorists Fisch and Karney. They pointed out that the inevitable reversed electric field is not harmful per-se. As this field slows the suprathermal particles, the loss of particle energy corresponds to the energy flow into the poloidal-field energy. They proposed a bookkeeping system for the energy flow which is shown in Fig. 10. A fraction η of the rf power does work in pushing suprathermal electrons. Some of this power P_{el} flows into the poloidal field and some is lost as the fast particles collide with the thermal background. The reversed electric field V drives a current, and the dissipation associated with it, V^2/R, represents a further detraction from the ramp-up efficiency. From this diagram it is shown that $d/dt\ (1/2\ LI^2) = P_{el} - V^2/R$. The Fisch-Karney theory showed that P_{el} is a calculable function of $V_{phase}/V_{Dreicer}$, where V_{phase} is the wave-phase velocity and $V_{Dreicer}$ is the electron runaway velocity in the electric field. In Fig. 11, P_{el} versus $V_{phase}/V_{Dreicer}$ is plotted for over 250 current-drive shots on PLT. In order to get this fit to the experimental data, it was assumed that $\eta \approx 0.75$.

During the past year, a 2.45-GHz, 1.5-MW system (source power) for furthering lower-hybrid studies was completed and installed on PLT. This system allows a significant extension of the parameters of current drive. The pulse-length capability of this new

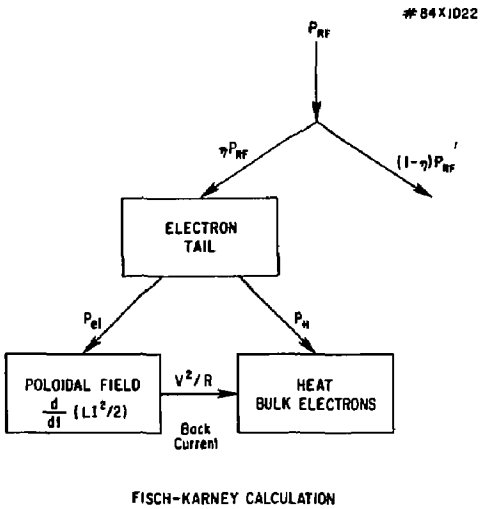

Fig. 10. Power-flow diagram for the rf ramp-up process.

system is more than ten times that of the older system; the power capability is about four times the previous typical operating power level; and the density at which it can operate should be well into the 10^{13} cm^{-3} range instead of below 7×10^{12} cm^{-7}, which has been the upper limit for effective operation until now.

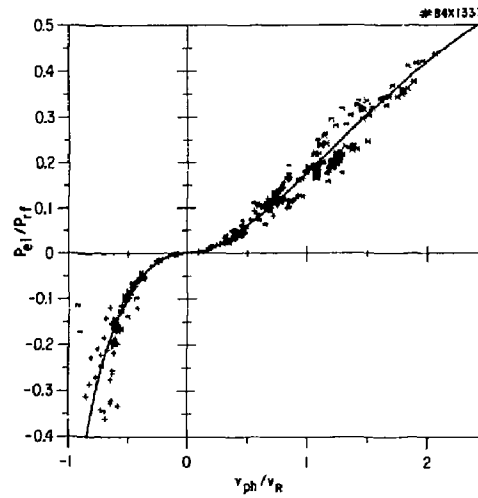

Fig. 11. Comparison between the experimental and theoretical efficiency of conversion of rf energy into electric field energy as a function of $V_{phase}/V_{runaway}$.

The 2.45-GHz system consists of three modules. The first module was attached at the equatorial plane of PLT in January, 1984. The second and third modules were attached at the so-called top launch position in August, 1984. Each module is capable of launching 400 kW of rf into the PLT plasma. The maximum power achieved to date in one port is ~250 kW and the maximum simultaneous power in two ports is 500 kW.

It has been learned that the first step in ascertaining if a lower-hybrid waveguide coupler is operating correctly is to make a measurement of the overall reflection coefficient for the coupler versus the phase difference between adjacent waveguides. Figure 12 shows the experimental and theoretical results for the eight-waveguide 2.45-GHz coupler. The n_e and $\nabla\bar{n}_e$ values shown are those assumed in the theory to exist at the plasma end of the coupler. The agreement between the theory and experiment indicates that the energy is being transmitted to the plasma (not areas inside the coupler) and that the phase shift calibration is correct.

Figure 13 shows current drive for an electron density of 1.4×10^{13} cm^{-3}. This density is twice as high as the density cutoff for the 800-MHz system. In this case the power through the top launch and the outside launch was 220 kW each for 0.2 seconds. The current drive in this case was less efficient in

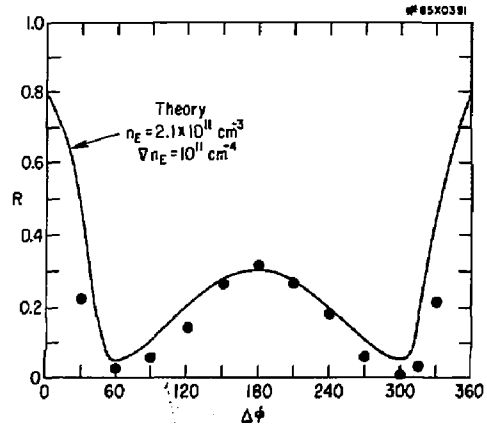

Fig. 12. Experimental results and theoretical predictions of reflected power versus waveguide phasing for an eight-waveguide, 2.45-GHz grill coupler.

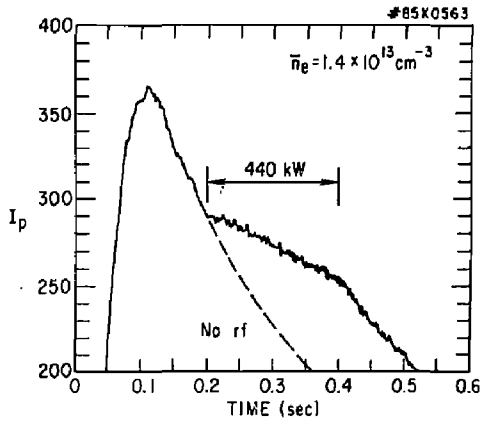

Fig. 13. Effect of 440 kW of 2.45-GHz power on the plasma current at $\bar{n}_e = 1.4 \times 10^{13}$ cm^{-3}.

terms of A/W per electron density than the efficiencies seen at lower densities. Whether this is a reproducible result remains to be seen.

Another early result of the 2.45-GHz experiment, which is perhaps surprising, is that the top launch is comparably efficient to the outside launch at densities below 10^{13} cm^{-3}. Preliminary results from another laboratory had indicated that top launch efficiency is much less than that for outside launch. Further studies of the relative effectiveness of the two couplers will take place in 1985.

In the coming year (1985) radial control of current drive and its effect on plasma stability will be given greater emphasis. In 1984 some very preliminary measurements of energy distribution versus plasma radius were made to initiate this new direction of study.

Radial studies of current-drive effects could have an important bearing on the understanding of the physics of current drive and the effect of current drive on plasma stability. Figure 14(a) and 14(b) show X-ray measurements of bremsstrahlung radiation during current drive on PLT. Data through four chords of the PLT plasma was taken. In Fig. 14(a) curves indicating that the energy distribution is independent of minor radius are shown. Figure 14(b) shows similar data for a slightly higher density. In this case, the lower-energy photons fall off quickly with minor radius while the higher-energy photons are down by only a factor of 3 at r = 30 cm, indicating a broad or even hollow distribution for the most energetic electrons. Although systematic studies are just beginning, it is clear that the new multichannel hard X-ray system will allow the study of the extremely important radial variations of current drive in the coming year.

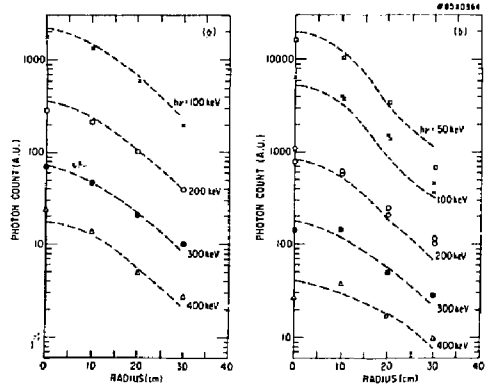

Fig. 14. (a) Perpendicular hard X-ray emission at four viewing chords with $\bar{n}_e \simeq 3 \times 10^{12}$ cm^{-3}. (b) Same as (a) except $\bar{n}_e \simeq 4.0 \times 10^{12}$ cm^{-3}.

Plasma Materials Interaction and Rotating Limiter[6-9]

A limiter with a specially contoured front face and the ability to rotate during tokamak discharges was installed in a PLT pump duct (Fig. 15). These features were selected to handle the unique particle and heat load requirements of ICRF heating and lower-hybrid current-drive experiments. The limiter shape was chosen so that runaway electrons and energetic ions impact on the front face while the bulk plasma impacts primarily behind the limiter where a restricting collar and a pumping duct act to prevent particles from reentering the plasma. The heat load impacting the front face can be distributed over a large surface area by rotating the limiter. The limiter was conditioned by irradiation with 1-MW, 200-msec duration, 40-keV

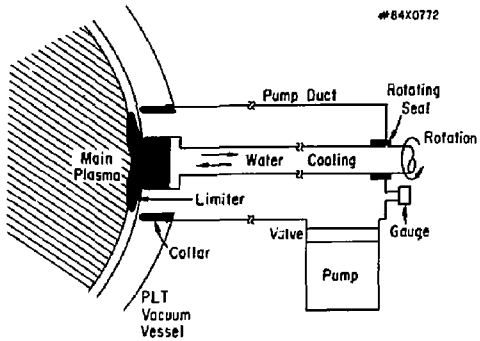

Fig. 15. Schematic drawing of the rotating pump limiter on PLT.

ion beam pulses. With the limiter rotating, a 50% increase in lower-hybrid pulse duration was achievable at $\bar{n}_e \sim 2 \times 20^{12}$ cm^{-3} without the uncontrolled density rise experienced previously.

Aspects of plasma materials interactions connected with impurity control and antenna power handling are discussed in the sections dealing with ICRF and LH.

Fusion Products

New diagnostic techniques for measuring the ion temperature and poloidal-field profiles using 3-MeV protons created by d(d,p)t fusion reactions were invented and tested. The fusion protons leave the plasma on trajectories determined by the position of their birth and by the poloidal magnetic field. Pitch-angle resolution of the escaping 3-MeV protons can separately resolve the spatial distribution of d(d,p)t fusion reactions and the poloidal-field distribution inside the tokamak. Figure 16 shows a fusion emission profile measured with an array of collimated

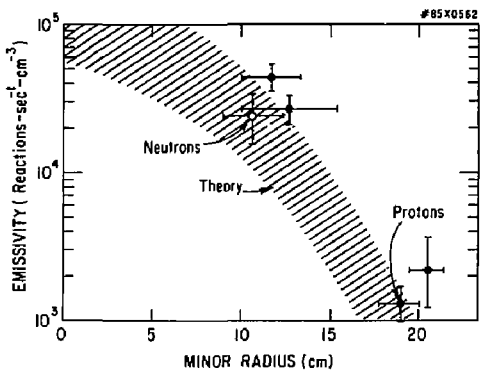

Fig. 16. Fusion emissivity profile measured during ohmic heating in deuterium PLT discharges. The theoretical emissivity is from neoclassical calculations of the ion temperature profile.

surface barrier detectors during ohmic heating in deuterium. The measurements indicated that with modest improvements quite accurate (±5% in T_i; ±2 cm in position) determination of the deuterium ion temperature profile is possible.[10] With detectors similar to our prototype detectors, measurements of the poloidal field at r/a = 0.5 to ±25% also appear possible. New physics results obtained with the 3-MeV proton detectors include accurate measurements of the emission profile during deuterium neutral-beam and lower-hybrid heating that showed that the beam ion deposition and damping on ions peak strongly near the magnetic axis.[11]

Charge-Exchange

A bounce-averaged quasilinear operator that properly treats ICRF heated ions with banana orbit tips near the resonance layer was implemented in a Fokker-Planck code in order to compare the predictions of the theory with charge-exchange measurements of the energy and angle distribution of the fast ions. Although detailed comparisons are still in progress, good qualitative agreement between the theory and the experiment was found, as shown in Fig. 17. These measurements were made during fundamental cyclotron heating of a ^{3}He minority in a ^{4}He majority plasma. A ^{4}He plasma was used instead of the usual D plasma to take advantage of the double charge-exchange reaction $^3He^{++} + {}^4He \rightarrow {}^3He + {}^4He^{++}$ to produce a measurable flux of energetic ^{3}He neutrals. The largest neutral flux was seen at an intermediate viewing angle, corresponding to particles whose banana tips lie near the resonance layer and whose banana orbit carries them to the high-neutral-density region in the edge of the plasma.

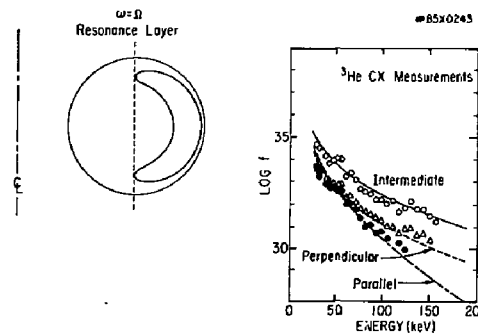

Fig. 17. Charge-exchange measurement of the ^{3}He energy distribution during ^{3}He minority heating in a ^{4}He majority plasma at three different viewing angles: near-parallel (R_{tan} = 102 cm), near-perpendicular (R_{tan} = 35 cm), and intermediate (R_{tan} = 82 cm). The large neutral flux at the intermediate viewing angle corresponds to particles whose banana tips lie near the resonance layer and whose orbit carries them to the high-neutral-density region in the edge of the plasma.

Charge-exchange measurements during H-minority heating show an even stronger pitch-angle anisotropy and more energetic tail than the ^{3}He measurements in Fig. 17. This can be explained by the higher collision frequency of ^{3}He, and this helps explain why ^{3}He-minority heating, is more efficient at heating the bulk plasma than H-minority heating since the less energetic ^{3}He tail transfers a larger percentage of its energy to ions instead of electrons and suffers less from fast-ion losses due to unconfined orbits.

Spectroscopy[12-20]

Tokamak plasmas generally contain neutral hydrogen far in excess of what would be appropriate in coronal ionization equilibrium at the prevailing electron temperature. This is especially true during neutral (hydrogen) beam heating of the plasma, where the neutral hydrogen density may be augmented by several orders of magnitude in the path of the beam. Among other effects, this hydrogen will interact in near-resonance with various impurity ions, giving rise to prompt radiation between highly excited Rydberg levels of the ions. The study of the space- and time-dependence relative to the beam injection can thus provide valuable information both on the spatial dependence of fully stripped ions and the behavior of the beam, information on which is not directly available by any other means. In addition, such measurements can provide spatial dependence of ion temperatures from Doppler profiles and other spectroscopic diagnostics. Measurements of this type have been performed in the ORMAK, TM-4, ISX-B and PDX (Poloidal Divertor Experiment) tokamaks, mostly on OVIII and CVI radiation in the vacuum-ultraviolet wavelength range.

However, the charge-exchange process also causes radiation by these ions at wavelengths above the air cutoff at 8000 Å. Although the radiation is weaker, this could be made up by the greater versatility of the instruments at these wavelengths. The OVIII radiation at 2976 Å ($n = 8 \rightarrow 7$ transition) and CVI at 3434 Å ($7 \rightarrow 6$) and 5291 Å ($8 \rightarrow 7$) was indeed observed in PLT discharges and applied to the measurement of central ion temperature and of the neutral-beam profile.

Also observed were radiation from the highly excited levels of AlXI and of ScXIX following charge-exchange of beam hydrogen and the corresponding helium-like ions, AlXII and ScXX, with aluminum or scandium injected by the laser-ablation technique during the hydrogen-beam heating.

These observations of charge-exchange-related radiations between highly excited levels are particularly applicable to conditions of high neutral hydrogen density, such as exist in neutral-beam heating, and fairly high-ion density of elements such as carbon and oxygen as well as other light elements, and are thus complementary rather than competitive with the near-ground-level excitations.

Radiation of the latter type were used in a comprehensive study of ion transport during neutral-beam heating. Scandium and molybdenum were injected into a variety of beam-plasma combinations, with the results indicating that the ion motion was very similar for both elements and independent of the heating neutral-beam direction as long as the amount of injected molybdenum or scandium was small enough not to cause appreciable perturbation of the temperature profile.

Also studied were the changes of impurity radiation during ICRF heating with different antennae configurations.

The spectra and atomic structure of various impurity and diagnostic elements continued from previous years, with substantial progress especially in the germanium and selenium spectra and in the configurations of phosphorus-like and silicon-like systems of elements up to molybdenum. Some measurements were also performed on silver ions in order to clear up some uncertainties of the observations of lighter elements.

References

[1]J. Hosea *et al.*, "PLT Ion Cyclotron Range of Frequencies Heating Program," in *Heating in Toroidal Plasmas* (Proc. 4th Int. Symp., Rome, 1984), edited by H. Knoepfel and E. Sindoni, Vol. *I*, International School of Plasma Physics and ENEA, Vienna (1984) 261.

[2]E. Mazzucato *et al.*, "Ion Cyclotron Heating Experiments in PLT," in *Plasma Physics and Controlled Nuclear Fusion Research 1984* (Proc. 10th Int. Conf., London, 1984), Vol. *I*, IAEA, Vienna (1985) 433.

[3]R. Motley, *et al.*, "Lower Hybrid Current Ramp-Up in the PLT Tokamak," in *Plasma Physics and Controlled Nuclear Fusion Research 1984* (Proc. 10th Int. Conf., London, 1984), Vol. *I*, IAEA, Vienna (1985) 473.

[4]T.K. Chu *et al.*, "Current Ramp-Up and Plasma Formation in the PLT Tokamak by Lower Hybrid Waves," in *Heating in Toroidal Plasmas* (Proc. 4th Int. Symp., Rome, 1984), edited by H. Knoepfel and E. Sindoni, Vol. *I*, International School of Plasma Physics and ENEA, Vienna (1984) 571.

[5]C.F.F. Karney, N.J. Fisch, and F.C. Jobes, "Comparison of the Theory and Practice of RF Current Drive," Princeton University Plasma Physics Laboratory Report PPPL-2152 (1984) 12 pp; to be published in Phys. Rev. A (Rapid Communications).

[6]S.A. Cohen *et al.*, "The PLT Rotating Pumped Limiter," J. of Nucl. Mater., *128&129* (1984) 430.

[7]S.A. Cohen *et al.*, "Plasma-Materials Interactions During RF Experiments in Tokamaks," J. Nucl. Mater. *128&129* (1984) 280.

[8]D.M. Manos *et al.*, "Studies of the Edge Plasma of RF Heated PLT Discharges," J. Nucl. Mater. *129* (1984) 319.

[9]W.R. Wampler and S.A. Cohen, "Energetic Neutral Particles Behind the PLT Pumped Limiter," Nucl. Fusion *25* (1985) 771.

[10]W.W. Heidbrink and J.D. Strachan, "Tokamak Ion Temperature and Poloidal Field Diagnostics Using 3 MeV Protons," Rev. Sci. Instrum. *56* (1985) 501.

[11]W.W. Heidbrink, "Tokamak Diagnostics Using Fusion Products," Ph.D. Thesis, Princeton University, June 1984.

[12]C.H. Skinner *et al.*, "Direct Spectroscopic Observation of Charge-Exchange Recombination of Medium-Z Elements in the PLT Tokamak," Phys. Rev. Lett. *53* (1984) 458.

[13]S. Suckewer *et al.*, "Observation of Lines Above 2000 Å in OVIII and CVI in the Princeton Large Torus Due to Charge-Exchange Processes: Diagnostic Applications," Appl. Phys. Lett. *45* (1984) 236.

[14]B. Denne, E. Hinnov, S. Cohen, and J. Timberlake, "The Ground Configuration of Highly Ionized Silver," to be published in Phys. Rev. A.

[15]A. Compant La Fontaine *et al.*, "Q = 1 Magnetohydro-Dynamic Activity in PLT Studied with Aluminum Impurity Injection as a Diagnostic Tool," submitted to J. of Plasma Phy.

[16]B. Denne, E. Hinnov, S. Suckewer, and J. Timberlake, "On the Ground Configuration of Phosphorus Sequence from Copper to Molybdenum," J. Opt. Soc. Am. *B1* (1984) 296.

[17]L.J. Curtis, J. Reader, S. Goldsmith, B. Denne, and E. Hinnov, "Empirical Evaluation of the $4s^24p\ ^2P$ Intervals in the Isoelectronic Sequence From Rb^{+6} to In^{18+}," Phys. Rev. *A29* (1984) 2248.

[18]S. Suckewer *et al.*, "Ion Transport Studies on the PLT Tokamak During Neutral Beam Injection," Nucl. Fusion *24* (1984) 815.

[19]B. Denne and E. Hinnov, "Intercombination Lines of AlVIII, AlIX, and AlX Ions," Phys. Rev. *A29* (1984) 3442.

[20]E. Meservey *et al.*, "Conductivity and Transport in Neon-Deuterium Discharges in the PLT Tokamak," Nucl. Fusion *24* (1984) 3.

PRINCETON BETA EXPERIMENT

MAJOR ACTIVITIES

The Princeton Beta Experiment (PBX) is a project with the broad goal of producing plasmas with β values well beyond those attained in conventional tokamaks. Beta is a measure of the heat content of the plasma relative to the confining magnetic field strength, and it is one of the important parameters that determine the economic feasibility of fusion reactors. Several ideal MHD instabilities that limit plasma heating must be overcome in order to produce high-β plasmas. This would be necessary even if the plasma were to become so hot and electrically well-conducting that the resistive instabilities common to present tokamaks would all vanish.

The ballooning instability is a short-wavelength mode, mostly internal to the plasma, that is driven unstable by the plasma pressure. This instability is theoretically expected to limit β: the maximum attainable β is the upper limit of the so-called first region of stability. All tokamaks, so far, have operated in this region. A conventional approach to increasing β in the first region has been to keep the plasma minor radius from being too small relative to the major radius.

The PBX tokamak will instead attempt to overcome the ballooning instability by unconventional cross-sectional shaping: the plasma cross section is indented on its inboard side so that its shape is like that of a kidney bean. As the degree of indentation increases beyond a certain critical value, the β limit set by the ballooning instability becomes very large, or disappears altogether. To reach this so-called second region of stability is an ultimate goal of the PBX Project. All other instabilities that may set a limit lower than that of the ballooning mode must also be overcome to reach the second stability region.

The fishbone instability is another pressure-driven mode internal to the plasma but with a long wavelength. It has a strong tendency to expel energetic plasma-heating ions from the plasma and thus to limit the efficacy of neutral-beam injection (NBI) heating. This instability was found to limit plasma heating in the PDX (Poloidal Divertor Experiment) tokamak. Fortunately, the theory predicts that bean shaping will help suppress this instability by strengthening the MHD stability properties of internal flux surfaces where the instability originates.

The external kink instability is a long-wavelength mode driven primarily by the plasma current. A conducting shell tightly surrounding the plasma would help stabilize this instability, but it would also severely limit the operational flexibility. The PBX, in its initial configuration, has opted to preserve the flexibility in order to establish the ability to form and maintain a bean-shaped plasma.

One instability which arises as a consequence of the plasma cross-sectional shaping is the vertical instability. The very force that produces the indentation and elongation by pulling and pushing various parts of the plasma also cause it to be vertically unstable. This positional instability must also be brought under control for the PBX tokamak to succeed.

In addition to helping suppress the various instabilities, cross-sectional shaping has the added benefit of enhancing the current-carrying capacity of the plasma and reaping any advantages that may be associated with a large plasma current. For example, higher current increases the β limit in the first region of stability for plasmas of any shape. Since the energy confinement time of NBI-heated plasmas in most tokamaks is proportional to the plasma current, the higher current-carrying capacity leads to a better confinement time.

In order to test these theoretical expectations within a relatively short time and at a modest cost, the PBX device was created by reconfiguring its predecessor device, the PDX tokamak. The reconfiguration primarily involved rearrangement of internal coils and reorientation of two of the four neutral beamlines from near perpendicular to tangential direction. The other two beamlines remained in the near-perpendicular direction. The first six months of FY84 were spent completing the conversion of PDX to PBX which had begun in the previous fiscal year. A poloidal cross section of the device is shown schematically in Fig. 1 and a photographic view of the interior in Fig. 2.

On April 6, 1984 the first plasma was produced, and on May 8th NBI heating experiments were commenced. On September 14th PBX achieved a volume-averaged toroidal β value ($<\beta_t>$) of 5.3%—a record to date for major tokamaks. At the end of October PBX was shut down for two months for internal hardware repair and new diagnostics installation. Activities during the month of October are included in this report for the sake of continuity. Over this seven-month period PBX operated on 56 days including 28 days with NBI-heating.

The experimental program during this period first focused on learning to produce and sustain a bean-shaped plasma in a controlled manner. The effort then shifted toward producing plasmas with high $<\beta_t>$. Studies of how bean shaping influenced the greatest achievable current density, $<\beta_t>$, and the fishbone

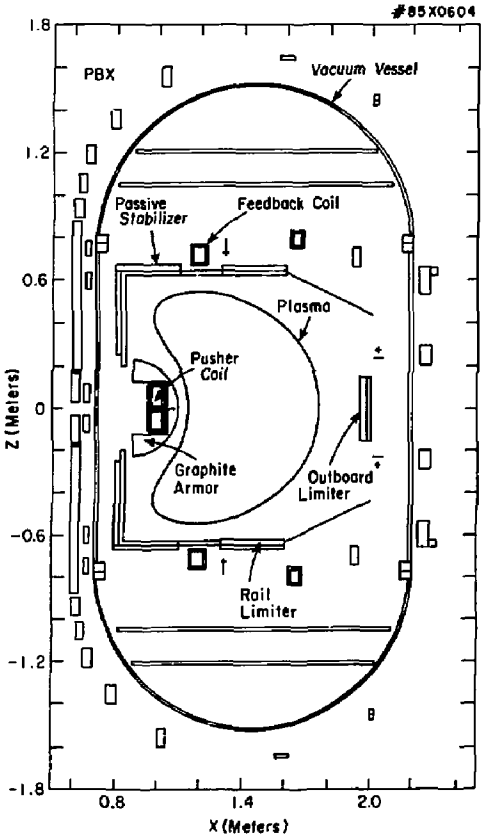

Fig. 1. Schematic diagram of a poloidal cross section of the PBX showing several major components. The tokamak center is to the left of the figure.

Fig. 2. Photograph of the interior of the PBX from a tangential view. Semicircular graphite armor (b) protects the pusher coil (a) from direct contact with the plasma. The upper and lower stabilizer plates (c) are each protected by four graphite rail limiters. One is visible on the upper stabilizer plates. The cylindrical stabilizers (c) on the inboard side are visible at left. The upper and lower active feedback coils (d) are visible between the inner and outer passive stabilizer plates.

instability followed. The H-mode (high-mode)—a regime of high energy confinement time—and fueling by pellet injection were also investigated briefly.

Interim results were reported at the 10th International Conference on Plasma Physics and Controlled Nuclear Fusion Research (London).[1] Many introductory materials on the topics covered in this article can be found in earlier Princeton University Plasma Physics Laboratory Annual Reports.[2] Materials on the PBX device can be found in the PBX section of the 1983 Annual Report and in the theory section of the 1982 report. The fishbone instability is covered in the PDX and theory sections of the 1982 report, and the H-mode is discussed in the PDX section of the 1983 report. Theoretical and engineering aspects of PBX are also described in detail in the project proposal.[3]

PLASMA CROSS-SECTIONAL SHAPING

The PBX is the first tokamak designed to produce a plasma with the unconventional bean-shaped cross section. The initial experimental program therefore addressed the issues of whether a bean-shaped plasma with a desired degree of indentation can be produced and maintained, and what parameters are important in determining the degree of indentation.

The PBX operates routinely with the magnetic decay index (n-index) around -2.0, and the plasma is subject to a strong vertical (axisymmetric) instability. Passive stabilizers and a modest active feedback amplifier act to stabilize this vertical instability. This stabilization proved adequate both in the plasma start-up phase and during the main discharge phase under moderate conditions. A TV photograph of a stable bean-shaped plasma is shown

in Fig. 3. Under more severe conditions, e.g., at very high indentation or during high-power NBI heating, loss of the plasma through the vertical instability has been observed. In some cases the instability appeared to be the cause of the loss, while in other cases the instability appeared to be the terminal phase of the plasma which had disrupted and whose current channel had shrunken.

For the geometrical arrangement of shaping coils in PBX, the radial plasma position and the strength of the indentation field (or "pusher coil") current (I_{IF}) in relation to the plasma current (I_p) are important elements that determine the degree of indentation. It is possible to maintain a well-indented plasma in steady-state for over 400 msec, nearly one-half the entire discharge length, by controlling these quantities with feedback systems. However, fine control of the precise shape and location of the separatrix surfaces is not possible with the present PBX configuration because all of the shaping coils are powered by a single generator, and their currents are not individually adjustable.

Further improvement in the indentation comes from the plasma current profile: a broad current profile results in a more bean-shaped plasma. In such a plasma both the plasma outer boundary and the inner flux surfaces are well elongated and indented. In this sense, good MHD properties of such shaped surfaces are strengthened in a plasma with a broad current profile.

The desired broad current profile is realized in PBX partly by operating at low q values at the plasma edge (high I_p at low toroidal magnetic field B_t). The dependence of indentation on the edge q value (q_{edge}) is shown in Fig. 4. The q_{edge}, evaluated on the surface enclosing 95% of the poloidal flux, was varied here by changing B_t while holding all other parameters the same. The data were taken in the steady-state phase of the discharges. A clear trend toward higher indentation is seen in this figure as q_{edge} becomes smaller and the current profile becomes broader.

The broad current profile is obtained also by ramping up I_p rapidly (high dI_p/dt) to take advantage of the skin-current effect, i.e., time delay associated

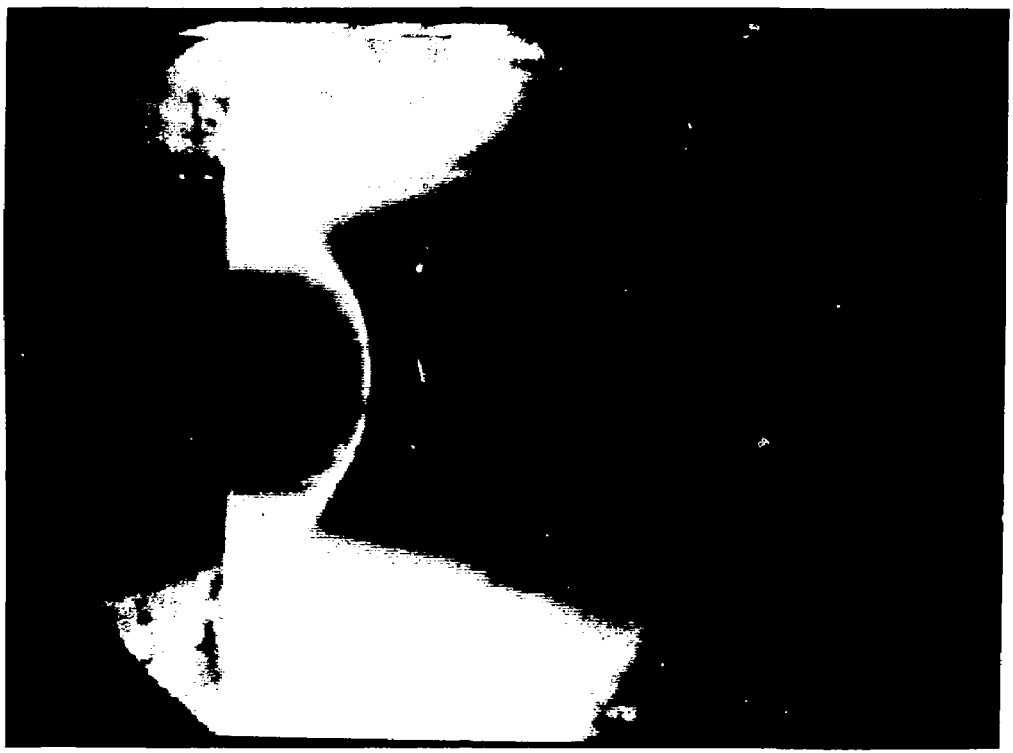

Fig. 3. A TV picture of a stable bean-shaped plasma from a tangential view. The light kidney-bean-shaped area is the image of the plasma. The inner passive stabilizer cylinders and the pusher coil are visible at left. In this L-mode (low-mode) discharge the outline of the plasma, especially on the outboard side (at right), appears fuzzy. The color photograph on the front cover of this report is an example of an H-mode (high-mode) discharge. The sharply defined outline reflects the steeper gradient of plasma parameters near the edge. (84X2160)

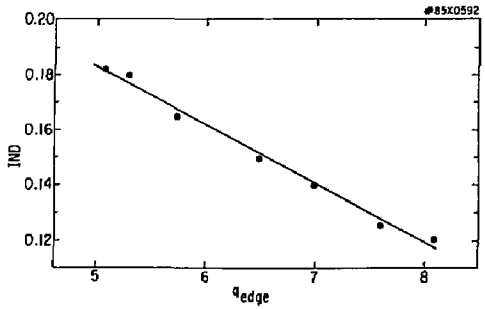

Fig. 4. Variation of indentation as a function of the q value at the plasma edge (q_{edge}). The q_{edge} was varied by changing B_t while holding all other parameters the same. As the q_{edge} becomes smaller and the plasma current profile broadens, the indentation becomes deeper.

with the diffusion of the current from the plasma edge to the center. The resultant current profile is broader than one expected from the classical resistivity based upon the electron temperature profile. A comparison between the toroidal current profile produced in PBX using the skin-current effect and a typical profile in PDX, both as functions of major radius, is shown in Fig. 5(a). The same comparison as a function of the normalized flux $\tilde{\psi} \equiv (\psi-\psi_o)/(\psi_{edge}-\psi_o)$, where ψ_o and ψ_{edge} are, respectively, values of the poloidal magnetic flux function ψ at the magnetic axis and plasma edge, is shown in Fig. 5(b) along with the profile used in the PBX project proposal.[3] The profiles obtained to date in PBX are much broader than those of PDX but are not quite as broad as anticipated.

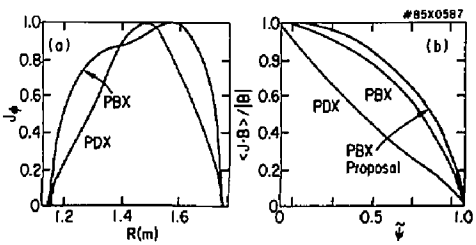

Fig. 5. Plasma current profile comparisons. (a) Plasma current profiles of PBX and PDX as a function of the major radius. (b) The same comparison as a function of the normalized poloidal flux function together with the plasma current profile anticipated in the PBX Project proposal. The magnetic axis is at the left and the plasma edge at the right in this graph. The PBX skin-effect current profile shown here is much broader than a typical PDX profile but not quite as broad as the PBX proposal.

MODE OF OPERATION

The present PBX design accommodates a wide range of operating modes in order to evaluate their relative advantages. For example, nearly circular and "D"-shaped plasmas, which may be needed as transitional states before reaching the final bean shape, can also be produced. This means, however, lack of optimization under some circumstances. For example, a tightly fitting conducting shell on the plasma outboard side is theoretically expected to help suppress the external kink mode, but it has not been employed to allow for a wider range of plasma shape and location.

Two different methods to form an indented plasma are used: the first method is to initially form a fully developed circular plasma and then slowly indent it by increasing I_{IF}, and the second method is to elongate and indent the plasma during the start-up phase. The latter process is subject to greater vertical instability because the passive stabilizers are less effective for the small current channel of start-up plasmas. The PBX experiments have, nevertheless, demonstrated successfully both methods of forming indented plasmas.

Either a material surface or magnetic separatrix can define the plasma outline in the PBX tokamak. In limiter plasma operation, graphite limiters on the inboard or outboard midplane, or graphite limiters on the top and bottom passive stabilizers define the plasma boundary. In separatrix operation, the absence of any material limiting surfaces allows the so-called H-mode—a regime of improved energy confinement time.

Table I summarizes the range of parameters of PBX operation to date. Many parameters are close to their design values. The plasma current, for example, reached 560 kA in comparison with the design value of 600 kA. The indentation reached 0.22 in both ohmically and NBI-heated plasmas, somewhat below the design value of 0.30. The difference has most likely arisen because the plasma current profile was not quite as broad as originally hoped for. On the other hand, the elongation reached routinely its maximum value of 1.8, a high value for tokamaks. The indentation and strong elongation of PBX plasmas facilitate an increased current-carrying capacity. This, in turn, leads to an increased β limit and higher energy confinement within the first region of stability.

An alternative way of expressing the enhanced current-carrying capacity is in terms of the equivalent cylindrical q value, defined as $q_{cyl} \equiv 2\pi \langle a\rangle^2 B_t(0)/(\mu_o R_p I_p)$, where R_p is the plasma major radius, $B_t(0)$ is the toroidal magnetic field at the geometrical axis, and $\langle a\rangle$ is the radius of a circular plasma that would have the same cross-sectional area as the indented plasma. For PBX q_{cyl} reached as low as 1.04, whereas q_{edge} remained equal to or above 3.0. While indentation and elongation, and their effect on the lowest achievable q_{cyl}, are closely coupled for PBX, no other major tokamak has attained this low value of q_{cyl}, even at elongations comparable to those of PBX.

The operating range in terms of the dimensionless parameters, β_p and $\langle\beta_t\rangle$, is shown in Fig. 6. The β_p is the β value based upon the poloidal component

Table I. Definition and Range of Parameters Covered to Date by the PBX Tokamak.

Parameter	Range	Definition
$B_t(0)$	0.7-1.4 T	Toroidal magnetic field at geometrical center
I_p	≤560 kA	Plasma current
dI_p/dt	≤1.5 MA/sec	Rate of rise of plasma current
R_p	1.43-1.55 m	Major radius
a_{mid}	0.30-0.45 m	Midplane half-width
P_b	≤5.5 MW	Injected neutral-beam power
q_{edge}	≥3.0	Edge q-value (on 95% flux surface)
q_{cyl}	≥1.04	Equivalent cylindrical q value
n-index	≥-2.5	Magnetic field decay index
i	≤0.22	Indentation
κ	≤1.8	Elongation
δ	≤0.3	Triangularity
$<\beta_t>$	≤5.3%	Volume-averaged toroidal β
$\beta_t(0)$	≤16.2%	On-axis toroidal β
β_c	≤2.4	Critical β [$= \mu_o I_p / a_{mid} B_t(0)$]
β_N	≤2.5	Normalized β ($= <\beta_t> / \beta_c$)
β_p	≤1.5	Poloidal β

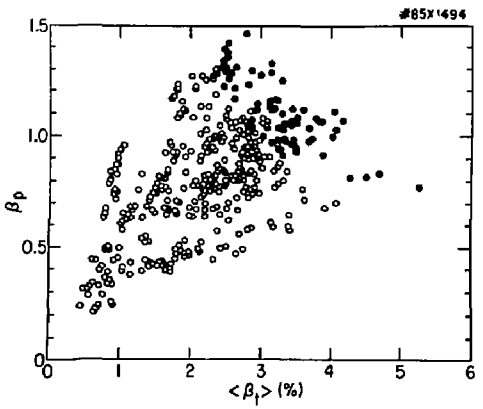

Fig. 6. Operating range of PBX in terms of dimensionless parameters β_p and $<\beta_t>$. The data points fall roughly within an area of triangular shape. The data around the lower right-hand side of the triangle are near the low-q (high I_p, low B_t) disruption limit. The data around the upper left-hand side are near the low-I_p heating limit. The data around the upper right-hand side are near the boundary of the first region of stability. The data points with $\beta_N \geq 2.0$ are identified by a different symbol (solid) and they all lie in the vicinity of the upper right-hand limit.

of the magnetic field. The data points fall roughly within a triangular region. The data points around the lower right-hand side of the triangle are near the low-q (high I_p, low B_t) disruption limit. The points around the upper left-hand side are near the low-I_p heating limit: as I_p is reduced, hot heating ions will increasingly be lost through large unconfined orbits. The data around the remaining upper right-hand side are near the boundary of the first region of stability. Discharges with the normalized β_N (see below) greater than 2.0 are indicated by the solid dots in the figure. Not all of these boundaries have been seriously tested yet because of the relatively limited period that PBX has been in operation. The region of operable parameter space is likely to be extended in the future. In particular, the ultimate goal of the PBX—to enter the second region of stability—means breaking through the upper right-hand side of the triangle.

BETA SCALING

As fusion research enters into a more technologically oriented phase, the issue of attaining higher β values has become increasingly more important. The volume-averaged toroidal β value is a dimensionless ratio of the plasma pressure to the confining toroidal magnetic field pressure. The generation of toroidal field is a costly element of the reactor, and

the magnitude of $\langle\beta_t\rangle$ has a direct impact on the economic feasibility of the fusion power generation.

Much experimental data goes into the determination of $\langle\beta_t\rangle$. They are poloidal flux (measured by flux loops), displaced toroidal flux (by diamagnetic loop), coil and plasma currents (by Rogowski coils and shunts), central ion temperature (by charge-exchange recombination spectroscopy), impurity levels (by spectroscopy), and electron temperature and density profiles (by TV Thomson scattering). The $\langle\beta_t\rangle$ is calculated using some or all of the above data by several different methods. A fast between-shot moments code called SURFAS (see below) calculates $\langle\beta_t\rangle$ for the majority of discharges. A full MHD equilibrium code (Grad-Shafranov equation solver) is also used for selected shots. In computing $\langle\beta_t\rangle$ both the plasma and magnetic pressures were averaged over the plasma volume rather than choosing the magnetic pressure at a reference point (e.g., magnetic axis) as has been sometimes done.

One example of a $\langle\beta_t\rangle$ determination is summarized in Fig. 7. The central graph (a) shows the time evolution of $\langle\beta_t\rangle$, β_p, and $\Lambda \equiv \ell_i/2 + \beta_p$ computed by the SURFAS code, where ℓ_i is the dimensionless internal inductance. The inset (b) shows the electron temperature and density profiles measured at one time point two-thirds of the way into the NBI phase of the discharge. Based upon these profiles and the diamagnetic measurement and other kinetic data, the full MHD equilibrium code calculation also determined $\langle\beta_t\rangle$. The two calculated values at this time point agree well with each other as indicated in the graph. The full MHD calculation was repeated at a later time point near the disruptive end of the discharge. The profiles were not measured at this point and were assumed unchanged from the previous time point. The inset (c) shows the central ion temperature variation, and the inset (d) compares the toroidal flux measured by the diamagnetic diagnostic with that computed by SURFAS.

The peak volume-averaged toroidal β value for the discharge shown in Fig. 7 achieved a value of $\langle\beta_t\rangle$ = 5.3% according to the SURFAS calculations. The on-axis $\beta_t(0)$ was 16.2% and β_p was 0.77. The

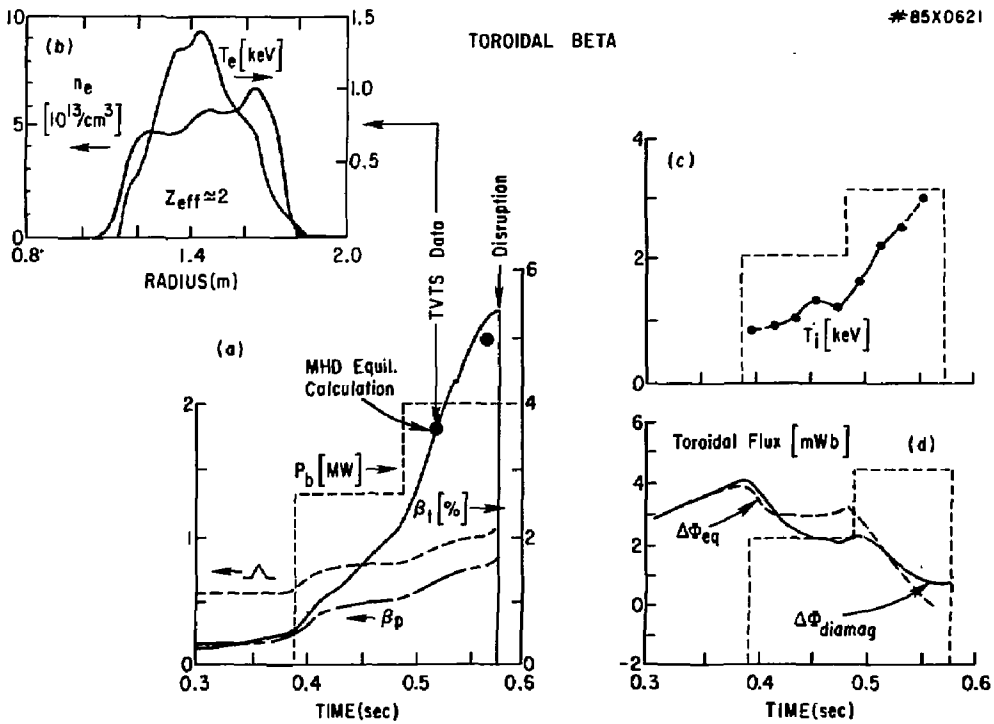

Fig. 7. Summary of the data and analysis of the highest $\langle\beta_t\rangle$ discharge. (a) Time variations of $\langle\beta_t\rangle$, β_p, and $\Lambda \equiv \ell_i/2 + \beta_p$ computed by the SURFAS code. The $\langle\beta_t\rangle$ values computed by the full MHD equilibrium code are also shown. (b) The TV Thomson scattering (TVTS) profiles of the electron temperature [$T_e(R)$] and density [$n_e(R)$] at one time point. (c) The central ion temperature variation with time. (d) Time variation of the displaced toroidal flux measured by the diamagnetic diagnostics and computed by the SURFAS code. The highest $\langle\beta_t\rangle$ reached in this discharge is 5.3%—a record for major tokamaks. The on-axis $\beta_t(0)$ reached 16.2%.

indentation was 0.19 and total heating power (NBI plus ohmic) was 4.5 MW.

Concerted efforts to raise $\langle\beta_t\rangle$ by many tokamak installations around the world produced a striking result[4]: the highest achievable $\langle\beta_t\rangle$ is bounded by a critical value determined by some combination of plasma parameters. Theorists have proposed that this so-called β scaling reflects a limitation on $\langle\beta_t\rangle$ caused by ideal MHD instabilities. The limit is the boundary of the first region of stability when the underlying instability is the ballooning mode. The limit set by the external kink mode may be lower or higher depending upon the proximity of the plasma to a conducting shell.

Many researchers have conducted numerical experiments to determine the parametric dependence of the critical β. One formula obtained by Troyon *et al.*[5] for the external kink instability has a particular appeal in its simplicity. It states that the maximum achievable $\langle\beta_t\rangle$ depends upon the plasma current (I_p), toroidal field (B_t), and the plasma size (a) in accordance with the formula: $\langle\beta_t\rangle \leq C\mu_o I_p/(aB_t)$, where $\langle\beta_t\rangle$ is in percent and C is a numerical constant. Troyon and Gruber[5] chose *a* to be the half-width along the midplane (a_{mid}) and B_t to be the toroidal field at the geometrical axis [$B_t(0)$], and they determined C to be between 2.0 and 2.5.

In order to examine the β scaling for the PBX tokamak, $\langle\beta_t\rangle$ is plotted, in Fig. 8, against $\beta_c \equiv \mu_o I_p/a_{mid}B_t(0)$. The figure also shows the data from the predecessor PDX tokamak for comparison. Both groups of data essentially fall below the line $\langle\beta_t\rangle = 2.5\beta_c$, i.e., C = 2.5. The $\langle\beta_t\rangle$ near this line was usually limited by the disruptive termination of the discharge. The ballooning-mode limit is believed to lie higher than this line (i.e., C > 2.5). Neither the ballooning mode nor the external kink mode, however, has been positively identified to date. Determining the underlying physical mechanism of the disruptive β limit in PBX will be the central research subject in the coming months.

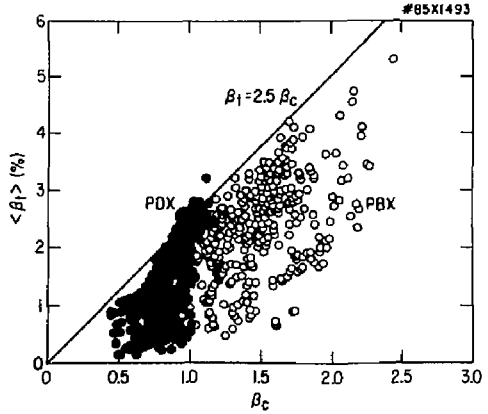

Fig. 8. Plot of $\langle\beta_t\rangle$ vs $\beta_c \equiv \mu_o I_p/a_{mid}B_t(0)$ for the PBX and PDX tokamaks. The data for both groups are essentially bounded by the Troyon and Gruber[5] limit $\langle\beta_t\rangle \leq 2.5\beta_c$ and are in the first region of stability. However, the operating range within this region has been doubled in PBX in relation to PDX.

The right-hand edge of the PBX data group in Fig. 8 at $\beta_c \approx 2.4$ is greatly extended from that of PDX at $\beta_c \approx 1.2$. The nearly twofold increase in maximum attainable β_c reflects the enhanced current-carrying capability of PBX plasmas. The PBX tokamak has thus not yet demonstrated access to the second region of stability, but has significantly extended the operating range in terms of β_c.

Discharges in PBX with high β_c were mostly highly indented plasmas and all had a high rate of rise of the plasma current to take advantage of the skin current in generating a broad current profile. Some high-$\langle\beta_t\rangle$ plasmas also had pellet injection to further influence the plasma profiles. This promising alternative, which was studied briefly during this reporting period, will be one of the major topics in the coming year.

FISHBONE INSTABILITY

The fishbone instability is an MHD activity that alternates between rapid growth and quenching in repetitive bursts of a few millisecond duration. Loss of fast ions and a drop in neutron production occur coincident with each burst. The instability was first discovered in the PDX tokamak.[6] The fast-ion loss due to the instability was believed to be the cause of reduced heating efficiency in PDX as the NBI power was increased. The current theoretical understanding is that the fishbone instability is the pressure-driven ideal internal kink mode, and that the triangularity of inner magnetic surfaces in a bean-shaped plasma helps suppress the instability.

Observation to date indicates that the fishbone instability is generally much less pronounced in PBX than in PDX and, in fact, is nearly absent in some cases. The Mirnov coil signal, which measures fluctuations in the poloidal magnetic field, is shown in Fig. 9 (top) for a PBX discharge with the fishbone instability. Many bursts of oscillations, mostly due to the fishbone instability but also partly due to the sawtooth relaxation, can be seen in the figure. A drop in neutron emission associated with each of the fishbone bursts and sawtooth relaxations is shown in Fig. 9 (bottom). This is an example of bean-shaped plasmas with a relatively narrow current profile, a modest indentation ($i \approx 0.12$), medium $\langle\beta_t\rangle \leq 3.7\%$, and a moderate plasma current rise rate ($dI_p/dt \approx 0.9$ MA/sec). It represents a class of discharges with fishbone activity which is large by PBX standards. The Mirnov coil and neutron emission signals shown, respectively, in Fig. 10 (top) and 10 (bottom) are for a PBX discharge with a broad current profile, a strong indentation ($i \approx 0.19$), high $\langle\beta_t\rangle \leq 5.3\%$, and a large plasma current rise rate ($dI_p/dt \approx 1.5$ MA/sec). The discharge is nearly free of the fishbone instability in spite of higher $\langle\beta_t\rangle$. Both discharges were heated

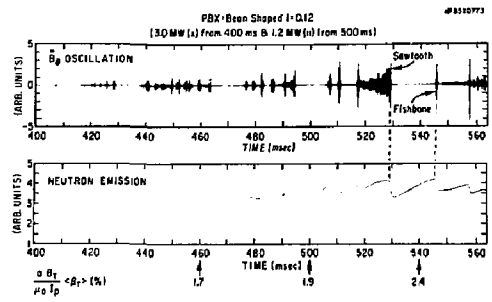

Fig. 9. The fishbone instability and its effects on the neutron emission in a discharge with narrow current profile in PBX. (Top) Fluctuations in the poloidal magnetic field measured by a Mirnov coil showing bursts associated with the fishbone instability and the sawtooth relaxation. (Bottom) Neutron emission rate showing a drop at each of the fishbone bursts as well as the sawtooth relaxations.

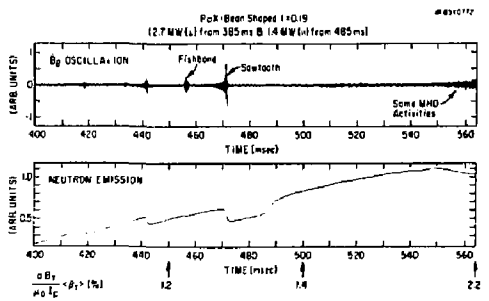

Fig. 10. The fishbone instability and its effects on the neutron emission in a discharge with broad current profile in PBX. (Top) Fluctuations in the poloidal magnetic field measured by a Mirnov coil showing bursts associated mostly with sawtooth relaxation. Only one fishbone burst is recognizable in this discharge. (Bottom) Neutron emission rate showing a drop at the sawtooth relaxation.

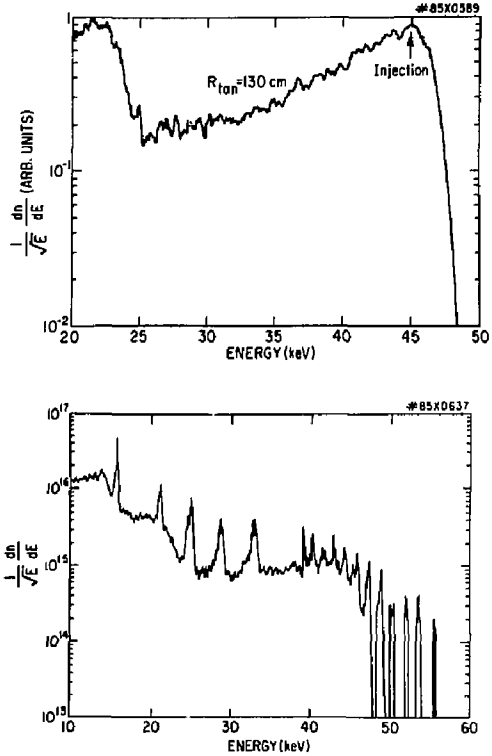

Fig. 11. Fast-ion slowing-down spectra measured by charge-exchange diagnostics. (a) Smooth classical slowing-down spectrum for a PBX discharge. (b) PDX spectrum with spikes corresponding to fast-ion loss at the time of each fishbone burst.

with two perpendicular beams and one tangential beam at a comparable power level.

The fast-ion loss is much less important in PBX than in PDX, reflecting in part the lower level of the fishbone instability. A slowing-down spectrum of fast ions measured by the electrostatic charge-exchange analyzer of the Fast Ion Diagnostic Experiment (FIDE) is shown in Fig. 11(a) for a high-$\langle\beta_t\rangle$ PBX plasma. Three deuterium beams (two perpendicular and one tangential) with a total power of 4.0 MW were injected into a hydrogen plasma with I_p = 516 kA and $B_t(0)$ = 0.86 T. The slowing-down spectrum is smooth and there is no evidence of beam-ion loss due to fishbone activity. A PDX slowing-down spectrum with a spiky structure is shown in Fig. 11(b). Three deuterium beams (all perpendicular) were injected into a hydrogen plasma with I_p = 400 kA and $B_t(0)$ = 1.2 T. The slowing-down spectra were obtained by varying the analyzer detection energy in time so that the fast-ion loss appears as a spike in the charge-exchange signal at each fishbone burst.

The severity of the fishbone instability can be characterized in a semiquantitative manner by noting how frequently the bursts occur and how great the drop in neutron emission associated with them: the neutron loss rate may be defined in terms of quantities defined in Fig. 9 (bottom) as $\nu_{loss} \equiv (\Delta I/I)/T$. The reciprocal of ν_{loss} is a qualitative estimate of the fast-ion confinement time. The ν_{loss} in PBX and PDX is plotted in Fig. 12 against the normalized $\beta_N \equiv \langle\beta_t\rangle/\beta_c$. The reduction in neutron loss in PBX relative to PDX, as seen in the figure, is due in part to the fact that two of the PBX neutral beams inject in the tangential direction. In PDX all four beams injected in the near-perpendicular direction. According to the theory, it is the perpendicularly injected particles which are affected most by the fishbone instability: therefore, some reduction of fast-ion loss

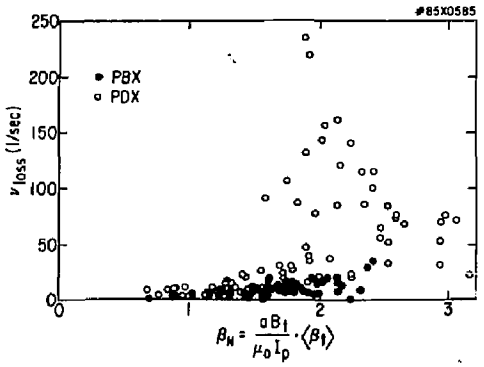

Fig. 12. Neutron loss rate ν_{loss} as a function of the normalized β_N for PBX and PDX. The reciprocal of ν_{loss} is a qualitative estimate of the fast-ion confinement time. The PDX data are plotted against slightly different abscissa $\beta_N(q_{shaf}/q_{cyl})$, where q_{shaf} is the true MHD q value at the plasma edge. However, the ratio q_{shaf}/q_{cyl} is not far from unity for all PDX data for the purpose of this comparison.

is expected merely from the reorientation of two of the four PBX beamlines. However, more detailed comparisons between PBX and PDX with just the two perpendicular beams appear to indicate that beam-shaping is also responsible for reducing fast-ion loss associated with the fishbone instability.

H-MODE OPERATION

The separatrix-defined plasma in PBX can undergo transition into the H-mode when the neutral-beam power (P_b) is above a threshold value, as observed in many other tokamaks. The H-mode plasma is of interest to the PBX project in three ways. First, its higher confinement time may help to raise $\langle\beta_t\rangle$ for a given NBI power. Second, rapid density build-up associated with the H-mode serves as an efficient fueling mechanism and also may help to raise the $\langle\beta_t\rangle$. Third, high electron temperature at the plasma edge can lead to a broader current profile needed for high indentation. Studies of the H-mode discharges in the PBX are, however, still preliminary.

The H-mode transition manifests itself in many different diagnostics. One of the more striking examples is the appearance of the plasma seen through the plasma TV: the outer edge becomes much more sharply defined as the plasma goes through the transition. The photograph in Fig. 3 shows a plasma before the H-mode transition (so-called L-mode) with diffuse outline, especially on the outboard side. The color photograph on the front cover of this report is the same plasma after the H-mode transition. The plasma outline is now sharply defined, possibly reflecting steep density and temperature gradients at the plasma edge.

The time variation of the H_α emission signal from the upper separatrix region is shown in Fig. 13(a) and the signal from the midplane region in Fig. 13(b). Both signals show a characteristic drop at the transition, but the separatrix signal appears to indicate repeated transitions back and forth between the L- and H-modes. Close tolerance between the separatrix and the rail limiters and lack of fine control of the separatrix position may be responsible for this behavior.

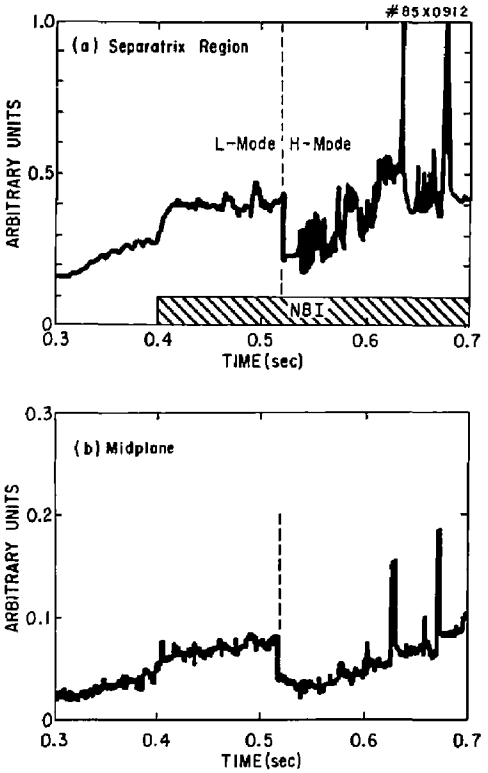

Fig. 13. Time variation of the H_α signals during the L- and H-mode from (a) the upper separatrix region and (b) the midplane region. The separatrix signal appears to indicate repeated transitions back and forth between the two modes.

An initial jump in the energy confinement up to 70% of the pretransition value can occur at the H-mode transition in PBX. However, it falls gradually back to the pretransition value in a few hundred milliseconds. (See the top right graph in Fig. 14). The errant separatrix location may in part be responsible for this degradation, and finer control of the separatrix is an important agenda item in the future experiments.

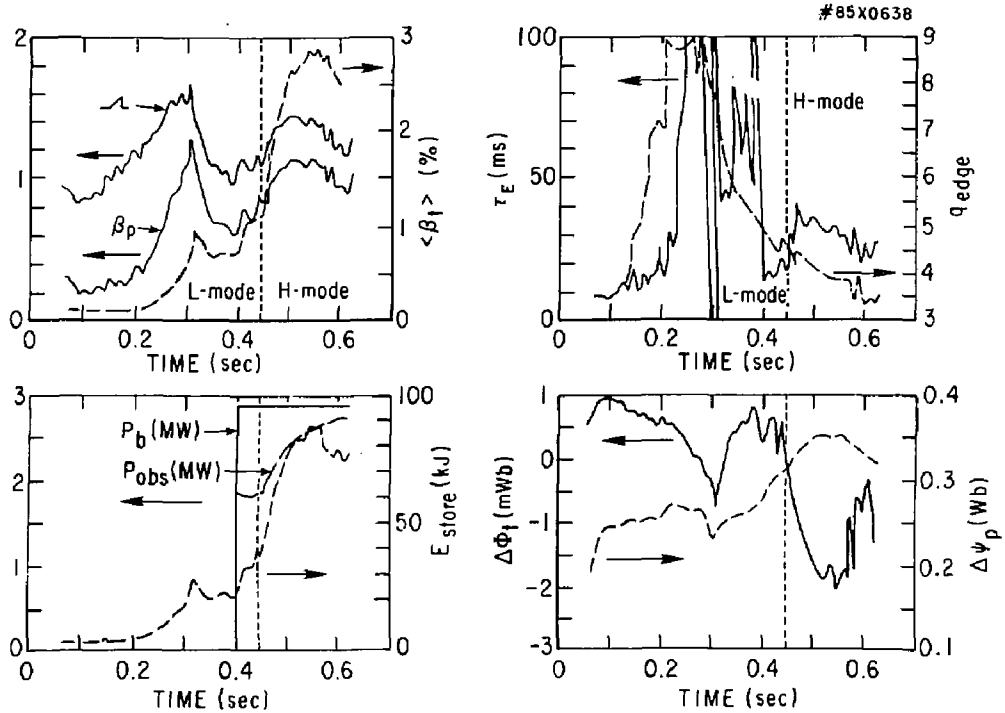

Fig. 14. A sample page of the multipage output of the SURFAS code for the same discharge shown in Fig. 13. Sharp breaks in curves at 300 msec and 400 msec were caused by initiation of inward radial motion of the plasma and onset of NBI heating, respectively. The discharge had an H-mode transition at about 445 msec and was terminated disruptively at about 625 msec. This example also shows a jump in the energy confinement time τ_E at the H-mode transition (top right graph).

DIAGNOSTIC DEVELOPMENT

Some new diagnostic techniques have been developed during this reporting period. They include a plasma TV system that enables visual observation of the plasma shape and a new ion temperature diagnostic.[7] The most important development from both the machine operational and plasma analysis standpoints is the SURFAS code. Plasma parameters, such as the plasma major and minor radii, q_{edge}, and ℓ_i, are readily obtainable for circular plasmas from geometrical and magnetic data. The β_p and $\langle\beta_t\rangle$ can also be easily calculated for circular plasmas from diamagnetic measurements. For bean-shaped plasmas all of these quantities are more intricately related to the plasma shape and are not as apparent as for circular plasmas.

The SURFAS code was developed to provide a quick between-shot analysis of these parameters. The code determines the shape of the plasma surface using measured magnetic data as boundary conditions, computes the magnetic field components on the surface and relates them to useful MHD and kinetic properties of the plasma. The reliability of this shorthand analysis was checked for selected discharges against the full MHD equilibrium code using the same set of boundary conditions and additional magnetic and kinetic data. The SURFAS analysis proved to be an indispensable tool for guiding the machine operation as well as for building a data base for a large number of discharges.

A sample page of this multipage SURFAS output is shown in Fig. 14 for the same discharge whose H_α signals are given in Fig. 13. Sharp breaks in curves at 300 msec and 400 msec were caused by initiation of inward radial motion of the plasma and onset of NBI heating, respectively. The discharge had an H-mode transition at about 445 msec and was terminated disruptively at about 625 msec.

A new technique to measure the ion temperature and plasma-rotation speed was also implemented during this reporting period. The technique relies on charge-exchange recombination of impurity ions with neutral particles of the heating beams, and it is

capable of measuring the radial profiles of these parameters. An example of the time variation of the central ion temperature is shown in Fig. 7(c).

References

[1]M. Okabayashi, P. Beiersdorfer, K. Bol, *et al.*, "Studies of Bean-Shaped Tokamaks and Beta Limits for Reactor Design," in *Plasma Physics and Controlled Nuclear Fusion Research 1984* (Proc. 10th Int. Conf., London, 1984), Vol. *I*, IAEA, Vienna (1985) 229.

[2]Princeton University Plasma Physics Laboratory Annual Report PPPL-Q-40 (October 1, 1981 to September 30, 1982) 52 and PPPL-Q-41 (October 1, 1982 to September 30, 1983) 54.

[3]K. Bol, M. Chance, R. Dewar, et al., "PBX: The Princeton Beta Experiment," Princeton University Plasma Physics Laboratory Report PPPL-2032 (1983) 120 pp.

[4]R.D. Stambaugh, R.W. Moore, L.C. Bernard, *et al.*, "Tests of Beta Limits as a Function of Plasma Shape in the Doublet III Device," in *Plasma Physics and Controlled Nuclear Fusion Research 1984* (Proc. 10th Int. Conf., London, 1984), Vol. *I*, IAEA, Vienna (1985) 217; M. Keilhacker, G. Fussmann, G. von Gierke, *et al.*, "Confinement and β-limit Studies in ASDEX H-mode Discharges," *ibid.*, 71; D.C. Robinson, N.R. Ainsworth, M.W. Alcock, *et al.*, "Limiting β Investigations at Low Collisionality," *ibid.*, 205.

[5]F. Troyon, R. Gruber, H. Saurenmann, *et al.*, "MHD Limits to Plasma Confinement," Plasma Physics and Controlled Fusion *26* (1984) 209; F. Troyon and R. Gruber, "A Semi-Empirical Scaling Law for the β-Limit in Tokamak," Ecole Polytechnique Fédérale de Lausanne Report LRP 239/84 (1984) 13 pp.

[6]K.M. McGuire, "Observation of Finite-β MHD Phenomena in Tokamaks," in *Plasma Physics* (Proc. Int. Conf., Lausanne, Switzerland, 1984), M.Q. Tran and O.J. Verbeek, Eds., Invited Papers Volume, Commission of the European Communities, Directorate General XII-Fusion Program, Brussels (1984) 123.

[7]K.P. Jaehnig *et al.*, "Charge Exchange Recombination Spectroscopy Measurements of Ion Temperature and Plasma Rotation in PBX," Rev. Sci. Instrum. *56* (1985) 865; R.J. Fonck, "Charge Exchange Recombination Spectroscopy as a Plasma Diagnostic Tool," Rev. Sci. Instrum. *56* (1985) 885.

S-1 SPHEROMAK

The spheromak, a type of compact toroid with an internal toroidal-field component created by currents within the plasma, does not require external toroidal-field coils, and therefore allows a simple wall and blanket topology. The primary objectives of the S-1 Spheromak experiment are to investigate confinement and MHD-stability properties of the spheromak configuration, while providing plasma equilibrium and stability by means of an external poloidal magnetic field and loose-fitting conducting walls. The formation scheme is based on inductive transfer of toroidal and poloidal magnetic fluxes from a flux core.[1]

If the two coil currents in the flux core are properly timed, spheromak configurations resembling the Taylor minimum-energy state are created, with major radii of 45-65 cm, minor radii of 30-50 cm, and toroidal plasma currents of 200-350 kA. The S-1 Spheromak device[2] was completed and started full operation in September, 1983.

After early difficulties with the flux-core liner were corrected, base pressures of 5×10^{-8} to 2×10^{-7} Torr were regularly obtained. The major activity during this reporting period was concentrated on the study of the plasma in a manner described in the S-1 proposal. Stable, low-q, toroidal pinch configurations with zero externally applied toroidal fields were created and studied with the aid of a passive figure-8 coil system which stabilized global tilt and shift instabilities.

S-1 OPERATIONS WITHOUT FIGURE-8 COILS

In the first half of FY84, S-1 was operated without passive stabilizing coils.[3] Spheromak plasmas were formed on time scales of 0.1, 0.2., 0.5, and 0.8 msec with various equilibrium-field modes (Modes A, B, C, D, and E). Spheromak plasmas were created that had toroidal currents up to 350 kA and typical configuration lifetimes of about 0.3 msec. In most discharges, the plasma was unstable against gross MHD modes such as shift/tilt instabilities, as predicted by MHD theory. In these discharges, the electron temperatures were limited to under 50 eV with a density of $0.3\text{-}3 \times 10^{14}$ cm^{-3}.

GENERATION OF STABLE SPHEROMAK PLASMAS WITH FIGURE-8 COILS

In order to stabilize the plasma against the gross MHD modes, a figure-8 coil system (named according to its eddy current pattern) was designed, based on theoretical studies and the results from the Proto S-1 devices,[4] and installed in S-1.[5] The first figure-8 coil system was designed primarily to stabilize the shift modes of a plasma with a major radius of 45-65 cm. As shown in Fig. 1, two pairs of figure-8 coils were installed on each side of the midplane of the flux core so that the cross points of the coils were 60 cm (≃1.5 plasma radii) away from the midplane. The outermost circumference of the coil system has a major radius of 75 cm. The present passive coil system is made of (2 cm × 3 cm cross section) oxygen-free copper bars.

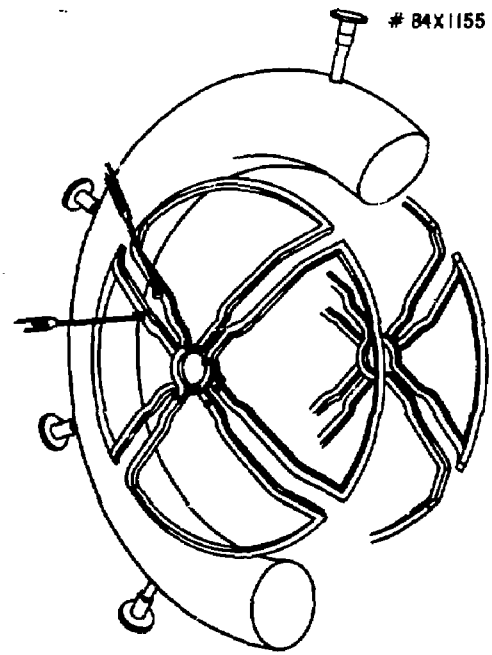

Fig. 1. Schematic diagram of the figure-8 coil system installed on S-1 device.

The installation of the figure-8 coil system made a significant change in the stability features of the formed spheromak plasma.[5] The left side of Fig. 2 shows the time evolution of the radial profile of the B_z field in the midplane (i.e., the z component of the

poloidal field where the z axis is the major symmetry axis) for a plasma shot taken without the stabilizing system. Immediately after the plasma is formed it starts shifting in the midplane with a speed of $0.2\text{-}0.5 \times 10^6$ cm/sec. With the figure-8 coil system installed, the spheromak plasma is kept in a stable equilibrium position for more than a half millisecond, an order-of-magnitude improvement in the duration of the stable quiescent period. The plasma configuration is that of a spheromak, with a low-current density region in the vicinity of the major axis.

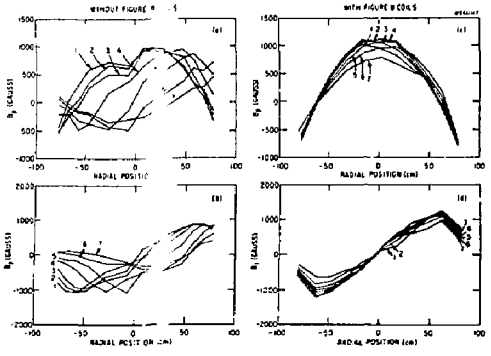

Fig. 2. Evolution of the radial profile of the magnetic field taken between 0.3 msec and 0.6 msec after the initiation of discharges (curves 1-7 are taken every 0.05-msec interval during this time). Plots (a) and (b) correspond to toroidal field (B_t) in the absence of the figure-8 coil system and plots (c) and (d) to B_t, B_z with the installed figure-8 coil system.

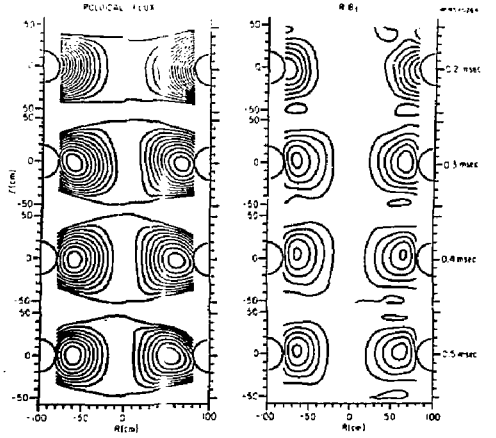

Figure 3. Time evolution of poloidal magnetic flux plots obtained by internal magnetic probe data from 40 consecutive and reproducible shots. The probe is scanned through -25.5 cm < Z <52.5 cm and -77.5 cm < R < 77.5 cm. The separatrices of the spheromak configuration are shown by the outmost solid lines around the plasma.

To date, gross-MHD-stable spheromaks have been obtained with up to 85% of the poloidal flux detached from the flux core, a significant improvement from previous discharges without figure-8 coils where 10-50% detachment was obtained. Reproducible plasmas were obtained with the figure-8 coil system. The time evolution of the global magnetic field structure can be mapped out using data from magnetic probes inserted into the plasma. In particular, a cross section of the plasma in a chosen toroidal plane can be obtained by scanning a multicoil radial-arm probe in the z direction; spatial grid size is between 7.5 and 15 cm. Figure 3 presents the time evolution of poloidal and toroidal flux plots taken 0.2, 0.3, 0.4, and 0.5 msec after the start of the discharge. An excellent match of the $\psi_{poloidal}$ flux plots with the RB_t (poloidal current) flux plots supports a low-β stable spheromak configuration during the whole period.

INVESTIGATION OF GROSS MHD-STABLE SPHEROMAKS WITH FIGURE-8 COILS

Plasma reproducibility has allowed the study of more detailed features of the spheromak plasma.[6-8] The radial q profiles, which correspond to the magnetic field profiles shown in Fig. 3, are shown in Fig. 4. After the formation of the spheromak plasma ($t \geq 0.3$ msec), the q profile remains unchanged in time and varies monotonically from $q_s = 0.6$ at the separatrix ($R = \pm 80$ cm) to $q_a = 0.73$ at the magnetic axis ($R = \pm 60$ cm), which compares favorably with the q profile for the ideal spheromak plasma ($q_s = 0.72$, $q_a = 0.82$). In addition, the value of q at the magnetic axis increases from zero (at $R = \pm 80$ cm) to 0.6 during the formation of the spheromak plasma. This agrees with the time behavior of the observed toroidal modes.

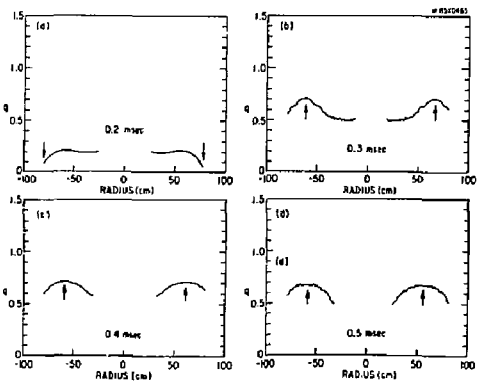

Fig. 4. Radial q profiles obtained from the internal magnetic probe data from Fig. 3. The q profiles are calculated 0.2, 0.3, 0.4, and 0.5 msec after the start of the discharge.

Magnetic fluctuations of the S-1 spheromak plasma have recently[8,9] been resolved into toroidal n-number modes. The figure-8 stabilization coil system provided well-detached plasmas of sufficiently long lifetimes to allow the observation of modes with $n > 1$. Previously, without the stabilization, the plasma shifted soon (~0.2 msec) after the start of the discharge. Modes with n = 1, 2, 3, 4,... have been observed with peak amplitudes of the n = 2, 3, 4 perturbations as high as 20% of the unperturbed field. A significant finding[8] is the temporal progression through the n = 4, 3, 2 mode sequence during formation. This is directly correlated with the time evolution of the $q(\psi)$ profile with q_0 on axis rising through 1/4, 1/3, 1/2 integral fractions.

The behavior of the spheromak plasma with and without passive stabilizing coils was studied; Figure 5 compares these two conditions. The first four panels summarize the spectroscopic data obtained with visible monochromators.[6] Note that the emission due to metals (Fe, Ni, Ta) ejected from the walls was substantially reduced after the stabilizing coils were installed. Copper emission also appears, as expected, but after the collapse of the formation. The H_β emission is quantitatively similar for both cases, although the fluctuation level is noticeably reduced with figure-8 coils.

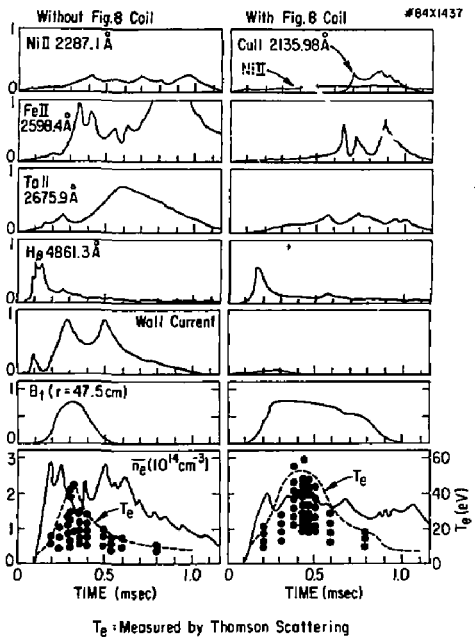

Fig. 5. Comparison of S-1 Spheromak data before (left-hand side) and after (right-hand side) installation of the figure-8 coil system.

A Rogowski coil was used to monitor current conducted along the open field lines at the plasma edge through the vacuum vessel wall; a dramatic decrease in the magnitude of this current after figure-8 coil installation can be seen. This is consistent with the above-mentioned spectroscopic data.

As described earlier, internal magnetic pickup coils were used to monitor the toroidal field inside the plasma. The data showed that the spheromak configuration is maintained for a substantially longer time after the stabilizing coils were installed. Thomson scattering at R = 45 cm indicates a corresponding increase in the lifetime of the peak electron temperature. A single-channel CO_2 interferometer measured line-averaged density at R = 45 cm. Prior to the figure-8 coil system installation, the interferometer showed high-fluctuation levels; these were reduced in amplitude for the stabilized case.

In this fiscal year the S-1 Thomson scattering system has been improved significantly by increasing laser energy to 15 J. Before the installation of the figure-8 coil system, the 10-45 eV electron temperatures and electron densities were observed to decay in less than 0.2 msec. Subsequent to the coil installation, measured electron temperatures have risen to 30-70 eV and above. The scatter of the T_e data for the same firing condition is attributed to the fluctuations of electron temperature together with errors in the Thomson scattering measurement. Relative errors for those measurements plotted are less than 30%. In addition, the electron density has been observed to remain steady for 0.3-0.5 msec. A combination of greater detachment of the poloidal flux from the core, increased stabilization, increased plasma current, and improved vacuum conditioning contributed to the marked increase in the electron temperature.

COMPLETION OF BASIC S-1 DIAGNOSTICS

In this reporting period, basic S-1 diagnostics to measure the main plasma parameters were nearly completed. The diagnostics completed in FY84 included the single-point Thomson scattering system with automatic data acquisition, the vacuum-ultraviolet spectrometer, the single-channel CO_2 laser interferometer, the computer-based external field monitoring system (N probe), the multichannel soft X-ray imaging system, and the triple Langmuir probe.

References

[1] M. Yamada *et al.*, "Quasistatic Formation of the Spheromak Plasma Configuration," Phys. Rev. Lett. *46* (1981) 188.

[2] R. Ellis, Jr. *et al.*, "Status of Fabrication of the S-1 Spheromak Device," in *Physics and Technology of Compact Toroids in the Magnetic Fusion Energy Program* (Proc. 5th Symp., Bellevue, WA, 1982), Mathematical Sciences Northwest (1982) 39.

[3]A.C. Janos *et al.*,"Summary of Initial S-1 Experiments," in *Sixth U.S. Symposium on Compact Toroid Research and the Fifth U.S.-Japan Joint Symposium on Compact Toroid Research*, Princeton Plasma Physics Laboratory (1984) 9.

[4]C. Munson *et al.*, "Experimental Control of the Spheromak Tilting Instability," Phys. Fluids *28* (1985) 1525.

[5]M. Yamada *et al.*, "Initial Results from S-1 Spheromak," in *Plasma Physics and Controlled Nuclear Fusion Research 1984* (Proc. 10th Int. Conf., London, 1984), Vol. *II*, IAEA, Vienna (1985) 535.

[6]M. Yamada *et al.*, "Stabilization of Gross MHD Instabilities of S-1 Spheromak by Passive Figure-8 Coils," in *Compact Toroid Research* (Proc. 6th U.S.-Japan Joint Symp., Hiroshima, Japan, 1984) to be published.

[7]S.F. Paul *et al.*, "Characterization of the Spheromak Plasma in the S-1 Device," in *Compact Toroid Research* (Proc. 6th U.S.-Japan Joint Symp., Hiroshima, Japan, 1984) to be published.

[8]A.C. Janos *et al.*, "Global Magnetic Fluctuations in S-1 Spheromak Plasmas and Relaxation toward a Mininum-Energy State," Princeton University Plasma Physics Laboratory Report PPPL-2214 (1985) 31 pp.

[9]A.C. Janos, "Relaxation Phenomena and Flux Conversion in S-1 Spheromak," in *6th U.S. Symposium on Compact Toroid Research and the Fifth U.S.-Japan Joint Symposium on Compact Toroid Research*, Princeton Plasma Physics Laboratory (1984) 97; Princeton University Plasma Physics Laboratory Report PPPL-2066 (1985) 55 pp.

ADVANCED CONCEPTS TORUS-I

The Advanced Concepts Torus-I (ACT-I) is a steady-state, 5-kG toroidal device with minor and major radii of 10 cm and 59 cm, respectively. Research on ACT-I in 1984 covered a wide spectrum of wave physics, from fundamental studies such as the backward branch of the electrostatic ion cyclotron wave to advanced reactor-relevant radio-frequency (rf) wave concepts including the ion Bernstein wave heating and an α-particle diagnostic using lower-hybrid test waves. Supportive experiments for the ongoing major rf wave experiments, such as the parasitic ion Bernstein wave excitation for the ICRF heating and the electron-beam physics for the rf current drive, were also vigorously pursued.

PARASITIC LOADING OF THE ICRF ANTENNA

Fast-wave heating in the ion cyclotron range of frequencies (ICRF) is a leading candidate for bringing reactor plasmas to ignition temperatures. A typical ICRF antenna is oriented in such a way as to couple predominantly to the fast wave. In addition, the antenna has an electrostatic "Faraday shield" to suppress electrostatic wave excitation. This suppression of the "wrong mode" is quite important not only for improved heating efficiency but also for avoiding potentially serious edge heating. In the ACT-I warm-ion hydrogen plasma, the physics of this parasitic excitation was investigated using a Faraday-shielded ICRF antenna similar to that in tokamak ICRF experiments. It was found that even with a Faraday shield, parasitic excitation of the electrostatic ion Bernstein wave (IBW) occurs over a wide range of plasma parameters.[1,2] In Fig. 1 a two-dimensional wave interferogram of the excited IBW is shown. The nonuniform excitation pattern may be attributed to the nonuniform density gradient along the antenna surface. The excitation process appears to be so strong that at high density ($n_e \simeq 10^{11}$ cm^{-3} at the edge) parasitic loading can extract over 90% of the rf power from a 0.25 Ω antenna circuit! A theory based on a local analysis of the Vlasov-Maxwell equations including the effect of the plasma density gradient was developed and was found to be in very good agreement with the experimental observation. Physically speaking, the $\vec{E} \times \vec{B}$ plasma response in the density gradient region converts the E_y (poloidal) field of the antenna into an E_x (radial) field which then couples to the ion Bernstein wave.

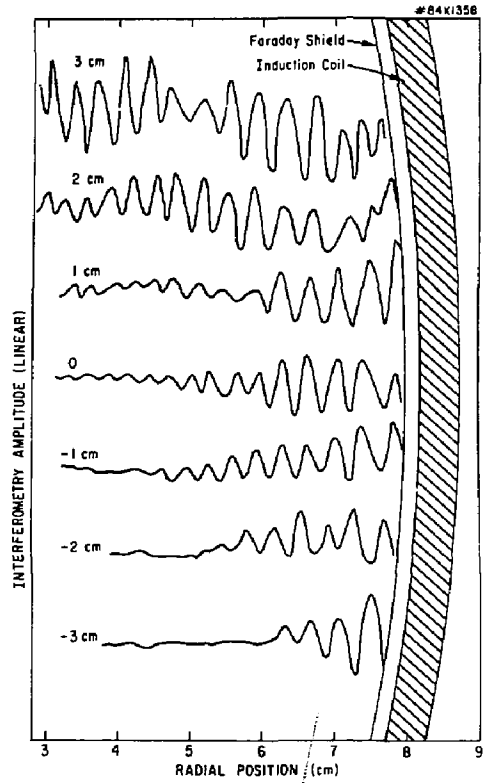

Fig. 1. Ion Bernstein wave interferograms over a poloidal section of the plasma. In the toroidal direction, the probe is located downstream from the antenna by two ports ($\simeq$ 34 cm).

BACKWARD BRANCH OF THE ELECTROSTATIC ION CYCLOTRON WAVE

The backward branch of the electrostatic ion cyclotron wave was measured for the first time.[3] This branch was predicted some twenty years ago when finite-Larmor-radius (FLR) effects were included in the electrostatic ion cyclotron wave dispersion relation. The verification of this hot-ion branch was

made possible by the creation in the ACT-I device of a low-collision, finite-ion temperature neon plasma. In the experiment, a phased antenna structure immersed in the plasma was used to define the parallel wave phase velocity necessary to satisfy the stringent conditions for the wave propagation. In Fig. 2 the measured wave dispersion relation is shown by the open triangles and dots, and the theoretical solution of the dispersion relation is shown as a solid curve. The part of the dispersion curve which has a negative slope is the backward branch. The experimental data are seen to provide very good agreement with the theoretical curve.

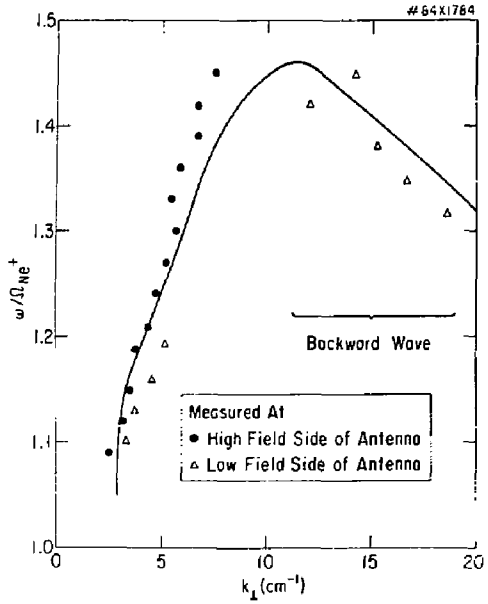

Fig. 2. Wave dispersion relation of the electrostatic ion cyclotron wave in a neon plasma. Solid dots and open triangles display experimentally measured values while the solid curve is a numerical solution based upon $k_{\parallel} = 1.0$ cm^{-1}, $T_e = 2.1$ *eV, and* $T_i = 0.4$ *eV. The negatively sloped part of the wave dispersion curve is the backward branch.*

LOWER-HYBRID CURRENT DRIVE

The ACT-I uses an electron beam injected into the torus to create a target plasma with sufficient seed current for lower-hybrid current drive. For this scheme to work efficiently, it is important for the beam-created plasma to interact strongly with lower-hybrid waves. In the ACT-I experiment, the electron-beam velocity distribution has been measured using a multigrid electron-energy analyzer. It has been found that the beam quickly relaxes into a Maxwellian-like monotonically decreasing velocity distribution which extends up to twice the injected energy. This stable velocity distribution is very desirable for good electron-beam penetration and for strong wave absorption. Two-dimensional computer particle simulation experiments of the electron beam have been able to reproduce the observed beam velocity distribution and to show that the beam-plasma instability is responsible for this distribution.[4]

ION BERNSTEIN WAVE HEATING

Ion Bernstein wave heating, developed by ACT-I, continues to appear as a promising reactor heating concept. In 1983 this heating concept was successfully tested in the JIPPT-II-U tokamak,[5] and testing has now moved on to a larger and more well-diagnosed tokamak, the Princeton Large Torus. In 1984 IBW launching by a $B\theta$ loop antenna, the same as that being used in PLT and JIPPT-II-U IBW-heating experiments, was investigated in ACT-I. The antenna-IBW coupling problem was solved using integral equations, and this newly developed theory is in very good agreement with antenna-loading measurements obtained in ACT-I.[1] A computer code based on this theoretical model is now being developed for tokamak IBW-heating experiments.

In 1984 during a collaborative project with the Kyoto University simulation group, a new resonant ion-heating mechanism at the ion cyclotron subharmonic frequencies ($\omega \simeq 3\Omega_i/2, 5\Omega_i/2$, etc.) was uncovered while carrying out particle simulation for ion Bernstein wave heating.[6] This IBW-heating mechanism causes the wave power to be absorbed in the bulk distribution of the majority ions, which is advantageous for better thermalization and confinement of heated ions in fusion applications.

ALPHA-PARTICLE DIAGNOSTIC USING LOWER-HYBRID TEST WAVES

Measurement of the fusion-produced, 3.5-MeV alpha particles will be a necessary diagnostic for reacting fusion plasmas, and it now presents a challenging problem since the conventional charge-exchange approach is very expensive. In 1983 ACT-I investigated, through a theoretical model, the effect of ion cyclotron harmonic damping on slow and fast waves in the lower-hybrid range of frequencies. It was found that these waves can be heavily damped by energetic alpha particles.[7] Measurement of this wave damping can help determine both the α-particle density and the α-velocity distribution.

References

[1] F. Skiff, "Linear and Non-Linear Excitation of Slow Waves in the Ion Cyclotron Frequency Range," Ph.D. Thesis, Princeton University, January 1985.

[2]F. Skiff, M. Ono, P. Colestock, and K.L. Wong, "Parasitic excitation of Ion Bernstein Waves From a Faraday Shielded Fast Wave Loop Antenna," Phys. Fluids *28* (1985) 2453.

[3]J. Goree, M. Ono, and K.L. Wong, "Observations of the Backward Electrostatic Ion Cyclotron Wave," Princeton University Plasma Physics Laboratory Report PPPL-2178 (1984) 10 pp.

[4]H. Okuda, R. Horton, M. Ono, and K.L. Wong, "Theory and Simulations of Current Drive via Injection of and Electron Beam in the ACT-I Device," Princeton University Plasma Physics Laboratory Report PPPL-2197 (1985) 34 pp.

[5]M. Ono, T. Watari, *et al.*, "Ion-Bernstein-Wave Heating in the JIPPT-II-U Tokamak Plasma," Phys. Rev. Lett. *54* (1985) 2339.

[6]H. Abe, H. Okada, R. Itatani, M. Ono, and H. Okuda, "Resonant Heating Due to Cyclotron Subharmonic Frequency Waves," Phys. Rev. Lett. *53* (1984) 1153.

[7]K.L. Wong and M. Ono, "Effects of Ion Cyclotron Harmonic Damping on Current Drive in the Lower-Hybrid Frequency Range," Nucl. Fusion *24* (1984) 615.

X-RAY LASER STUDIES

Stimulated emission at 100 times the intensity of spontaneous emission with a gain-length of 6.5 was among the substantial advances achieved in the Soft X-Ray Laser Experiment in 1984.[1] This result was obtained by focusing a ~1 kJ CO_2 laser onto a carbon disc, creating a carbon plasma which was confined in a magnetic field (B = 90 kG). The plasma cooled rapidly by radiation losses, and rapid recombination generated a population inversion between levels n=3 and 2 in hydrogen-like CVI. Gain-lengths of up to 6.5 at 182 Å were measured along the plasma column. Very recently, extreme ultraviolet (XUV) mirrors have become available and are expected to greatly ease the difficulties of obtaining laser action at XUV wavelengths. In initial experiments with an XUV mirror of measured effective reflectivity of 12%, a 120% increase in the intensity of the CVI 182-Å line in the axial direction was observed. This is a clear demonstration of the amplification of stimulated emission.

In the 1983 Annual Report,[2] time-resolved measurements of axial enhancement of CVI 182-Å emission in carbon discs and carbon fiber targets corresponding to a one-pass gain-length $k \times \ell \lesssim 3.5$ were presented. Since then, major progress in the area of target development[3] has led to a greatly increased enhancement of stimulated emission over spontaneous emission. In addition, amplification of stimulated emission by the use of soft X-ray mirrors has been demonstrated.

EXPERIMENTAL SETUP

In the Soft X-Ray Experiment (Fig. 1), the XUV spectroscopic diagnostic instruments were converted from the photographic-plate mode to the time-resolved mode.[4] An XUV grazing incidence duochromator, which viewed the transverse, mainly spontaneous, plasma emissions in the 10-350 Å spectral range, was equipped with two channel-electron multipliers with rise time approximately 10 nsec. In the axial direction, the XUV spectrograph was converted to a monochromator with a 16-stage electron multiplier with rise time 20 nsec. A grazing incidence mirror was used to image the plasma on the monochromator entrance slit. Disc targets (mostly of carbon) were used with carbon blades attached perpendicular to the target surface to improve the laser-target interaction. In addition, fiber targets were investigated. In some cases, both disc and fiber targets were coated with a thin layer of aluminum to enhance the radiation cooling.

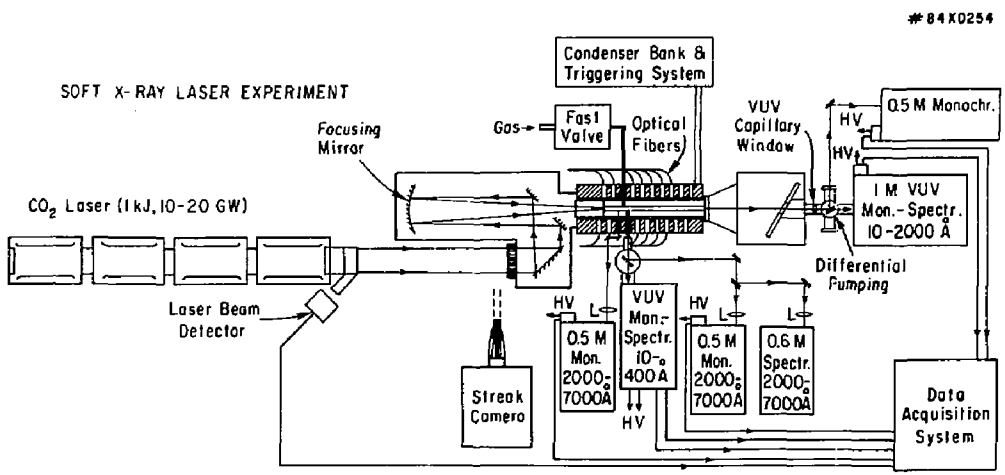

Fig. 1. Experimental arrangement of the Soft X-Ray Laser Experiment.

CARBON FIBER TARGETS

A natural way to achieve a long thin plasma geometry suitable for laser development is to produce a plasma from a long thin target.[5,6] Thermal conduction to the solid surface can increase the cooling above that due to radiation losses in the important region below 50 eV. The carbon fiber targets ranged in diameter from 13 to 350 μm and in length from 2 to 10 mm and were supported by spider webs.

Figure 2 shows framing camera images in the visible wavelength range of the laser-axial fiber interaction, with and without the magnetic field present. In both cases, the plasma extended along the length of the fiber. For B = 90 kG the plasma was well contained and elongated, while for B = 0 kG the plasma extended over a larger volume and much of the support strands were heated. Since the lower-charge states of carbon have stronger radiative transitions in the visible wavelength range, care must be taken in interpreting the framing images in terms of the CVI geometry. In particular, the plasma generated by the support strands is only heated to low-charge states by the fringe of the laser beam but, nevertheless, appears with high intensity in the B = 0 kG image (at B = 0 kG the plasma expanding from the fiber appears to increase the interaction of the laser beam fringe with the support strands). The transverse width of the plasma image is also weighted to the lower-charge states and is much larger than the region containing CVI. However, the framing images do give a qualitative picture of the plasma and show a long thin plasma geometry suitable for generating high gain. The laser interaction along the fiber is not, at present, well understood and may be facilitated by a hollow electron density profile produced at the fiber tip or may be promoted by hot electrons generated in the laser-plasma interaction.

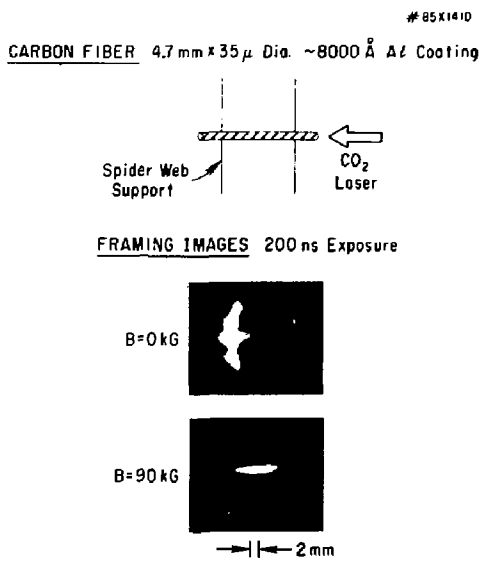

Fig. 2. Carbon fiber target coated with a thin layer of aluminum for which the highest gain was observed. Framing images of the CO_2 laser-fiber interaction at B = 0, 90 kG.

The population inversion between CVI levels n=3 and 2 and the enhancement of the CVI 182-Å line intensity were measured for different experimental conditions.[7] Enhancement is defined as $E = [I(182)_{axial}/I(182)_{transverse}] \times R$, where R is the relative instrumental sensitivity. E > 1 means that the axial intensity is enhanced over that expected from spontaneous emission. With a magnetic field B = 90 kG, the enhancement was less than two and no population inversion was measured. However, in the B = 0 kG case with the fiber target coated with a thin (~8000 Å) layer of aluminum, population inversions and enhancements of up to 6 were obtained, corresponding to a gain of 6 cm^{-1} (Fig. 3).

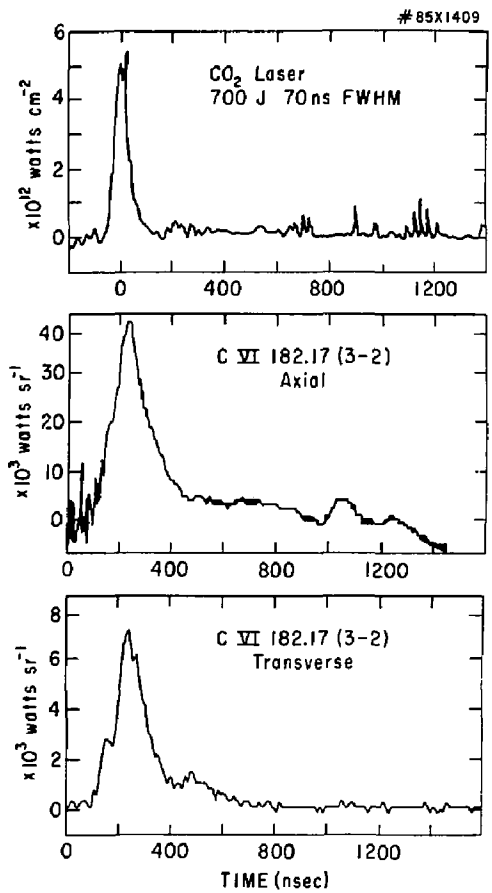

Fig. 3. CVI 182-Å intensities for the fiber target in Fig. 2 with an enhancement E = 7.2 and a gain of 6 cm^{-1}.

The improved results at B = 0 kG may be due to better thermal conduction cooling or to the absence of the deleterious effects of collisional mixing of level populations present at the higher densities maintained in the 90 kG case. The overall plasma geometry, obtained with the framing camera, was longer and more uniform at B = 90 kG, and it is expected that refinements in the experimental arrangement will lead to high gain at B = 90 kG. The gain obtained from the CVI 182-Å enhancement was checked by calculating the gain from the measured n=3 and 2 level populations. For the measured n = 3 population of 2×10^{15} cm^{-3}, the calculated gain is 8 cm^{-1}, in excellent agreement with the gain measured from the enhancement.

CARBON DISC TARGETS

In the 1983 Annual Report,[2] CVI 182-Å emission in a magnetic field B = 90 kG with an enhancement E = 10 corresponding to a gain-length product G = $k \times \ell \approx 3.5$ was reported. Since then substantial progress was made in refining the target configuration to improve the laser-target interaction in the presence of magnetic field B = 90 kG.[8-10] This has resulted in an enhancement of stimulated emission to spontaneous emission of ~100, corresponding to a gain-length product of 6.5.[1]

In the early experiments, carbon discs with 1.5-mm hole targets were used. Gain was measured along the axis of the plasma column (the axis of the column was close to the center of the hole). However, radial profiles of the CVI line radiation, measured by a shot-to-shot vertical scan[8] with the transverse XUV duochromator, indicated that much better conditions for maximum gain should exist in the off-axis region of the plasma column—in agreement with theoretical expectations. In the center of the plasma column the temperature is at a maximum and decreases rapidly in the outer region, whereas, the electron density reaches a maximum off-axis. In this way, C^{6+} ions are created mainly in the center of the plasma column and recombine to CVI in the outer region where the electron density is at a maximum and the temperature is significantly lower than on the axis. The carbon disc target was masked to enable the axial and transverse spectrometers to observe only the off-axis region of the plasma. Figure 4 shows such a carbon disc target with a thin carbon blade attached to improve the laser-target interaction. With this target, the axial CVI 182-Å enhancement increased by an order of magnitude.

The enhancement of the CVI 182-Å line was measured in two ways. The first method was based on the comparison of the ratio of the intensities of the CVI 182-Å line recorded simultaneously by the axial and transverse XUV instruments (first laser shot) with the ratio of the intensities of the CVI 135-Å line (4—2 transition) also recorded simultaneously by the axial and transverse XUV instruments (second laser shot). The CVI 135-Å line was chosen for such a comparison because it has the same lower level and an upper level close in energy to the 182-Å line. The

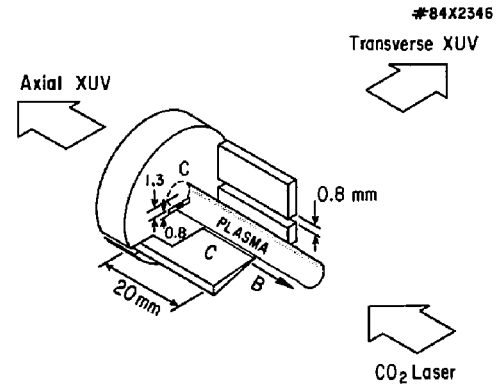

Fig. 4. A carbon disc target with a 0.8 mm × 4 mm horizontal slot and with a thin carbon blade 20 mm long.

transverse intensities of the 182-Å and 135-Å lines compared to the 33.7-Å line indicated a population inversion of levels n=3 and 4 relative to level 2, hence, the 182-Å and 135-Å lines were not affected by optical trapping. In the transverse direction, the intensities of both lines were mainly due to spontaneous emission because of the small plasma thickness.

In the second method, the intensity of the CVI 182-Å (and 135-Å) line in the axial direction relative to the same line in the transverse direction was compared using the relative intensity calibration data from spark and vertical fiber plasmas.[5,6] The enhancement E is related to the one-pass gain-length G by E = (exp G - 1)/G. The peak of the CVI line intensities was observed during plasma recombination. In the recombination phase, the electron temperature $T_e \approx$ 10-20 eV was measured from the slope of CVI and CV recombination continua. In the same phase, the maximum electron density $n_e \approx (6\text{-}7) \times 10^{18}$ cm^{-3} was measured from the intensity ratio of the CV satellite lines from $2p^2\ ^3P - 1s2p\ ^3P$ and $2s2p\ ^3P - 1s2s\ ^3S$ transitions.

Figure 5 shows an example, from a series of measurements of the time evolution, of the CVI 182-Å and CVI 135-Å line intensities in the axial and transverse directions. The enhancement E ≈ 95 of the CVI 182-Å line (corresponding to a gain of G ≈ 6.5) was measured by the first method described above. This value is close to that required for laser action (G ≈ 10)! The CO_2 laser was focused at $r \approx 1.3$ mm from the edge of the slot, which corresponded to the maximum enhancement region for the blade position shown in Fig. 4. The transverse instrument viewed 5 mm of plasma length where the intensity of the CVI lines was strongest (the region 1-6 mm from the disc surface). Measurement of the CVI line intensities at different distances from the carbon disc revealed that the effective length of the plasma, where the CVI ion density was sufficiently large and uniform to produce significant gain, was $\ell_{eff} \approx 1$ cm. The enhancement,

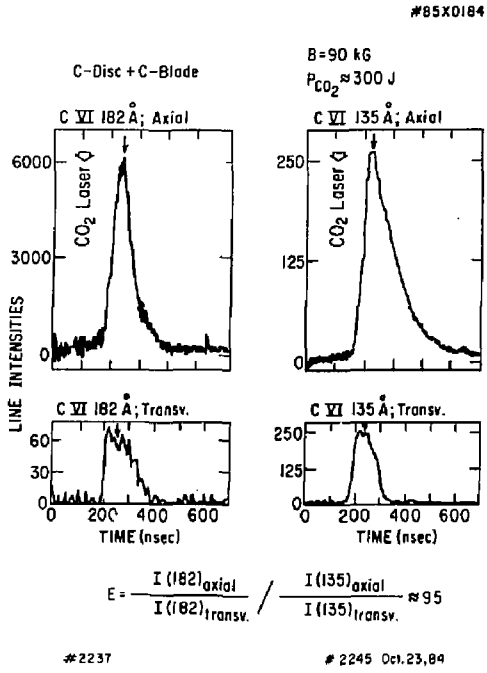

Fig. 5. Time evolution of CVI 182-Å and 135-Å line intensities. The enhancement for the 182-Å line was E ≈ 100 corresponding to a one-pass gain-length k × ℓ ≈ 6.5.

measured by the second method described above, was E ≈ 120, about 25% higher than that measured by the first method. This small difference is due to the enhancement E ≈ 1.3 (G ≈ 0.5) of the CVI 135-Å line.

Two additional checks confirmed the enhancement measurement. First, the population of level n = 3 of the CVI ion was measured from the 182-Å line emission in the transverse direction to be $N_{3,transverse} \approx 1.1 \times 10^{15}$ cm^{-3}, which is in good agreement with the population obtained from the 182-Å line spontaneous emission in the axial direction ($\sim I_{axial}/E$), $N_{3,axial} \approx 1.3 \times 10^{15}$ cm^{-3}. Such populations correspond to the gain k ≈ 5.5-6.5 cm^{-1} for a Doppler-broadened 182-Å line at 10 eV and well support the measured gain. Second, the blackbody brightness temperature $T_B \approx 25$ keV, obtained from the 182-Å line axial brightness of $I = 2 \times 10^6$ W/sr, was much higher than the temperature of the recombining plasma that was emitting this radiation.

Strong enhancement was also measured with a carbon disc target without a carbon blade. The maximum obtained enhancement was E ≈ 100, although intensities of the 182-Å and 135-Å lines in the axial direction were approximately four times lower than for the carbon disc with a carbon blade.

An exciting result, obtained very recently using an XUV multilayer mirror, is the independent proof of the amplification of stimulated emission. The experimental setup is shown in Fig. 6. The XUV mirror had a radius of curvature r = 200 cm and was placed 200 cm from the carbon target in the center of the annular CO_2 laser beam. A small, pulsed vacuum spark was used to measure the effective reflectivity (including the ratio of solid angles towards the detector and mirror) of the XUV mirror *in situ*. The effective reflectivity of the mirror at 182-Å was measured to be 12%. Figure 7 shows an example, from a series of preliminary measurements, of the amplification of stimulated emission from the CVI 182-Å line due to the XUV mirror. A series of 4 to 5 reproducible shots was made with the XUV mirror shutter in a "closed-open" sequence for a gain k × ℓ ≈ 4.3. (This gain was measured with the shutter closed; the gain was lower than in Fig. 5 due to a CO_2 laser problem.) Although

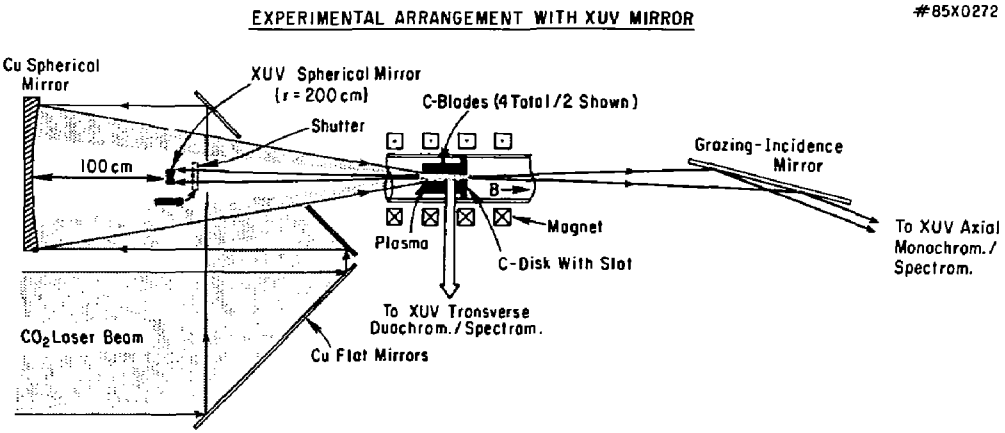

Fig. 6. Experimental setup with the XUV spherical mirror.

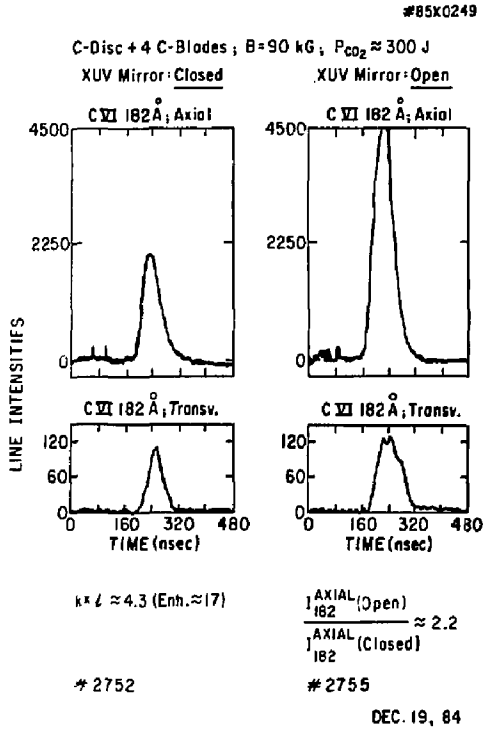

Fig. 7. Time evolution of CVI 182-Å line intensities in the axial direction with the XUV mirror closed (first discharge; gain $k \times \ell \approx 4.3$) and open [second discharge; $I(182)_{axial}$ (open)/$I(182)_{axial}$(closed) ≈ 2.2]. Effective reflectivity of the XUV mirror at 182 Å is less than 12%).

the effective reflectivity of the mirror was less than 12%, the axial intensity of the 182 Å-line increased by ~120% when the shutter was open, while the intensity of this line in the transverse direction was essentially the same. This is a clear demonstration of the amplification of stimulated emission. With an XUV mirror of smaller radius of curvature and with further experiments at higher gain, it is expected to obtain an amplification several times higher.

References

[1]S. Suckewer, C.H. Skinner, H. Milchberg, C. Keane, and D. Voorhees, "Amplification of Stimulated Soft X-Ray Emission in a Confined Plasma Column," submitted to Phys. Rev. Lett.; "Soft X-Ray Laser Gain Measurements in a Recombining Plasma Column," Princeton University Plasma Physics Laboratory Report PPPL-2207 (1985) 22 pp.

[2]Princeton University Plasma Physics Laboratory Annual Report PPPL-Q-41 (October 1, 1982 to September 30, 1983) 62.

[3]Patent Disclosures: *Soft X-Ray Laser*, S. Suckewer; *Disc-Blade X-Ray Laser Target*, S. Suckewer, C.H. Skinner, and D. Voorhees; *Axial Thick-Fiber Target for X-Ray Laser Production*, H. Milchberg, S. Suckewer, and D. Voorhees; *Annular X-Ray Target*, H. Milchberg.

[4]S. Suckewer, and C. Keane, H. Milchberg, C.H. Skinner, and D. Voorhees, "Recent Experiments on Soft X-Ray Laser Development in a Confined Plasma Column," in *Laser Techniques in the Extreme Ultraviolet*, Eds. S.E. Harris and T.B. Lucatorto (AIP, New York, 1984) 55.

[5]H. Milchberg, J.L. Schwob, C.H. Skinner, S. Suckewer, and D. Voorhees, "Soft X-Ray Spectra, Population Inversions and Gains in a Recombining Plasma Column," *Ibid.*, 379.

[6]H. Milchberg, Ph.D. Thesis, "Studies of Population Inversions and Gains for XUV Laser Development in a Recombining Plasma Column," Princeton University, 1985.

[7]H. Milchberg, C.H. Skinner, S. Suckewer, and D. Voorhees, "Measurements of Population Inversion and Gain in Carbon Fiber Plasmas," to be published in Appl. Phys. Lett.

[8]C.H. Skinner, C. Keane, H. Milchberg, S. Suckewer, and D. Voorhees, "Spatial Profiles and Time Evolution of Plasmas which are Candidates for a Soft X-Ray Laser," in *Laser Techniques in the Extreme Ultraviolet*, Eds. S.E. Harris and T.B. Lucatorto (AIP, New York, 1984) 372.

[9]C. Keane, C.H. Skinner, and S. Suckewer, "Line Coincidence Experiment in the XUV Spectral Region Using a CO_2 Laser Produced Plasma," Bull. Am. Phys. Soc. 29 (1984) 1211.

[10]C. Keane and C.H. Skinner, "Radiative Power and Electron Cooling Rates for Oxygen in Steady State and Transient Plasmas at Densities Beyond the Coronal Limit," submitted to Phys. Rev.

THEORY

The theoretical program has three aspects: the development of new theoretical concepts and computational capabilities, the suggestion of experiments which may lead to improvements in toroidal plasma confinement, and the provision of computational and interpretive support to the experimental program of the Laboratory. Each research program generally has elements of all three. For example, the continuing theoretical program in current drive and ramp-up has led to new current-drive and ramp-up concepts, new methods of analyzing the Fokker-Planck equation, and a physical understanding of the high efficiency of current ramp-up in the Princeton Large Torus (PLT) device. During the past year, advances have also been made in the computation of the equilibrium and start-up of axisymmetric plasmas as well as their stability to axisymmetric perturbations. Such computations play a critical role in both the tokamak and the spheromak programs. Further studies have been made on the stability properties of tokamaks in which the plasma has a bean-shaped cross section and on the spectrum of shear Alfvén waves. New transport scaling laws have been developed which are based on the properties of the trapped-particle instabilities. A better understanding of the break-up of magnetic surfaces in toroidal devices has come from the study of stellarators, and related efforts on the break-up of magnetic surfaces in tokamaks (tearing modes) continues. The Theoretical Division has a small program in space plasma physics which fosters the exchange of information between the space and laboratory plasma research efforts.

CURRENT RAMP-UP

Recent current-drive experiments on PLT have converted lower-hybrid wave energy to poloidal-field energy with the remarkable efficiency of 25%. To explain this experiment, and to see whether it might be extrapolated, a theory of radio-frequency (rf) driven plasmas was developed.[1]

First the physical picture. Suppose rf waves push an electron in velocity space against a dc electric field. If the electron is fast, and therefore relatively collisionless, it is primarily affected by the dc field, and increments in the kinetic energy of such electrons are efficiently converted to field energy. For slow electrons collisions dominate, and energy invested in slow electrons is quickly randomized and not converted to field energy. The runaway speed v_R is roughly the dividing line between these two regimes.

To explain the experiments, two response functions are important. One is the rf-induced runaway rate. A confined runaway electron is a constant and serious drain of energy as it is accelerated by the electric field. Suppose an electron has velocity $\vec{v}$ and the probability of its running away is $R(\vec{v})$, Fig. 1. Current ramp-up will be inefficient if the rf pushes electrons to regions of high R, producing numerous runaways. The second important response function is $W(\vec{v})$, the energy transferred to the field by a stopped electron as it stops, Fig. 2. As outlined above, W goes to zero in the collision-dominated regimes, but W goes to $mv^2/2$ in the electric-field-dominated regime giving an efficient ramp-up. By comparing Figs. 1 and 2, it is shown that there is a window around $v_\parallel \gtrsim v_R$ where efficient ramp-up is possible without incurring a large production of runaways. The high efficiency PLT ramp-up experiments operated in this regime.

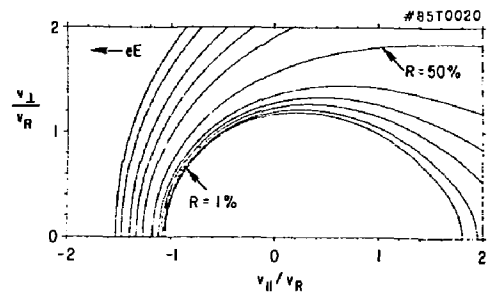

Fig. 1. Probability of an rf-driven electron running away in energy as a function of its parallel and perpendicular velocities divided by the velocity v_R at which the collisional drag force equals the force of an applied electric field.

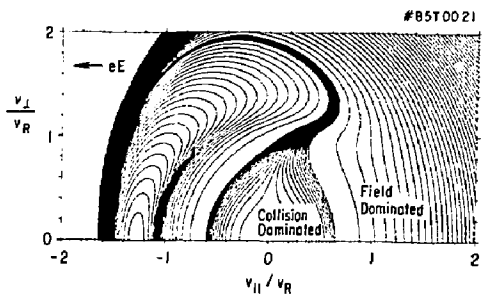

Fig. 2. Energy transferred to the magnetic field by the slowing down of an rf-driven electron as a function of its initial velocity.

In order to apply the theory to the lower-hybrid ramp-up experiments on PLT,[2] it is necessary to express the experimental data in terms of the theoretical variables. The theoretical efficiency is defined as

$$\frac{P_{el}}{P_{in}} = \frac{\vec{\Gamma} \cdot \partial W/\partial \vec{v}}{\vec{\Gamma} \cdot \partial \epsilon/\partial \vec{v}}$$

where P_{in} is the rf power absorbed by the hot electrons, P_{el} is power converted into electromagnetic energy (mostly poloidal magnetic field energy), ϵ is the electron kinetic energy $mv^2/2$, and $\vec{\Gamma}$ the rf-induced flux in velocity space. The important theoretical dimensionless parameter is v_{ph}/v_R, where v_{ph} is the wave parallel phase velocity. In Fig. 3 P_{el}/P_{rf} is plotted against v_{ph}/v_R as determined from the PLT experimental data. These data include all the shots over a two-month period in which the duration of the rf exceeded 200 msec. The lack of scatter indicates that the correct dimensionless parameter has been identified. With few assumptions, the theoretical prediction is given by the solid curve. The fit is outstanding over a wide range of current-drive experiments, namely, where the current is decreasing ($v_{ph}/v_R < 0$), steady ($v_{ph}/v_R = 0$), and increasing ($v_{ph}/v_R > 0$).

The comparison of theory with data shows that the high PLT efficiencies can be explained using the ramp-up theory, which means that larger experiments can be designed with a higher degree of confidence than was previously possible.

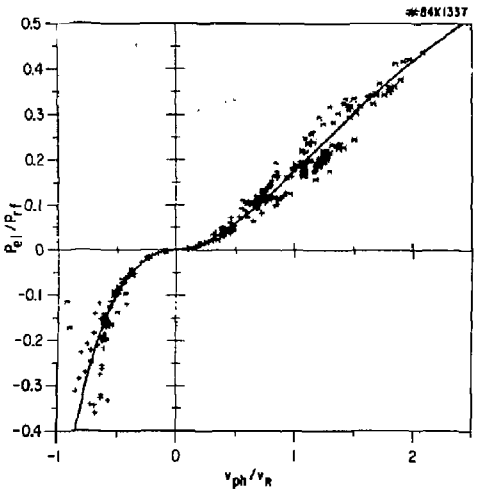

Fig. 3. Comparison of PLT data (dots) with the theory of an rf driven-current ramp-up (solid curve).

AXISYMMETRIC MAGNETICS

The interest in plasmas with a noncircular cross section, plasma compression, and the spheromak device has led to the development of the STARTUP code,[3] which evaluates free-boundary axisymmetric equilibria and transport. The code uses ordinary spatial rather than magnetic coordinates. The numerical method allows an implicit treatment of the fast wave and the field diffusion through the high-resistivity region which simulates the vacuum. This leads to a much larger stable time step allowing longer time simulations. The boundary flux computation uses a multipole moments expansion of the plasma current. A new form for the artificial viscosity maintains numerical stability with a smaller coefficient, and thus yields better resolution of instability growth rates.

The STARTUP code utilizes surface averaging for the pressure, density, and transform so that accurate transport simulations can be performed. A generalized feedback control system has been implemented so that complicated, realistic tokamak feedback control systems can be modeled. Also, an improved vacuum vessel model has been incorporated, which takes into account the possibility of high-resistance bellows regions or toroidally axisymmetric gaps.

Besides fundamental and code verification runs, the code has been supporting the Tokamak Fusion Test Reactor (TFTR), Princeton Beta Experiment (PBX) and S-1 Spheromak experiments, both in modeling existing machines and in the design of upgrades and modifications, Fig. 4. It has been used for axisymmetric stability and electromagnetic transient analysis of the proposed International Tokamak Reactor (INTOR) experiment. It has also been used in collaboration with the Center for Research in Plasma Physics in Lausanne, Switzerland in the design of a highly-elongated-racetrack cross-section experiment.

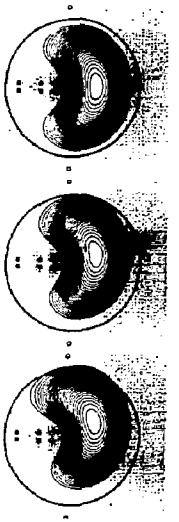

Fig. 4. The STARTUP code simulation of the vertical instability of a bean-shaped plasma without passive or active feedback. (85T1008).

SHAPED-TOKAMAK STUDIES

Theoretical[4] and PBX experimental results have indicated that plasmas with a bean-shaped cross section have favorable stability properties. During the past year, theoretical investigations have been made of the effects of the safety factor and the pressure profile as well as the aspect ratio on stability. Preliminary work has also been carried out on the tearing modes and on the internal modes which arise if the central value of the safety factor is below unity. Variation of the safety factor profile showed that the second stable region increased as the edge safety factor q was raised, although the critical indentation needed for accessibility also increased. Raising q at the magnetic axis helped to alleviate this problem. Variation of the pressure profile showed that an unfavorable profile can eliminate the second stable region, but that a favorable profile strongly enhances the stability properties by reducing the critical indentation needed to reach favorable high-β configurations, Fig. 5. These calculations underestimate the stability since near the stability boundaries the ballooning modes have very short wavelengths and kinetic effects exert a significant stabilizing influence.

High-β values can be reached by either operating in the first stable region at small aspect ratio and low q, or in the second region at larger aspect ratios and higher q. Given a favorable scaling of confinement time with aspect ratio, large aspect ratio (A~6-10) bean-shaped tokamaks operating in the second stable region are interesting reactor candidates. In addition to providing the local shear, which improves the stability properties, the identation strengthens the poloidal field on the field on the outboard side enhancing the confinement properties. The n = 1 tearing modes were considered and indentation was found to have a stabilizing effect on some of these modes. Finally, the low-n internal modes with q(0)<1 were considered and found to be unstable at a relatively low value of β. These modes probably prevent access to the second stable region unless q(0) is kept above unity.

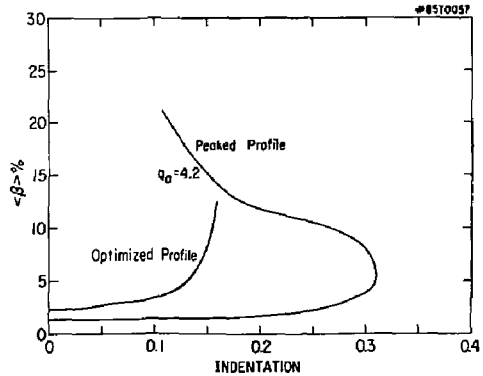

Fig. 5. Effect of configuration indentation on the critical beta for ballooning modes with different plasma-current profiles.

SHEAR ALFVEN SPECTRUM

Numerical studies of the spectrum of low-n global shear Alfvén waves have been carried out using both the PEST code and a new nonvariational MHD stability code, which is being developed to study nonideal-MHD effects. Both codes indicate the presence of a new type of mode, a discrete, global, shear Alfvén mode that lies inside the gaps of the Alfvén continuum. The global extent of these modes make them attractive for plasma heating. Also, they may be driven unstable by interacting with energetic particles such as beam or alpha particles. Indeed, these modes may account for the observations of high-frequency oscillations (f ≈ 100 kHz, m ≈ n ≈ 5) during neutral-beam injection on the PLT and Poloidal Divertor Experiment (PDX) devices.

SCALING LAWS

Classical transport coefficients are calculated by linearizing the Fokker-Planck equation about a Maxwellian distribution. Unfortunately, the electron thermal transport in ohmically heated tokamaks is about two orders of magnitude larger than that predicted by classical calculations. Ohmic tokamak plasmas are known to be subject to both microscopic trapped-electron instabilities and macroscopic tearing instabilities, but a self-consistent transport model containing these effects remains to be developed. Consequently, the development of semiemperical transport models is important for scaling new experiments and for determining the dominant physical processes which contribute to transport.

Two approaches to the problem have been adopted. One approach[5] concentrates on ohmically heated quasistationary tokamak discharges, Fig. 6. In this approach, a current profile is assumed which is consistent with macroscopic stability, and the electron temperature profile is determined from the current profile by the classical Ohm's law. The existence of a thermal equilibrium determines the radial dependence of the coefficient of thermal conductivity, and the magnitude of the coefficient is determined by the familiar $\gamma/k_\perp^2$ estimate using the trapped-electron drift instability.

In the second approach,[6] heuristic arguments are used to construct the coefficient of thermal conductivity except for an unknown multiplicative factor which is expected to be of order unity. The second approach has been applied to both ohmically heated tokamak plasmas and to neutral-beam-heated tokamak plasmas in the so called L-mode, Fig. 7. Both approaches support the view that drift wave turbulence is responsible for the anomalous thermal conductivity in tokamaks.

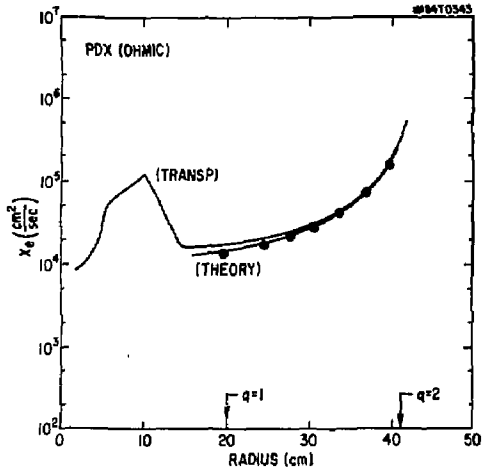

Fig. 6. Comparison of PDX ohmic discharges, as reduced by the TRANSP code, with a theoretically predicted thermal diffusivity

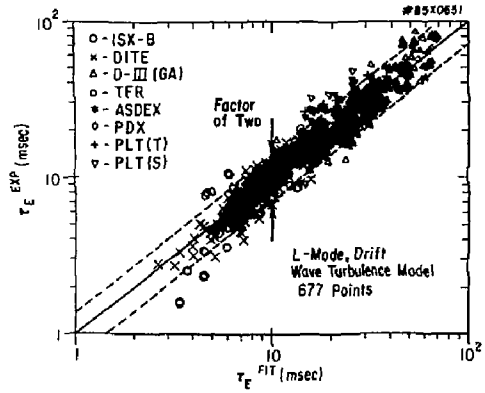

Fig. 7. Comparison of the observed L-mode energy confinement time in a number of tokamaks with a theoretically predicted confinement time.

THREE-DIMENSIONAL EQUILIBRIA AND TRANSPORT

Magnetic field line trajectories are guaranteed to form perfect surfaces in purely two-dimensional equilibria, such as axisymmetric tokamak equilibria. That is not the case in three-dimensional equilibria, for which the existence of magnetic surfaces is a critical issue. The issue is a relevant one not only for intrinsically three-dimensional devices, such as stellarators, but also for nominally two-dimensional devices, such as tokamaks, which are actually three dimensional due to MHD instabilities and field ripple.

The distortions of the magnetic or flux surfaces with finite plasma pressure can cause enhanced transport and at high enough pressure the break-up of the flux surfaces. Considerable progress has been made in studying these questions in the context of stellarators.

Stellarator vacuum fields are designed to have good flux surfaces. Adding plasma with finite pressure gives diamagnetic and Pfirsch-Schlüter currents, which modify the magnetic field. The resulting field may have islands and regions with stochastic field lines. There are three ways in which this may happen. First, the pressure-driven current on any given flux surface may resonate with the rotational transform of a surface elsewhere in the plasma. This effect tends to be particularly serious in devices with large transform per period where the transform per period tends to be near a low-order rational. This effect has been studied using an expansion in beta, with an auxiliary expansion about the magnetic axis.[7] For an early Heliac design, for example, the flux surfaces break up at $\beta \sim 0.3\%$.

Second, the change in rotational transform due to finite beta can introduce low-order rational surfaces not in the vacuum field. Third, finite beta distorts the flux surfaces so that magnetic fields which would be nonresonant at zero beta can have resonant terms at high beta. The last two effects are particularly severe in stellarators with low-rotational transform and low shear. For stellarators with small transform per period, the surfaces can be studied using the stellarator expansion equilibrium code to calculate the magnetic field. The field lines are then followed to produce Poincaré, plots of the surfaces.[8] Such Poincaré plots are shown in Fig. 8 for Wendelstein VII-A parameters with $\beta(0) = 1\%$ and $\beta(0) = 2\%$. The Shafranov shift is large even at these low values of β, and at $\beta(0) = 2\%$ a bad island structure can be observed.

The distortion of the flux surfaces by finite plasma pressure can not only destroy the flux surfaces, but even at lower values of beta it can significantly modify the transport.[9] Unfortunately, this finite-beta effect tends to enhance the transport coefficients. However, the increase can be nullified or even reversed through careful design of the vacuum fields.

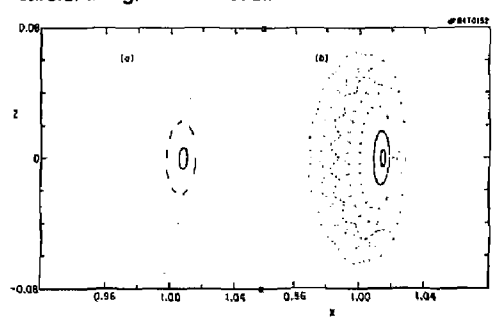

Fig. 8. Magnetic surface break-up in calculations with increasing central beta in a stellarator with Wendelstein VII-A parameters: (a) $\beta_0 = 1\%$ and (b) $\beta_0 = 2\%$.

RESISTIVE MAGNETOHYDRODYNAMICS

The equations of MHD provide a simple single fluid description of plasma dynamics, but they are complicated by the presence of multiple time scale phenomena. When studying the stability of tokamak equilibria, it is beneficial to remove analytically the fastest time scale from these equations, that is, the time scale of the fast compressible magnetosonic wave. Since there are no unstable modes on this time scale, the elimination simplifies numerical calculations without removing relevant physics from the MHD model. A commonly used method of filtering out the fast wave is to expand the equations of MHD in powers of the inverse aspect ratio ϵ, which gives the so-called reduced equations. By ordering the plasma beta to be of $0(\epsilon)$, a set of equations can be generated which, to leading order $[0(\epsilon^2)]$, has been used to study the linear and nonlinear ideal or resistive stability of finite-beta tokamak plasmas. If a more realistic ordering with $\beta \sim 0(\epsilon^2)$ for present-day tokamaks is assumed, pressure does not enter the equations in leading order $[0(\epsilon^2)]$. The resulting set of equations has been used to study external kinks and tearing modes in low-beta tokamaks treated as straight cylinders. This lower order set of reduced equations has been compared with the full MHD equations in a cylinder. Toroidal and finite-beta effects enter in the next order $[0(\epsilon^3)]$. The third-order equations have been used to study the behavior of resistive tearing modes in finite aspect ratio zero-beta tokamaks. Including the next higher order $[0(\epsilon^4)]$ corrections introduces substantially new physics. The correct Mercier stability criterion to ideal interchange modes is recovered. Also the linear and nonlinear dynamics of ideal internal kink modes is accurately modeled. Taking the expansion one order further, $[0(\epsilon^5)]$, the effects of finite beta on the linear and nonlinear evolution of resistive modes for tokamak plasmas of finite aspect ratio can be studied. This fifth-order set of reduced equations has been coded by extending the initial value code HIB.

The modified HIB code, called HILO, has been checked by comparing its results with those from an exact code for cylindrical tearing modes.[10] The results are in excellent agreement and show that the analytic theory of tearing modes has limited validity.

In addition to being useful for tokamak studies, this reduced set of equations can be used to find stellarator equilibria and the HIB code has also been modified for this purpose.[11] An application of this modification of the HIB code, called HIBS, is for the evaluation of equilibria of the Heliac stellarator and is illustrated in Fig. 9. The Heliac has an aspect ratio of five and five field periods. In Fig. 9(a), the central beta value is 10%. However, at a central beta of 12% a ballooning-like mode appears [Fig. 9(b)], which probably limits the beta obtainable in this configuration.

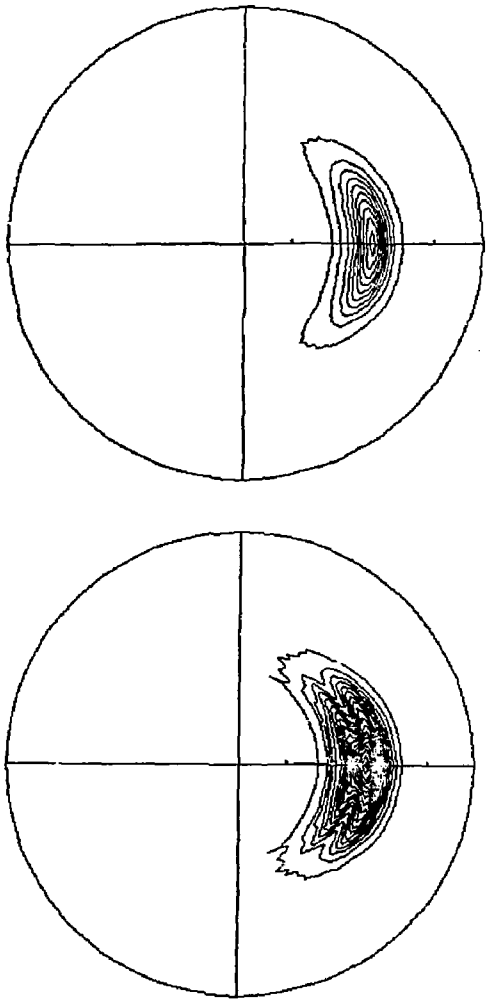

Fig. 9. Heliac equilibria with five field periods and an aspect ratio of five showing the development of a ballooning mode at high central beta: (a) β_0 = 10% and (b) β_0 = 12%. (85T1004 and 85T1007).

SPACE PLASMA PHYSICS

The two major areas of plasma physics research are space and fusion plasmas. Although the theoretical program of the Princeton Plasma Physics Laboratory is concentrated on fusion plasmas, a small, National Science Foundation supported effort is maintained in space plasmas to foster the

interaction between the two research areas. The space plasma research effort includes work on double layers, ion conics, beam-plasma interactions, and the formation and stability of the geomagnetic tail.

Strong macroscopic double layers have been shown to occur in a dipole magnetic field as a result of plasma injection from both the equator and the ionospheric boundaries. This strong double layer, whose electrostatic potential is of the order of a few keV, is in contrast to the ion acoustic double layers previously found, and it is believed to be responsible for the acceleration of auroral particles.

Another important and interesting observation on auroral field lines is the "ion conics," in which cold, ionospheric ions are heated perpendicular to the dipole magnetic field to a few hundred electron volts as they stream up the field lines. Since this differs from the prediction of adiabatic theory, some nonadiabatic process must be in operation. A model has been developed in which the electrostatic ion cyclotron waves are destabilized by the field-aligned current in order to heat the ions transversely.[12] In contrast to quasilinear theory, this model allows the presence of ionospheric electrons, thereby giving rise to an ion temperature of a few hundred electron volts, which is close to what has been observed. Similar electrostatic ion cyclotron waves have been utilized in the ACT-I device for ion heating.

In collaboration with the ACT-I group, it has been shown (recently) that an electron beam injected into a plasma can propagate a much longer distance than predicted by quasilinear theory. This has been seen in the electron-beam current-drive experiments on the ACT-I device and has been confirmed by the numerical simulations as well as by analytic theory.[13] Beam electrons, once injected, will generate beam-plasma instabilities which in turn accelerate a considerable fraction of the beam and background electrons to high energy. These accelerated electrons suffer little collisional slowing down.

A two-dimensional high-β MHD simulation code has been used to study the formation and stability of the geomagnetic tail. Results of this simulation, which starts with a vacuum dipole field, are that after the tail configuration is formed, plasma acceleration and slow shock formation develop as a result of magnetic reconnection.[14] These results are in good agreement with satellite observations.

References

[1]N.J. Fisch and C.F.F. Karney, "Conversion of Wave Energy to Magnetic Field Energy in a Plasma Torus," Phys. Rev. Lett. *54* (1985) 897.

[2]C.F.F. Karney, N.J. Fisch, and F.C. Jobes, "Comparison of the Theory and the Practice of RF Current Drive," Princeton University Plasma Physics Laboratory Report PPPL-2152 (1984) 12 pp; to be published in Phys. Rev. A (Rapid Communications).

[3]S.C. Jardin, "Multiple Time-Scale Methods in Tokamak Magnetohydrodynamics," in *Multiple Time Scales*, Brackbill and Cohen, Eds., Academic Press (1985) 185.

[4]R.C. Grimm *et al.*, "MHD Stability Properties of Bean-Shaped Tokamaks," *Nucl. Fusion 25 (1985) 805.*

[5]W.M. Tang *et al.*, "Anomalous Transport and Confinement Scaling Studies in Tokamaks," in *Plasma Physics and Controlled Nuclear Fusion Research 1984* (Proc. 10th Int. Conf., London, 1984), Vol. *II*, IAEA, Vienna (1985) 213.

[6]F.W. Perkins, "Confinement Scaling in Tokamaks: Consequences of Drift Wave Turbulence," in *Heating in Toroidal Plasmas* (Proc. 4th Int. Symp., Rome, 1984), Edited by H. Knoepfel and E. Sindoni, International School of Plasma Physics and Italian Commission of Nuclear and Alternative Energy Sources (ENEA), Vol. *II* (1984) 977.

[7]A.H. Reiman and A.H. Boozer, "Island Formation and Destruction of Flux Surfaces in Three-Dimensional MHD Equilibria," Phys. Fluids *27* (1984) 2446.

[8]J.L. Johnson *et al.*, "Study of Stellarator Devices by Expansion Techniques," in *Plasma Physics and Controlled Nuclear Fusion Research 1984* (Proc. 10th Int. Conf., London, 1984), Vol. *II*, IAEA, Vienna (1985) 41.

[9]H.E. Mynick, "The Effect of Finite β on Stellarator Transport," Phys. Fluids *28* (1985) 1139.

[10]R. Izzo *et al.*, "Reduced Equations for Finite Beta Tearing Modes in Tokamaks," Phys. Fluids *28* (1985) 903.

[11]W. Park *et al.*, "Three-Dimensional Stellarator Equilibrium as an Ohmic Steady State," Princeton University Plasma Physics Laboratory Report PPPL-2234 (1985) 19 pp.

[12]H. Okuda and M. Ashour-Abdalla, "Acceleration of Hydrogen Ions and Conic Formation Along Auroral Field Lines," J. Geophys. Res. *88* (1983) 899.

[13]H. Okuda, R. Horton, M. Ono, and K.L. Wong, "Theory and Simulations of Current Drive via Injection of an Electric Beam in the ACT-I Device," Princeton University Plasma Physics Laboratory Report PPPL-2197 (1985) 34 pp.

[14]K. Min, H. Okuda, and T. Sato, "Numerical Studies on Magnetotail Formation and Driven Reconnection," J. Geophys. Res. *90* (1985) 4035.

TOKAMAK MODELING

The Tokamak Modeling Group is concerned with modeling plasma transport and impurity control methods in both current tokamak experiments and future tokamak reactors. The Group has developed several major computer codes for this work. Chief among these is BALDUR, a multispecies plasma transport code which incorporates a wide variety of models for sources, sinks, diffusion and convection of plasma energy and particles.[1] The DEGAS code calculates the three-dimensional transport of neutral gas species as they evolve off the chamber walls and interpenetrate with a given plasma. The PLANET code, which models the plasma in the scrape-off layer running into the limiter or a divertor chamber, is designed to be run together with DEGAS. The MIST code follows impurity species through various stages of ionization, charge-exchange, radiation and transport within the plasma. In each of these codes, the models for transport, atomic physics, the effects of plasma instabilities, and a wide variety of processes that affect plasma confinement are refined by using the codes to analyze present experiments.[2-6] The models are then used to predict the performance of future tokamaks which are in the planning stage.[7-11]

DIVERTORS AND PUMP LIMITERS

Two codes are being actively developed to predict the ability of divertors and limiters to remove thermal power and impurities from the edge of the plasma in tokamaks. The DEGAS code, which calculates the transport of neutral gas for a specified plasma, has been successfully applied to the PDX, ISX, ALT-I[10] pump limiters, the TFTR limiters and ZrAl getters, and the PDX, DITE, D-III, and ASDEX divertors. It is in use at UCLA, ORNL, GA, LLNL, LANL (on Reversed-Field Pinches) and PPPL in the U.S. and at Garching, Culham, JAERI, and Nagoya abroad. The PLANET code, which calculates two-dimensional transport of plasma coupled to the DEGAS code, has been successfully applied to PDX and D-III and has been useful in design studies for INTOR, TFCX, and FED tokamak reactors.[5,8] Examples of divertor simulations using DEGAS and PLANET are shown in Figs. 1-3.

These codes predict that divertors should be able to operate in a high-recycling regime in which a low-temperature, high-density plasma forms in front of the neutralizer plate, thus lowering the sheath potential and reducing sputtering. The INTOR poloidal divertor, for example, has been modeled using realistic geometry.[7,8] Results indicate that the plasma temperature can be reduced below 20 eV at the neutralizer plate while maintaining an acceptably high-electron density of 6×10^{13} cm^{-3} in most of the scrape-off region. The electron density in the divertor chamber, shown in Fig. 2, reaches peak values of 2×10^{14} cm^{-3}. As a result of the low temperature and high density, erosion rates were found to be negligible for the steel vacuum wall and the tungsten neutralizer plate. Particular attention has to be paid to the magnetic geometry and to the neutralizer plate orientation, to keep the peak power flux to a tolerable level. Radial particle transport combined with high-recycling rates near the neutralizer plate were found to cause flow reversal (away from the plate) over a considerable part of the scrape-off region. These findings reemphasize the need to treat the whole scrape-off region simultaneously when divertors are modeled.

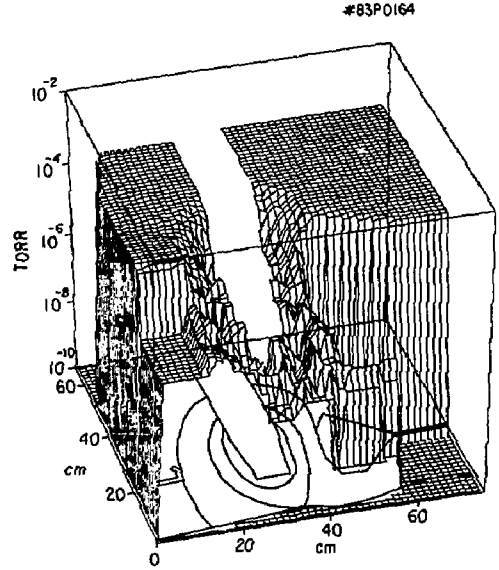

Fig. 1. Two-dimensional variation of the molecular D_2^0 pressure in the divertor as predicted by the DEGAS code during the ohmic phase of a PDX discharge. The geometry of the magnetic flux surfaces, centrally located neutralizer plate, and divertor throat are indicated at the bottom. The pressure drop from the dome to the main vacuum vessel is clearly shown.

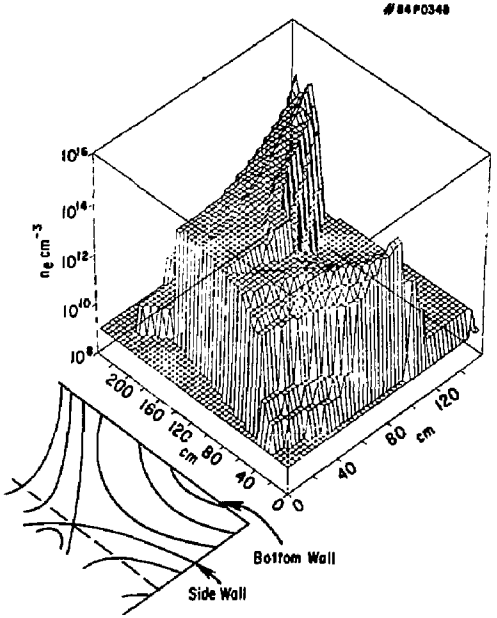

Fig. 2. Electron density predicted by the PLANET code in the INTOR poloidal divertor. The shapes of the magnetic surfaces going into the divertor are shown at lower left.

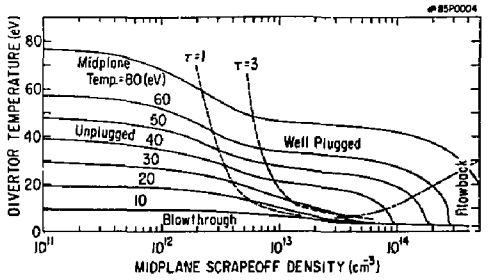

Fig. 3. The divertor temperature is plotted as a function of density for a range of midplane temperatures. Various operating regimes and plasma conditions are indicated qualitatively. The opacity τ of the divertor to neutral being ionized is indicated for τ = 1 and 3, as is the boundary for a collisional plasma. This plot shows the divertor temperature dropping significantly when plasma recycling becomes important (in the regime where the opacity to the neutrals is large).

To complement the above work, a relatively simple two-chamber model of the plasma scrape-off layer was developed[12] and incorporated in the BALDUR transport code in order to approximate particle and heat loss terms at the edge of a tokamak with divertor or pumped limiter. Typical results from this model, shown in Fig. 3, characterize four divertor operating conditions for beam-heated plasmas—plugged, unplugged, blowthrough, and blowback. As a consequence of increased recycling, the midplane Mach number M and the temperature in the divertor are found to decrease with increasing density until the divertor becomes plugged (M = 0). Results from the simple analytic model are found to be in reasonable agreement with detailed numerical calculations using the PLANET code for the PDX divertor.

ATOMIC PHYSICS

Tokamak modeling requires a detailed understanding of atomic processes such as ionization, recombination, charge-exchange, radiation, and the interaction of ions and atoms with material walls.[2,13-15] The Group has compiled extensive atomic data sets which are used in BALDUR, DEGAS, PLANET, MIST, and other transport codes.[16]

Occasionally, newly discovered features of the atomic data yield striking changes in predictions for tokamaks and other fusion devices. For example, when *multiple processes* involving excited atomic states are included in the calculation of neutral-beam penetration into plasmas, it is found[14] that the computed penetration distance is reduced by 30-40% for the current generation of large tokamaks, such as TFTR, JET, and JT-60. The effective stopping cross section is enhanced by these multiple collision processes by 30% to 150% depending upon beam energy, plasma density, and plasma impurity level. The resulting heating efficiency of neutral beams may, therefore, be lower than previously calculated.

Atomic processes have a direct impact on plasma diagnostic techniques. For example, exploiting the relative simplicity of the atomic processes of fully-ionized helium made it possible to carry out a precise determination of impurity transport in the PDX tokamak.[6] An empirical transport parameterization, initially motivated by analysis of the experimental data from this experiment, has recently been further developed and successfully applied to modeling the transport of other light and heavy impurities in tokamaks.[2] For example, one-dimensional modeling of radial impurity transport is being used to analyze X-ray and bolometer data of impurity radiation cooling in the TFTR tokamak.

PLASMA TRANSPORT

Semiempirical plasma transport models are being developed by the Tokamak Modeling Group to combine the best experimental evidence with the most relevant theoretical predictions.[2,3] For example, energy transport models have been developed which incorporate a two-regime electron thermal conductivity motivated by the observed energy confinement time reduction in auxiliary-heated tokamaks, the internal profile modifications and consequent global effects of recurring instabilities such as sawtooth

oscillations, the scaling laws from microinstability-driven turbulence which are theoretically predicted to enhance transport over portions of the plasma profile, and the effect of divertors at the edge of the plasma which, under some conditions, can result in a substantial improvement in the energy confinement time. The goal is to find one combination of models which most reliably and accurately reproduces existing experimental data, in an effort to find a convincing extrapolation to future tokamak reactor conditions.

The BALDUR transport code[1] is continually being improved and used to study new conditions. It has been used to estimate the net beam-driven current in low-density TFTR plasmas and the net lower-hybrid current to be expected during the current ramp-up phase of the TFCX reactor design.[9] A time-dependent sawtooth mixing model was implemented in BALDUR and used to study the effects of sawtooth oscillations on current-profile relaxation in TFCX[9] and on the global energy confinement time of both TFCX and ohmically heated TFTR plasmas.[2] A new survey of the D-T performance in TFTR was carried out with BALDUR to aid an assessment of the possible effects on Q of a variety of machine upgrades.[17] It was found that the fusion power output could be significantly increased by making the tritium density profile more peaked (Fig. 4); this profile modification may be produced by the proposed tritium pellet injector for TFTR. In addition to the original large plasma and strong compression configurations, a new high-current configuration was studied in this survey.

Fast MHD equilibrium routines for plasma with noncircular cross section and modifications for flux-surface averaged transport equations have recently been incorporated into a version of the BALDUR code and are undergoing verification.[18] The object is to extend the capability of BALDUR to better simulate adiabatic compression, triangular and bean-shaped plasmas, and the toroidal effects of high-beta plasmas.

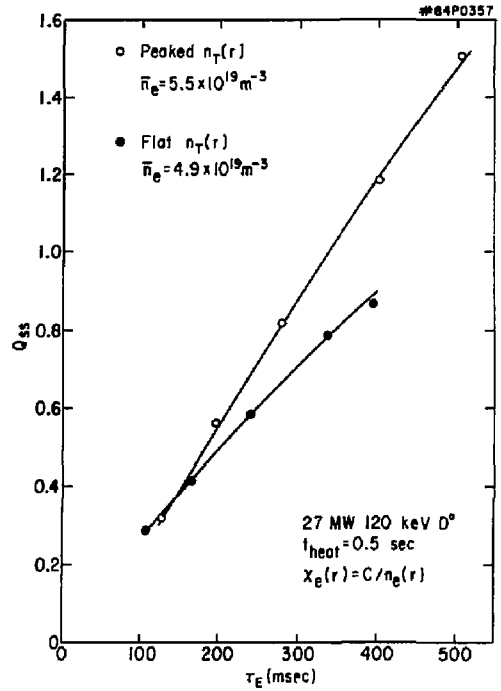

Fig. 4. Estimated steady-state Q, which is the ratio of total fusion output power to heating input power, is plotted, as a function of thermal energy confinement time, from BALDUR simulations of TFTR for two tritium density profiles.

References

[1]C.E. Singer *et al.*, "BALDUR: A One-Dimensional Plasma Transport Code," Computer Physics Communications, in press (1986).

[2]C.E. Singer, editor, "TFTR/JET INTOR Workshop on Plasma Transport in Tokamaks," Princeton University Plasma Physics Laboratory Report No. PPPL-2182 (1985) 147 pp.

[3]C.E. Singer, "Semiempirical Transport in Tokamaks," Princeton University Plasma Physics Laboratory Report No. PPPL-2055R (1984) 24 pp; J. Fus. Energy 3 (1983) 231.

[4]M. Petravic, D. Heifetz, S. Heifetz, and D. Post, "Recent Progress in the Tokamak Edge Modeling," J. Nucl. Mater. *128&129* (1984) 91.

[5]M. Petravic, D. Heifetz, and D. Post, "Modeling Analyses of Tokamaks with Divertors and Pumped Limiters," in *Plasma Physics and Controlled Nuclear Fusion Research 1984* (Proc. 10th Int. Conf., London, 1984), Vol. *II*, IAEA, Vienna (1985) 103.

[6]R.J. Fonck and R.A. Hulse, "He** Transport in the PDX Tokamak," Phys. Rev. Lett. *52 (1984)* 7.

[7]INTOR Group, prepared by D. Post, "INTOR: Impurity and Particle Control," in *Plasma Physics and Controlled Nuclear Fusion Research 1984* (Proc. 10th Int. Conf., London, 1984), Vol. *III*, IAEA, Vienna (1985) 207.

[8]M. Petravic, D. Heifetz, G. Kuo-Petravic, and D. Post, "INTOR Divertor in a Realistic 2-D Geometry," J. Nucl. Mater. *128&129* (1984) 111.

[9]TFCX Preconceptual Design Report, Princeton University Plasma Physics Laboratory Report, F-Axxxc-8406-007 (1984) Sec. 5.

[10]C.D. Boley, D.B. Heifetz, D.E. Post, and M.E. Malinowski, "Neutral Transport in the ALT-I Limiter," Princeton University Plasma Physics Laboratory Report No. PPPL-2043 (1983) 20 pp; J. Nucl. Mater. *121 (1984) 316.*

[11]B.J. Braams and C.E. Singer, "Low Temperature Plasma Near a Tokamak Reactor Limiter," Princeton University Plasma Physics Laboratory Report No. PPPL-2191 (1985) 21 pp.

[12]W.D. Langer and C.E. Singer, "Two-Chamber Model for Divertors with Plasma Recycling," Princeton University Plasma Physics Laboratory Report No. PPPL-2160 (1984) 15 pp; IEEE Trans. Plasma Sci. *PS-13* (1985) 163.

[13]C.E. Singer, K. Mann, K. Rauh, and D. Heifetz, "New

Recycling Model for Light Ions and Atoms," Princeton University Plasma Physics Laboratory Report No. PPPL-2102 (1985) 16 pp; J. Vac. Sci. Technol. *A3* (1985) 1183.

[14]C.D. Boley, R.K. Janev, and D.E. Post, "Enhancement of the Neutral-Beam Stopping Cross Section in Fusion Plasmas Due to Multistep Collision Processes," Phys. Rev. Lett. *52* (1984) 534.

[15]F.W. Perkins and R.A. Hulse, "On the Murakami Density Limit in Tokamaks and Reversed-Field Pinches," Princeton University Plasma Physics Laboratory Report No. PPPL-2087 (1984) 31 pp.

[16]R.K. Janev *et al.*, "Survey of Atomic Processes in Edge Plasmas," Princeton University Plasma Physics Laboratory Report No. PPPL-2045 (1983) 20 pp; J. Nucl. Mater. *121* (1984) 10.

[17]H.P. Eubank *et al.*, "Neutral Beam Heating in TFTR—Projections and Initial Results," in *Plasma Physics and Controlled Nuclear Fusion Research 1984* (Proc. 10th Int. Conf., London, 1984), Vol. *I*, IAEA, Vienna (1985) 303.

[18]M.H. Redi, "Solevev Analytic Test Case Results for the Princeton EQ Code," Princeton University Plasma Physics Laboratory Report No. TM-362 (1984) 15 pp.

REACTOR STUDIES

Reactor studies efforts not covered elsewhere in this Annual Report included:

1) Contributions to the FINESSE Project, a multi-institutional study whose purpose is to determine how to satisfy the development and testing requirements for fusion-reactor blankets;
2) Contributions to the conceptual design program led by the Massachusetts Institute of Technology (MIT) for copper-coil tokamak reactors, ranging from ignition test reactors to commercial power reactors;
3) Work with the Lawrence Livermore National Laboratory (LLNL), TRW, and GA Technologies, Inc. (GAT) on the design of a tokamak-hybrid reactor with a fast-fission blanket.

NUCLEAR TECHNOLOGY TEST FACILITY (FINESSE PROJECT)

The principal performance requirements for a nuclear test facility include a neutron wall loading of at least 1 MW/m^2, a lifetime neutron fluence capability of 10 MW-yr/m^2, a test volume with at least 10 m^2 exposed to the fusion neutron current, and a burn time of at least several hundred seconds with a dwell time between pulses of less than 100 sec. The capital cost should be less than $1 billion for the complete facility. The electrical power consumption should be less than 200 MW and the tritium consumption less than 5 kg per annum. The last constraint implies a fusion power less than 200 MW, assuming a capacity factor near 0.5.

A relatively compact tokamak configuration was derived that gives a wall loading of 1.3 MW/m^2, with both the fusion power and circulating electric power near 185 MW. The principal features of this configuration are the following:

- Copper toroidal-field coils.
- Ignition achieved mainly by ohmic heating, assisted by 5 MW of radio-frequency power (ion cyclotron waves). Quasi-ohmic heating to ignition can be achieved by operating the magnetic field during start-up at nearly twice its steady-state value.
- Pulsed operation, with 1,000-sec pulses and a duty factor >0.9.
- Location of the ohmic-heating coils in the toroidal-field coil bore, to maximize the available flux swing.
- High-beta (23%) operation during the burn, which requires an elongated bean-shaped plasma.

This tokamak concept meets the neutron wall loading, fluence, and burn cycle requirements, although the wall loading is at the lower end of the range of interest. The circulating electrical power and annual tritium consumption are at the higher ends of the acceptable ranges, and the capital cost would probably exceed $1 billion. Thus the most important obstacles to adapting the tokamak as a nuclear technology test facility appear to be its very high capital and operating costs.

COPPER-COIL TOKAMAK REACTORS

Work with the MIT Plasma Fusion Center included design concepts for commercial-scale tokamak reactors using water-cooled-copper toroidal-field coils. Potential advantages over superconducting coils include physically smaller machines, shorter time for reactor maintenance, possible use of demountable joints for ease of access, and relative insensitivity to rapidly changing fields. A further advantage is that toroidal-field coils made of plates can be factory manufactured and shipped to the reactor site.

The designs were scaled up in size from the LITE (Long-Pulse Ignited Test Experiment) test reactor concepts, which use quasi-continuous copper plate magnets. It was found that the coil power dissipation is acceptably low, even with moderate beta (6-8%) reactors having dee-shaped plasmas and major radii 6 m. The reactor size and recirculating power are reduced significantly by going to higher beta (~15%) bean-shaped plasmas. One disadvantage of this system is the large "pusher coil" that must be located in the midplane on the inboard side of the plasma in order to produce the bean indentation. Consideration was given to the use of toroidal-field coils with inboard legs bowed outward in the form of an arch; this configuration allows the pusher coil to be located in the throat of the tokamak outside the toroidal-field coil bore but still adequately close to the plasma, provided that the inboard blanket/shield is relatively thin.

Plant efficiencies, defined as net electrical power to total thermal power, are in the range 0.25-0.29 for these systems.

HYBRID REACTORS

A tokamak with a fast-fission depleted-uranium blanket can have much smaller fusion power and physical size than a "pure fusion" reactor or a fuel breeder with suppressed-fission blanket, in order to produce a given level of net electrical power. The configurations studied in conjunction with groups at LLNL, TRW, and GAT used a mobile blanket material, namely a U-Mo pebble-bed with helium cooling. The pebble-bed is compatible with rapid fuel exchange to remove bred material, which is desirable to minimize variation in average blanket power density. Tritium breeding is carried out in nearly stagnant liquid lithium contained in tubes within and behind the U-Mo pebble-bed.

Transient thermal analysis showed that upon loss of coolant the mobile fuel can be gravity-dumped to a separately cooled dump tank before excessive temperatures are reached.

A systems study analysis indicated that the least expensive machine, measured by direct cost per net kW-electric, has an ignited plasma with inductive current drive and approximately 5 m major radius. The plasma has the standard dee shape with a moderate beta, producing a fusion power of 520 MW and a neutron wall loading of 1.2 MW/m^2. The average blanket multiplication is 11, giving a net electrical power of about 1300 MW. This concept offers a potentially economic tokamak application using machine parameters of the same order as those presently envisaged for fusion test reactors of the late 1990s period, such as the International Tokamak Reactor (INTOR).

SPIN-POLARIZED FUSION PROGRAM

The goal of the spin-polarized fusion program is the development of an intense source (10^{21} sec^{-1}) of spin-polarized hydrogen for eventual test in a fusion reactor. Funding for this program from the Department of Energy began in 1984. This allowed continuation of laboratory experiments to study the physics and technology of optical pumping production of spin-polarized hydrogen in small closed pyrex cells. In addition to supporting one physicist, several undergraduate and graduate students were hired. An additional experimental apparatus was built to allow several experiments to be performed simultaneously.

Optical pumping converts the angular momentum of circularly polarized laser light into hydrogen spin. Rubidium is initially pumped by the laser and the hydrogen atoms are polarized by subsequent spin-exchange collisions.[1] Atomic hydrogen is produced by a pulsed radio-frequency discharge. Cells containing various pressures of hydrogen (1-20 Torr) were studied as functions of the rubidium density and discharge characteristics. Figure 1 shows the hydrogen Zeeman signal obtained in a 10 Torr cell being pumped by 100 mW. Analysis of the difference in the strengths of the $F=1$, $m_F=1 \rightarrow 0$ and $m_F=0 \rightarrow -1$ signals yields a hydrogen polarization of 28%.[2] The atomic hydrogen density was determined to be 10^{12} cm^{-3} in this cell.

In order to increase the polarization and atomic density of the hydrogen, experiments were undertaken to understand the relaxation mechanisms and discharge characteristics. Figure 2 shows the measured rubidium relaxation rate as a function of the hydrogen pressure. As the hydrogen pressure increases, the diffusion to the walls is decreased until volume depolarization due to Rb-H_2 collisions becomes dominant above one atmosphere. Studies of the discharge show that the hydrogen atoms relax in a similar manner, but that the hydrogen atomic density produced by the discharge drops very sharply with increased hydrogen pressure. These results showed that while the utilization of hydrogen as a buffer gas was suitable to obtain the initial hydrogen signals, it is not compatible with both a high degree of polarization and a large atomic density. Fortunately, it is possible to use wall coatings such as a paraffin to reduce the relaxation rates by several orders of magnitudes in low-pressure cells (<1 Torr) where efficient discharges are possible. Work is continuing to further understand these relaxation rates and to determine the optimum wall coating.

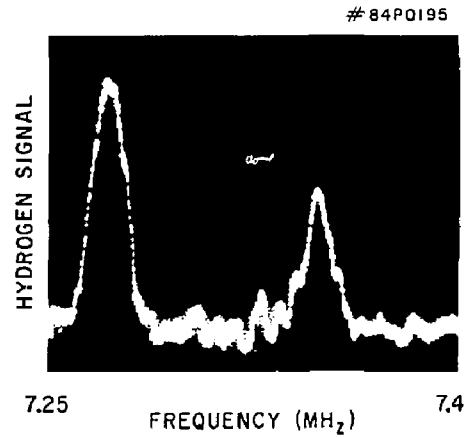

Fig. 1. Hydrogen Zeeman Signal for pumping with σ^+ light. The two observed signals correspond to the different $F=1$, $m_F=1 \rightarrow 0$, and $m_F=0 \rightarrow -1$ transactions. Analysis of these data yield a hydrogen polarization of 28%.

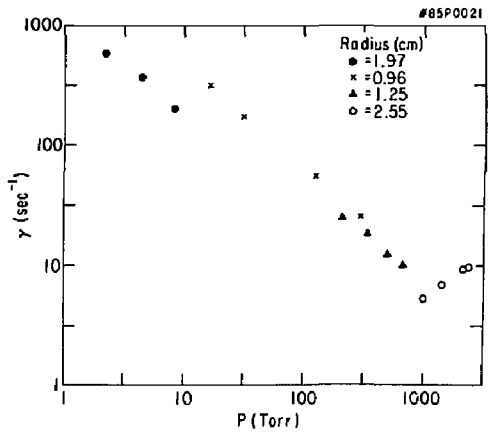

Fig. 2. Rubidium relaxation rate as a function of hydrogen buffer gas pressure. The low-pressure regime is diffusion dominated corresponding to a diffusion coefficient of $D=500\,P^{-1}cm^2sec^{-1}\,Torr^{-1}$. The high-pressure relaxation rate is due to Rb-H_2 electron randomization collisions with a cross section $\sigma=2\times10^{-23}\,cm^2$.

References

[1]W. Happer, E. Miron, R. Knize, and J. Cecchi, "Spin Exchange Optical Pumping to Produce Large Amounts of Polarized Nuclei," Polarized Proton Ion Sources, AIP Conference Proceedings No. 117 (AIP, New York, 1984) 114-122.

[2]R.J. Knize, W. Happer, and J.L. Cecchi, "Optical Pumping Production of Spin Polarized Hydrogen," Princeton University Plasma Physics Laboratory Report PPPL-2125 (1984) 15 pp; also Argonne National Laboratory Report No. ANL-84-50 (1984) 343-357.

TOKAMAK FUSION CORE EXPERIMENT

In October 1983 the Tokamak Fusion Core Experiment (TFCX) Project Group was officially established at the Princeton Plasma Physics Laboratory (PPPL). This action was in response to the U.S. Department of Energy's (DOE) request, late in FY83, that an organization be established at PPPL to pursue and direct a national effort in the planning and preconceptual design of the TFCX. A small number of staff from the other national fusion laboratories were assigned to work at PPPL, while a large number of personnel remained at their home institutions to contribute to the TFCX effort. The institutions participating in the TFCX Project, in addition to PPPL, were: the Argonne National Laboratory (ANL), the Fusion Engineering Design Center (FEDC) at Oak Ridge, the Idaho National Engineering Laboratory (INEL), the Lawrence Livermore National Laboratory (LLNL), the Massachusetts Institute of Technology's (MIT) Plasma Fusion Center, and the Oak Ridge National Laboratory (ORNL). Table I outlines the TFCX tasks assigned to each institution.

The mission of the Tokamak Fusion Core Experiment is to achieve the goal of plasma ignition and self-sustaining equilibrium burn. This is the most

Table I. TFCX Task Assignments.

Major Organizational Elements	Subsystems	Fusion Laboratory Assignments
Systems Engineering	Systems Engineering	MIT/PPPL
	Radiation Analysis	PPPL
	Electromagnetics	PPPL/MIT/FEDC
Plasma Engineering	Plasma Modeling	FEDC
	Magnetic Analysis	FEDC
Tokamak	PF Coils	MIT/FEDC/LANL
	TF Coils	MIT/PPPL/FEDC/LLNL
	Impurity Control	
	Analysis	PPPL/ANL/FEDC
	Design	PPPL/ANL/FEDC
	Structure	PPPL
	Vessel	PPPL
	Shielding	PPPL
Remote Handling	Remote Handling	INEL
Electrical & Plasma Heating	Low-Frequency Electrical	PPPL
	Radio-Frequency Heating	FEDC
Special Systems	Cooling	PPPL
	Cryogenics	MIT
	Tritium System	PPPL/LANL
	Buildings & Facilities	INEL/PPPL/FEDC
Diagnostics	Diagnostics	PPPL
R&D	R&D	ORNL
Safety	Safety	INEL

important scientific goal of the fusion program today. The TFCX will support the fusion program's mission by providing a facility in which all of the remaining plasma physics issues associated with the leading fusion device concept, the tokamak, will be addressed and resolved at one time. The TFCX Project is needed because there are, at this time, no facilities in the world that are capable of achieving the level of performance required to accomplish the TFCX mission.

MACHINE DESIGN OPTIONS CONSIDERED

Early in the preconceptual design phase, consideration was given to a wide range of device configurations including copper toroidal-field (TF) devices, superconducting TF devices, and hybrid (copper and superconducting) TF devices. The decision was made to focus on four primary design options, with additional trade-off studies branching from these options. It was concluded that hybrid TF devices fell within the range of the design options being considered in both cost and performance, and that further consideration of this design option could be of benefit during the conceptual design phase. In addition, it was concluded that other reasonable alternatives, such as placing the poloidal-field (PF) coils inside the TF coils, should be considered during the conceptual design as possible refinements of the four design options considered. Of the four primary design options to be studied, two incorporate superconducting TF coils and two incorporate copper TF coils. The options within each of these sets differ primarily in the extent that the performance of the TF is increased by more exotic approaches to the TF design. The primary difference between the copper and superconducting alternatives, however, is the nuclear shielding required. Increases in shielding thickness are amplified by plasma-aspect-ratio considerations and produce increases in overall machine sizes. The nuclear shield for configurations employing superconducting TF coils must be sized to control the nuclear heat load on the coils. Increased nuclear heat load complicates the design of the coil cooling system and requires increased external refrigeration.

The two superconducting TF options are designated as "nominal" and "high performance," respectively. The element in the design basis that separates these options is the 1 mW cm^{-3} maximum heat load for the nominal superconductor and the 50 mW cm^{-3} heat load for the high-performance option. The design studies have demonstrated that it is feasible to design for high nuclear heat load, while incurring some complications because of the need for high helium throughput. Although the refrigeration requirement for high-duty factor operation at these heat loads would be prohibitive, the refrigeration is tractable at the low-duty factor (3%) planned for TFCX.

The two copper TF options are distinguished by the mechanical design and materials used in the TF coils. The nominal copper TF option employs complete coil cases, a central bucking cylinder for the TFs, and oxygen-free, high-conductivity (OFHC) copper for the conductors. (An artist's concept of the nominal-performance copper option of TFCX is shown in Fig. 1.) The high-performance configuration employs wedging to react against the centering force without a bucking cylinder or coil case in the central region. A "strong-back" coil case configuration confines the case to the outboard regions of the coil where more space is available. In addition, the high-performance copper TF option features a high-strength copper allow (beryllium copper) to minimize the space required for material to react on the magnetic forces. This approach to the high-performance copper TF design minimizes the tokamak size, although it increases the complication of the TF coil design.

Table II lists the characteristic parameters of the four primary design options considered for the TFCX device.

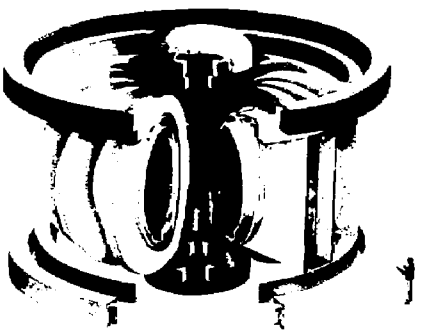

Fig. 1. Artist's concept of nominal-performance copper option of the TFCX device. (IL84001)

RISKS AND BENEFITS

There are several levels of benefits associated with the TFCX Project. All of the design options being considered as candidates for the TFCX device satisfy the basic mission of the Project. All the TFCX options are designed for ignited, long-pulse operation and will provide development and demonstration of the physics associated with achieving the mission, a significant step beyond the achievements of TFTR and the Joint European Torus (JET).

The program for designing and constructing any one of the four TFCX options will bring with it all

Table II. Characteristic Parameters of the Four Primary Design Options under Consideration for the TFCX Device.

Parameter	Superconducting		Copper	
	Nominal	High Performance	Nominal	High Performance
Major Radius (m)	4.08	3.61	3.35	2.60
Minor Radius (m)	1.52	1.30	1.30	1.04
Aspect Ratio	2.69	2.77	2.58	2.49
Field-on-Axis (T)	3.73	4.23	4.00	4.50
Inboard Shielding (m)	0.62	0.36	0.12	0.015
Fusion Power (MW)	267	270	229	197
Wall Load (MWm^{-2})	0.69	0.92	0.85	1.17
Plasma Current (MA)	11.2	10.5	10.9	10.4
Pulse Length (sec)	618	452	458	298
LHRF Power (MW)	32	26	26	19
ICRF Power Initial/Final (MW)	6/31	10/36	7/28	7/26
TF/PF Power (MW))	—	—	405/51	333/108
Beta (%)	5.51	5.35	5.76	5.95
Ign Mirnov	1.5	1.5	1.5	1.5

of the technological advances associated with the development of the TFCX subsystems. Included will be development of magnetic systems, device configuration and remote handling, impurity control and helium removal systems, tritium cooling and safety systems, and overall project facilities. Although all the TFCX options will produce substantial technological development, the magnitude of this technological development differs according to the design option chosen. The design basis for the high-performance copper and high-performance superconducting TF options was chosen with the objective of reducing the cost of the devices by incurring increased but, hopefully, acceptable risk. The TFCX design team believes these risks are acceptable for the fusion program to bear.

ENGINEERING DEPARTMENT

Fiscal year 1984 was a period of moderate transition for the Engineering Department. Its function as a service and support organization for the Laboratory Experimental Program shifted toward operation activities and away from design and fabrication activities. This included direct support of PLT, PBX, S-1 Spheromak, and the smaller devices and the maintenance of power supplies and cooling systems. In addition, overall responsibility continued for the operation and maintenance of all primary electrical power supplied to PPPL by PSE&G. The major design and fabrication work during FY84 was centered on diagnostics and neutral beams for PLT. Details of these activities are covered in the following pages.

During the year, PPPL's first Computer-Aided Design and Drafting (CADD) facility was put into service. The initial installation consisted of a four-terminal Computervision System with supporting mainframe hardware and printers. After sufficient personnel are trained, it is planned to expand this system at PPPL and to interconnect with other fusion community sites and activities. This will include direct use of the National Magnetic Fusion Energy Computer (NMFEC) network, providing immediate access to engineering design and analysis systems such as NASTRAN.

The Engineering Analysis Division was heavily committed to work in the design of a new experimental device called the Tokamak Fusion Core Experiment (TFCX). This work was in conjunction with the Fusion Engineering Design Center (FEDC) at the Oak Ridge National Laboratory (ORNL) and the other national fusion laboratories. A more complete description of this work is covered in the Engineering Analysis Division section.

Another cooperative effort with fusion-related experimental work was the beginning of design and fabrication of the poloidal-field coils for ORNL's Advanced Toroidal Facility machine. These coils are to be fabricated in the PPPL Coil Shop with a completion date of the end of the next fiscal year (FY85).

A major effort was expended by the Engineering Department to increase safety awareness by all of its members. An organization of area safety coordinators was established, training was increased, and the central theme of "safety first" was emphasized.

With the Laboratory shift toward more operations and less new design and fabrication, substantial numbers of the Engineering Department were transferred to the TFTR Project. This is in keeping with the PPPL matrix-oriented organization that provides for direct assignment to projects where such activity is appropriate. The result has been a decrease in the Engineering Department staff level from 585, as presented in the FY83 Annual Report, to 518 at the end of FY84.

ENGINEERING ANALYSIS DIVISION

The role of the Engineering Analysis Division (EAD) is to support the Laboratory's physics programs and the national fusion effort by providing planning and evaluation of new and upgraded experiments, conceptual and preliminary engineering design services, and systems engineering services. The EAD also develops and maintains computer programs for design and analysis and performs engineering and scientific analyses in specialized areas of technology such as radiation, solid and fluid mechanics, heat transfer, vacuum and cryogenics, superconductivity, electromagnetics, and field design. The EAD consists of the Division Office and four technical units. They are the Electromagnetics Branch, the Thermomechanical Branch, the Radiation Analysis Group, and the Systems Group.

Electromagnetics Branch

The Electromagnetics Branch carries out design and analysis activities related to magnetic field systems and their interaction with the associated electrical and mechanical systems.

Eddy current analysis capabilities were substantially increased during FY84. The EAD-developed computer code "SPARK" underwent significant development in FY84. The program "SPARK" is a finite element eddy current analysis code in which the geometry of a model is defined in a manner similar to NASTRAN. Eddy current forces are output in a format compatible with NASTRAN inputs. During FY84, the user-interface portions of the code were extensively refined. A "SPARK" reference manual was published[1] and the code was installed on the CRAY at the NMFECC. A user's manual for the NMFECC version was also made available. The execution speed of the code was increased through vectorization. Figure 1 shows typical results from a "SPARK" run.

The EAD successfully conducted a theoretical and experimental investigation into the coupling between mechanical dynamics and induced electrical currents.

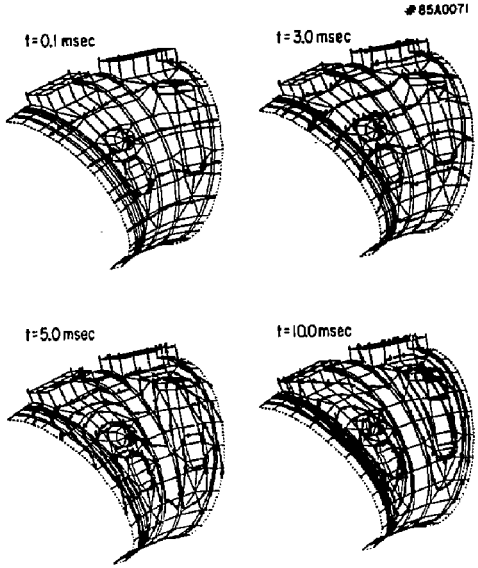

Fig. 1. Eddy current streamlines for a stationary disruption of a 3-MA plasma.

This work originated during the analysis of the TFTR bumper limiter. Several metallic plates and loops were theoretically analyzed, then mounted on a test stand and subjected to a pulsed magnetic field while immersed in a constant background field. Figure 2 shows the excellent match typically obtained between the experimental observations and theoretical

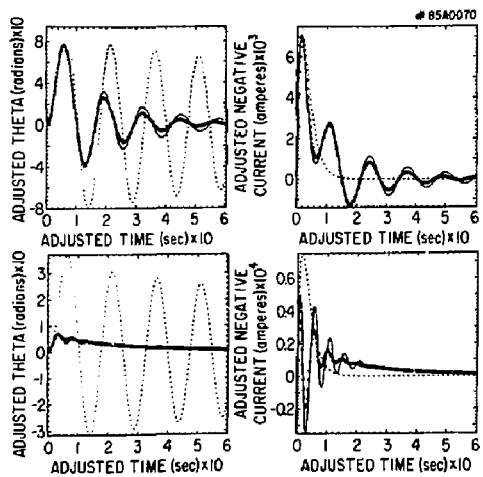

Fig. 2. Combined field tests of a copper plate. Asterisks indicate observed data, the dashed line the uncoupled numerical solution including mechanical damping, and the solid line the simplified analytic solution.

predictions. These results confirmed the assumptions about magnetic damping in the analysis of the TFTR bumper limiter and protective plates.[2,3]

A magnetic coordinates version of the HELIAC simulation program which can evaluate beta limits from resonant magnetic fields was written. It was used to find and evaluate configurations with n = 5, n = 6, and n = 8 periods.

Power sources for the four versions of the Tokamak Fusion Core Experiment (TFCX) Preconceptual Study were investigated. The feasibility of pulsing the National Electric Grid at PPPL up to 650 MW for 5 minutes was verified. Public Service Electric and Gas Co., the local utility, spearheaded the investigation. Their effort provides a benchmark for pulse loading at other locations. A generic model of the National Electric Grid was developed to assist quick determination of the location dependence of the pulse loading capability.

Systems Group

The Systems Group provides overall systems support for large experiments, from the preconceptual design stage to the start of operation. Most of the efforts of the Systems Group for this fiscal year were focused on the TFCX design, with some continuing support for TFTR.

During the preconceptual design of the TFCX, a computer program was developed to determine the point designs of the nominal and high-performance copper devices. The Preconceptual Design Specification of TFCX was incorporated into the code. The code will generate radial-build and vertical-build layouts to comply with the design specification and input parameters. For example, a run will produce a layout showing the plasma, scrape-off region, first wall, vacuum vessel, shielding, toroidal-field coil and case, bucking cylinder, prescribed tolerances and thermal barriers, and the central solenoid poloidal field. The technique of fittings to multipoles[4,5] is used to determine the currents needed to shape the plasma, and from this an optimal set of poloidal-field coil locations can be found for any combination of superconducting and copper coils. This code was used extensively in trade-off studies that were performed during the TFCX preconceptual design.

Also as part of the TFCX preconceptual design, a study was performed which established a defensible cost basis for TFCX buildings and facilities. The sections on costing in the TFCX final report and the design and cost reviews were generated in the Systems Group.

Thermomechanical Branch

The Thermomechanical Branch provides a broad spectrum of capabilities in engineering mechanics, finite element analysis, thermal analysis, and mechanical design. The primary activities of the Branch included engineering analysis and design

support for the TFTR Project and the TFCX preconceptual study.

Thermal analysis capabilities were enhanced by the addition of several new computer codes. Also, in cooperation with the Electromagnetics Branch, a series of experiments was performed at the Argonne National Laboratory to verify the predicted effects of magnetic damping and magnetic stiffness on the mechanical vibration of metallic plates and loops in a magnetic field.

During the year, one member of the Branch spent three months working in the diagnostics group (Project Office 3) of the JT-60 Project at the Japan Atomic Energy Research Institute (JAERI) as part of the U.S.-Japan Exchange Program.[6]

TFTR Diagnostics

Engineering support for TFTR Diagnostics was provided in several areas. The impurity injector was installed and operated. Numerous short-term design and installation tasks in the category of general engineering support were completed. A dynamic analysis and design upgrade was performed for the TFTR X-ray crystal spectrometer collimator support structure. Supplemental dynamic finite element analyses were performed for the TFTR diagnostic support structure.

PLT

Work was completed on a 500-node, three-dimensional nonlinear thermal model of the PLT rotating limiter.[7] A more detailed 1000-node model was also developed.

TFTR/TFM/OSES

Many structures and components of TFTR were studied by the Branch. A detailed simulation of an uncased TFTR toroidal-field coil was developed. The examination of the dynamic behavior of the TFTR phase II bumper limiter continued. The response of the TFTR bellows to bakeout and pulse-discharge cleaning was analyzed, and allowable temperature envelopes for the bellows and adjacent rings were determined. A detailed and reliable dynamic analysis of the TFTR vacuum vessel, under various plasma disruption scenarios, was completed. The first three-dimensional (3-D) TFTR toroidal-field coil thermal analysis was completed. The model included temperature-dependent 3-D thermal conductivity, time and temperature-dependent I^2R heating, and temperature dependent cooling water properties. Conversion of the Grumman vacuum vessel model to PPPL format was accomplished. Several members of the Branch lent support to the Operations System Engineering Support (OSES) Project, an in-depth analysis of the poloidal-field coils on TFTR by Grumman.

In addition to these analytical tasks, assistance was given to the development of a viable strain gauge system for TFTR. Presently, some 1500 strain gauges are installed on TFTR.

TFCX

A major amount of effort was devoted to the TFCX preconceptual design proposal. Proposed configurations of the machine were designed, analyzed, and optimized using finite element modeling (FEM).

Radiation Analysis Group

The Radiation Analysis Group provides radiological and radiation-related analyses and evaluations and assessments for the design, operation, and instrumentation of the fusion devices at PPPL. At the beginning of FY84, the manpower of the group was increased by 50%. The responsibilities of the group were extended to include analysis of on-site meteorological data in preparation for the radiological assessment of TFTR tritium operations and analysis of the experimental shielding in an effort to validate the model calculations. Also, a considerable amount of time was devoted to the radiation characterization of TFCX.

Radiation Analysis for TFTR

The Radiation Analysis Group assisted the TFTR Project in several different areas. One was to provide, according to prescribed scenarios, radiation dose and flux maps for low-power D-D (deuterium-deuterium) operation. The analysis considers the shielding configuration pertaining to different stages of operation. The data constitute part of the input for operational planning.

Design analysis for major Test Cell labyrinths continued during the year. The final design ultimately evolved from these area analyses.

A trade-off study of the advantages of having boron coating on the Test Cell wall was performed. The study led to the decision to put off the boration, both for the Test Cell and for the data acquisition room (DARM). As a result of this study a method of calculating, at an early stage of a fusion reactor design, the effectiveness of boration was investigated.[8]

The impact of major Test Cell floor penetrations was analyzed, and shielding design studies for these penetrations were provided.

Radiation Analysis for TFTR Diagnostics

The objectives of this work were to provide estimates of radiation-induced noise in different diagnostics and to define the shielding requirements or to assess the adequacy of existing shielding designs. Analyses to determine radiation-induced noise were performed for the X-ray pulse-height analyzer, the X-ray imaging system,[9] and the charge-exchange microchannel plate. The analysis technique was improved so that the 3-D effect could be considered. Shielding optimization for polyethylene/lead and water extended polyester/lead two-layer systems was also carried out using realistic response functions. Some of the analysis also included the

details of electron-photon coupling and the effect of local geometric perturbations.

Meteorological and Radiological Analysis

In the meteorological analysis, on-site weather data collected are categorized according to wind speed, wind direction, and the stability class. The stability class is a measure of the dispersion of an effluent injected into the local atmosphere. These data are essential for predicting the impact of long-term and accidental releases of radioactive effluents. Figure 3 shows an example of the wind-rose plot for TFTR.

In addition to the meteorological data analysis, work was done on a comprehensive radiological assessment analysis software package. The source evaluation package, established this fiscal year, calculates the outgassing of tritium from machine components and the build-up of radioactive nuclides in air due to neutron activation. The dispersion package evaluates the consequences of the release of a radioactive effluent, using the on-site meteorological data. These calculations yield direct effects such as inhalation and indirect effects such as precipitation, deposition, and transmission through the food chain. This year's effort established a foundation upon which the radiation safety aspects of TFTR tritium operation can be correctly evaluated.

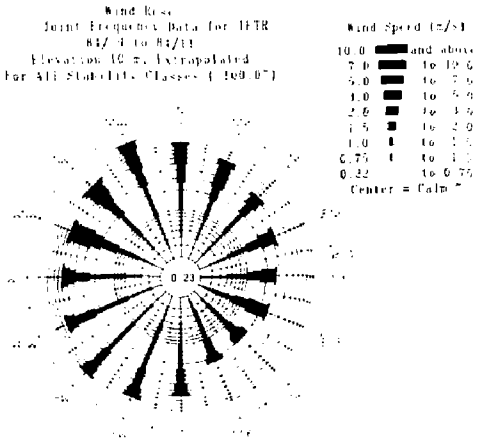

Fig. 3. Wind-rose plot for TFTR. (85X3066)

Experimental Shielding Analysis

The Experimental Shielding Program, a joint effort by the Nuclear Engineering Branch of the TFTR Technical Systems Division and the Radiation Analysis Group, was initiated this year. The primary objective is to validate the theoretical transport calculations and predictions for TFTR. Most of the activities this year were organizational and planning. However, the calibration analysis was performed to determine the best water moderator thickness for the roughly 600 thermal luminescence dosimeter pairs which will be used for part of the neutron dose measurement.

Radiation Analysis for TFCX

A considerable amount of effort was devoted to the radiation characterization of TFCX. The attenuation properties of different shielding configurations were studied. The nuclear heating and damage levels were established. These levels, along with the system design, determined the shielding thickness requirement and the machine operational characteristics. The building wall thickness requirement was analyzed, and the results were used as the input for radiation safety studies and the facility design studies.

ELECTRONIC AND ELECTRICAL ENGINEERING DIVISION

Fiscal Year 1984 witnessed several major developments in the Electronic and Electrical Engineering Division. A significant radio-frequency (rf) system, the 2.45-GHz lower-hybrid current-drive (LHCD) system, was successfully commissioned and operated into the Princeton Large Torus (PLT). Several of the internal shops were merged and restructured to standardize quality assurance procedures and to adapt to an increased use of outside vendors.

The Division staff played an expanded role in the management of a broad range of Laboratory programs. Important among the programs were the TFTR motor generator (MG) upgrade, the Subcontractor Proposal Evaluation Board (SPEB) management of helium refrigeration support, and the TFTR lower-hybrid (LH) study. The latter program was highly commended for its technical excellence and cost and schedule performance.

During FY84 a significant effort was expended in strengthening and modernizing Division safety programs. New training courses were introduced, and employees were encouraged to update their safety skills. Numerous inspection programs were initiated, and existent inspection programs were reevaluated. As a consequence of the heightened attention focused on safety, an improved record in this area of performance is anticipated.

Of major importance to the Laboratory is a new role being performed by the Division. This role is a systems-level cognizance which crosses Division branch boundaries in establishing multidisciplined electrical engineering teams for the improvement and upgrading of existent project equipment. The Electronic and Electrical Engineering Division teams are currently at work in this role on the neutral beam, energy conversion systems (ECS), and pellet injector programs.

Electronics Section

Most FY84 electronics engineering was devoted to the design and construction of diagnostic and control systems for TFTR. Projects started in FY83 for TFTR neutral beams and completed in FY84 include: the fault detector system, the sequence timer system, and the gas valve driver system. New projects completed in FY84 are described below.

The TFTR vertical plasma position controller is an analog-to-digital feedback unit that dynamically controls the vertical position of the TFTR plasma during a discharge. All the variables in the unit's transfer function are controlled by the CICADA computer system.

The TFTR neutral-beam plasma-disruption monitor (Fig. 4) provides a hardwired interlock between 12 neutral-beam sources and several monitoring systems to prevent damage to the vacuum vessel, which could result if the beams were not shut down when the plasma disrupts.

The TFTR neutral-beam power monitor (Fig. 4) is an analog computer that calculates the instantaneous power supplied by each neutral-beam source. It provides voltages representing power versus time for each beamline and for the total injected power.

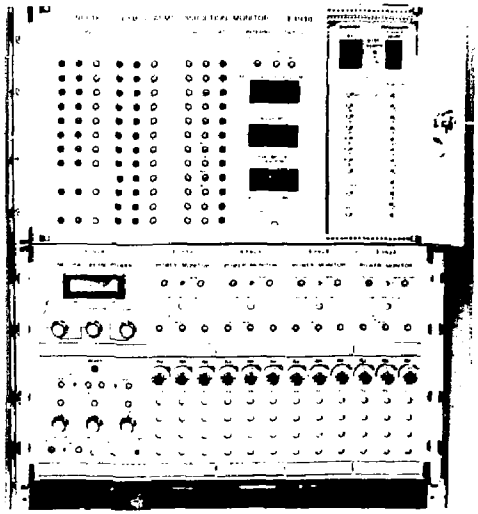

Fig. 4. The TFTR neutral-beam plasma disruption monitor and TFTR neutral-beam power monitor. (85E0363)

The PLT sniffers monitor stray radiation from the 2.45-GHz rf heating systems. If the stray radiation is excessive, the power amplifiers are shut down. This protects personnel and equipment from possible harm.

Two major TFTR neutral-beam projects in FY84, scheduled to be completed in FY85, are the fiber-optic analog data links and the water instrumentation system. The data links provide safe and accurate transmission of analog signals originating from points at high voltage with respect to control room ground. The water instrumentation system accurately measures very small changes in temperature of water cooling the neutral beams. When the beams are pulsed water temperature increases and measurements are made at a number of points in the water flow path. The beam power injected into the plasma is calculated from temperature measurements.

Electro-Optics Section

A spectrograph for measuring the hydrogen species in the neutral beam was assembled and tested in the Laboratory. A fiber-optic lens system was designed and built for carrying light from the neutral beams to the neutral-beam control room where the spectrograph is located.

Work began on a disruption thermal monitor, a 15-channel, two-color photometer operating near 900 nm. Fiber-optics carry the coarse image of the limiter to the lower data acquisition room where the output of each fiber is split and imaged in narrow boards onto silicon photodiodes.

The Interstellar Medium Absorption Profile Spectrograph (IMAPS), a 900 to 1200 Angstrom Echelle spectrograph sounding rocket payload, was launched in October 1984. This astronomical instrument employs a windowless image intensifier charge-coupled device (CCD) developed by the Electro-Optics Section. Further flights are planned for FY85, and this instrument is a candidate for a space shuttle payload.

Analog Engineering Section

The TFTR neutral-beam pyrometer interlock system was designed, assembled, and tested. This system will be used to obtain temperature information from the tokamak walls due to shine-through of the neutral beams and will provide an interlock if the wall temperature exceeds the threshold setting. Four wide-angle bolometer systems and a bolometer array were also built, tested, and installed on TFTR.

A second charge-exchange analyzer was added to the horizontal charge-exchange diagnostic on TFTR. This analyzer is similar to the unit installed last year except that its mounting support is capable of changing the elevation of the analyzer, thereby permitting a wide range of viewing angles into the plasma. A remotely controlled actuator system was designed for this new analyzer. It will permit position control and position readout from the control room.

Construction began on an isolation system for the TFTR neutral beams. This system will provide fiber-optic isolation between the beamlines and the control room for the control and monitoring signals.

A monitor subsystem was constructed for the 48 power detectors in the PLT 2.45-GHz arc protection system. Eight on each of three sources monitor forward power and eight monitor reverse power. If the ratio of reverse-to-forward power exceeds a CAMAC [Computer-Automated Measurement and

Control (System)] threshold, the rf power is blanked for 50 microseconds. If this occurs more than a preset number of times during a shot, the rf source is shut down.

Instrumentation Section

The control and signal processing electronics for the multichannel infrared interferometer (MIRI) were fabricated, tested, and installed on TFTR. The MIRI simultaneously measures line-averaged electron density and poloidal-field distributions along ten vertical chords at Bay S. The probing beams are produced by dual 100-mW far-infrared methyl alcohol lasers (118.8 μm) pumped by a single 100-W CO_2 laser. The electronics that were developed perform control and monitoring functions for the lasers and support equipment. They also detect (using Schottky diodes) and process the 1-MHz beat signals produced by the probing beams. Presently, five density channels and one breadboard poloidal channel are operational. Figure 5 shows a recent density measurement.

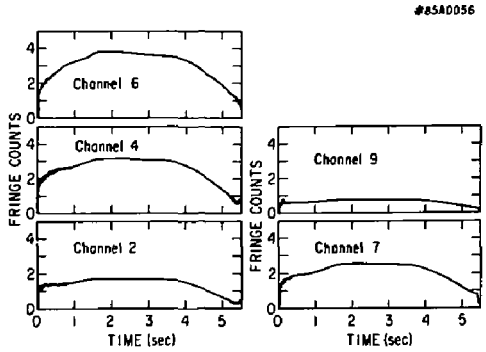

Fig. 5. A MIRI density plot (1 fringe count = 0.935 × 10^{15} electrons/cm^2).

The torus vacuum pumping system cabling on TFTR Bays C and R was redesigned and rewired and a watchdog timer and Test Cell audible alarm were installed. A plan was generated to document the basement cabling and to upgrade the control room computer system.

Vacuum control systems were built and installed on five TFTR diagnostics. Cabling for 26 torus interface valve systems was installed; 14 systems are now operational.

Three spectrometry systems for TFTR were completed: VIPS (Visible Impurity Photometric Spectrometer)-1 (visible); multichannel SOXMOS (Soft X-Ray Monochrometer Spectrometer)-1 (soft X-ray); and FLOPSY (Flexible Optical Path Systems) (scanning ultraviolet and visible). The first two are now operating on TFTR.

Block transfer modules (BTM) were installed on three PLT systems. This fast, direct-memory-access interface, designed last year, replaces the slow, cumbersome parallel data channel. Additional printed circuit BTM units are being fabricated to replace all parallel data channels.

Baseline designs were made for the control electronics for the TFTR repeating pneumatic injector (scheduled for FY85), deuterium pellet injector (scheduled for FY86), and the tritium pellet injector (scheduled for FY88). Detailed design of the repeating pneumatic injector was started.

AC Power Section

The AC Power Section continued to provide support to TFTR from installation through operation, including significant support for the synchronizing tests of 475-MVA motor generator (MG) sets Nos. 1 and 2. In addition, wide-ranging support for the total Laboratory program included the following efforts:

- The installation and energization of a second 138-kV service entrance breaker was completed which provides the Laboratory with significant power system flexibility. This addition allows the operational removal of the original 138-kV service breaker—for the purpose of extensive breaker maintenance—without adversely impairing Laboratory operations.
- The electrical design, engineering, and procurement for the repeating pellet injector system—the forerunner of the tritium pellet injector system—was started.
- A backup supply source was provided for the 4.16-kV buses Nos. Q1, Q2, and Q6 and for the installation of new 4.16-kV feeders for the ion cyclotron radio-frequency heating system and emergency vehicle building loads.

Involvement continued in construction activities including design review, inspection, and supervision of numerous installation packages and field change requests. Also included was the installation of energy management instrumentation and engineering evaluation of various energy saving proposals.

Motor Generator Section

During FY84 all large dc (direct current) pulse-power generators were undercut, finished, reprogrammed, and run-in. The Radio-Frequency Test Facility (RFTF) MG power supply was finished and all power testing was completed.

A procurement was placed for ten motor-operated safety disconnects with ratings of 5,500 continuous amperes dc at 1,000 volts. These units were received.

During the year high-power tests were successfully concluded for all the loads on the Princeton Beta Experiment (PBX).

Computer studies were made that confirmed the idea of running PBX using only two of the three MG

sets, thereby, producing a savings of at least 800 kWh for every hour of run time of the generators, as long as the S-1 Spheromak and the RFTF were not running. This also made it possible for the S-1 Spheromak and the RFTF to run when either PBX or PLT was operating.

An engineering and manufacturing procurement was placed for constant-current regulators for the high-speed breakers' calibration coils.

Neutral-Beam Power Section

The PLT and PBX continued to utilize neutral-beam heating during FY84, and some effort was required from the Section to support those operations. During the last quarter, however, all of the day-to-day support was assumed by the Experiment Operations personnel. The diagnostic neutral beams on both machines were supported, and continue to be supported, by the Section. In addition, the Section supplied the design and specification effort required to provide the electrical portion of the TFTR diagnostic neutral beam.

Most of the Section's efforts during FY84 were devoted to the manufacture, installation, and start-up of the electrical systems required by the TFTR heating neutral beams.

Specifications and drawings required to allow Ebasco to install the apparatus and its accompanying cabling were completed for power systems 5, 4, and 3.

The remanufacture of apparatus received in kit form from Transrex/Aydin, as originally contemplated in FY83, was completed in October and November. However, the requirements for new functions to be installed in the high-voltage enclosures (HVEs) resulted in continuing manufacturing type work being performed on them. This effort involved design and fabrication of mounting facilities, installation and manufacturing test of vendor-supplied arc modulators, and optical link instrumentation.

Start-up of the power supplies for the various systems proceeded throughout the year. The first system to be started was System 5 (for the Neutral Beam Test Cell), comprising three (5A, 5B, 5C) power supply subsystems. In January 1984, power supply No. 5C was used to power the first ion source operated into a TFTR beamline. In March, System 5 was started up and was capable of operating ion sources.

As the heating beamlines were installed in the tokamak Test Cell, the Section provided support in installation of the HVEs and the connecting cables (Fig. 6). As a consequence, the System 3 power supply subsystems (3A, 3B, and 3C) were put under operational test in July and operated into the heating beamlines in August.

By September Systems 3, 4, and 5 were installed and seven of the nine power supply subsystems involved started up. Of the seven, six were operating sources and one was commencing operations test.

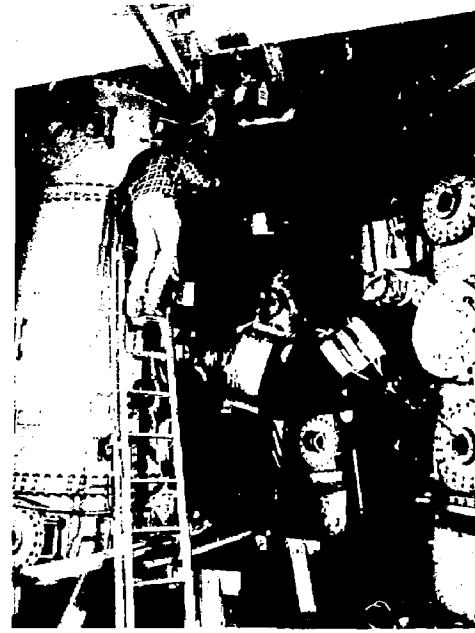

Fig. 6. Installation of "elephant trunk" power cable at a TFTR neutral-beam high-voltage enclosure (HVE). (84E0822)

Rectifier Section

The Rectifier Section continued to support operations of the PLT, PBX, and S-1 Spheromak machines by providing the service, maintenance, and repair of the rectifier systems involved. These include the ohmic-heating and equilibrium-field rectifiers, the redesigned radial field supply, and the S-1 Spheromak capacitor charge and ignitron switching system.

The TFTR motor generator flywheel No. 2 cycloconverter, exciter, and liquid rheostat were brought into operation to supply full power to TFTR.

Safety requirements received new emphasis this year. All power supplies and energy storage devices were evaluated with respect to personnel and equipment safety. Entrance and test procedures were written and personnel were trained.

A system for decreasing the peak power drawn from the utilities and thus decreasing the cost of electrical power was conceived. This program was submitted to DOE through the Energy Conservation Group. The system uses electricity at a low rate at night, stores this energy in batteries, and supplies the high peak power during daytime operations.

High-Frequency Radio-Frequency Section

The 800-MHz Lower-Hybrid Resonance System

The program to improve operation and reliability of the 800-MHz lower-hybrid resonance heating (LHRH) system was completed this year. Several design changes were made in the capacitor bank to reduce the amount of stored energy and to decrease the power supply impedance. These changes lessened the stress on the modulators and the crowbar during emergency or fault-induced shutdowns. Portions of the control console were redesigned to make the system more self-sufficient and to reduce the burden on Operations personnel. A spare tube dolly (complete with focus magnet and klystron) for the high-power amplifier (HPA) assembly was constructed to allow rapid replacement and minimize downtime in the event of an HPA failure.

In preparation for next year's fast-wave current-drive experiments, a contract was signed for the production of the coupler needed for this project.

The 2.45-GHz Lower-Hybrid Current-Drive System

The construction phase of this project was completed this year, and the system began operations in the high-density current-drive experiments mode on PLT. Figure 7 shows one of the system's three HPAs with rear doors removed to show its Varian VKS 8269 klystron. By the end of FY84, all three of the HPAs of this system had been operated into their respective dummy loads at full power (500 kW each), and HPAs No. 1 and No. 2 were operated into the PLT tokamak at levels up to 100 kW each. Extensive modifications to the high-voltage safety system for this project were made.

Fig. 7. The 2.45-GHz high-power amplifier with klystron installed. (83E1268)

The 60-GHz Electron Cyclotron Resonance Heating System

During FY84, the 60-GHz electron cyclotron resonance heating (ECRH) transmission line system was transferred from PBX to PLT. The high-voltage power supply and the modulator/regulator portions of the 60-GHz system and their controls were modified so that they could be shared by the 2.45-GHz lower-hybrid current-drive system.

Low-Frequency Radio-Frequency Section

Modifications were completed on the two cavity-tuned ion cyclotron radio-frequency (ICRF) amplifiers to shift the frequency from 42 MHz to 30 MHz. Both systems were tested successfully to 2.5 MW into dummy loads. The third, older, ICRF amplifier was upgraded and converted to 30 MHz. Dummy load tests on this amplifier were run successfully up to 1.6 MW. Experimental operations into PLT are now possible up to a full 6.0 MW using all three ICRF systems.

Two 80-MHz rf systems, to provide 1.5 MW of power, were acquired from the Hanford Electronic Development Laboratory. Installation of these systems is nearing completion. These sources will be used for ICRF harmonic-heating experiments on PLT. A photograph of the 80-MHz equipment is shown in Fig. 8.

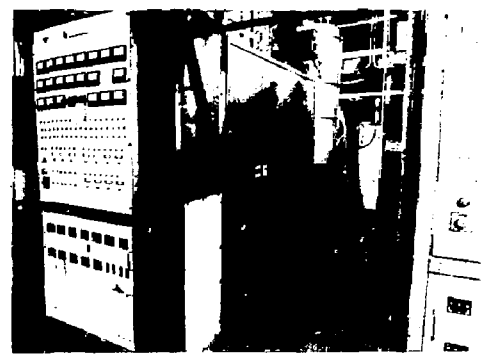

Fig. 8. The 80-MHz 1.5-MW ion cyclotron radio-frequency generator. (85E0302)

Several programs to design and develop high-power rf feed-thru bushings for PLT were completed. All high-power rf bushings on PLT were changed to the new design and are operating reliably and successfully at maximum power levels available from rf sources. Two additional bushing programs were started to develop a high-current four inch bushing for center fed antennas and a water-cooled six-inch bushing for high-energy, long-pulse applications. The programs are scheduled for completion in mid-FY85.

MECHANICAL ENGINEERING DIVISION

The Mechanical Engineering Division (MED) provides engineering and technical services to the many projects and programs at the Laboratory. The Division consists of three branches: the Mechanical Technology Branch, the Vacuum and Cryogenic Branch, and the Coil Systems Branch. In addition to the branches there is a Special Projects Group and an independent Engineering Services Group. The Division's major efforts and activities during FY84 were for TFTR, with the needs of the remaining research programs being met as required.

The Special Projects Group is available to the MED and others for technical support. Major efforts this past year concerned studies of the problems facing the TFTR Project. The study of the MG No. 1 and No. 2 rotor runout was one of the major contributions of this Group. Another major task is the program to provide mechanical supports for the poloidal-field leads.

The Engineering Services Group provides skilled technicians to work for the various MED branches and for other organizational groups at the Laboratory. Included in this group are carpenters, electricians, metalsmiths, pipe fitters, welders, millwrights, and general technicians.

Mechanical Technology Branch

During FY84 the Mechanical Technology Branch combined two separate engineering sections to create the Diagnostics and General Fabrication (D&GF) Section. Other sections of the branch include the Drafting, Machine Design, and Materials Test Section.

Diagnostics and General Fabrication Section

One of the most complex diagnostics on TFTR, the Multichannel Infrared Interferometer (MIRI), was completed and installed in FY84. The MIRI diagnostic will be used to monitor TFTR plasma density. The total system weight of this laser-based instrument exceeds 30 tons. The D&GF Section designed, tested, and installed the interferometer which is shown in Figs. 9, 10 and 11. The system is currently operating in a "shakedown" test mode using five data channels

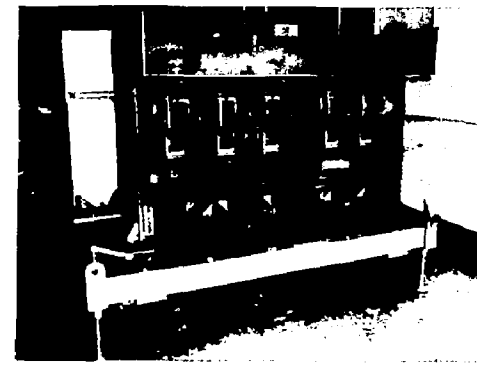

Fig. 9. Four levels of the Multichannel Far-Infrared Interferometer (MIRI). (1) Power division, (2) power division and heterodyne detection, (3) density, and (4) Faraday rotation. (84E0871)

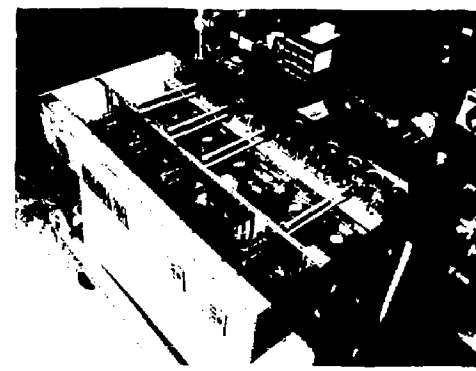

Fig. 10. Top section of the MIRI showing motorized laser-beam steering mirrors. (84E1051)

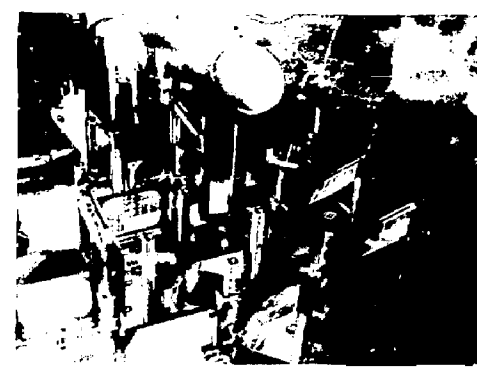

Fig. 11. First level (power division) of MIRI. (The small white spots are a diffraction pattern from an alignment laser beam passing through the system.) (84E0828)

and is expected to be commissioned early in FY85. Five additional data channels will also be added to the MIRI system in FY85.

In other TFTR diagnostic work, an additional charge-exchange analyzer was installed on the horizontal charge-exchange system, and the vertical charge-exchange system was installed in the TFTR Test Cell Basement.

In the area of X-ray diagnostics, two vacuum chambers were fabricated for use on the TFTR pulse-height analyzer (PHA) system. A PHA support structure framework was designed and fabrication started to allow installation of two PHA chambers in FY85.

The horizontal X-ray imaging system (XIS) was upgraded in FY84 to include more data gathering channels and the addition of remotely selectable attenuator filters. By changing filters, different regions of the X-ray spectrum can be studied. The filters, which are located inside the XIS vacuum chamber along two tracks positioned directly in front of the X-ray sensing detectors, are shown in Fig. 12.

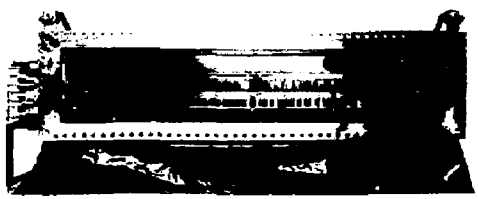

Fig. 12. The X-ray filters located inside the instrument X-ray imaging system vacuum chamber. (84E0969)

The D&GF personnel were also involved with work on the Princeton Large Torus (PLT) in FY84.[10] Mechanical engineering for the PLT rotating pump limiter, shown in Figs. 13 and 14, included design, fabrication, and installation. The PLT rotating pump limiter has a contoured front face of graphite and rotates during plasma discharges. The limiter is located within the PLT pump duct and can be moved fore and aft as required. It was preconditioned for use on PLT by mounting it on a water-cooled support placed in an ion beamline and by irritating it, head-on, by short pulses of 1-MW hydrogen-ion-beam shots. This caused the limiter to reach a peak temperature in excess of 2000°C and a bulk temperature greater than 600°C.

Drafting Section

The Drafting Section continued to provide design and drawing support to all on-going programs at the Laboratory. In addition, the Section also provided conceptual design support for study projects such as TFCX. The Section has also been responsible for writing the first comprehensive Drafting Standards Manual for the Laboratory.

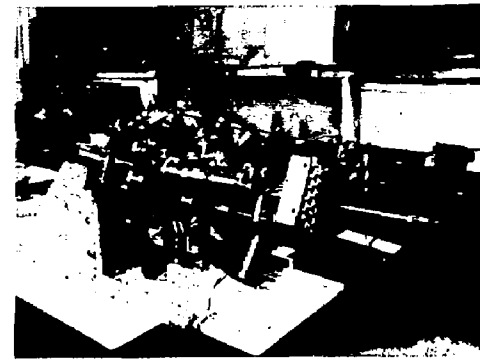

Fig. 13. The PLT rotating pump limiter assembly. (83E1578)

Fig. 14. The PLT rotating graphite limiter.

Machine Design Section

The Machine Design Section continued to be involved in a number of tasks which were started the previous fiscal year. The majority of these tasks concerned the design, procurement, and installation of TFTR vacuum vessel internal components and their associated cooling systems. The initial protective plates were fabricated, delivered, and installed in the TFTR vacuum vessel, and the cooling water system for the initial protective plates was completed on schedule. Concurrently, the design of the cooling water systems for the final protective plates and the bumper limiter was also completed.

Testing the TFTR movable limiter actuators continued after the installation of the movable limiter last fiscal year. Life cycle tests indicated a potential problem in the drive mechanism of the actuator. This problem was resolved utilizing a ball-screw replacement drive.

The Machine Design Section provided mechanical design assistance in a number of areas including continued support of neutral-beam activities. There were also a number of tasks which fall into a miscellaneous design category. A typical example is the design, fabrication, and installation of a bakeout

blanket for the torus vacuum pumping system (TVPS) ducts. Figure 15 shows a TVPS duct after the assembly of the wire mesh and bakeout tubing. Figure 16 shows the TVPS duct after wrapping with aluminum foil, fiber glass insulation, and a protective outer covering layer of PVC.

Fig. 15. The torus vacuum pumping system duct at an early stage of assembly showing wire mesh and bakeout tubing. (84E0791)

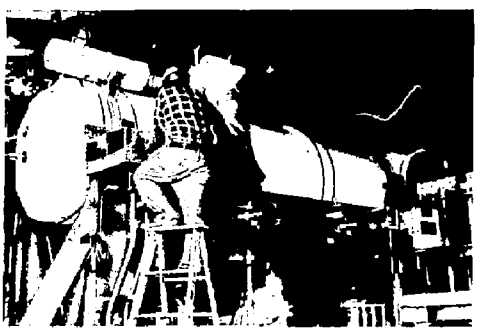

Fig. 16. The torus vacuum pumping system duct wrapped with protective PVC covering. (84E0927)

Materials Test Section

In FY84, the Material Test Laboratory (MTL) performed a total of 92 tasks, primarily for TFTR. In addition, the Laboratory facilities were used by several other groups at PPPL for investigating the effects of magnetic fields on TFTR components.

Major accomplishments during this period include the design of supporting fixtures for the mechanical instrumentation of TFTR MG No. 2, the expansion of the TFTR data acquisition system (developed by MTL in FY83) to include MG No. 2, and the installation of strain gauge rosettes on all TFTR toloidal-field coils. Other tasks performed during this period include proof testing of lifting fixtures and providing instrumentation and transducer support for other groups.

Vacuum and Cryogenic Branch

Vacuum Section

The Vacuum Section of the Vacuum and Cryogenic Branch supported a variety of project needs for the TFTR, PLT, PBX, and S-1 Spheromak during FY84.

Most of the Vacuum Section resources (about 70%) were devoted to the TFTR during this reporting period; with neutral beam and facility operations the major users. Work continued on the neutral-beam assemblies in the 1-H Building, and system No. 4 was delivered to the tokamak Test Cell during the winter shutdown. Vacuum lines were completed before the shutdown, and modifications were made in the roughing pump liner during the shutdown. From January through March almost all of the Section's resources were involved in the TFTR shutdown. Repairs were made to pumping ducts, defective gate valves were replaced, and assistance was given to diagnostics and bakeout.

The fabrication of a new flux core liner for the S-1 Spheromak was completed during FY84. This liner was mechanically ground to the desired 0.020-inch thickness. Figure 17 shows this activity. The Vacuum Section was also involved in the PLT 2.45-GHz program; brazing windows and supplying engineering and design assistance.

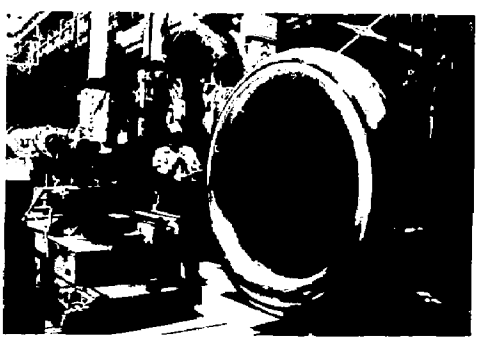

Fig. 17. Grinding the S-1 Spheromak flux core liner to 0.020-inch wall thickness. (84E1281)

Cryogenics Section

The Cryogenics Section was primarily involved with the many aspects of the 1070-watt helium refrigerator system for TFTR. This included installation and leak and vacuum testing of approximately 4,500 ft of ambient piping and cryogenic transfer lines in the cold-box/dewar area and in the Test Cell.

The cold-box work platform was modified to accommodate the turbine housing vacuum jacket isolation extension. Under the Cryogenics Section direction, Ebasco Services installed all electrical power services (4160 V, 480 V, and 110 V) to the compressor skids. They also installed all control and instrumentation wiring for the complete refrigerator system. A Request for Proposal[11] was issued to qualified bidders to operate and maintain PPPL's 1070-watt helium refrigeration system. Final selection of a qualified bidder and issuance of a one-year contract should be finalized early in FY85.

Coil Systems Branch

During FY84 the Coil Branch was selected as contractor for design and fabrication of the Oak Ridge National Laboratory's Advanced Toroidal Facility (ATF) coils. The program consisted of designing and fabricating six water-cooled coil stacks. Four are single coils and two are three coil units within a stack. The largest coil measures 20 ft in diameter. All six coil stacks use approximately 50,000 pounds of copper for fabrication. Figure 18 shows the winding of one coil. This is the first time the Coil Branch has undertaken a job of this magnitude for an outside laboratory. Completion of the job is scheduled for mid-FY85.

Fig. 18. Winding operation of a coil for the Advanced Toroidal Facility. (84E1490)

The Coil Branch was involved in a considerable amount of work for TFTR during FY84, some of which was "on call" work and some scheduled. A major scheduled job occurred during the TFTR shutdown. At that time, the entire toroidal-field lead and ring bus systems were checked and refurbished to bring them within a high level of insulation and contact integrity.

Coil Branch personnel fabricated and installed the mechanical support structures for the PF bus and lead systems. The effort will be continued and completed during the FY85 shutdown.

A total of 14 coaxial busbars were designed and fabricated for TFTR surface pumping panels. Multilam™ plug-in connectors are used to make the electrical connection between the busbars and panel (Fig. 19).

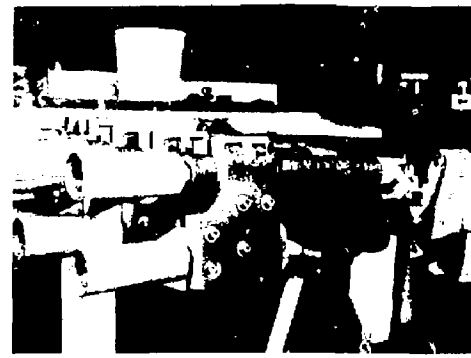

Fig. 19. Multilam™ plug-in connectors to make the electrical connection between the busbars and panel used in the TFTR surface pumping system. (84E0748)

Coil Branch personnel were also involved, during the fiscal year, in the proposal, development, manufacturing, testing, and installation of major components housed within the TFTR vacuum vessel. One area of endeavor has been the bumper limiter, which was designed to protect the inner wall of the vacuum vessel during operation when plasma flux densities reach up to 420 W cm^{-2} and local diagnostic neutral-beam depositions reach up to 1.2 kW cm^{-2}.

The bumper limiter consists of a backing plate with associated hardware that mounts the plate to the inner wall of the vessel. The facial surface of the backing plate is covered with compressed micrograin carbon graphite tiles which are covered with a titanium carbide film. A bar code system was procured to be used in tracking the 2,500 tiles, each with a specific installation location, through the processing and checking system. The programming and computer work was developed at PPPL.

Work began on the replacement of the defective S-1 Spheromak flux core liner (vacuum boundary) in early March (Fig. 20). The new liner to be installed on the flux core had one characteristic not shared with the original failed liner. The original liner spinning had been chemically etched from the inside to its final thickness. It was decided that, given the grain size of the "as supplied" Inconel 601, a slightly thicker unit was desired. In contrast to the chem-etching, the new liner halves were ground from the exterior to achieve final mean thickness. The Engineering Analysis Division proposed a 100-mil glass reinforced

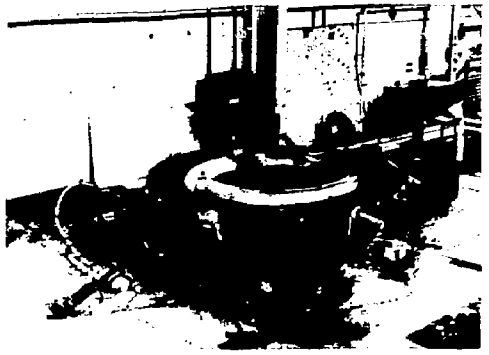

Fig. 20. Replacement of the defective S-1 Spheromak flux core liner. (84E0746)

polyester lining for application to the interior of the liner set. Their model demonstrated that the service life of the liner set could be substantially increased by the use of this suggestion. The Coil Branch chose to include the composite with the other modifications and, to date, the liner has served in a much improved manner when compared to the original set, thus allowing the S-1 Group to set new records in plasma temperatures and densities.

The Coil Branch participated in the design effort for the proposed Tokamak Fusion Core Experiment, which, in 1984, was a multi-laboratory effort centered at Princeton. This project developed four separate designs, all of which were to achieve ignition and long-pulse burn using standardized design constraints and assumptions. In two of the designs the toroidal-field coils were superconducting, while in the other two designs they were copper. The Coil Branch was a prime contributor to the copper toroidal-field coil designs. All the designs contained at least some superconducting poloidal-field coils. One of the chief objectives of this study was to reduce the overall cost by reducing the size (primarily major radius) of the machine.

Although the detailed superconducting design was done elsewhere [especially at the Fusion Engineering Design Center (FEDC) and the Massachusetts Institute of Technology (MIT)], the Coil Branch developed a method for determining the allowable current density of Nb_3Sn forced-flow conductors. The method is more comprehensive than previous ones and is implemented using spreadsheet software on a personal computer.[12] The resulting cavity current density is more ambitious than present-day Large Coil Program (LCP) coils.

COMPUTER DIVISION

During FY84 the Computer Division provided support to physicists and engineers at PPPL in many different areas. In support of TFTR, the amount of data acquired rose to 7.5 megabytes per shot, a VAX-based data reduction system was added, neutral beams were supported, and overall reliability was increased. In support of PLT/PBX/S-1 Spheromak, a supplementary VAX-based system was added to provide relief for the Digital Equipment Corporation KL-10 system and to provide a migration path for future system evolution. The personal computer is now being utilized as both a technical aid and a management tool.

A listing of publications by Computer Division personnel is given in Refs. 13-22.

New Software and Hardware for TFTR Support

The CICADA Central System

The CICADA (Central Instrumentation, Control, and Data Acquisition) system currently supports over 35 distinct systems of diagnostic and engineering applications on TFTR. Over 6,000 points in a total of 160 CAMAC [Computer Automated Measurement and Control (System)] crates are monitored every two seconds, and almost 4,000 points are controlled. For each shot, about 150 waveforms are automatically computed and available for display on 90 graphics screens or for transmission to another computer system for additional analysis.

The CICADA system was upgraded and enhanced to better support TFTR applications, and over all system reliability was improved. The following new system software support features were added in FY84:

- Software was developed for a block transfer system, which allows blocks of data to be shipped from CAMAC crates on TFTR over a communications link to central application computers;
- Software was added which allows a subset of the TFTR shot data acquired on the Gould-based CICADA system to be automatically transmitted to the DEC-based High-Level Data Analysis (HAX) system;
- A periodic scheduler was provided to permit trending of device values and periodic scanning and alarming;
- A prepulse data base was installed to record the status of all diagnostic devices at the time of a TFTR shot. It is used for physics interpretation;
- A crate status support system was developed to permit the user to be informed of the link status of a crate associated with a specified device.

Upgrades to CICADA systems software were performed in the following areas:

- Graphics speed to the operating stations was increased;
- Intercomputer task scheduling and synchronization support was streamlined, and action flexibility was increased;

- Data acquisition was accelerated by incorporating the high-speed communications block transfer path paralleling the CAMAC highway and the subsystem computers.

Hardware support in FY84 focused on enhancing and expanding the existing computer resources to better meet the needs of the TFTR Project. A major effort was devoted to providing support for neutral beams and diagnostics. Fiscal year 1984 enhancements were as follows:

- The CICADA hardware personnel installed 11 Terminal Operating Stations (TOS) and 8 Console Operating Stations (COS), bringing the total to 31 TOSs and 28 COSs;
- Seven and one-half megabytes of memory were added to the CICADA system in support of neutral beams and diagnostics. The shared memory was expanded from 2.5 megabytes to 3.5 megabytes;
- An additional subsystem computer was added;
- The block transfer host interface multiplexor was installed on the central level computers. This allows TFTR shot data to be transmitted from the tokamak to the CICADA system over a synchronous data link in large groups or "blocks." This transmission method improves the speed of the acquisition process and at the same time reduces the archiving process;
- More than 60 CAMAC crates were added to the on-line system, bringing a total of 160 crates on-line.

CICADA Neutral Beam, Diagnostics, and Facilities Support

The first two neutral-beam injectors were made operational in 1984. The CICADA system provides control and synchronization, as well as data acquisition and display, of the neutral beams. Through CICADA, the neutral-beam calorimetry system operates to measure the injected neutral-beam power and beamline power losses. And, the neutral-beam thermocouple system was installed to measure temperatures of various components affected by the neutral-beam injector.

The protective plate cooling system is now operating on TFTR. This system exists to cool down the tiles (or plates) that protect the inner wall of the TFTR vacuum vessel against damage that could result from neutral-beam injection. The CICADA system provides remote computer capability to control the cooling system.

The discharge fault system was implemented. This system monitors the TFTR discharge, and it sends signals to the other TFTR systems whenever there are any faults (or abnormalities) during a discharge. These abnormalities might include, for example, failures in the power supply system or the gas injection system.

Strain gauges were installed on TFTR to measure stresses on the experimental device. Readings are set and acquired via the CICADA system to allow cognizant personnel to study the structural characteristics of TFTR.

The TFTR safety system, which provides fire alarms and security alarms, was enhanced. The CICADA system can now detect a hazard in approximately 600 areas on TFTR. In addition, the radiation monitoring system was installed. This system consists of stand-alone PDP-11 microcomputers that detect and record the gamma and neutron radiation on the TFTR site.

The following new diagnostics were added to TFTR in support of plasma impurity studies: SOXMOS (Soft X-Ray Monochromator Spectrometer), the Impurity Injection System [also called the LITE, or Laser Injected Trace Element (system)], and VIPS (Visible Impurity Photometric Spectrometer).

The following diagnostics were implemented to support electron density and temperature studies: Michelson Interferometer (electron temperature), Fast Scanning Heterodyne Radiometer (electron temperature), MIRI, or Multi-Channel Far-Infrared Interferometer System (electron density), and Thomson Scattering (electron temperature and density).

The X-Ray Crystal Spectrometer diagnostic was installed to measure ion temperature.

The movable limiter position and water monitoring system is on-line.

Support of PLT, PBX, S-1 Spheromak, and RFTF

Software Support

During FY84 the DAS (Data Acquisition System) computer facility continued to operate at or near saturation; the PLT and PBX regularly averaged one and one-half to two megabytes or more per plasma discharge, and the S-1 Spheromak averaged approximately one-half to one megabyte per discharge. The DAS DEC System-10 achieved the first operational support of two experimental machines (PLT and S-1 Spheromak) running in real time, simultaneously. The DAS also achieved the first real-time operational use of the DAS VAX computer system (for S-1 Spheromak).

New diagnostics for the several experimental projects continued to be implemented at a rate of approximately two per month.

The DEC-based computers were all updated to incorporate UNIX software tools, which are user-friendly, state-of-the-art operating tools.

S-1 Spheromak Support

During FY84 a CAMAC "mailbox memory" interface was designed to allow the transfer of important parameters from the S-1 Spheromak control system to the DAS. An alarm system was developed and partially implemented to improve troubleshooting on

S-1 Spheromak. This system provides hardcopy reports for permanent record keeping. Gas pressure remote readouts are now available on the operating console display.

Radio-Frequency Test Facility Support

The programmable controller-based controls system installation was completed in FY84, followed by a successful power test.

New Computer Systems

Two new VAX computer systems were installed in FY84: the TFTR Off-Line Data Reduction System (RAX), and the DAS Supplemental System (DAX). These two computers, along with the High-Level Data Analysis System (HAX), are configured into a "cluster" network, such that they can share most disk storage capabilities and can also communicate with the large computing facilities at the National Magnetic Fusion Energy Computer Center.

The primary purpose of the RAX system is to reduce raw data acquired during TFTR shots to physics results. The primary purpose of the DAX system is to complement the DAS, which is the computer system utilized in PLT, PBX, and S-1 Spheromak experiments.

Use of the Personal Computer

The IBM Personal Computer (PC) is utilized as an engineering and scientific workstation and as a management tool. As an engineering tool, the PC is used as a stand-alone controller for TFTR vacuum vessel bakeout operations and for power conversion stand-alone testing. The IBM PC has been developed into a single user workstation computer/controller. It is used for performing off-line testing and development for other CAMAC (Computer Automated Measurement and Control) systems, and it is also used for stand-alone graphics.

References

[1]D. Weissenburger, "SPARK Version One: Reference Manual," Princeton University Plasma Physics Laboratory Report PPPL-2040 (1983) 228 pp.

[2]D. Weissenburger *et al.*, "Experimental Observations of the Coupling Between Induced Currents and Mechanical Motion in Torsionally Supported Square Loops and Plates, Part 1: Experimental Analysis," Princeton University Plasma Physics Laboratory Report PPPL-2158 (1984) 50 pp.

[3]D. Weissenburger *et al.*, "Experimental Observations of the Coupling Between Induced Currents and Mechanical Motion in Torsionally Supported Square Loops and Plates, Part 2: Data Inventory," Princeton University Plasma Physics Laboratory Report PPPL-2159 (1984) 100 pp.

[4]G.V. Sheffield, "Closed Expressions for the Magnetic Field of Toroidal Multipole Configurations," Nucl. Fusion *23* (1983) 1039.

[5]A.B. Ehrhardt, "An Application of Toroidal Multipoles to Facilitate Tokamak Reactor Studies," Princeton University Plasma Physics Laboratory Report PPPL-2112 (1984) 15 pp.

[6]R. Ellis, III and H. Yokomizo, "Design of Viewing Dumps for JT-60 Thomson Scattering System," Japan Atomic Energy Research Institute Report JAERI-M 84-157 (1984) 33 pp.

[7]S. Cohen *et al.*, "The PLT Rotating Pumped Limiter," Princeton University Plasma Physics Laboratory Report PPPL-2123 (1984) 16 pp.

[8]L.P. Ku, J. Kolibal, and S.L. Liew, "The Effectiveness of Building Wall Boration in Controlling the Neutron Responses in a Fusion Facility," in *Technology of Fusion Energy* (Proc. 6th Topical Mtg., San Diego, 1985), to be published.

[9]S.L. Liew, L.P. Ku, J. Kolibal, and K.W. Hill, "Shielding Analysis for the Horizontal X-Ray Imaging System," in *Technology of Fusion Energy* (Proc. 6th Topical Mtg., San Diego, 1985), to be published.

[10]S.A. Cohen, R.V. Budny, V. Corso, *et al.*, "The PLT Rotating Pump Limiter," *J. of Nucl. Mater. 128 & 129* (1984) 430.

[11]Request for Proposal 84-239G, "Services to Maintain PPPL's 1000 Watt Helium Refrigeration System," published by PPPL Procurement Section.

[12]P. Materna, "Comprehensive Design Procedure and Spreadsheet for Internally Cooled Cable Superconductors," IEEE Trans. Magn. *MAG-21* (1985) 1091.

[13]G. Bates, S. Bodine, T. Carroll, and M. Keller, "DAS Performance Analysis," Princeton University Plasma Physics Laboratory Report PPPL-2092 (1984) 47 pp.

[14]H.K. Feng and G.J. Bradish, "High Speed, Locally Controlled Data Acquisition System for TFTR," in *Fusion Engineering* (Proc. 10th Symposium, Philadelphia, 1983) Vol. *1*, IEEE Cat. No. 83CH1916-6 NPS, New York (1983) 345.

[15]K.W. Hill, M. Bitter, M. Tavernier, *et al.*, "The TFTR Horizontal High-Resolution Bragg X-Ray Spectrometer," Princeton University Plasma Physics Laboratory Report PPPL-2173 (1984) 19 pp.

[16]K.W. Hill, S. von Goeler, M. Bitter, *et al.*, "The Tokamak Fusion Test Reactor X-Ray Imaging Diagnostic," Rev. Sci. Intrum. *56* (1985) 830.

[17]J. McEnerney, G. Christianson, J. Montague, *et al.*, "TFTR Master Control and Master Clock System," in *Fusion Engineering* (Proc. 10th Symposium, Philadelphia, 1983) Vol. *1*, IEEE Cat. No. 83CH1916-6 NPS, New York (1983) 501.

[18]J. Montague, "Tokamak Fusion Test Reactor Facility Clock System," in *Fusion Engineering* (Proc. 10th Symposium, Philadelphia, 1983) Vol. 2, IEEE Cat. No. 83CH1916-6 NPS, New York (1983) 1965.

[19]L. Ratzan, "Towards a More Human Equation," in *Smithsonian Magazine*, Spring, 1984.

[20]N.R. Sauthoff, R.E. Daniels, and the PPL Computer Division, "TFTR Diagnostic Control and Data Acquisition System," Rev. Sci. Instrum. *56* (1985) 963.

[21]G.F. Schobert, "TFTR Hardwired Interlock System for Personnel Access Control," in *Fusion Engineering* (Proc. 10th Symposium, Philadelphia, 1983) Vol. 2, IEEE Cat. No. 83CH1916-6 NPS, New York (1983) 1238.

[22]G. Taylor, P. Efthimion, M. McCarthy, *et al.*, "Fast Scanning Heterodyne Receiver for the Measurement of the Time Evolution of the Electron Temperature Profile on TFTR," Rev. Sci. Instrum. *55* (1984) 1739.

PROJECT PLANNING AND SAFETY OFFICE

The Project Planning and Safety Office has three distinct organizational units for carrying out its responsibilities. These three units are the Planning Office, the Project Management Systems Group, and the Project and Operational Safety Office.

PLANNING OFFICE

In FY84, the Planning Office reviewed and updated the PPPL Technology Program Plan and prepared PPPL's FY83 *Technology Transfer Report*. These actions enabled PPPL to comply with Department of Energy Order DOE 5800.1, which implements Public Law 96-480 (The Stevenson-Wydler Technology Innovation Act of 1980). This Act requires government-funded research and development laboratories to establish a formal technology transfer program.

The Planning Office also served as a single point of contact for the Department of Energy concerning PPPL computer matters. A long-range automated data processing (ADP) plan was prepared, which outlined PPPL's FY85 to FY90 computing needs and proposed methods for satisfying those needs. A short-range plan, which addressed FY84 ADP procurements, was also prepared. At the beginning of the year, all ADP equipment and software purchases were reviewed by the office to assure that they were consistent with PPPL's ADP plans. Midway through the year, this responsibility was transferred to the Computer Division and Information Resource Management (IRM). In FY84 work was started on the preparation of a "PPPL Site Statement of Strategy for Microprocessors and Personal Computers."

Also in FY84, the Planning Office analyzed the anticipated work load on the technical labor force by reviewing the budget and personnel data bases. The analysis compared the projected FY84, FY85, and FY86 work loads with the current staff. Recommendations were then made concerning adjustments to the work load and/or staff so that a balance between the two could be achieved.

PROJECT MANAGEMENT SYSTEMS GROUP

Significant progress was made during the year towards the establishment of PPPL's Progress Measurement System (PMS) as a management tool which is used by both the project and engineering departments for cost and schedule control.

Four essential elements of the system are currently in place which provide PPPL with the vehicle to organize, plan, monitor, and control the work loads. Specific introductions during the year include:

- Standard software systems for estimating, monitoring, and reporting. Standard performance reports are issued monthly;
- Monthly progress statusing of each job by the cognizant engineer utilizing the bar chart progressing technique;
- Monthly variance analysis. Significant cost (earned value-actual expenditures) or schedule (earned value-plan) variances are formally analyzed and reported by the job engineer. Variances are highlighted and discussed at monthly management meetings;
- Baseline change control. Revisions to scope, schedule, or cost must be approved by management before changing the PMS/accounting data base.

Implementation of these subsystems now allows PMS to provide:

- Engineering Department management with staffing forecasts based on detailed, integrated, and computerized work estimates. This "first" at PPPL allows early identification of manpower requirements and potential manpower shortages which could impact project milestones (Fig. 1).

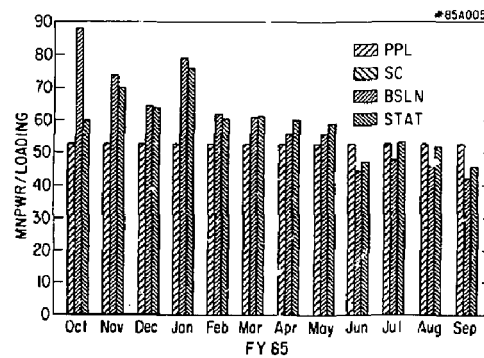

Fig. 1. Manpower distribution curve for Computer Division engineering labor. Note that the planned work (BSLN = Baseline) is in excess of on-board staff (PPL). This information triggered an in-depth review of this division's work plan and its impact on the TFTR Project.

JOB VARIANCE ANALYSIS REPORT

CC= 1350 WP= CV00 JOB#= 0110 TUPS DESCRIPTION 8/1/84 AS OF

T. STANKO JOB ENGINEER ( ) INITIAL REPORT ( ) FOLLOW UP

CUMULATIVE COST/SCHEDULE PERFORMANCE DATA

	PLAN	EARNED	ACTUAL	SCHEDULE VARIANCE	COST VARIANCE
	BCWS	BCWP	ACWP	BCWP-BCWS	BCWP-ACWP
	120 K	112 K	202 K	-8 K	-90 K

BUD= 154 K LRE= 243 K SPI= 0.93 CPI= 0.55

*** JOB EXCEEDS COST THRESHOLDS ***

PREPARED BY JOB ENGINEER:

VARIANCE DESCRIPTION - (cause & impact)

The cost and schedule variance were caused by a change in job scope which was requested by Operations. This new task involved the re-design and re-wiring of the cabling at B & C bay. This had highest priority and was completed in time to meet the scheduled TFTR pump down.

IMPACT ON OTHER JOBS? NO ( ) YES Diagnostic termination were delayed two weeks because all available manpower was used for this task.

RECOMMENDED CORRECTIVE ACTION PLANS

None

JOB ENGINEER DATE 8-25-84 DIVISION HEAD DATE 8/28/84

PREPARED BY CC MANAGER:

DIRECTED ACTION

COST CENTER MANAGER DATE

ATTACHMENTS:

( ) PMS '0 REPORT ( ) ACCOUNTING REPORT ( ) _____

( ) BARCHARTS ( ) PRIOR REPORTS ( ) _____

Fig. 2. Typical detailed variance report used to highlight cost and schedule variances, their causes, impact on other work, and corrective action.

- Management with an early warning of potential cost or schedule impacts at the summary or detail level (Fig. 2).
- Line managers, physicists, and engineers with a plan and schedule to work by and monitor (not just milestone date "promises"). By the end of FY84, 98% of DOE FY85 guidance had already been planned and approved, marking the first time in PPPL history that work was formally preplanned before entering the new fiscal year. This work is represented by over 650 project jobs with a total dollar value of $113.7 M (including G&A burdens equipment, and operating budgets). These budgets are based on integrated activity schedules, manpower estimates, and nonlabor estimates (Fig. 3).
- Divisions and projects with a formal method for requesting and authorizing new or revised work. This subsystem is electronically tied to accounting so as to prevent unauthorized work from accruing costs. This is another first which forces preplanning of work.
- The PPPL and DOE management with project status with respect to both cost and schedule, including projected year end costs (Fig. 4).
- Engineering and project managers with monthly charges to their divisions and projects.

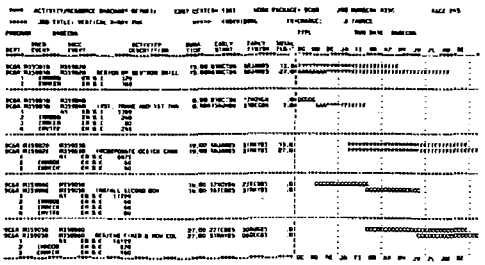

Fig. 3. Detailed work plan and current progress status for typical job. (Over 650 jobs exist within the Progress Measurement System data base.)

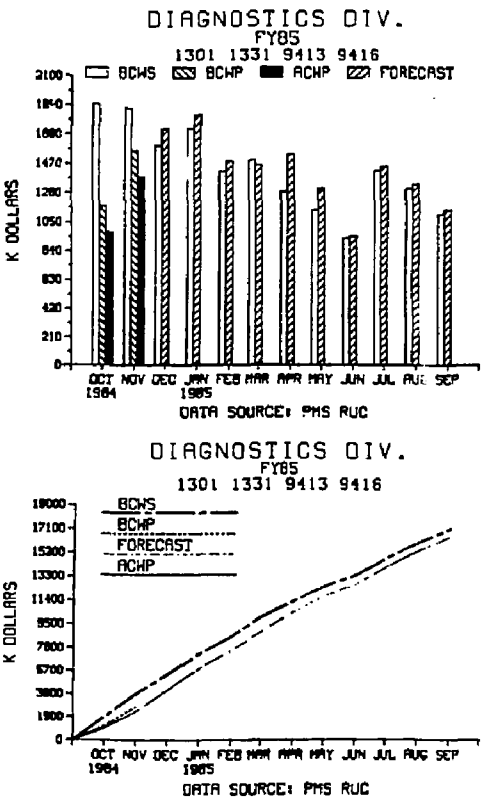

Fig. 4. Typical cumulative and incremental performance curves.

PROJECT AND OPERATIONAL SAFETY OFFICE

The Project and Operational Safety Office (P&OS) worked closely with TFTR and other PPPL projects; a heavy emphasis was placed on day-to-day

interactions and on close support of project personnel. A mechanical/cryogenic safety engineer was added to the professional staff. The second "Annual Environmental Report" was published. This document reported on PPPL's environmental monitoring program, on PPPL's compliance with government regulations and requirements, and on proposed expansion of the program.

Work was completed on Safety Assessment Documents (SAD's) for the PBX and the Radio-Frequency Test Facility. A system of active participation in timely reviews was implemented by P&OS for Facility Advisory Notices, Engineering Review Board Processes, Design Reviews, Installation Procedures, and Operational Procedures. The standard electrical construction specification was upgraded and expanded to streamline the review process for outside vendor specifications. The P&OS entered into an agreement with the Quality Assurance Program where Nonconformance Reports could be generated by P&OS on safety related deficiencies.

Radioactive analysis, which was initiated earlier, was done solely in-house starting in March. A review of the radiological environmental monitoring program was completed by the Idaho National Engineering Laboratory/EG&G, with minor recommendations from this review being placed into schedules for implementation. Discussions for a groundwater monitoring program were initiated, with plans for initiation in FY85.

QUALITY ASSURANCE AND RELIABILITY

The Quality Assurance (QA) Program, initiated in mid-1983, entered 1984 with an organizational structure, objectives, and a core group staff. The broad objectives were the implementation of selected control systems having obvious economic benefit and the building of the structure necessary for support of the then projected ignition device. While the changed fusion research environment had an impact upon 1984 QA organization and staffing plans, there were achievements in a number of areas that were of significant and lasting benefit to the Laboratory's existing projects. Several such enhancements, new services, or expansion of existing controls include:

- A new Receiving Inspection Facility (Fig. 1), located adjacent to the Warehouse 4 receiving area, was built, equipped, staffed with trained inspection personnel, and integrated into the procurement system. This activity is selectively utilized for the acceptance of critical or troublesome parts and assemblies, and it has resulted in measurable improvement in vendor quality levels for such items as vacuum components and assembled printed circuit boards.

Fig. 1. The Quality Assurance Program's Receiving Inspection Facility. (85A0284)

- Other elements of a purchased item quality control system were implemented and integrated into the total procurement system. These are (a) incorporation of appropriate provisions into contract documents during the preprocurement phase that provide increased control and management visibility, (b) selective vendor inspection and surveillance activities by PPPL Quality Assurance personnel, (c) utilization of DCAS (a DOD inspection agency related to DOE via an interagency agreement) inspection personnel at remote supplier facilities (this did provide expert source inspection and rapid problem feedback, essentially extending supplier control without simultaneously diluting technical or financial resources), and (d) a policy of QA telephone communication with suppliers immediately following the discovery of a discrepancy, resulting in increased supplier responsiveness and corrective action.

- A formal PPPL nonconformance reporting system was implemented to facilitate tracking of corrective actions and, via analysis of repetitive events, to identify those areas where management action could prevent recurrence.

- The TFTR Trouble Report system, the result of a joint QA and Project effort, became an important management tool. Weekly meetings of an ad hoc Working Group, consisting of the TFTR Project Manager, his key branch managers, and Quality Assurance were initiated. These meetings address all Trouble Reports (TR's) issued during the preceding week, assess the immediate response, and identify those areas where technical resources must be tasked to identify an underlying cause and to determine a long-term fix.

- The scope of routine inspection and quality control activity was expanded to support shop, construction, engineering, and project management need for independent verification and feedback. Given staffing constraints, the tailored application of resources and control strategies is determined by a simple, but formal risk assessment procedure.

Quality-related services in support of PPPL's primary objectives were markedly improved and expanded during 1984 (without an accompanying increase in staff) by extensive training of existing personnel and limited outside recruiting of missing technical skills.

ADMINISTRATIVE OPERATIONS

In FY84 the emphasis within Administrative Operations was on improving the quality of administrative and support services while reducing Laboratory overhead costs.

A program to reduce the discretionary overhead expenses of the Laboratory by 10% was established and discussed with DOE in August 1984. Examples of the cost control measures are: the integration of the emergency services and security forces; vigorous energy saving programs; better planning and scheduling of plant maintenance projects; tightened overtime controls; use of user-access data files for budgeting, accounting, and personnel activities; and implementation of a decentralized administrative computer network. These and other cost reduction activities are described more fully below.

Other actions of note in FY84 are:

- Management by objectives was introduced throughout Administrative Operations.
- A Laboratory Institutional Plan, setting forth program and administrative support options for the five-year period FY84-89, was prepared and forwarded to DOE.
- Quarterly reviews of indirect costs of the Laboratory were initiated. They involved project and departmental managers throughout the Laboratory, as well as overhead managers.
- A top-level Budget and Manpower Committee was established. Improvements in the manpower and budget controls and the decision process were made.

In FY84 the total Laboratory staff increased by 30, from 1,257 to 1,287, and was composed as follows:

Faculty	2
Physicists	119
Engineers	275
Technicians	561
Other	330
TOTAL	1,287

The direct employment increase was related to the skills required for planned improvements in TFTR capabilities and for meeting the demanding research milestones on TFTR and other experimental devices. In April 1984, temporary subcontractor employment at PPPL peaked at 315 and declined to 151 six months later. At year's end, reduction in both the direct and subcontractor staffs was underway, commensurate with the decline in funding available to the Laboratory.

ADMINISTRATION DEPARTMENT

Plant Maintenance and Engineering

The Plant Maintenance and Engineering (PM&E) Division is a technical and administrative support organization. Its function and purpose is to support the Laboratory's research programs by operating, repairing, constructing, and modifying physical facilities, systems, and equipment at A-, C-, and D-Sites and at several buildings at B-Site. Table I shows the gross square feet (GSF) maintained by PPPL at each site during FY84.

Table I. Gross Square Feet (GSF) by Site Maintained by PPPL during FY84.

Location	GSF
A-Site	209,911
B-Site	140,088
C-Site	450,363
D-Site	214,173
Trailers (C- and D-Sites)	18,470
TOTAL	1,032,905

Project Engineering

During the year, the Project Engineering Branch was reorganized and expanded to provide more effective project coordination and control and the timely implementation of projects. Two new engineering managers were added: one to manage the energy program and the heating, venilation, and air conditioning (HVAC)/mechanical projects, and one to manage building projects (civil/structural function).

The Project Engineering Branch assumed, during FY84, the responsibility for planning, engineering, and coordinating GPP (General Plant Projects)-funded

projects. Table II summarizes the number and value of active projects at midyear.

Table II. Project Summary.

	Number of Projects	Value ($K)
Energy Conservation		
Retrofits		
Previous fiscal years	9	$ 991
Current FY84	4	773
Studies	4	209
	17	1,973
General Plant Projects (GPP)		
Authorized		
Previous fiscal years	3	1,504
Current FY84	10	1,085
Proposed FY85/86		
Conceptual Design Studies	12	130
	25	2,719
Other Engineering Support	44	1,055
TOTAL	86	$5,747

Energy Conservation

The Laboratory's energy management and conservation activities increased significantly in FY84. This was primarily due to the increased implementation of energy retrofit projects and an intensified effort to address energy conservation opportunities in physical plant preventative maintenance operations. The results of these intensified activities produced a 42% reduction in the FY84 Laboratory Buildings Energy Utilization Index (Btu/ft^2) versus the 1975 Base Year. Thus, PPPL not only met but exceeded the energy use reduction goals established in Executive Order 12003 on July 20, 1977. This reduction, when normalized (FY84 versus 1975), resulted in a savings of $917.4 K in electric and $1.2 M in fuel oil costs. It is evident that this achievement required: the full commitment and support of management; the cooperation and efforts of a large number of Laboratory personnel employed in all disciplines at the Laboratory; implementation of many cost-avoidance projects; and the use of innovative engineering techniques during the year.

Energy conservation efforts in physical plant equipment operations resulted in: improvements in the quality of chilled water and make-up water delivery, improvements in the fresh air economizer systems/cycles, improvements in overall HVAC surveillance and inspections, and improvements in boiler efficiency by central plant oxygen trimming; a reduction in steam and condensate losses; the implementation of an off-hour light-extinguishing program by the Security Office.

Examples of energy retrofit projects under way in FY84 are: the energy monitoring and control system, the outside air economizers, the night temperature setback systems, the C-Site lighting efficiency upgrade, the central chiller plant optimization controls, and the efficient boiler chemical feed tanks.

To keep maintenance personnel up to date in energy conservation equipment operations and procedures, periodic training sessions were conducted. In addition, special in-depth energy conservation symposia/seminars were attended by PPPL engineers in order to further enhance and to implement energy management and conservation measures. Throughout the Laboratory, the employee energy awareness program provided additional energy savings and cost avoidance. In recognition, commendation letters were issued to employees making energy savings suggestions.

During FY84, nine employees received drivers energy conservation awareness training (DECAT). The Laboratory also encouraged employee ride sharing/car pooling. Out of approximately 1,270 Laboratory employees, approximately 203 participated in this form of energy conservation, and a survey showed that an additional 58 employees were interested in participating in the program.

Public relations interface with Laboratory staff was maintained through the *PPL Hotline* newsletter. With the DOE theme, "Partners in Energy," Energy Awareness Week was conducted at the Laboratory in October. Posters encouraging energy conservation were displayed on bulletin boards throughout the Laboratory. Overall, employee cooperation and energy conservation awareness was high. All of this contributed to an effective Laboratory-wide energy management and conservation program.

Plant Maintenance

The PM&E Division's work load has increased significantly over the past five years, with the construction of the Tokamak Fusion Test Reactor (TFTR) and the addition of numerous support facilities. Fiscal year 1984 saw 4,467 service calls, 3,024 major (requiring more than eight hours of labor to complete) work orders, and 1,318 preventative maintenance (PM) work orders, for a total of approximately 94,000 scheduled man-hours, as compared to approximately 65,000 scheduled man-hours in FY78. In addition, during FY84, organizational restructuring throughout the Laboratory resulted in approximately 214 office moves. With many of these moves, renovation and facility upgrading were incorporated to enhance the working and safety environment.

A computer-based work order system, capable of handling the increased demand for planning and scheduling of the work load, was developed in-house and was operational as of October 1, 1983. It provides for instant call-up of any project and reports its status with weekly updates. Monthly status reports are sent to each requestor. This system enabled plant management to accumulate various information

accurately for the first time. Examples of the types of information available are: listings of work orders by requestor, by site location, by safety-related items, by estimated hours, by actual hours, and by percentage of work orders completed within an allotted time frame. This information is used to measure management-by-objectives goals. It also gives accurate accountability of work load by each craft group. Weekly schedules based on computerized backlogs were established with improved accuracy. By charting the backlog and by using temporary employees during peak periods, Plant Maintenance reduced the peaks in the backlog. Total backlog and ready-to-run (all materials are in stock and work scheduling can occur when craftsmen are available) backlog were reduced from a high of 12 weeks and 8 weeks to 6 weeks and 3 weeks, respectively. Additionally, using a basis of ready-to-run and total backlogs allowed a quicker and more accurate prediction for requestors of when service could be provided.

A word-processor-based preventive maintenance (PM) program for C-Site was designed and developed during FY84. The system automatically schedules and prints out routine preventative maintenance tasks for 580 pieces of equipment at C-Site. These tasks represent 374 work orders per year and 5,206 man-hours of effort. A D-Site computerized PM program, which is a purchased system, generates 622 work orders and 9,000 man-hours of effort per year. An in-house manual (to be computerized in FY85) PM program for A- and B-Sites generates 322 work orders and 4,400 man-hours of effort per year. All site systems retain a maintenance history of each piece of equipment with detailed information on description of work done and costs of labor and material. Periodic review of the history now enables maintenance management to analyze equipment in relationship to cost of upkeep, durability, and predictive replacement. When consolidated into one computerized system of improved, well-defined PM procedures and finite scheduling, equipment downtime will be reduced to an absolute minimum and will save approximately 6,000 man-hours of labor a year.

A physical plant upgrading of the facilities at C-Site was undertaken with the replacement of roofs at C-Site. Thirty-six thousand square feet of built-up roofing were replaced with single-ply roofing systems. These roof replacements of the Lab Wing, RF 3rd floor, RF 4th floor, and the PLT/PDX Control areas have resulted in no major roof leaks or downtime in the affected buildings. Because of the amount of roof-mounted equipment and the heavy pedestrian traffic, the single-ply system with ballast overlay has proven invaluable in low-cost roof maintenance.

Maintenance Training

In-house training in maintenance procedures continued to receive strong support in FY84. Ten PM&E employees attended in-house classes for two hours, twice weekly for an eight month period. This was the seventh year that these vendor-designed (Technical Publishing Company) courses were given. Safety training continued to receive strong emphasis, with all PM&E mechanics attending monthly training sessions on various safety-related subjects. Additionally, the need for special instruction on specific equipment was recognized, with training provided for pyrotronics and radiation safety.

A general apprentice program, with emphasis on training minorities, planned by a group of PM&E managers, supervisors, and technicians, completed its second year. The program is specifically designed to produce well-rounded general maintenance mechanics, and it is the first of its kind in New Jersey to receive State and Federal certification. The program is well organized and established, and there have been noticeable advancements in the work of the apprentices.

Maintenance Safety Support

An intensified safety program in FY84 resulted in 409 safety-related work orders being issued that totaled 2,887 man-hours of effort. These identified safety work orders were completed in the minimum amount of time, with accurate tracking and reporting made possible with the computerized work order system. This effort contributed to a drop in the Laboratory-wide Safety Performance Index from 7.5 to 1.9. The PM&E Division established a record of 243 days without a lost-time accident.

Library

This was a year of transition for the PPPL Library as Elizabeth Graydon, Plasma Physics Librarian for 22 years, retired on 30 June 1984. Her position was assumed by Jane Holmquist, and Rhoda Stasiak was hired as the new Assistant Librarian.

Library operations and activities continued apace as approximately 3,000 books and 600 technical reports were circulated to the PPPL staff. A total of 325, or 9% of these materials were borrowed from other libraries. Also obtained from outside sources for the PPPL staff were 2,300 journal articles. Computerized literature searches increased by 80% to a total of 275, and the DOE/RECON and LOCKHEED/DIALOG bibliographic systems were also used extensively to answer reference questions.

A total of 225 new books, 305 bound journals, and 2,100 microfiche were added to the PPPL collection, bringing the cumulative totals to 10,000 bound volumes and 31,400 microfiche. A total of 1,300 journal articles and 800 technical reports were cataloged by the PPPL librarians, and cards were produced for the card catalog and monthly acquisitions lists.

The possibility of cataloging the journal articles and technical reports on-line and providing Laboratory-wide access to this file is currently being investigated.

Telecommunications

The role of the Telecommunications Office is to provide the Laboratory voice communication services that are cost-effective and efficient. With this as its goal, the Telecommunications Office completed the following:

- Radio communication studies for the conversion of the existing VHF system to UHF. The studies were started in FY83, with DOE consultants, and established the need to convert radio coverage in all areas of the Laboratory. Installation and implementation is expected to be completed in FY85.
- Specifications for the proposed digital telephone system to replace the current Centrex. Approved by the DOE, the contract will be awarded during the third quarter of FY85 and the system installed during early FY86.
- Cost-effectiveness tests of the Federal Telecommunication System (FTS). The results indicated better costs control using commercial lines versus FTS, with marginal savings. Comparison data was provided to the DOE; it was decided that FTS would be reinstalled while the DOE and General Services Administration continued their studies.
- Contract award for an emergency evacuation system. The system will have the capacity to interface with the public address system at D-Site; thus C- and D-Sites will be assured personnel safety in the event of emergencies resulting from fire, smoke, fumes, power failure, or natural calamities. Contract is scheduled for completion in FY85.
- Studies to install a 30-station intercom system in the TFTR complex Approved by DOE, the system will be installed during FY85.
- Thirty-five hundred requests for moves, installations, and changes in the telephone service.

The impact of deregulation and divestiture of AT&T, effective January 1, 1984, has had a major effect on the Telecommunications Branch. Changes in policies and procedure occurred at that time and have continued throughout the year. The need for more complex record keeping, coordination between the many vendors, and budgetary problems have contributed to a challenging environment.

Information and Administrative Services Branch

The Information and Administrative Services Branch includes all Laboratory services supporting the preparation and dissemination of information pertaining to PPPL's program. Included are photography, graphics arts and technical illustration, word processing, printing, technical information, and public and employee information. Also, various administrative services—specifically, reception, mail, travel, and food services—are also provided. In FY84 a conference coordination service was added.

Public and Employee Information

The Public and Employee Information Section of Information and Administrative Services is responsible for providing up-to-date information on PPPL's program for members of the general public, the press, representatives of government and industry, and employees of the Laboratory. The section maintains an information kit consisting of brochures and information bulletins that are written for the layman. An employee newsletter, *PPL Hotline*, is published twice monthly. The staff coordinate an active speakers bureau, Laboratory tour program, as well as press relations and community outreach activities.

In October 1983, PPPL hosted a meeting of the New York area section of the National Association of Science Writers (NASW). A day-long briefing on the U.S. fusion program was conducted. The meeting was well attended by members of the state and local press.

The press were also invited to a news conference held at PPPL in January 1984, in conjunction with a meeting of the International Atomic Energy Agency (IAEA) Technical Committee on Operating Plans for Large Tokamak Experiments. The attendees were given an opportunity to learn the status of the large Tokamak programs, including the Joint European Torus (JET), Japan's JT-60, the U.S. TFTR, and the Soviet Union's T-15. Representatives of these programs were available for interviews at the news conference.

In January 1984 an updated version of the TFTR brochure, originally issued in FY76, was published. Printing this four-color brochure was made possible by grants from Ebasco Services, Inc., Grumman Aerospace Corp., Pennsylvania Power and Light Co., and Public Service Electric and Gas Co. The objective of the book was to familiarize the general public and industry with the TFTR device and its objectives.

In late FY84, the updating and upgrading of PPPL's slide/sound show for public tours was undertaken. Plans called for the original single-slide/sound system, produced in 1978, to be replaced by a multi-image show. The goal is to provide a clear, concise introduction to PPPL's fusion program for visitors, including community groups and area school students. Completion was scheduled for mid-FY85.

The Princeton Plasma Physics Laboratory's Community Outreach Program, established in FY82, was continued in FY84. The goal of the program is to foster a broad base of local public understanding of the work at PPPL and to forge closer communication links with local government, industry, and educational groups.

Fiscal year 1984 Community Outreach activities included the continuation of the popular monthly

TFTR Open Houses, attended by an average of approximately 100 people each month. The Open House tours were held in addition to PPPL's existing tour program. During CY84, 300 tours for approximately 6,000 visitors were arranged upon request. Meetings with representatives of local business and government were continued to provide these groups with an overview of PPPL's fusion program and a tour of TFTR. Several groups of teachers from area schools attended similar programs throughout the year.

As in the previous year, PPPL participated in the Scientist-Science Teachers Interaction Project during the summer of 1984. A physics teacher from a nearby high school spent one week at the Laboratory interviewing and working with a variety of technical specialists. On the basis of his experience, the teacher developed a series of lesson plans on fusion energy for use in the classroom.

The Princeton Plasma Physics Laboratory's Summer Work Grant program was started during the summer of 1984. Under this program, five outstanding high school students were provided work experience assisting PPPL scientists or engineers in research or technical projects. The students and their Laboratory supervisors found the program to be extremely beneficial. Plans were developed to expand this program to include more students and schools during summer 1985.

Graphic/Photographic Services

Fiscal year 1984 saw a continued increase in the volume of production in the graphic and photographic services provided by the Information and Administrative Services Branch. Production in the Graphic Services Section increased approximately 23% over FY83. The demand for photographic services was up 10.2%. Both of these increases came on top of increases during FY83 over FY82 of 18% for graphics and 5.5% for photography. The significant rise in demand for services in the last two years is attributable to increased volume in the documentation of experimental results.

Printing Services

In the printing services area during FY84, some of the offset press equipment was phased out and replaced with a modern, high-speed Xerox 9500, V.R. duplicator. This enabled two high-speed duplicators, the Xerox 9200 and Xerox 9500, V.R., to operate at the same time, with a stripped down version of the remaining offset press used for forms production and equipment backup. Having two high-speed duplicators increased turnaround capability, improved quality, and provided for greater control of various printing features (reduction, density, contrast, etc.).

Total Print Shop production increased from 4,089,805 impressions in FY83 to 5,564,093 impressions in FY84, an increase of 36%.

Word Processing Activities

The configuration of the word processing network at PPPL, in place at the end of FY83, remained essentially the same throughout FY84. This included two physically separate NBI networks: one large NBI OASys 64 network that serves C-Site and another smaller OASys 64 that serves A- and B-Sites.

Links to the word processing networks, however, continued to increase in FY84. Approximately 14 terminals and nine printers were added to the NBI network, which brought the total number of word processing peripherals to 92. This provided additional word processing capability in the following areas: TFTR Operations, Academic Affairs, the Research Department, Plant Maintenance, Technical Systems Division, PLT, PBX, TFCX, Quality Assurance, and Personnel.

The additional capacity for word processing at the Laboratory resulted in a total production of 164,240 pages, which was a 313% increase over FY83. Of this total, the Word Processing Center contributed 26,295 pages or 16% of the total as compared to 53% of the total in FY83. Although the Word Processing Center share of the total decreased as expected, the Center's FY84 production remained roughly equal to its FY83 production.

In-house training on NBI equipment was provided by Word Processing Center personnel. Approximately 19 new operators were trained in FY84. Training included both basic word processing functions and advanced features such as equations, records sort, statistical math, spelling verification, and communications.

Both NBI networks have dial-up communications capabilities that enable the electronic transfer of documents from NBI-to-NBI as well as between different makes and models of word processors and personal computers. In FY84, PPPL demonstrated successful communications between NBI and NBI, Wang, Micom, the Commodore 64, and the IBM PC. In addition, the C-Site NBI network is hardwired to PPLNET, the Laboratory computer network, which enables the transfer of documents with the USC and VAX cluster. A formatting program, resident on the USC, was developed allowing PPPL staff to make the cleanup of documents downloaded from the computer easier and more efficient.

In January 1984, a detailed maintenance log was created for all NBI equipment. From these records it was determined that during normal working hours the average up-time for each OASys 64 unit was: MUTT, 96.4%; JEFF, 99%; and A-Site, 99%.

Administrative Services

The Administrative Services Section also experienced an overall increase in activities during FY84. Mail deliveries were increased from one to two daily

in four buildings, due to relocations of key groups and the volume of mail generated by them. The mail route was also extended to service nine buildings and trailer units not previously served. Trips arranged through Travel Services increased in number by approximately 38% over the previous year. Equipment activities included acquisitions to upgrade copiers in key areas and to provide equipment in areas not previously served.

Conference Coordination

In January 1984, a conference coordination function was established within the Information and Administrative Services Branch, recognizing the need for a centralized service to support large PPPL-sponsored technical meetings held both on and off-site. The responsibilities of the new office include: assistance in the selection of locations for off-site conferences; negotiation with hotels; administration of conference budgets; coordination of arrangements including mailings, transportation, security, food service, and publications; and supervision of support staff during the meetings.

During FY84, four meetings were coordinated on-site: The IAEA Technical Committee on Operating Plans for Large Tokamak Experiments, 16-20 January; the US-Japan Joint Symposium on Compact Toroid Research, 20-23 February; the TFCX Preconceptual Design Review, 6-8 June; and the TFTR/JET INTOR Workshop on Plasma Transport in Tokamaks, 9-10 June.

One meeting was coordinated off-site: the NATO Advanced Study Institute's International Course on the Physics of Plasma-Wall Interactions in Controlled Fusion, 30 July-10 August in Val-Morin, Québec, Canada.

Patent Awareness Program

During FY84 there were thirty-five Invention Disclosures submitted to DOE. Based on previously submitted PPPL Invention Disclosures, DOE prepared seven patent applications, which were executed by the PPPL inventors and then filed with the U.S. Patent and Trademark Office. Five patents were issued to DOE for PPPL inventions during this time period. As part of the Patent Awareness Program initiated in 1981, the Committee on Inventions awarded 64 PPPL inventors with cash and certificates and honored the inventors at an Annual Awards Banquet. The invention disclosure titles and inventors for FY84 are listed in the Table on PPPL Invention Disclosures.

Personnel

Major programs and activities of the Personnel Division enacted during FY84 were the following:

- Princeton University introduced Health and Dependent Care Expense Accounts, which were implemented by the Benefits Section. Employees were also given the option of participating in the programs provided by Health Maintenance Organizations (HMOs) of New Jersey/Pennsylvania.
- The Compensation Section revised and expanded its market survey base and effected several new procedures for analyzing compensation survey data, including the benchmarking approach. Also, the annual merit review cycle was streamlined and computerized along with the annual University Personnel Audit.
- The Employment Section coordinated and implemented a Job Training Program for Minority and Economically Disadvantaged Youths. The program is guided by the Job Training Partnership Act and is the principal statute authorizing job training and other employability development programs for the unemployed. During the summer of 1984, four youths were employed and given extensive on-the-job training.
- The Employment Section implemented the Minority College Recruiting Program in order to identify qualified female and minority undergraduates in the disciplines of Computer Science, Electrical Engineering, and Mechanical Engineering.
- Employee Relations initiated a Laboratory-wide development program, Managing Personal Growth (MPG), with Blessing-White, Inc. Emphasizing personal growth in staff members' present positions, the program stresses strengthening communications between staff/managers to enhance the value of work performance and productivity of employees. A version of the MPG process was tailored for secretaries and office support positions and offered during October-November 1984.
- The Employee Relations Section reestablished the Work Area Visit Program. The Manager of Employee Relations made scheduled visits to work areas, informally meeting and speaking with employees to discuss individual concerns.
- The Employee Relations Section and Occupational Medicine and Safety implemented an Employee Assistance Program whereby staff members are helped to resolve personal problems when those problems affect their work performances. In this joint venture with the Family Service Agency of Princeton, an employee may elect to receive assistance—limited to three counseling sessions—with marriage problems, marital separations/divorce, difficult parent-child relationships, alcohol or drug abuse, and other emotional difficulties.

Occupational Medicine and Safety

The Occupational Medicine and Safety Division (OM&S) continued to institute new programs and to

adjust them to meet more closely the needs of the Laboratory.

As a result of the combined efforts of management, employees, and OM&S, a significant decrease in serious injuries and in all injuries was realized. The Safety Performance Index used by DOE, an integrated accident frequency and severity rate, fell from 8.3 for FY83 to 2.5 for FY84. The lower the figure, the better the accident experience.

Major projects addressed by the various components of the Division are described below.

Medical Branch

A manual system of identifying and tracking individual employees, who require specific periodic medical surveillance procedures, was devised and implemented. Eligible staff were members of the Emergency Services Unit and employees with potential exposure to harmful agents, such as noise, radio-frequency energy, tritium, and lasers. In the future, this tracking system will be automated.

The diagnostic and therapeutic capabilities of the dispensary were enhanced by the installation of physical therapy equipment, a computerized electrocardiographic analysis system, and the use of a contract analytical laboratory for blood tests.

In cooperation with the Emergency Services Unit, a computerized cardiopulmonary instruction and examination system was installed on a trial basis. More instructional flexibility and economies in personnel time are anticipated from its use.

In cooperation with the Personnel Division, an assessment was made of the needs of and advantages to the Laboratory for a therapeutic program for employees whose productivity and effectiveness are impaired by emotional and/or social problems. The University's program for such needs was reviewed. Based on the Medical Branch's findings and recommendations, management approved such a program for PPPL, and an outside organization was retained to provide counseling services. Employees who express a desire for such assistance are evaluated by the Personnel Division or the Medical Branch and, if approved, are referred to the counseling organization.

Safety Branch

An experienced safety professional with a graduate degree in industrial safety joined OM&S and was later promoted to Manager of the Safety Branch. An analysis of the Laboratory's accident experience and the priorities and orientations of the existing safety program suggested a redirection of efforts from the construction and project-oriented areas to that of industrial safety. This has been done in cooperation with the Project and Operational Safety Office and with the Department Safety Officers.

The Deputy Departmental Safety Officer of Administrative Operations, with the support of OM&S, undertook the expansion of the Safety Manager/Area Safety Coordinator system to a Laboratory-wide program. This program places the emphasis for safe working conditions and procedures at the employee-immediate supervisor interface. Late in the year, direction of the program was gradually phased from Administrative Operations to OM&S.

The safety training program of the Laboratory was expanded and intensified through the use of outside instruction organizations. Classes in safe lifting techniques and advanced electrical safety were presented by contractors. As part of the lifting instruction program, several PPPL employees were trained as instructors and have since presented classes. The use of outside contractors for instruction will be increased in FY85.

Industrial Hygiene Section

New Jersey's Worker and Community Right-to-Know Law became effective August 29, 1984. As a research and development laboratory, PPPL is exempt from a number of its provisions. However, the Laboratory is required to label containers, to instruct employees in safe handling of chemicals and the signs and symptoms of overexposure, and to establish liaison with local fire services. Since the Laboratory has been doing much of this already, coming into full compliance presented no difficulty. Plans have been made to computerize the hazardous materials control system in FY85.

A hazardous materials purchase control procedure, in cooperation with Purchasing, was implemented and requires reviews of potentially injurious materials by the Industrial Hygiene Section. Arrival of hazardous material is noted, screened for unsafe qualities, and, if approved, members of the Industrial Hygiene Section advise supervisors of safe handling procedures.

Emergency Services

Fiscal year 1984 was a significant year for the Emergency Services Unit (ESU); the ESU consolidated with Security personnel to form one diversified group, Emergency Service Officers trained to respond to fire, first aid, and hazardous material incidents and to provide security coverage to Forrestal Campus. This program will optimize use of personnel and reduce costs of two labor-intensive organizations. It has, in fact, reduced the ESU/Security expenses by $250,000.

During this period, the ESU purchased a new Rapid Intervention Vehicle (RIV) which carrys a payload of fire extinguishing agents consisting of 100 gallons of Aqueous Film-Forming Foam and 450 pounds of Purple K Dry Powder. Application may be implemented by either a twin-agent, front-mounted automatic turret or manually, using a twin-agent fire hose from the rear of the vehicle. In addition, the ESU obtained a used rescue truck from the Brookhaven National Laboratory and two vans—one for a mobile command post and the other for hazardous material response

purposes. The procurement of these excessed, used vehicles provided the ESU with special emergency equipment for response to all emergency situations and, at the same time, reduce purchase expenditures.

During FY84, the ESU loaned employees to various divisions and departments throughout the Laboratory to assist in special assignments and authorized work and to fill in whenever a nonemergency job was required. This work-loan program accounted for a 75% productive time disbursement to various units, such as TFTR, Security, Receiving Warehouse, Stockroom, Occupational Medicine & Safety, Plant Maintenance and Operations, and other offices that needed additional manpower. Further, the ESU conducted a comprehensive survey identifying all hazardous chemicals and their locations within PPPL.

Other tasks performed by the Unit during the year include:

- Certifying 275 employees in CPR,
- Recertifying 178 employees in CPR,
- Training 38 employees in basic first aid,
- Training 287 employees in basic fire extinguisher usage,
- Issuing 1,244 flame permits,
- Issuing 51 penetration permits,

and responding to:

- 58 first aid calls,
- 63 fire calls, and
- 3 hazardous material calls.

The ESU provided an update of the Emergency Preparedness Plans which involved implementing 54 individual building evacuation routes and preparing assembly area placards throughout Forrestal Campus.

Procurement

In October the Procurement Division was represented at an Office of Fusion Energy (OFE)-sponsored Fusion Procurement Seminar held in Oakland, California. The seminar was beneficial in that personal contacts and relationships were established among the participants, and a better understanding was gained of the procurement practices, successes, and problems at each of the other laboratories.

In February the Procurement Division held an open-house for Small Socially and Economically Disadvantaged and Women-Owned Businesses. This provided the attendees an opportunity to tour the facilities and to meet one-on-one with procurement and technical personnel from the Laboratory, as well as representatives of the Small Business Administration from the Department of Labor and representatives of the Department of Energy. A total of 175 people representing 127 businesses attended. As a result, 70 new businesses were added to PPPL's bidders' list.

In March the Procurement Division published a *Requisitioner's Manual.* The purpose of the manual is to provide requisitioners with a guide for the proper completion of a requisition so that the goods and services required may be obtained in a timely manner.

In May a surveillance review of the procurement system was conducted by the Princeton Area Office of the DOE. As a result of this review, the adjectival rating was upgraded from Satisfactory to Good. Subsequently, in July, the Laboratory's authorization to enter into fixed-price competitive procurements without prior DOE approval was increased from $250,000 to $500,000. All other previously approved authorization levels were unchanged.

Materiel Control

The primary focus of Materiel Control's efforts during the past year was again on improving the Laboratory's control of capital and sensitive property. A comprehensive property management plan was developed and implemented, and the Laboratory Council endorsed a property accountability policy that was issued as a directive. The first Laboratory-wide equipment custodian meetings were held, with periodic meetings scheduled throughout 1985. A key Laboratory objective is the DOE's approval, late in FY85, of the Laboratory's property management system.

Stockroom sales for FY84 reached $1.9 M with 126,000 stockroom withdrawals being made by users. The turnover ratio of inventory was an improved 2.1 to 1, and the reorganization of the stockroom inventory is 90% complete. Storage of bulky items continued to be a problem; the C-Site storage shed scheduled for completion in mid-1985 will help alleviate this problem.

In the Warehouse, over 20,000 receipts, deliveries, and shipments were made in support of Laboratory requirements. Storage space needs for equipment and supplies being held for projects continued to grow, and projects were undertaken to identify and obtain new storage areas. The Spares Parts Section, consisting of process, device, and maintenance spares, processed $2.3 M in withdrawals, $2.5 M in receipts, and had a combined inventory value of $9.3 M with 12,000 line items.

Walk-through inspections were conducted within the Laboratory to identify and dispose of excess/surplus property. During the year, over $184,000 in materiel and property were excessed to other laboratories or retired. The Excess Property Section brought in (for the cost of transportation only) 26 items valued at $183,000 to apply against Laboratory requirements. Effective controls over the disposal of scrap material resulted in $29,000 being received from the sale of scrap. The Hazardous Materiel Section disposed of 429 capacitors, 2 PCB transformers, and other types of hazardous material, while making 17 shipments to approved disposal facilities. Property administration processed over 10,000 equipment transactions in support of the Laboratory's efforts to control property and completed physical inventories of all capital and sensitive assets in accordance with DOE requirements.

CONTROLLER'S OFFICE

In FY84, the Controller's Office continued its effort to integrate the financial management procedures of the Laboratory and to pursue a systematic approach to data management. The integration of the various management systems that exist in the organization has offered interesting challenges and has sometimes resulted in unexpected advantages. Serious attempts have been made to address the problem of data mismatch or divergence. When the same data is entered into two systems independently with a different objective, for example between payroll and the personnel system, it often results in divergent data. The integration of the data into PUBSYS, a system accessible by most PPPL staff members, has largely eliminated these problems. In addition, most of the Laboratory data management systems have been organized through a public data base so as to make available current data to most users.

Accounting and Financial Control Division

The new Accounts Payable System, which permits direct computer transmission of accounting information from the PPPL Computer System to the Princeton University Main Campus Computer System, was implemented in October 1983. This has resulted in decreased processing time for payments and has improved coordination of the data in the two systems. The PPPL Accounting Procedures were revised in anticipation of the new DOE Letter of Credit to be used by Princeton University starting January 1, 1985.

Various segments of PUBSYS were used in account analysis and report preparation. This included down loading of PUBSYS accounting data into spreadsheet software such as Lotus 1-2-3 for use on personal computers. During fiscal year 1984, new quality assurance systems and procedures were designed and installed for data entry, software additions and improvements, and financial reporting.

The Draft of the Accounting and Financial Control Manual was reviewed with DOE, approved, and distributed. A system and procedures to keep the Manual up to date were established.

Table III shows a summary of the financial activities at the Laboratory for the last five years.

Budget and Manpower Planning Office

The Budget System, which has been in place for several years, continues to improve as users become more familiar with it as a management tool. The Laboratory personnel demographic data continues to improve as users realize the importance of maintaining these data. Monthly financial closings have become routine, due mainly to improvements to operating software installed during fiscal year 1984. A draft Budget Manual was completed and is in review prior to being forwarded to the DOE for its comments and approval. Important steps were taken to improve budget data discipline and the usefulness of the budget system to management for budget status and control. The preparation of Field Task Proposals from the budget data base improved in efficiency and effectiveness.

Information Resource Management

Emphasis was directed toward efficiency and cost saving in fiscal year 1984. The IBM 4331 at the Laboratory was upgraded to an IBM 4361, with the goal of improving response time and reducing both cost and the dependence on Princeton University for data processing services. During fiscal year 1984, a new center for administrative computing was established and the computer equipment and terminal links installed. A study has commenced to select and move operating systems from the University's IBM 3081 to the IBM 4361.

PUBSYS, a system that provides a high degree of flexibility to users requesting reports, was made operational. The first phase was directed toward providing the accounting reports, and as work continues into fiscal year 1985, budget, payroll, and personnel will be includ d. The introduction of PUBSYS provided a twofold gain: in addition to allowing the user to request reports, it has reduced our dependence on CICS, a rather expensive teleprocessing monitor. Users may now display, through CMS/RAMIS—the command processor for PUBSYS—the data that were provided on CICS screens. This will eventually eliminate the need for CICS and provide substantial and recognized cost savings.

An IBM 3270 computer communications service was extended to Laboratory managers at C-Site through the installation of coaxial cables between their offices and the C-Site IBM 3274 control unit. The control unit is programmed to provide access to PUBSYS and other VM/CMS time-sharing applications.

A guided Learning Center was established and outfitted with hardware to educate users in the use of PUBSYS. The system will be expanded to include budget, payroll, and personnel, and new enhancements will be added that increase the usefulness of the Learning Center. As the effort is directed toward cost containment and the transfer of processing from the Princeton University computer to the IBM 4361, the Learning Center's responsibilities will continue to expand in fiscal year 1985.

Development and enhancements were continued on the Work Approval Form and the Automatic Work Approval Form Transfer, a system to transfer Performance Measurement System job budgets to the

Balance Forward Accounting file. The system has been made operational; enhancements will continue in fiscal year 1985.

Work was completed on the overnight network processor. The system processes cost center allocations, calculates General and Administrative expenses and Tech Center overhead, and synchronizes budget entries in both the accounting and budget systems.

The study and specifications for point-of-receipt processing of receiving reports, corrections and returns was completed. However, system development is temporarily held in abeyance while a study of personal computer networking and the availability of personal computers to the Laboratory is completed.

Personal computer technology has evolved so rapidly in the last three years that the evolution has left little experience to draw upon. The Laboratory has procured a limited number of personal computers to enable an evaluation of their effectiveness in administrative data processing. Once the evaluation is completed in fiscal year 1985 and, if it proves to be an effective tool, system development will move forward taking advantage of the new technology.

Table III. PPPL Financial Summary.
(Thousands of Dollars)

	FY80	FY81	FY82	FY83	FY84
OPERATING (Actual Costs)					
Department of Energy					
TFTR Res and Develop Operations	$ 4,744	$ 2,314	$ 2,945	—	—
TFTR Facility Operations	5,587	11,832	10,424	18,029	16,725
TFTR Tokamak Flexibility Mod	4,885	13,951	13,033	17,725	19,358
TFTR CICADA	1,184	2,437	4,044	8,588	10,327
TFTR Neutral Beams	—	1,870	6,253	24,410	22,166
TFTR Experimental Research	1,768	2,081	2,835	5,682	5,422
TFTR Diagnostics	5,832	7,706	8,973	14,143	13,146
TFTR Remote Handling	—	—	—	65	813
TFTR Tritium Systems	—	—	—	301	2,628
TFTR Pellet Injector System	—	—	—	—	129
PLT/PDX/PBX	21,050	23,271	18,893	17,846	18,501
RF Development	—	—	—	742	617
ACT-I	398	438	443	458	408
S-1	1,565	3,223	3,254	3,703	3,561
Ignition Studies Project	—	—	—	—	2,744
Theory	2,437	2,643	2,488	2,808	3,061
Applied Physics	396	807	1,280	1,352	655
Other Research	290	364	495	418	457
Fusion Engineering Device	—	125	412	—	—
Change in Inventories	2,305	1,922	(237)	(3,169)	(599)
X-Ray Laser Development	160	251	266	313	16
Energy Management Studies	—	170	197	47	125
SRSA	1	—	—	—	—
Department of Defense	88	280	297	77	278
Other Contracts	491	563	565	893	1,880
Total Operating	$53,185	$76,248	$76,860	$114,431	$122,418
EQUIPMENT (Budget Authorization)					
Capital Equipment not Related to Construction	$ 6,974	$ 8,237	$ 9,272	$ 10,285	$ 8,896
CONSTRUCTION (Budget Authorization)					
TFTR	$19,361	$25,000	$31,600	$ 1,800	$ 255
PDX Neutral Beams	1,100	—	—	—	—
General Plant Projects	1,000	610	1,400	1,000	1,000
Energy Management Projects	558	115	—	499	1,049
Total Construction	$22,019	$25,725	$33,000	$ 3,299	$ 2,304

PPPL INVENTION DISCLOSURES FOR FY84

Title	Inventor(s)
High Resolution Multichannel Spectrometer (HIRUM)	S. Suckewer J. Schwab
Multiple Lockin Method for rf Signal Detection Amidst rf Pickup and Broadband Noise	J. Goree
Process for Controlling the Plasma Energy Flux to a Limiter by Varying the Plasma Elongation	J. Cecchi B. Coppi
Direct Generation of Electricity from a Magnetized Plasma Using Finite Ion Larmor Radius and/or Ion Sheath Thickness Effects	P. Stangeby
Inductive Steady-State Spheromak Maintenance without Electrode	A. Janos M. Yamada S. Jardin
Helium Ash Monitor	R. Fonck R. Goldston R. Kaita D. Post
Plasma-Deposited Hydrogenated and Deuterated Amorphous Semi-Conductors for First-Wall Materials and Coatings in Polarized Fusion Reactors	H. Greenside R. Budny D. Post
Practical Access to Very High Beta Tokamak Operation Through Bean Shaping	M. Chance S. Jardin T. Stix R. Grimm J. Manickam M. Okabayashi
Rotating Indented Limiter	S. Cohen J. Timberlake J. Hosea
Generation of X-Ray Lasing Action in Confined Plasma Column by Picosecond Laser	S. Suckewer
External Pusher Coil Stabilizer for High-Shear Torsatron	J. Johnson G. Rewoldt
Steady-State Maintenance and Current Drive of Spheromaks by Continuous Inductive Ψ - Φ Pumping	A. Janos
Liquid-Metal First-Wall/Blanket for Magnetic Fusion Reactors	H. Furth D. Post D. Jassby M. Yamada
Ion and Atomic Beam Limiter Conditioning	D. Mueller L. Grisham
E $\parallel$ B Ion Mass/Energy Spectrometer	S. Medley R. Kaita A. Roquemore
TPX Vacuum Window	J. Goree B. Blanchard

PPPL INVENTION DISCLOSURES FOR FY84

Title	Inventor(s)
Transport Reducing Vertical Field Coil	H. Mynick
Push-Pull Circuit with Integrated Transition to Waveguide Output Terminal for Use in ICRF Plasma Heating Equipment	W. Bennett
Enhancement of Stellarator Confinement by Operation at Positive Ambipolar Potential	H. Mynick
Ground Monitoring Device	G. Cutsogeorge M. Viola R. Woolley
Electro-Magnetic Transparent Electrostatic Faraday Shields	D. Hwang C. Fortgang J. Hosea
Symmetric Tandem Mirror	S. Yoshikawa
Disruption Control Passive Conductors	J. Murray
Tokamak Poloidal Field Diagnostic Using Fusion Products	W. Heidbrink
Tokamak Ion Temperature Diagnostic Using Charged Fusion Products	W. Heidbrink
Method and Apparatus for Fast Ramp-up of Tokamak Current with Waves	N. Fisch C.F.F. Karney
Protection for Probes, Limiters, etc., in Toroidal Fusion Devices	S. Yoshikawa D. Manos
Compact Torus Stellarators Hybrid Configuration	H. Furth C. Ludescher
Bonding of Powders to Substrates by Plasmas	S. Cohen S. Yoshikawa
Coil to Maintain Equilibrium in Stellarators with Large Transform Per Period at High Pressure	A. Reiman A. Boozer
Laser Optical Pumping—Spin Exchange Production at Large Quantities of Highly Polarized Hydrogenic Isotopes	R. Knize W. Happer J. Cecchi
Cross Potential in Tokamak Configuration	J. Murray G. Bronner
Current Maintenance by Charged Fusion-Product Particle Production in Fusion Devices	S. Cohen R. Budny S. Yoshikawa
Carbon-Heated Lanthanum Hexaboride Cathode	J. Goree R. Horton M. Ono
Toroidal Mid-Plane Neutral Beam Armor and Limiter for Indented Bean-Shaped Plasmas	H. Kugel S. Hand H. Ksayian

GRADUATE EDUCATION: PLASMA PHYSICS

The program of graduate education in plasma physics bridges two institutions: Princeton University and the Princeton Plasma Physics Laboratory (PPPL), which provides a major center of excellence for the University. Shortly after the declassification of the fusion energy research effort in 1959, the Plasma Physics Program was first offered at Princeton University in the Department of Astrophysical Sciences. The Program has evolved and adapted, over its twenty-five years of life, to provide pertinent graduate education in an environment that has seen enormous changes in the fields of plasma physics and controlled fusion. In this period, the Program has established its own traditions of education—centered on fundamentals in physics and applied mathematics—and training—based on intense exposure to the cutting edge of research in plasma physics.

Graduate students entering the Plasma Physics Program at Princeton University spend the first two years in classroom study, laying a firm foundation in the many disciplines which make up plasma physics: classical and quantum mechanics, electricity and magnetism, fluid dynamics, hydrodynamics, atomic physics, applied mathematics, statistical mechanics, and kinetic theory. Table I lists the Departmental courses offered this past academic year. Many of these courses are taught by the members of PPPL's research staff who also comprise the fifteen member plasma physics faculty (see Table II). The curriculum is supplemented by courses offered in other departments of the University and by a student-run seminar series in which PPPL physicists share their expertise with the graduate students.

Most students hold Assistantships in Research at PPPL through which they participate in the continuing experimental and theoretical research programs. In addition to formal class work, first and second-year graduate students work side by side with the research staff, have full access to laboratory facilities, and learn firsthand the job of a research physicist. First-year students assist in experimental research areas,

Table I. Plasma Physics Courses Offered and Instructors.

Course Number	Course Title	Instructor
	Fall 1983	
AS 551	General Plasma Physics I	T.H. Stix and S.E. von Goeler
AS 553	Plasma Waves and Instabilities	F.W. Perkins, Jr.
AS 557	Advanced Mathematical Methods in Astrophysical Sciences	J.A. Krommes
AS 558	Seminar in Plasma Physics	C.R. Oberman
AS 561	Special Topics in Magnetic Confinement	P.H. Rutherford and S. Yoshikawa
	Spring 1984	
AS 552	General Plasma Physics II	R.M. Kulsrud and W.M. Tang
AS 554	Irreversible Processes in Plasma	C.F.F. Karney
AS 556	Advanced Plasma Dynamics	C.R. Oberman and H. Okuda
AS 558	Seminar in Plasma Physics	G. Rewoldt

Table II. Astrophysical Sciences/Plasma Physics Faculty.

Faculty Members	Title
Thomas H. Stix	Associate Chairman, Department of Astrophysical Sciences, and Associate Director for Academic Affairs, PPPL
Liu Chen	Principal Research Physicist and Lecturer with rank of Professor
Harold P. Furth	Professor of Astrophysical Sciences
Charles F.F. Karney	Research Physicist and Lecturer with rank of Associate Professor
John A. Krommes	Research Physicist and Lecturer with rank of Associate Professor
Martin D. Kruskal	Professor of Mathematics and Astrophysical Sciences
Russell M. Kulsrud	Principal Research Physicist and Lecturer with rank of Professor
Carl R. Oberman	Principal Research Physicist and Lecturer with rank of Professor
Hideo Okuda	Principal Research Physicist and Lecturer with rank of Professor
Francis W. Perkins, Jr.	Principal Research Physicist and Lecturer with rank of Professor
Gregory Rewoldt	Research Physicist and Lecturer in Astrophysical Sciences
Paul H. Rutherford	Principal Research Physicist and Lecturer with rank of Professor
William M. Tang	Principal Research Physicist and Lecturer with rank of Professor
Schweickhard E. von Goeler	Principal Research Physicist and Lecturer with rank of Professor
Shoichi Yoshikawa	Principal Research Physicist and Lecturer with rank of Professor

including TFTR diagnostics development, PLT, PBX, ACT-I, S-1 Spheromak, and the X-Ray Laser Project. In a similar fashion, second-year students assist members of the Theoretical and Applied Physics Divisions. Often the results of this work are documented by the students and published in professional journals. Following the two years of class work, students concentrate on the research and writing of a Ph.D. thesis. This research is under the guidance of a member of the PPPL staff, although thesis students bear a greater responsibility for the content of their projects than do first and second-year students. Of the forty-two graduate students in residence this past year, twenty-five were engaged in thesis projects—fourteen on theoretical topics and eleven on experimental topics. Table III lists the doctoral thesis projects completed this fiscal year under the Plasma Physics Program.

Outside support for the graduate program came, in part, from the Westinghouse Educational Foundation. A grant from this Foundation has permitted the Department of Astrophysical Sciences to offer prizes to outstanding applicants to the Plasma Physics Program. In addition, some students were awarded fellowships by the National Science Foundation, the Fannie and John Hertz Foundation, the State of New Jersey Department of Higher Education, and the National Science and Engineering Research Council of Canada. In most cases these fellowships are supplemented by partial research assistantships.

Overall, the plasma physics graduate studies program in Princeton's Department of Astrophysical Sciences has had significant impact on the field of plasma physics: More than 100 physicists have now received doctoral degrees in this field. Many of them have become leaders in plasma research and technology in academic, industrial, and government institutions. Even now the process goes on. The Laboratory continues to train the next generation of scientists, preparing them to take on the challenging problems of the future.

Table III. Recipients of Ph.D. Degrees.

Daniel E. Dubin		
	Thesis:	Perturbation Methods and Closure Approximations in Nonlinear Systems, May 1984
	Advisor:	John A. Krommes and Carl R. Oberman
	Employment:	University of California, San Diego
Taik S. Hahm		
	Thesis:	Theory of Weakly Collisional Modes in Magnetically Confined High Temperature Plasmas, August 1984
	Advisor:	Liu Chen
	Employment:	Institute for Fusion Studies, University of Texas, Austin
William W. Heidbrink		
	Thesis:	Tokamak Diagnostics using Fusion Products, April 1984
	Advisor:	James D. Strachan
	Employment:	Princeton Plasma Physics Laboratory
Alice E. Koniges		
	Thesis:	MHD Equilibrium in Toroidal Systems with a Helical Magnetic Axis, September 1984
	Advisor:	John L. Johnson
	Employment:	Lawrence Livermore National Laboratory
Bradley J. Micklich		
	Thesis:	Control of Neutron Albedo in Toroidal Fusion Reactors, November 1983
	Advisor:	Daniel L. Jassby
	Employment:	Nuclear Engineering Program, University of Illinois
David L. Ruzic		
	Thesis:	Total Scattering Cross-Sections and Interatomic Potentials for Neutral Hydrogen and Helium on Some Noble Gasses, February 1984
	Advisor:	Samuel A. Cohen
	Employment:	Nuclear Engineering Laboratory, University of Illinois
Harold R. Thompson		
	Thesis:	Second Harmonic Ion Cyclotron Resonance Heating by the Fast Magnetosonic Wave on the PLT Tokamak, December 1983
	Advisor:	Joel C. Hosea
	Employment:	University of California, Irvine

GRADUATE EDUCATION: PLASMA SCIENCE AND FUSION TECHNOLOGY

The collaborative effort between the Princeton Plasma Physics Laboratory and Princeton University's School of Engineering and Applied Science (SEAS) has evolved during the past fiscal year with the appointment of an Interim Committee for Graduate Study in Plasma Science and Fusion Technology to plan the formation of an Interdepartmental Program in Plasma Science and Fusion Technology. An outgrowth of the Fusion Reactor Technology Program, which was established more than a decade ago in the Department of Chemical Engineering, the new endeavor will be broadened to include all four departments of SEAS: Chemical Engineering, Civil Engineering, Electrical Engineering and Computer Science, and Mechanical and Aerospace Engineering.

An important event for the Program occurred at the end of FY84 when the State of New Jersey, through the Governor's Commission on Science and Technology, furnished the University with a $100,000 grant, one-half of which is intended for graduate support. The other half will support the Cooperative Industrial Program in Plasma Science and Fusion Technology (formerly the Industrial Training Program). Support for participation of two mid-career industrial engineers in the Program is now ensured, and increased recruiting activities are being undertaken.

PROGRAMS

Princeton continues as a participating university in the U.S. Department of Energy's Magnetic Fusion Energy Technology Fellowship (MFETF) Program, an affiliation begun when that program was initiated four years ago. During FY84 three students in the interdepartmental program were supported by this Fellowship: one has received his degree (while completing his master's program here, this student contributed to two publications describing early work on TFTR[1,2] and wrote his dissertation[3] on an allied subject), one anticipates it shortly, and the third has returned for his second-year work. He has been joined by a recent MFETF recipient, making the current number in residence two.

The Cooperative Industrial Program in Plasma Science and Fusion Technology, after a successful beginning, was largely dormant during the past year due to the lack of success in attracting participants. As a result of the recent State grant, the employer of a participant in the Program is now responsible for only one-half of the visiting engineer's salary instead of the full amount. A new brochure emphazing this feature has been prepared, and it is hoped that this will help in the recruitment of new participants.

ACTIVITIES

In FY84 the number of supported graduate students increased from six to ten, with two more expected as a result of the State grant. Two students in the Program completed Ph.D. degrees, one finished his master's work, and a fourth will receive his doctorate shortly. Four students are supported by Fellowships and six are receiving PPPL support. Their activities are detailed in Table I.

Faculty members played a greater role in the Program during the last fiscal year with their support increasing approximately 20% over the previous year. Several areas of study for students and of mutual interest to SEAS and PPPL were explored including: Nuclear Instrumentation, Computer-Assisted Data Reduction, Radiation Damage Studies, Coupled Mechanical/Electrodynamic Analysis, Fast Response Detectors, and Submillimeter Laser Development.

PROJECTS

The new Chemical Engineering Laboratory completed its first full year of operation, during which two graduate students pursued their research topics and published their findings.[4,5] One dissertation was completed.[6]

Establishment of a second laboratory, this one for polymer research, was undertaken during the period, and its completion is expected in the Spring of 1985. Also located on the Forrestal Campus near the Chemical Engineering Laboratory, the new facility will accommodate studies involving the effects of radiation on polymers.

DEPARTMENT CURRICULUM

In addition to the graduate program, the Chemical Engineering Department offers a strong undergraduate curriculum to stimulate interest in fusion. A

Table I. Graduate Students in the Plasma Science and Fusion Technology Program.

J.V. Foley[a]	
Thesis Topic:	Neutronic Instrumentation
Advisor:	H. Hendel/R.G. Mills
Department:	Chemical Engineering
K.W. Goossen[a]	
Thesis Topic:	Fast Response Detectors
Advisor:	S.A. Lyon
Department:	Electrical Engineering and Computer Science
F. Auzerais[b]	
Thesis Topic:	
Advisor:	Undecided
Department:	Chemical Engineering
G. Dhondt[b]	
Thesis Topic:	Radiation Damage
Advisor:	A.C. Eringen
Department:	Civil Engineering
E. DiPesquole[b]	
Thesis Topic:	Computer Assisted Data Reduction
Advisor:	E.J. Durbin
Department:	Mechanical and Aerospace Engineering
M. Grant[a]	
Thesis Topic:	Hydrogen-Metal Interaction
Advisor:	Undecided
Department:	Chemical Engineering
J.S. Lee[b]	
Thesis Topic:	Coupled Mechanical/Electrodynamic Analysis
Advisor:	J.H. Prevost
Department:	Civil Engineering
R. Myers[b]	
Thesis Topic:	Plasma Propulsion
Advisor:	R.G. Jahn
Department:	Mechanical and Aerospace Engineering
P. Pang[b]	
Thesis Topic:	Polymers
Advisor:	J.K. Gillham
Department:	Chemical Engineering
John F. Quanci[a]	
Thesis Topic:	Tritium Recovery Experiments
Advisor:	R.G. Mills/D.L. Jassby
Department:	Chemical Engineering

[a]Supported by Fellowship.
[b]Supported by PPPL.

minicourse on fusion is included in Chemical Engineering 101. It is designed primarily for A.B. students to satisfy their science requirement but is frequently elected by entering freshman engineering students. Junior and Senior independent work in fusion is also sponsored. The undergraduate course Introduction to Fusion Power (CHE 417) is suitable for both undergraduate and graduate students, and it has been elected by graduate students of four different departments.

Each year Chemical Engineering 417 welcomes as auditors several members of the professional engineering staff of the Laboratory. These people are specialists seeking a broader understanding of aspects of the Laboratory work that differ from their professional specialty. Since FY79 this arrangement has provided a unique opportunity for students to associate with working professionals in the topic of the course. To reinforce this opportunity, a key feature of the course is a machine design project. The class

is divided into two teams for a competition. The professional staff members are divided into three groups, two sets of consultants for the teams and a selection board to evaluate the final design. In some years younger staff members are assigned as members of the teams. Oral presentations before the board are a fairly realistic preview of the "real world's" contractor selection procedures.

Chemical Engineering courses relating to the Plasma Science and Fusion Technology Program are given in Table II.

With the addition of the remaining SEAS departments to the Program, other pertinent courses, both on the graduate and undergraduate level, are recommended to the students. These are listed in Table III, together with three courses of interest in Astrophysical Sciences.

References

[1]K.M. Young, M. Bell, W.R. Blanchard, *et al.*, "TFTR Initial Operations," Princeton University Plasma Physics Laboratory Report PPPL-2051 (1983) 33 pp.

[2]R.J. Hawryluk, M.G. Bell, M. Bitter, *et al.*, "Recent Results from TFTR," in *Heating in Toroidal Plasma* (Proc. 4th Int. Symp., Rome, 1984), edited by H. Knoepfel and E. Sindoni, Vol. II, International School of Plasma Physics and ENEA, Varenna (1984) 1012.

[3]J.A. Isaacson, "Activation Analysis for Fusion Research Neutron Source Strength Measurement," M.S. Thesis, Princeton University, 1984.

[4]P.C. Bertone and D.L. Jassby, "Tritium Recovery from Lithium Oxide Pellets," J. Nucl. Mater. *122&123* (1983) 883.

[5]P.C. Bertone and T.M. Kasturirangan, "Fusion Blanket Design Fundamentals," in *Fusion Engineering* (Proc. 10th Symp., Philadelphia, 1983), Vol. 2, IEEE Cat. No. 83CH1916-6 NPS, New York (1983) 1148.

[6]T.M. Kasturirangan, "Slurry Blankets for D-T Fusion Reactors," Ph.D. Thesis, Princeton University, 1984.

Table II. Chemical Engineering Courses Relating to the Plasma Science and Fusion Technology Program and Instructors.

Course Number	Course Title	Instructor
CHE 351,352	Junior Independent Work	Staff
CHE 451,452	Senior Independent Work	Staff
CHE 417	Introduction to Fusion Power	R.G. Mills
CHE 418	Nuclear Engineering	R.C. Axtmann
CHE 550	Fusion Reactor Technology	R.C. Axtmann
		R.G. Mills

Table III. Pertinent Courses in Other SAES Departments.

Graduate Courses of Interest

Chemical Engineering

544	Chemical Reactor Engineering
545	Mathematical Methods of Engineering Analysis (also CE 502)
550	Fusion Reactor Technology

Civil Engineering

501	Mathematical Methods of Engineering Analysis I
502	Mathematical Methods of Engineering Analysis II (also CHE 545)
553	Advanced Structural Mechanics
576	Electromagnetic Interactions with Continua

Electrical Engineering and Computer Science

540	Solid State Electronics
541	Electronic Materials
542	Surface Properties of Electronically Active Solids
543	Transport Processes in Solids

Mechanical and Aerospace Engineering

511	Experimental Methods
513	Dynamic Data Analysis
528	Plasma Dynamics
547	Optics and Lasers
583	Electric Propulsion

Astrophysical Sciences

551	General Plasma Physics I
552	General Plasma Physics II
553	Plasma Waves and Instabilities

Undergraduate Courses of Interest

Chemical Engineering

417	Introduction to Fusion Power
418	Nuclear Engineering
441	Chemical Reactor Engineering
445	Process Control

Civil Engineering

310	Introduction to Numerical Methods for the Solution of Differential Equations
463	Finite Element Methods in Structures and Mechanics

Electrical Engineering and Computer Science

481	Introduction to Solid State Electronics
483	Microwave Electronics

Mechanical and Aerospace Engineering

433	Automatic Control Systems

SECTION EDITORS

Tokamak Fusion Test Reactor
S. Duritt, Jr.

Princeton Large Torus
J. Stevens

Princeton Beta Experiment
T. Takahashi

S-1 Spheromak
M. Yamada
A. Janos

Advanced Concepts Torus-I
M. Ono

X-Ray Laser Studies
C. Skinner

Theory
A. Boozer

Tokamak Modeling
G. Bateman

Reactor Studies
D. Jassby

Spin-Polarized Fusion Program
R. Knize

Tokamak Fusion Core Experiment
M. Machalek

Engineering Department

Engineering Analysis Division
R. Ellis, III

Electronic and Electrical Engineering Division
P. Murray

Mechanical Engineering Division
E. Moshey

Computer Division
S.A. Connell

Planning and Resource Management
A. Upperco

Quality Assurance and Reliability
H. Howard

Administrative Operations
O. Bernett
M. Iseicz

Graduate Education: Plasma Physics
T. Stix

Graduate Education: Plasma Science and Fusion Reactor Technology
R. Mills

GLOSSARY OF ABBREVIATIONS, ACRONYMS, SYMBOLS

A	Ampere
Å	Angstrom unit; 10^{-8} cm
ac	*Alternating Current*
ACT-I	Advanced Concepts Torus-I (at the Princeton Plasma Physics Laboratory)
A/D	Analog-To-Digital
ADP	Automated Data Processing
ADPE	Automated Data Processing Equipment
Alcator	A family of tokamak devices being developed and built at the Massachusetts Institute of Technology
ALT	Advanced Limiter Test on TEXTOR (Jülich, West Germany); Version I
ALT-I	Version II of ALT
amu	*Atomic Mass Unit*
ANL	Argonne National Laboratory
ASDEX	Axially Symmetric Divertor Experiment (Max-Planck-Institut für Plasmaphysik, Garching, West Germany)
ATF-1	*Advanced Toroidal Facility-1 (a stellarator at Oak Ridge National Laboratory)*
BALDUR	A Princeton Plasma Physics Laboratory one-dimensional tokamak transport code
BTM	Block Transfer Module
CADD	*Computer-Aided Design and Drafting (Facility)*
CAMAC	Computer-Automated Measurement and Control (System)
CAR	Computer-Assisted Retrieval
CAR	Cost Analysis Report
CCD	*Capacitor Charge/Discharge*
CFFTP	Canadian Fusion Fuels Technology Project
CICADA	Central Instrumentation, Control, and Data Acquisition System
CIPREC	Conversational and Interactive Project Evaluation and Control System
cm	Centimeter
COO	Chicago Operations Office
COS	Console Operating Station
CPSR	Contractor Procurement System Review
CRAY	A brand of computer made by Cray Research, founded by S. Cray
CTR	Controlled Thermonuclear Research
CY	Calendar Year
°	Degrees
°C	Degrees Centigrade
°K	Degrees Kelvin
D/A	Digital-To-Analog
D-D	*Deuterium-Deuterium*
D-III	Doublet-III. A tokamak located at GA Technologies, Incorporated
D-T	Deuterium-Tritium
DARM	*Data Acquisition Room*
DAS	Data Acquisition System (on PLT, PBX, S-1)
DAX	DAS supplemental system (uses a VAX computer)
dc	Direct Current
DECAT	Drivers Energy Conservation Awareness Training
DEGAS	A PPPL computer code for studying the behavior of neutrals in plasma
DEMO	Demonstration Power Reactor
D&GF	Design and General Fabrication (Section)
DITE	Divertor and Injection Tokamak Experiment (Culham Laboratory, United Kingdom)
DOD	Department of Defense
DOE	Department of Energy
DPI	Deuterium Pellet Injector

EAD	Engineering Analysis Division
ECE	Electron Cyclotron Emission
ECH	Electron Cyclotron Heating
ECO	Energy Conservation Opportunities
ECRF	Electron Cyclotron Range of Frequencies
ECRH	Electron Cyclotron Resonance Heating
ECS	Energy Conversion System
EF	Equilibrium Field
EPRI	Electric Power Research Institute
ERB	Engineering Review Board
ERP	Edge Relaxation Phenomena
ESU	Emergency Services Unit
ETACS	Equipment Tracking and Control System
ETR	Engineering Test Reactor
ETS	Engineering Test Station
eV	Electron Volt
EZB	Exclusion Zone Boundary
FAN	Facility Advisory Notices
FCPC	Field Coil Power Conversion
FED	Fusion Engineering Device
FEDC	Fusion Engineering Design Center (Oak Ridge National Laboratory)
FELIX	An experimental test facility under construction at the Argonne National Laboratory
FEM	Finite Element Modeling or Finite Element Method
FIDE	Fast Ion Diagnostic Experiment
FIR	Far-Infrared
FLOPSY	*Flexible Optical Path System*
FLR	Finite Larmor Radius
FSAR	Final Safety Analysis Report
FTS	Federal Telecommunications System
FY	Fiscal Year (October 1 to September 30)
G	Gauss
G&A	General and Administrative (cost or expense)
GAO	General Accounting Office
GAT	GA Technologies, Incorporated
GDC	Glow Discharge Cleaning
GE	General Electric Company
GHz	Gigahertz; 10^9 cycles per second
GJ	Gigajoule, a unit of energy; 19^9 joules
gpm	Gallons Per Minute
GPP	General Plant Projects
GSA	General Services Administration
GSF	Gross Square Feet
H	High-Confinement Mode
HAIFA	Hydrogen Alpha Interference Filter Array
HAX	High-Level Data Analysis (system); uses a VAX computer
HEDL	Hanford Engineering Development Laboratory
HLDAS	High-Level Data Analysis System; equivalent to HAX
H-mode	High-Confinement Mode
HPA	High Power Amplifier
HVAC	Heating, Ventilating, and Air Conditioning
HVE	High-Voltage Enclosure(s)
IBW	Ion-Bernstein Wave
ICH	Ion Cyclotron Heating
ICRF	Ion Cyclotron Range of Frequencies
ICRH	Ion Cyclotron Resonance Heating
IMAPS	Interstellar Medium Absorption Profile Spectrograph
INEL	Idaho National Engineering Laboratory
INTOR	International Tokamak Reactor
IPP	Initial Protective Plates
IPP	Institut für Plasmaphysik at Garching, West Germany
IR	*Infrared*
IRM	Information Resources Management

ISX	Impurity Study Experiment (at Oak Ridge National Laboratory)
ITR	Ignition Test Reactor
JAERI	Japan Atomic Energy Research Institute
JET	Joint European Torus
JT-60	JT stands for JAERI Tokamak and 60 means plasma volume in m^3. An energy breakeven plasma testing device in Japan
kA	Kiloamperes
keV	Kilo-Electron-Volts
kHz	Kilohertz
kG	Kilogauss
kJ	Kilojoule
kV	Kilovolt
kV A	Kilovolt Ampere
kW	Kilowatt
kW h	Kilowatt Hour
L	Low-Confinement Mode
LANL	Los Alamos National Laboratory
LBL	Lawrence Berkeley Laboratory
LBM	Lithium Blanket Module
LC	Inductance Capacitance
LCCs	Local Control Centers
LCP	Large Coil Program
LH	Lower Hybrid
LHCD	Lower Hybrid Current Drive
LHe	Liquid Helium
LHRF	Lower Hybrid Range of Frequencies
LHRH	Lower Hybrid Resonance Heating
LITE	Laser Injected Trace Element (System)
LITE	Long-Pulse Ignited Test Experiment (at the Massachusetts Institute of Technology)
LLNL	Lawrence Livermore National Laboratory
L-mode	Low-Confinement Mode
LO	Local Oscillator
LOB	Laboratory Office Building
μm	Micrometer; equivalent to micron
μsec	Microsecond
m	Meter
MA	Megamperes
MARS	Mirror Advanced Reactor Study (Lawrence Livermore National Laboratory)
Mb	Megabyte
MCNP	Monte-Carlo Neutron and Proton Code
MCP	Microchannel Plate
MED	Mechanical Engineering Division
MeV	Mega-Electron-Volt
MFAC	Magnetic Fusion Advisory Committee
MFETF	Magnetic Fusion Energy Technology Fellowship
MG	Motor Generator
MHD	Magnetohydrodynamics
MHz	Megahertz
MIRI	Multichannel Infrared Interferometer
MIST	A computer code which follows impurity species through various stages of ionization, charge-exchange, radiation, and transport within the plasma
MIT	Massachusetts Institute of Technology
MJ	Megajoules
mm	Millimeter
MPG	Managing Personal Growth
msec	Millisecond
MTL	Material Test Laboratory
MVA	Megavolt Ampere
mW	Milliwatt
MW	Megawatt
NASTRAN	A structural analysis code
NASW	National Association of Science Writers

NB	Neutral Beam
NBETF	Neutral Beam Engineering Test Facility
NBI	Neutral Beam Injection
NBLs	Neutral Beamlines
NBPS	Neutral Beam Power Supply
NBTC	Neutral Beam Test Cell
NCR	Nonconformance Report
nm	Nanometer
NMFECC	National Magnetic Fusion Energy Computer Center
nsec	Nanosecond
OFE	Office of Fusion Energy
OFHC	Oxygen-free high conductivity (copper)
OH	Ohmic Heating
OMA	Optical Multichannel Analyzer
OM&S	Occupational Medicine and Safety
ORC	Operations Review Committee
ORNL	Oak Ridge National Laboratory
ORR	Operational Readiness Review
OSES	Operations System Engineering Support
OSR	Operational Safety Requirements
PADS	Procurement Automated Data Processing System
PBX	Princeton Beta Experiment
pC	Pico Coulomb
PDC	Pulse Discharge Cleaning
PDR	Preliminary Design Review
PDX	Poloidal Divertor Experiment
PEST	Princeton Equilibrium, Stability, and Transport Code
PF	Poloidal Field
PFC	Plasma Fusion Center (at the Massachusetts Institute of Technology)
PHA	Pulse Height Analysis
PLT	Princeton Large Torus
PM&E	Plant Maintenance and Engineering
PMS	Performance Measurement System
PMS	Performance Management System
P&OS	Project and Operational Safety
PP&L	Pennsylvania Power and Light
PPPL	Princeton Plasma Physics Laboratory
PSE&G Co.	Public Service Electric and Gas Company
psi	Pounds Per Square Inch
PUBSYS	PPL Public Information System (installed on the Princeton University IBM 3081 computer)
QA	Quality Assurance
QA/R	Quality Assurance and Reliability
RAX	TFTR off-line data reduction system (uses a VAX computer)
RBT	Resonance Broadening Theory
rf	Radio Frequency
RFBA	Request for Baseline Adjustment
RFP	Request for Proposal
RFP	Reversed-Field Pinch
RFTF	Radio-Frequency Test Facility
RGA	Residual Gas Analyzer
RIV	Rapid Intervention Vehicle
rms	Root Mean Square
RPI	Repeating Pneumatic Injector
rpm	Revolutions Per Minute
S-1 Spheromak	A compact toroid device (at the Princeton Plasma Physics Laboratory)
SAD	Safety Assessment Document
SCR	Silicon Controlled Rectifier
SEAS	School of Engineering and Applied Science
sec	Second
SF	Shaping Field, equivalent to EF
SNAP	Time-independent power equilibrium code
SOXMOS	Soft X-Ray Monochromator Spectrometer

SPARK	A general geometry computer code that calculates transient eddy currents and the resulting fields
SPEB	Subcontract Proposal Evaluation Panel
SPICE	A general purpose circuit simulation code
SPRED	Survey, Power Resolution, Extended Domain Code
SPS	Surface Pumping System
Sr	Steradian
SR	Safety Requirements
STARTUP	A computer code which evaluates free boundary axisymmetric equilibria and transport
SURFAS	A fast between-shot moments code
TAC	Technical Advisory Committee
TBR	Tritium Breeding Ratio
TEXTOR	Tokamak Experiment for Technologically Oriented Research (Jülich, West Germany)
TF	Toroidal Field
TFCD	Tokamak Fusion Core Device
TFCX	Tokamak Fusion Core Experiment
TFM	TFTR Flexibility Modification
TFTR	Tokamak Fusion Test Reactor
TiC	Titanium Carbide
TLD	Thermoluminescent Dosimeters
TMPs	Turbo-Molecular Pumps
Torr	Torr
TOS	Terminal Operating Station
TPI	Tritium Pellet Injector
TR	Trouble Reports
TRANSP	Time-dependent transport analysis code
TSCALE	A computer code that scales plasma equilibrium parameters over a wide range of major radius and aspect ratio
TVPS	Torus Vacuum Pumping System
TVTS	TV Thomson Scattering
UCLA	University of California at Los Angeles
USC	User Service Center; implemented on a Digital Equipment Corporation (DEC) PDP-10 computer
UV	Ultraviolet
V	Volt
VAX	Digital Equipment Corporation computer; "Virtual Address Extention"
VIPS	Visible Impurity Photometric Spectrometer
VUV	Vacuum Ultraviolet
W	Watt
WBS	Work Breakdown Structure
WKB	Wentzel-Kramers-Brillouin. (A method for analyzing wave behavior if propagation characteristics depend on position.)
XIS	(Horizontal) X-Ray Imaging System
XUV	Extreme Ultraviolet
ZrAl	Zirconium-Aluminum